



The University of
Nottingham

UNITED KINGDOM • CHINA • MALAYSIA



BBSRC Doctoral
Training Partnerships

Understanding the use of sex pilus specific bacteriophages to reduce conjugative dissemination of antibiotic resistance

Ramon Pedraja Maluping

DVM, MS, MSc (*Cantab*), CSci FIBMS, CBiol MRSB

**Thesis submitted to the University of Nottingham
for the Degree of Doctor of Philosophy**

School of Veterinary Medicine and Science

University of Nottingham, UK

December 2022

Abstract

Antimicrobial resistance (AMR) is considered as one of the greatest threats to human public health and in agriculture and food security. To address this threat, a Global Action Plan encourages development of alternatives to antibiotics, including the use of bacteriophage to control infections. A large proportion of transmissible antibiotic resistance is encoded on conjugative plasmids. Transmission requires sex pili and a sex pilus targeting (SPS) phage could provide a selection against plasmid carriage.

The aim of this research is to isolate novel SPS phage to tackle AMR bacteria. Fifteen SPS phages were isolated, eleven were ssDNA phages in the *Inoviridae* family and four were ssRNA phages of the *Leviviridae* family. All phages were able to infect strains with the F plasmid but there was some phage plasmid specificity observed on different F like plasmid field isolates. Phylogenetic analysis of the 11 ssDNA phages genomes and protein pIII confirmed that they belong to genus *Inovirus* and are highly similar to filamentous (Ff) phages (M13, fd, f1). Three of the ssRNA phages were highly similar to genus *Levivirus* and the remaining ssRNA phage was similar to *Allolevivirus*. Two ssDNA phages R4 and R7, and ssRNA phage R13 represent a new species of *Inovirus* and *Allolevivirus*, respectively under ICVCN guidelines. All the phages demonstrated good stability under various conditions of temperature, pH and detergent.

One step growth analysis and plasmid loss kinetics of selected ssDNA and ssRNA phages were tested against strains containing derepressed and repressed plasmids. Phage growth on derepressed plasmid hosts had a

short latent period and large burst size compared to a longer latent period with shorter rise period and burst size observed on repressed plasmid hosts. Selected phages demonstrated *ca.* 60% plasmid loss on derepressed hosts. Selection was limited on more repressed plasmid hosts, with a minimum loss of 0% and a maximum loss of 14%. These results suggest that treatment with phage will have variable efficacy in reducing plasmid borne AMR and that repression may pose a limit on the effectiveness of this approach to treat or reduce infections by targeting the plasmids. However, further investigations are required to fully understand SPS phage impact under additional environmental selective conditions.

Declaration

I declare that the work in this dissertation was carried out in accordance with the regulations of the University of Nottingham.

The work is original and has not been submitted for any other degree at the University of Nottingham or elsewhere.

Name: Ramon Pedraja Maluping

Signature:

A handwritten signature in black ink that reads "Ramon P. Maluping". The signature is written in a cursive style with a prominent dot over the 'i' in "Maluping".

Date: March 9, 2022

Acknowledgments

My deepest gratitude goes to:

Dr. Michael A. Jones and Dr. Robert J. Atterbury, my supervisors, for accepting me in their research group, for their intellectual input to this research project, for the training and support they have given me throughout my PhD and for their careful reading of this dissertation. To Prof. Paul A. Borrow, former member of my supervisory team, for inspiring me to do phage research and for the friendship.

Dr. Janis Rumnieks for his advice and for unselfishly sharing his expertise in the field of single stranded bacteriophage. To Joan Colom, Adriano Gigante, Abiyad Baig and to everyone at the School of Veterinary Medicine for all the help and advice during this research.

To everyone at the University Disability Support Services especially to Caroline Adlam for the support, help and encouragement especially during those challenging times.

To my examiners Prof. Aidan Coffey, Prof. Malcolm Bennett and Dr. Sharon Egan, for their constructive comments, suggestions and advice for the improvement of this thesis.

The BBSRC DTP management headed by Prof. Zoe Wilson for the support throughout my PhD and especially during the Covid lockdowns. To all UK taxpayer for the financial support through the BBSRC DTP scholarship.

To my whole family and to all my friends for the unconditional love. To God Almighty for all these blessings.

Table of Contents

Chapter 1. Introduction	1
1.1 Antimicrobial resistance – the problem.....	1
1.2 <i>Escherichia coli</i> and the study of AMR	6
1.3 AMR and plasmids	7
1.3.1 Classification of plasmids.....	9
1.3.2 Incompatibility group and AMR.....	10
1.3.3 Incompatibility F (IncF).....	13
1.3.4 Repression and derepression in IncF plasmids.....	13
1.3.5 The fertility inhibition (FinOP) system	15
1.4 Bacteriophage.....	16
1.5 AMR, plasmid and the F pilus specific phage.....	22
1.5.1 Single-stranded DNA (ssDNA) bacteriophages.....	23
1.5.2 Single-stranded RNA (ssRNA) bacteriophages	27
1.6 Bacteriophage (phage) therapy.....	31
1.7 Inhibition of conjugation and plasmid DNA transfer	32
1.7.1 Pilus specific phage as inhibitor of conjugation.....	32
1.7.2 Other strategies to inhibit conjugation and plasmid DNA transfer.....	34
1.8 Other published reports on phage therapy	34
1.9 Advantages and disadvantages of phage therapy.....	37
1.10 Objectives of the study.....	39
Chapter 2. Materials and Methods	40
2.1 Bacterial strains and culture condition.....	40
2.2 Source and samples for phage isolation.....	42
2.3 Phage Isolation	45
2.4 Confirmation of sex (F) pilus specificity	45
2.5 Production of phage lysate	46
2.6 High titre phage propagation	47
2.7 Plaque assay and morphology.....	47
2.8 Polyethylene Glycol (PEG) precipitation	48
2.9 Phage purification by Caesium chloride centrifugation.....	49
2.10 Transmission Electron Microscopy	50
2.11 Sodium dodecyl sulphate polyacrylamide gel electrophoresis (SDS-PAGE)	51
2.12 Ribonuclease (RNase) sensitivity.....	51

2.13	Chloroform sensitivity	52
2.14	Thermal stability	52
2.15	pH stability	53
2.16	SDS stability	53
2.17	Genomic DNA and RNA extraction	55
2.18	Preparation of replicative form (RF) of ssDNA phage	56
2.19	Restriction digestion	57
2.20	cDNA synthesis of ssRNA phage genome	57
2.21	Phage genome sequencing	58
2.22	Genome sequence analysis	58
2.23	Protein and amino acid sequence analysis	60
2.24	Naming and classification of phage isolates.....	60
2.25	Phage host range in wild-type E. coli strains	60
2.26	Phage adsorption assay	61
2.27	One – step growth curve	62
2.28	Burst size determination	63
2.29	Plasmid population kinetics model with derepressed plasmid ..	63
2.30	Plasmid population kinetics model with repressed plasmid.....	64
2.31	Effect of R4 phage during conjugation.....	65
2.32	Statistical analysis	67
Chapter 3. Isolation and Characterisation of SPS Phages.....		68
3.1	Introduction	68
3.2	Results	69
3.2.1	Phage isolation	69
3.2.2	Plaque morphology.....	71
3.2.3	Ribonuclease sensitivity	71
3.2.4	Phage lysate characterisation CsCl purification	72
3.2.5	Purified phage staining in agarose gel.....	75
3.2.6	Virion morphology	75
3.2.7	Chloroform sensitivity	78
3.2.8	Restriction digestion	79
3.2.9	Structural proteins analysis by SDS–PAGE.....	80
3.2.10	Thermal stability	84
3.2.11	pH stability	86
3.2.12	Detergent stability.....	89
3.3	Discussion.....	91

Chapter 4. Genomic and Phylogenetic Analysis	96
4.1 Introduction	96
4.2 Results	96
4.2.1 ssDNA phage.....	96
4.2.1.1 Species identification and comparison to reference strains	96
4.2.1.2 Genome structure and organisation	100
4.2.1.3 Amino Acid and Protein Analysis.....	108
4.2.2 ssRNA phage.....	114
4.2.2.1 Species identification and comparison to reference strains	114
4.2.2.2 Genome structure and organisation	117
4.2.2.3 Amino Acid and Protein Analysis.....	118
4.2.3 Naming and classification of phage isolates	123
4.3 Discussion.....	125
4.3.1 ssDNA phage discussion	125
4.3.2 ssRNA phage.....	126
Chapter 5. Host range, growth, and plasmid loss kinetics	130
5.1 Introduction	130
5.2 Results	130
5.2.1 Phage host range on field strains of <i>E. coli</i>	130
5.2.2 Phage Adsorption and one-step growth curve	135
5.2.3 Plasmid loss kinetics with derepressed plasmid	142
5.2.4 Plasmid loss kinetics with repressed plasmid.....	146
5.2.5 Effect of R4 phage during conjugation	149
5.2.6 Replication of phage R4 on different bacterial species.....	149
5.3 Discussion.....	151
Chapter 6. General Discussion.....	158
Appendix A.	163
Appendix B.	171
Appendix C.	179
Appendix D.	183
Appendix E.	184
References	186

Tables of Tables

Table 1.1. Classification of selected β -lactamase & its substrates.	4
Table 1.2. Phage classification based on morphology & nucleic acid. ...	19
Table 1.3. The genes and proteins of filamentous (Ff) phage.	25
Table 1.4. Phage therapy reports in humans and animal models.	36
Table 1.5. The advantages and disadvantages of phage therapy.	38
Table 2.1. Bacterial strains used for SPS phage isolation.....	42
Table 2.2. Source and sample type for phage isolation.	43
Table 3.1. List of isolated SPS phages and their sources.	70
Table 3.2. Summary of the characteristics of the isolated phages.	90
Table 4.1. The ssDNA phages sequence characteristics.	97
Table 4.2. Identification of Ff phage based on nucleotide similarity.	98
Table 4.3. Novel Ff phage identified based on nucleotide similarity. ...	98
Table 4.4. Phage gene length and percent similarity to M13.	102
Table 4.5. Phage gene length and percent similarity to fd.	104
Table 4.6. Novel phage gene length and percent similarity to M13..	107
Table 4.7. The ssRNA phages sequence characteristics.	114
Table 4.8. ssRNA phages identified based on nucleotide similarity. ..	115
Table 4.9. Individual gene length and percent similarity to MS2.	117
Table 4.10. Individual gene length and percent similarity to Q β	118
Table 4.11. Individual protein length and percent similarity to MS2.	119
Table 4.12. Individual protein length and percent similarity to Q β . .	119
Table 4.13. Characteristics of the isolated phages.....	124
Table 5.1. Replication of ssDNA phages on field isolates.....	132
Table 5.2. Replication of ssRNA phages on field isolates.....	134
Table 5.3. Growth characteristics of SPS phages on <i>E. coli</i> with derepressed plasmid.	137
Table 5.4. Estimated number of phages secreted per unit time.	138
Table 5.5. Growth characteristics of SPS phages on <i>E. coli</i> with repressed plasmid.	141
Table 5.6. Plasmid transfer rate after conjugation with <i>E. coli</i> J62 Rif ^R with and without phage R4.	149

Tables of Figures

Figure 1.1. Resistance timeline in β -lactam antibiotics.	5
Figure 1.2. Resistance genes carried by plasmid Inc plasmid types.	12
Figure 1.3. Simplified diagram of the FinOP system.	16
Figure 1.4. Classification of bacteriophages.	20
Figure 1.5. Types of bacteriophage life cycle.	22
Figure 1.6. Electron micrograph & diagram of an ssDNA phage.	24
Figure 1.7. Schematic representation of <i>Leviviridae</i> virion.	29
Figure 1.8. Genetic map of a (A) <i>Levivirus</i> and (B) <i>Allolevivirus</i>	29
Figure 2.1. Site for phage isolation.	44
Figure 2.2. Diagram showing genomic and sequencing methods.	55
Figure 3.1. Spot test to demonstrate pilus specificity of phage.	70
Figure 3.2. Plaque morphology demonstrated by isolated phages.	71
Figure 3.3. Ribonuclease sensitivity of the phage isolates.	72
Figure 3.4. CsCl density gradient centrifugation of the phage lysate.	74
Figure 3.5. Selected dialysed phage visualised on an agarose gel.	75
Figure 3.6. TEM – negative staining images of phage.	76
Figure 3.7. ssRNA R13 phage attaching to the side of the F pilus.	77
Figure 3.8. Effect of chloroform on phage titres.	78
Figure 3.9. Restriction analysis of the RF of phage R1.	79
Figure 3.10. Restriction pattern of the RF of ssDNA phages.	80
Figure 3.11. SDS-PAGE analysis of ssDNA phages.	81
Figure 3.12. SDS-PAGE analysis of ssDNA phages.	82
Figure 3.13. SDS-PAGE analysis of ssRNA phages.	83
Figure 3.14. Thermostability of (A) ssDNA and (B) ssRNA phages.	86
Figure 3.15. pH stability of (A) ssDNA and (B) ssRNA phages.	88
Figure 3.16. SDS stability of selected ssDNA and ssRNA phages.	89
Figure 4.1. Phylogeny of ssDNA phage genome.	100
Figure 4.2. Genome organisation of phage R1.	103
Figure 4.3. Genome organisation of phage R8.	103
Figure 4.4. Genome organisation of phage R3.	105
Figure 4.5. Genome organisation of phage R10.	105
Figure 4.6. Genome organisation of phage R4.	107
Figure 4.7. Genome organisation of phage R7.	108
Figure 4.8. Phylogeny of ssDNA phage protein pIII.	109
Figure 4.9. Alignment of attachment protein (pIII) against M13.	110
Figure 4.10. Alignment of attachment protein (pIII) against fd.	112

Figure 4.11. Alignment of pIII of novel R4 & R7 phages against M13.	113
Figure 4.12. Phylogeny of ssRNA phage genome.....	116
Figure 4.13. Genome organisation of phages R5, R14 and R15.	117
Figure 4.14. Genome organisation of phage R13.....	118
Figure 4.15. Phylogeny of ssRNA phage maturation protein.	121
Figure 4.16. Phylogeny of ssRNA phage coat protein.	122
Figure 4.17. Phylogeny of ssRNA phage replicase protein.	123
Figure 4.18. Amino acid sequence of the minor coat protein (A1). ..	128
Figure 5.1. ssDNA phages replication against <i>E. coli</i> field strains. ...	133
Figure 5.2. ssRNA phages replication against <i>E. coli</i> strains.	134
Figure 5.3. One step growth curve of R4 in derepressed plasmid....	139
Figure 5.4. Effect of ssDNA phages on derepressed plasmid.	143
Figure 5.5. Effect of ssRNA phages on derepressed plasmid.....	145
Figure 5.6. Effect of ssDNA phages on repressed plasmid pF26.	146
Figure 5.7. Effect of ssRNA phages on repressed plasmid pF21.	148
Figure 5.8. Replication of phage R4 on different bacterial species. ..	150

List of Abbreviations

%	Percentage	FDA	Food and Drug Administration
% v/v	Percentage volume per volume	g	Gram
% w/v	Percentage weight per volume	g/RCF	G-Force/Relative centrifugal force
°C	Degrees Celsius	h	Hour
μL	Microlitre	ICTV	International Committee for the Taxonomy of Viruses
A ₆₀₀	Absorbance at 600 nm	ICVCN	International Code of Virus Classification and Nomenclature
ANOVA	Analysis of variance	IPTG	Isopropyl-β-D-thiogalactoside
ATP	Adenosine triphosphate	kb	kilobase pair
BLAST	Basic Local Alignment Search Tool	kDa	KiloDalton
bp	Base pair	kV	Kilovolt
CaCl ₂	Calcium chloride	LB	Luria-Bertani medium
cDNA	Complementary deoxyribonucleic acid	LPS	Lipopolysaccharide
CDS	Coding sequence	M	Molar
CFU	Colony-forming unit	m	Minute
cm	Centimetre	Mb	Megabase
CsCl	Caesium chloride	MDR	Multidrug resistant
Da	Dalton	mg	Milligram
DNA	Deoxyribonucleic acid	MgCl ₂	Magnesium chloride
DNase	Deoxyribonuclease	MgSO ₄	Magnesium sulphate
dNTP	2' deoxyribonucleotide 5' triphosphate	MH	Mueller-Hinton
ds	Double stranded	mL	Millilitre
DsDNA	Double stranded DNA	mM	Millimolar
DTT	Dithiothreitol	MOI	Multiplicity of infection
<i>E. coli</i>	<i>Escherichia coli</i>	mol	Mole
EDTA	Ethylene diamine tetra-acetic acid	MRD	Maximum recovery diluent
EU	European Union		

mRNA	Messenger ribonucleic acid	ssRNA	Single stranded RNA
NA	Nutrient agar	STs	Sequence types
NaCl	Sodium chloride	TAE	Tris acetate EDTA buffer
NaOH	Sodium hydroxide	TBS	Tris Buffered Saline
NCBI	National Center for Biotechnology Information	TE	Tris EDTA buffer
ng	Nanogram	TLA	Top layer agar
nm	Nanometre	Tris	Tris (hydroxymethyl) aminomethane
OD	Optical density	tRNA	Transfer RNA
OD ₆₀₀	Optical density 600	U	Unit
ORF	Open reading frame	UK	United Kingdom
PAGE	Polyacrylamide gel electrophoresis	UV	Ultraviolet
PBS	Phosphate buffered saline	V	Volt
PCR	Polymerase chain reaction	v/v	Volume for volume
PEG	Polyethylene glycol	w/v	Weight for volume
PFGE	Pulsed-field gel electrophoresis	WHO	World Health Organisation
PFU	Plaque-forming unit		
Phage	Bacteriophage		
ppm	Parts per million		
RNA	Ribonucleic acid		
RNase	Ribonuclease		
rpm	Revolutions per minute		
rRNA	Ribosomal ribonucleic acid		
S	Seconds		
SD	Standard deviation		
SDS	Sodium dodecyl sulphate		
SEM	Standard error of mean		
SM	Salt magnesium buffer		
SPS	Sex pilus specific		
Ss	Single stranded		
ssDNA	Single stranded DNA		

Chapter 1. Introduction

1.1 Antimicrobial resistance – the problem

Antimicrobial resistance (AMR) is considered as one of the greatest threats to human public health and has a significant impact in agriculture and food security (World Health Organization, 2016). This is due to the rapidly increasing number of antibiotic-resistant bacterial infections in humans and animals and reports of bacterial strains that are resistant to all clinical drug options available (Fernandes et al., 2016, Mediavilla et al., 2016, Pulss et al., 2017, Wang et al., 2018). It is estimated that a continued rise in resistance by 2050, would lead to 10 million people dying every year and a reduction of 2% to 3.5% in Gross Domestic Product (GDP) costing the world up to 100 trillion USD (O'Neill, 2014).

The appropriate and inappropriate constant use of antibiotics has exerted a strong pressure on bacteria to develop resistance (Cohen, 1992, Austin et al., 1999, Levy and Marshall, 2004). One of the mechanisms of antibiotic resistance is through acquired resistance - when antibiotic susceptible bacteria become resistant through the acquisition or gain of resistance genes (Rice, 2012). The overuse and misuse of antibiotics, which select for resistant bacteria has been identified as one of the drivers of acquired resistance. In humans, these include unnecessary prescription for viral infections, against which they have no effect; too frequent prescription of "broad-spectrum antibiotics"; and patients not adhering to the prescribed duration of medication (ECDC, 2014). In animals, the use of antibiotics as growth promoters may have contributed to the development of acquired resistance especially in low- and middle-income countries (LMICs). Since

2000, meat production has plateaued in high-income countries but accelerated in LMICs by more than 60% in Africa and Asia, and by 40% in South America, as countries in these regions shifted from low- to high-protein diets (Van Boeckel and Pires, 2019). Consequently, pressure to produce more meat to address this demand has risen resulting in the increase use of antibiotics to reduce infections and to increase body mass of livestock and poultry (Van Boeckel and Pires, 2019). A study has revealed that more than 131,000 tons of antibiotics were used in food animals worldwide and is estimated to increase up to more than 200,000 tons by 2030 (Van Boeckel et al., 2017, Van Boeckel and Pires, 2019). Another study conducted by Tiseo et al. (2020) on global trends in antimicrobial use in food animals from 2017 to 2030 estimated global antimicrobial sales in 2017 at 93,309 tonnes and predicted to rise by 11.5% in 2030 to 104,079 tonnes. Data from the US Food and Drug Administration (FDA) revealed that 80% of antibiotics were consumed in food animals; either to prevent disease or as growth promoters (Love et al., 2011). In the study conducted by Van Boeckel and Pires (2019) it was revealed that occurrence of antibiotic resistance has nearly tripled in disease-causing bacteria within the period of 18 years. Antibiotics that could be used for treatment failed more than half the time in 40% of chickens and 30% of pigs raised for human consumption. The highest resistance rates were observed with the most commonly used classes of antibiotics in animal production such as tetracyclines, sulphonamides, and penicillins (Van Boeckel and Pires, 2019).

Among the more than 15 classes of antibiotics, Beta lactams have been amongst the most successful for the treatment of bacterial infections

for the past 60 years (Bush and Bradford, 2016). The β -lactam antibiotics act by binding to cell wall trans-peptidases known as penicillin-binding proteins (PBPs) and disrupting peptidoglycan cross-linking during cell wall synthesis. Inhibition of PBPs weakens the cell wall, resulting in bacterial lysis and cell death (Ghuysen, 1991). The β -lactam antibiotics are the first drug of choice to treat most bacterial infections in humans and animals but have been plagued by the problem of increasing acquired resistance. The most common resistance mechanism to β -lactams occur through expression of β -lactamases - a group of enzymes that break down antibiotics belonging to the penicillin and cephalosporin groups. These enzymes are plasmid encoded and are the most frequently described enzymes conferring resistance to these antibiotics (Ghuysen, 1991).

The β -lactamases are classified based on either the revised Ambler classification scheme or the Bush–Jacoby system (Bonomo, 2017). The revised Ambler classification scheme classified β -lactamases from A to D based on amino acid sequence homology whereas, the Bush–Jacoby system classes these enzymes from group 1 to 4 based on its substrate hydrolysis profiles (Hall and Barlow, 2005, Bush and Jacoby, 2010). Table 1.1 provides a list of selected β -lactamases of Gram-negative bacteria and their updated classification; with the corresponding substrate (antibiotic) on which the enzyme acts (Jacoby and Munoz-Price, 2005, Bush and Jacoby, 2010, Bonomo, 2017) (Table 1.1).

Table 1.1. Classification of selected β -lactamase & its substrates.
 Adopted from (Jacoby and Munoz-Price, 2005, Bush and Jacoby, 2010, Bonomo, 2017).

β-lactamase	Bush-Jacoby (Ambler) group	Representative enzyme(s)	Distinctive substrate(s)	Defining characteristic(s)
Broad-spectrum	2b (A)	TEM-1, TEM-2, SHV-1	Penicillins, early cephalosporins	Similar hydrolysis of benzylpenicillin and cephalosporins
	2d (D)	OXA-1, OXA-10	Cloxacillin	Increased hydrolysis of cloxacillin or oxacillin
AmpC	1 (C)	ACT-1, CMY-2, FOX-1, MIR-1	Cephalosporins	Greater hydrolysis of cephalosporins than benzylpenicillin; hydrolyses cephamycins
Extended-spectrum	2be (A)	TEM-3, SHV-2, CTX-M-15, PER-1, VEB-1	Extended-spectrum cephalosporins, monobactams	Increased hydrolysis of oxyimino- β -lactams (cefotaxime, ceftazidime, ceftriaxone, cefepime, aztreonam)
	2de (D)	OXA-11, OXA-15	Extended-spectrum cephalosporins	Hydrolyses cloxacillin or oxacillin and oxyimino- β -lactams
Carbapenemase	2f (A)	KPC-1, KPC-2, IMI-1, SME-1	Carbapenems	Increased hydrolysis of carbapenems, oxyimino- β -lactams, cephamycins
	2df (D)	OXA-23, OXA-48	Carbapenems	Hydrolyses cloxacillin or oxacillin & carbapenems
	3a (B1)	IMP-1, VIM-1, CcrA, IND-1	Carbapenems	Broad-spectrum hydrolysis including carbapenems but not monobactams
	3b (B2)	CphA, Sfh-1	Carbapenems	Preferential hydrolysis of carbapenems

The development of resistance to β -lactam antibiotics is rapid with resistance reported less than 10 years since the introduction of a new β -lactam antibiotic (Medeiros, 1997, Levy and Marshall, 2004, Rice, 2012, Eiamphungporn et al., 2018) (Figure 1.1). The rapid emergence and spread of extended spectrum β -lactam resistant enterobacteria has resulted in the greater use of last resort antibiotics such as carbapenems for the treatment of infections caused by these ESBLs resistant bacteria (Paterson and Bonomo, 2005, Owens et al., 2011).

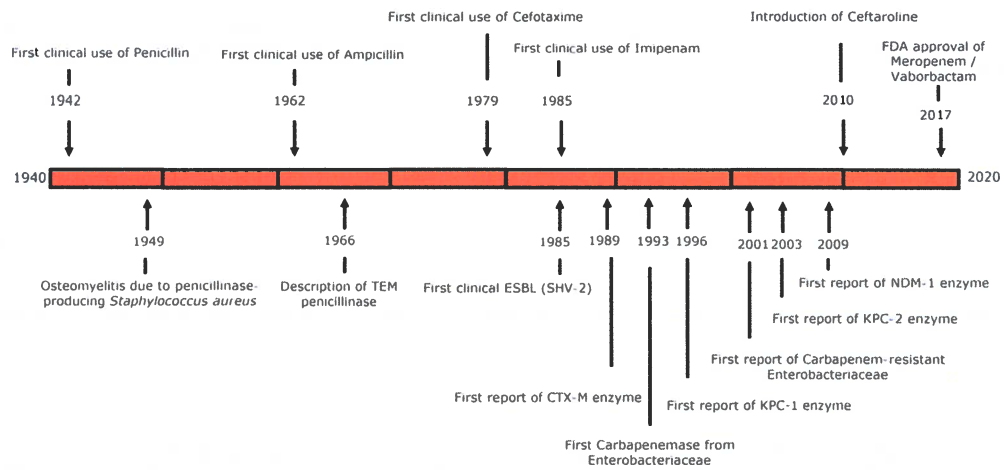


Figure 1.1. Resistance timeline in β -lactam antibiotics.

This figure demonstrates the development of acquired resistance years after the introduction of a new β -lactam antibiotic (Rice, 2012, Eiamphungporn et al., 2018).

1.2 *Escherichia coli* and the study of AMR

Escherichia coli is commonly used as a sentinel organism for monitoring AMR in faecal bacteria as it is found frequently in a wide range of hosts; constantly exposed to antimicrobials; acquires resistance easily; and is a reliable indicator of resistance in other bacteria (Markovska et al., 2014).

Several studies have looked at AMR in *E. coli* and how it changes in different hosts and environments. One study from the US investigated antibiotic susceptibility of 1,729 *E. coli* isolates isolated from humans, cattle, chickens, and pigs between 1950-2002. They found a clear correlation between commercial introduction of an antibiotic and subsequent increased prevalence of resistance (Tadesse et al., 2012). Prevalence of resistance was higher the longer antibiotics had been in use, such as tetracycline (40.9%) (introduced in 1948), sulphonamide (36.2%) (introduced in 1936), streptomycin (34.2%) (introduced in 1943), and ampicillin (24.1%) (introduced in 1961). This pattern was observed for both human and animal isolates (Tadesse et al., 2012). Among the tested antibiotics, human isolates were most resistant to sulphonamide, tetracycline and ampicillin, whereas animal isolates were most resistant to tetracycline, streptomycin, sulphonamide, kanamycin, and ampicillin (Tadesse et al., 2012). In contrast, the reduction of total antimicrobial consumption between 2010 and 2013 for veterinary use in Belgium in veal calves, chickens and pigs have been correlated with the reduction of antimicrobial resistance in commensal *E. coli* (Hanon et al., 2015). These studies have demonstrated that development of resistance may increase or

decrease after the introduction or withdrawal of every major class of antimicrobial drugs, respectively (Tadesse et al., 2012, Hanon et al., 2015).

1.3 AMR and plasmids

Genetic determinants of antibiotic resistance in enteric bacteria can be mediated via a mutation in the bacterial chromosome (mutational resistance) or by gene acquisition on a transmissible element; such as plasmid or transposon (transmissible or acquired resistance). Mutational resistance can only be transmitted to a progeny during replication hence its ability to spread between related organisms is limited. In contrast, transmissible resistance has the potential to spread resistance horizontally since intra-species, inter-species and inter-genera transfer can take place (Smith and Lewin, 1993).

Transmissible resistance in enteric bacteria, including *E. coli* is mediated by a plasmid, which is a circular, extra-chromosomal double-stranded DNA molecule that replicates autonomously in a host cell. They contain genes that are essential for plasmid maintenance, such as initiation and control of replication; and genes that are useful to their host such as antibiotic resistance (Thomas and Nielsen, 2005). Plasmids mainly act as vehicles for antibiotic resistance genes capture and dissemination between related bacteria through bacterial conjugation (Carattoli et al., 2005b, Carattoli, 2009). For instance, resistance to most commonly used antibiotics such as β -lactams, aminoglycosides, macrolides, sulphonamides, tetracyclines, chloramphenicol and trimethoprim were reported to be plasmid mediated (Smith and Lewin, 1993). The first report of plasmid mediated AMR transfer between *E.coli* was reported in 1969 (Smith, 1969).

The following year, AMR transfer from *E. coli* to *S. Typhimurium* was demonstrated to occur in the alimentary tract of chicken and calves (Smith, 1970). Recently, transfer of MDR plasmid from *Salmonella* to commensal *E. coli* was reported in an *in vitro* chicken gut model (Card et al., 2017). Furthermore, critically important antibiotics such as colistin once thought of as chromosomally mediated, have been identified more recently as plasmid-encoded resistance genes (Liu et al., 2016).

A major public health concern is that AMR plasmids can be transmitted to other opportunistic pathogens particularly important in human medicine, such as the ESKAPE pathogens (*Enterococcus faecium*, *Staphylococcus aureus*, *Klebsiella pneumoniae*, *Acinetobacter baumannii*, *Pseudomonas aeruginosa*, and *Enterobacter* species) (Founou et al., 2016, Santajit and Indrawattana, 2016). Consequently, the high proportions of resistance to third generation cephalosporins reported in these opportunistic pathogens means that treatment of severe infections caused by these bacteria must now rely mainly on another antibiotic family that is more expensive and may not be available in resource-constrained settings (Liu et al., 2016, Ye et al., 2016). The increase in resistance has led to an increased pressure to use antibiotics that are identified as critically important antimicrobials reserved for last resort use in for human medicine. However, pan drug resistant (PDR) bacteria including carbapenem-resistant and colistin-resistant *E. coli* are now being observed in clinical cases (Peng et al., 2019). The need for alternative approaches to treat increasing PDR bacterial infections is becoming more acute. This thesis describes the investigation of phage as a potential selective agent against bacteria with common AMR plasmids.

1.3.1 Classification of plasmids

There are two ways to classify plasmids. The first scheme is based on the plasmid's ability to be transferred from one bacterium to another. The second scheme is based on incompatibility grouping, which is the most frequently used scheme for classifying plasmids.

Based on the first scheme, plasmids can be grouped as either conjugative or non-conjugative. Plasmids that are conjugative enable conjugation to proceed, through a sex pilus that is expressed from the donor cell and binds to the recipient cell (Carattoli et al., 2005a). These plasmids contain transfer genes (*tra*) that allow plasmids to be transferred from one bacterium to another through conjugation. Bacteria containing these plasmids are indicated as F positive (F⁺), and bacteria lacking the plasmids are F negative (F⁻). When an F⁺ bacterium conjugates with an F⁻ bacterium, two F⁺ bacteria result (Ippen-Ihler and Minkley Jr, 1986). In contrast, non-conjugative plasmids cannot start the conjugation process solely on its own. These plasmids can only be transferred through sexual conjugation with the help of donor conjugative plasmids utilizing its transfer expressed conjugative plasmid components at high frequency (Kaiser and Suchman, 2013).

Plasmids can also be classified based on incompatibility (Inc), which is the failure of two co-resident plasmids to be stably inherited together in the absence of external selection. Inc is a universally inherited property by which plasmids control replication initiation and stable inheritance. Plasmids of the same incompatibility group share these functions and cannot be stably coinherited. Plasmids are incompatible if they have the same reproduction strategy or replication control in the cell. Therefore, if

the introduction of a second plasmid negatively affects the inheritance of the first, the two are considered to be incompatible (Novick et al., 1976). This is because the number of plasmids in a cell is governed by elements encoded within the origin of replication (*ori*) and it is not possible to maintain two plasmids that use the same mechanism for replication in a single cell.

1.3.2 Incompatibility group and AMR

Currently, there are 28 types of F conjugative Inc plasmids in Enterobacteriaceae (Helinski, 1996, Carattoli, 2009, Shintani et al., 2015). However, six types namely IncF, IncI, IncA/C, IncL (previously designated IncL/M), IncN and IncH, carry the greatest variety of AMR genes (Rozwandowicz et al., 2018). For instance, many of the genes encoding ESBLs, quinolone and carbapenem resistance genes found in Enterobacteriaceae are located on large plasmids that belong to the incompatibility groups IncF, IncH, and IncI (Cantón et al., 2008, Coque et al., 2008, Hawkey, 2008). These plasmids encode type IV secretion systems that enable conjugative transfer to other Enterobacteriaceae through horizontal gene transfer via bacterial conjugation (Su et al., 2008, Llosa et al., 2009). To determine the distribution of antimicrobial resistance genes that are carried by known Inc plasmid types in Enterobacteriaceae, a study by Rozwandowicz et al. (2018) comprehensively analysed all publications found in PubMed using the key words 'resistance plasmid' or 'Inc plasmid' as search criteria, One of the highlights from this study was the finding that ESBLs are the most frequent encoded resistance genes carried by plasmids regardless of the Inc type (Rozwandowicz et al., 2018). It was also shown that various plasmids seem to be associated to a specific

range of antibiotic resistance gene classes. For instance, IncF carry a wide variety of gene classes which include the β -lactams, extended-spectrum β -lactams and aminoglycosides, while IncI plasmids are only mainly associated with ESBLs. The figure below shows the Inc plasmids in Enterobacteriaceae and the resistance genes they carry (Rozwandowicz et al., 2018) (Figure 1.2).

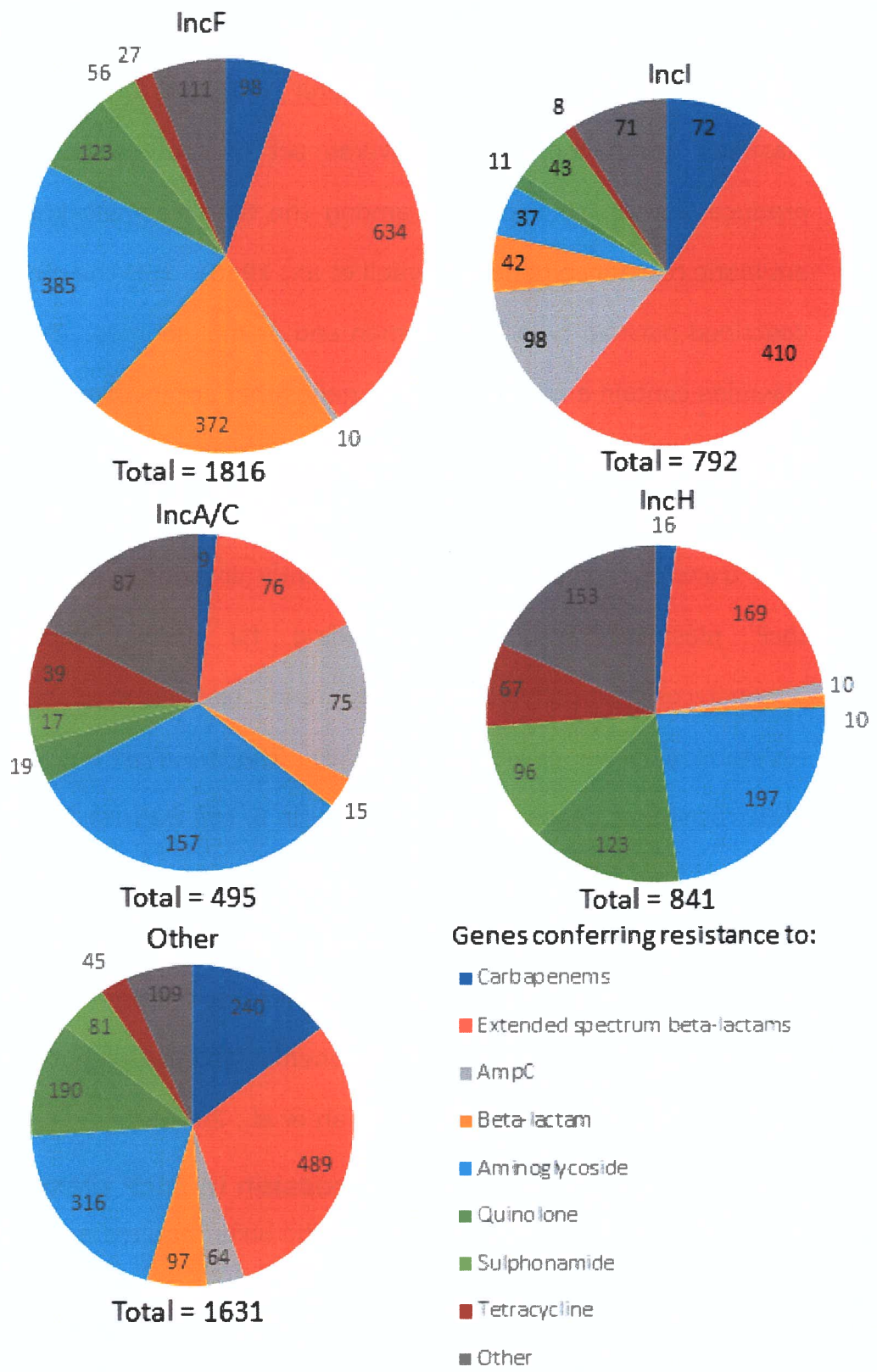


Figure 1.2. Resistance genes carried by plasmid Inc plasmid types. The distribution of antibiotic resistance genes carried by all known AMR-related Inc plasmid types in Enterobacteriaceae (Rozwandowicz et al., 2018).

1.3.3 Incompatibility F (IncF)

This project focuses on the IncF plasmids as they are a well characterised group with several useful constructs and tools. The IncF plasmids group comprises a diverse set of conjugative plasmids that produce type F pili and were among the first plasmids known to carry antibiotic resistance genes (Meynell et al., 1968). It is the most frequently described plasmid type from human and animal sources. Transmissible F plasmids contain a functional set of genes that are involved in conjugation, DNA transfer and autonomous replication (Helinski, 1996). They range between 45 and 200 kb in size and encode approximately 40 genes within their transfer region. The most frequently described resistance genes in IncF plasmids are those encoding for ESBL, carbapenemases, aminoglycoside-modifying enzymes and plasmid-mediated quinolone resistance (Rozwandowicz et al., 2018). The two most important of these ESBL resistance genes include *bla*_{CTX-M-15} in *E. coli* O25:H4-ST131 clone and *bla*_{NDM}. The former is mostly associated with ESBL production and fluoroquinolone resistance while the latter produces a metallo-beta-lactamase enzyme, which makes the bacteria resistant to almost all β -lactam antibiotics, including carbapenems (Leflon-Guibout et al., 2008, Nicolas-Chanoine et al., 2014, Rahman et al., 2014).

1.3.4 Repression and derepression in IncF plasmids

The survival of plasmids as genetic units requires a positive balance of factors that favour dissemination, such as the horizontal transmission via conjugation; and factors that lead to loss of plasmids in a population such as the fitness costs of maintaining conjugative plasmids and the attack of sex-pilus specific (SPS) phages (Bergstrom et al., 2000). As an effective

adaptation to the latter, many natural conjugative plasmids encode a fertility inhibition (FinOP) system that represses transfer gene expression in the majority of plasmid-carrying cells. The majority of native IncF and IncI plasmids possess such a fertility inhibition system, an example is the IncFII plasmid R1 (Koraimann et al., 1991, Koraimann et al., 1996). However, kinetic studies of plasmid transfer *in vitro* revealed that even if repressed plasmids are introduced at low frequencies in a bacterial population, transconjugants that have acquired the plasmids rapidly dominate the population (Lundquist and Levin, 1986). The successful spread of these plasmids in clinically relevant bacteria has been suggested to be supported by this transitory derepression and was suggested to last for *ca.* six generations before fertility inhibition is re-established in the transconjugant cell (Cullum et al., 1978, Lundquist and Levin, 1986, Simonsen, 1990).

Over the years, genetic modifications which are sometimes referred to as superspreader mutations, have dramatically enhanced the conjugation efficiency of naturally repressed conjugative plasmids belonging to diverse incompatibility groups (Virolle et al., 2020). This type of mutation was first characterised in the F plasmid, which carries an IS3 insertion sequence into the *finO* gene. FinO inactivation destabilizes the FinP-*traJ* mRNA duplex, thus resulting in the upregulation of *traJ* and the constitutive expression of *tra* genes resulting to derepression (Cheah and Skurray, 1986). This naturally occurring mutation accounts for the enhanced transfer efficiency of the F plasmid compared with the related IncF repressed plasmids in which the FinOP regulatory system is still active (Yoshioka et al., 1987). Both the repressed (or F-like) and derepressed IncF plasmids belong to same group

(MOB_{F12}) based on comparison and phylogenetic analyses of relaxase (*traI*) and coupling protein (*traD*) genes (Garcillan-Barcia et al., 2009).

Mutations in the FinOP regulatory system might not be the only mutations causes of derepression. It was also shown that insertion of the Tn1999 transposon into the *tir* (transfer inhibition of RP4) gene of the IncL/M-type plasmid pOXA-48a, responsible for the dissemination of specific ESBL genes in Enterobacteriaceae, increases the transfer efficiency by 50–100-fold without affecting *traM* expression levels (Potron et al., 2014). Finally, there are also other families of conjugative plasmids such as IncP and IncW plasmids, which are considered to be naturally derepressed, as they do not repress conjugative gene expression (Bradley et al., 1980).

1.3.5 The fertility inhibition (FinOP) system

The fertility inhibition (FinOP) system consists of an antisense RNA: FinP and a protein: FinO, which together repress TraJ expression (van Biesen and Frost, 1994) (Figure 1.3). The TraJ, a 27 kDa protein acts as a positive regulator of the *tra* operon, required for activation of high levels of transcription from the pY promoter (Willetts, 1977). The FinP, which is transcribed from the opposite strand and in a direction opposite to *traJ*, is a small 79 base antisense RNA molecule which is complementary to part of the 5' untranslated leader of *traJ* mRNA (Mullineaux and Willetts, 1985). The intracellular levels of FinP are dependent on co-expression of a 21.2 kDa protein FinO, which binds to FinP and prevents its degradation. FinO stabilizes FinP by protecting it from endonuclease, RNase E (Lee et al., 1992, Jerome, 1999). The untranslated leader of *traJ* mRNA forms a duplex with FinP resulting to duplex formation. This prevents *traJ* mRNA

translation through occlusion of its ribosome binding site, leading to repression of plasmid transfer (Lee et al., 1992, Jerome, 1999). Repression by FinOP leads to a 50-100-fold decrease in levels of plasmid transfer (van Biesen and Frost, 1994).

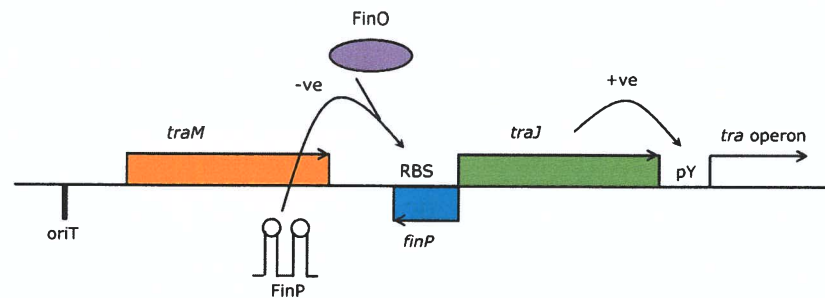


Figure 1.3. Simplified diagram of the FinOP system.

Transcription of the *tra* operon from pY is activated positively (+ve) by the *traJ* gene product, which in turn is negatively (-ve) regulated by the FinP antisense RNA and the FinO protein. **RBS**: ribosome-binding site; **pY**: promoter for the *tra* operon; **oriT**: origin of DNA transfer. Horizontal arrows indicate open reading frames. Adopted from (van Biesen and Frost, 1994).

1.4 Bacteriophage

General Characteristics

Bacteriophages or phages are viruses that exclusively infect bacteria and include viruses of eubacteria and archaea. Bacteriophages are ubiquitous in the environment and are considered one of the most abundant organisms on Earth (Sulakvelidze et al., 2001). Bacteriophages were first described in 1915 as lytic agents which are capable of self-amplification on a suitable bacterial host; and were eventually used in therapy to control bacterial infections (Twort, 1915, D'Hérelle, 1926).

The core structural components of bacteriophage include a capsid, which is a protein coat enclosing the nucleic acid (DNA or RNA) and may be further surrounded by a lipid layer (Chanishvili, 2012a). In addition to the capsid (head), tailed bacteriophages (order Caudovirales), possess a tail

which may either be contractile or non-contractile. Other structural components include collar, basal plate, spikes and tail fibres, which are involved in attachment and injection of the nucleic acid into the host (Ackermann, 2007, Ackermann, 2009).

Classification

The classification of phages carried out by the Bacterial and Archaeal Viruses Subcommittee (BAVS) of the International Committee on Taxonomy of Viruses (ICTV) was traditionally based on their genome type, viral morphology and host range (Ackermann, 2005, Ackermann, 2007). Since then, these criteria have been the basis for classifying phages (Adriaenssens and Brister, 2017)

Phage genomes are composed of either DNA or RNA, which may be double-stranded or single-stranded. This genetic material is packaged into a capsid that can be polyhedral (*Microviridae*, *Corticoviridae*, *Tectiviridae*, *Leviviridae* and *Cystoviridae*), filamentous (*Inoviridae*), pleomorphic (*Plasmaviridae*) or connected to a tail (Caudovirales) (Ackermann, 2007, Ackermann, 2009) (Table 1.2 and Figure 1.4). To date, the majority of the reported phages are tailed and have dsDNA genomes and classified under the Order Caudovirales, with the remaining Orders containing the polyhedral, filamentous and pleomorphic (PFP) phages (Ackermann, 2007).

The advancements in next generation sequencing methods have led to an increase in the use of phylogenetics to classify both culturable and uncultured phages rapidly broadening our understanding of phage in the environment (Cook et al., 2021). As more phages are being sequenced, the number of phage family and genus has dramatically increased in the

last 15 years. For instance, in the 8th ICTV Report, phages were classified into only one Order belonging to 13 Families but this has since increased into 14 Orders belonging to 145 Families (Fauquet et al., 2005, Walker and Siddell, 2020). In the ICTV's Bacterial and Archaeal Viruses Subcommittee latest update a further new order, 10 families, 22 subfamilies, 424 genera and 964 species were added (Adriaenssens et al., 2020).

Due to the advancement in metagenomics, there have been changes in the taxonomy of the ssDNA filamentous and ssRNA phages. A new Order Tubulavirales, was added in the group Family Inoviridae, together with Family Plectroviridae and a new Family Paulinoviridae (Knezevic et al., 2021). The Family Leviviridae has been reclassified into a Class Leviviricetes. As part of the reclassification, the genera Levivirus and Allolevivirus were renamed as Emesvirus and Qubevirus, respectively (Callanan et al., 2021). As these changes are very recent and are still not widely implemented in the phage scientific community, the current research will still refer to the previous and still more widely used phage taxonomy.

Table 1.2. Phage classification based on morphology & nucleic acid.
Adopted from (Ackermann, 2007).

Shape	Nucleic acid	Family	Characteristics
Tailed	dsDNA, linear	<i>Myoviridae</i>	tail contractile
	dsDNA, linear	<i>Siphoviridae</i>	tail long, noncontractile
	dsDNA, linear	<i>Podoviridae</i>	tail short
Polyhedral/ Spherical	ssDNA, circular	<i>Microviridae</i>	conspicuous capsomers
Spherical	dsDNA, circular	<i>Corticoviridae</i>	complex capsid, lipids
	dsDNA, linear	<i>Tectiviridae</i>	inner lipid vesicle
	ssRNA, linear	<i>Leviviridae</i>	poliovirus-like
	dsRNA, linear	<i>Cystoviridae</i>	enveloped, lipids
Filamentous	ssDNA, circular	<i>Inoviridae</i>	a. long filaments b. short rods
	dsDNA, linear	<i>Lipothrixviridae</i>	enveloped, lipids
Pleomorphic	dsDNA, circular	<i>Plasmaviridae</i>	enveloped, no capsid
	dsDNA, circular	<i>Fuselloviridae</i>	lemon-shaped
	dsDNA, linear	<i>Ampullaviridae</i>	bottle-shaped
	dsDNA, linear	<i>Globuloviridae</i>	paramyxovirus-like

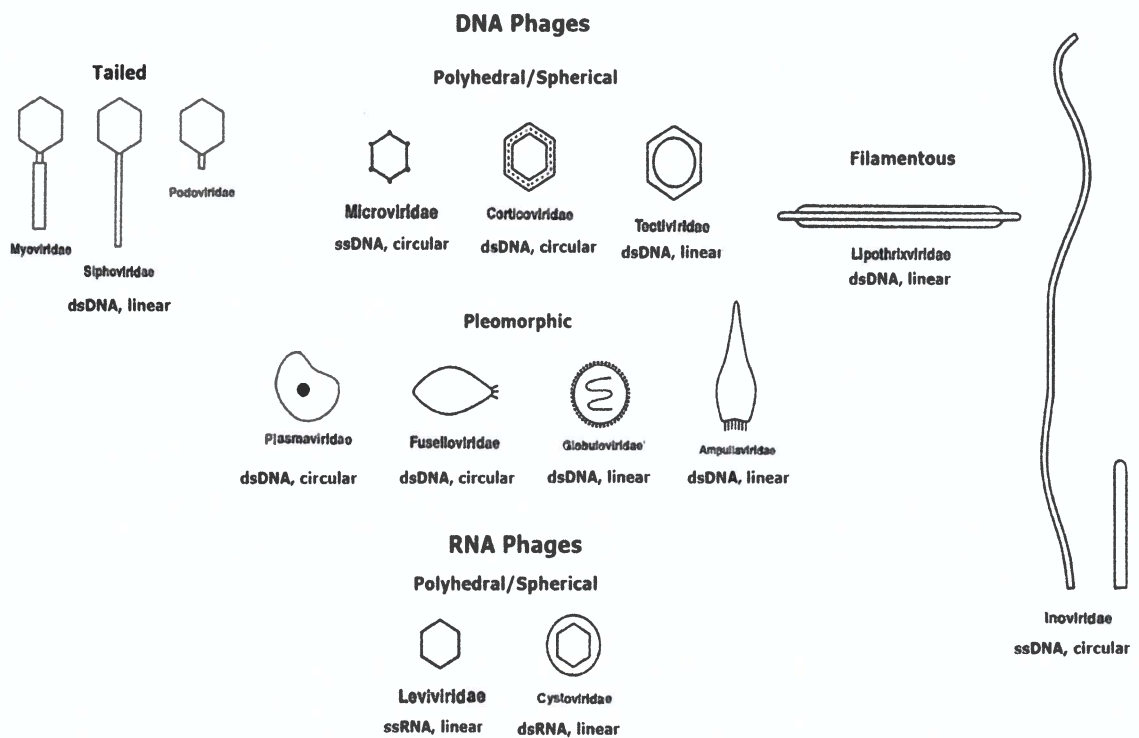


Figure 1.4 Classification of bacteriophages.

Bacteriophage family classified based on morphology and nucleic acid characteristics. Figure adopted from Ackermann (2007) with modifications.

Bacteriophage life cycle

Bacteriophages show several life cycles: lytic, lysogenic, chronic and pseudolysogenic infections (Ackermann, 1987, Miller and Day, 2008, Wernicki et al., 2017) (Figure 1.5). In a lytic cycle, a phage redirects the host's metabolism towards the production of new phages, resulting in lysis of the host cell and release of progeny virions (Ceysens and Lavigne, 2010). Phages that replicate only via the lytic cycle are also known as virulent phages. In the lysogenic cycle, the phage genome assumes a quiescent state called prophage. This prophage is often integrated into the host genome and replicates along with the host, until the lytic cycle is induced. A 'lysogenic decision', whether or not to establish a prophage state is made by the phage after infection (Ackermann, 1987). Phages using both lysogenic and lytic cycles are also known as temperate phages (Ripp and Miller, 1997).

There are also phages such as the filamentous ssDNA phages that are neither lytic nor lysogenic but follow a chronic life cycle. In the chronic life cycle, the host cell is infected, but unlike in the lysogenic cycle, the phage DNA does not form a stable relationship with host cell. However, the normal host cell processes still function alongside phage production. During chronic infection, phage progenies are constantly released from the host cell by budding or extrusion without lysing it (Ackermann, 1987, Russel et al., 2004). Lastly, in a pseudolysogenic infection (phage carrier state), phages multiply in a fraction of the population as phage nucleic acid simply resides within the host cell in a non-active state and may result in persistent infections (Ripp and Miller, 1997).

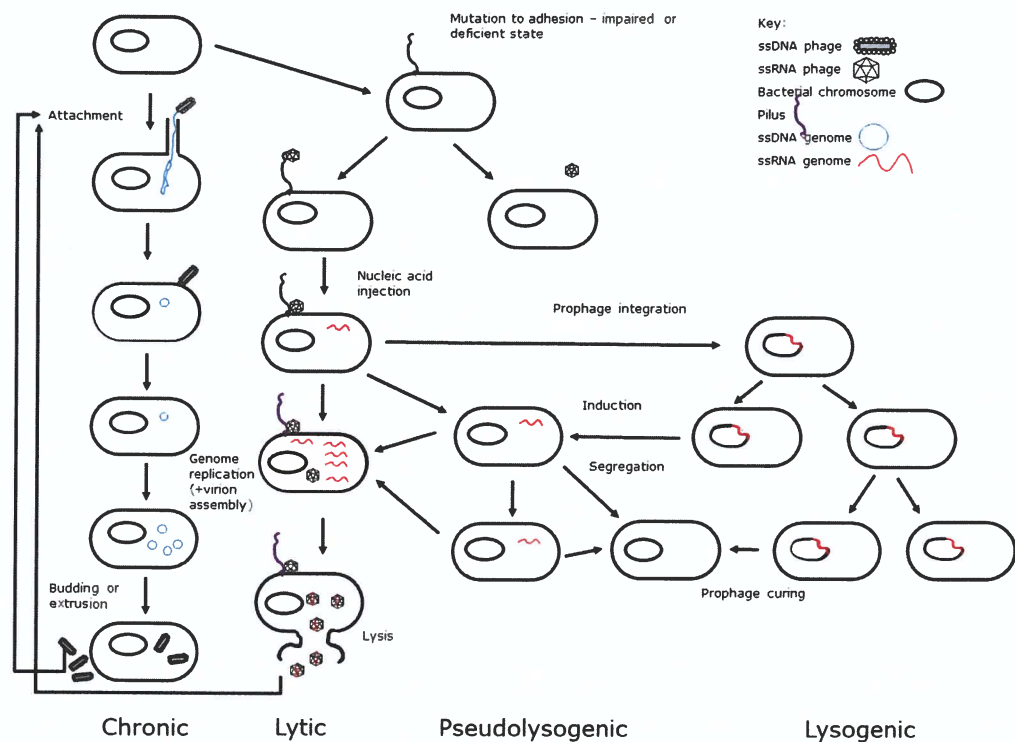


Figure 1.5. Types of bacteriophage life cycle.

The figure is adopted from Wernicki et al. (2017) with some modifications.

1.5 AMR, plasmid and the F pilus specific phage

The relationship between bacteria containing plasmids and bacteriophages is complex. Both plasmids and phages can confer phenotypic traits on recipient bacteria, including AMR; and both are involved in transmissibility (Rodrigue et al., 1992). Most of the more recent interest in phage has centred on their use to reduce levels of bacterial infection using phage which target surface structures, usually LPS or capsules (Sulakvelidze et al., 2001). Only few studies have investigated the use of phages, which specifically target the AMR plasmid-mediated sex pilus (Ojala et al., 2013, Ojala et al., 2016, Colom et al., 2019). One of the advantages of targeting the AMR plasmid mediated sex pilus is that the phage will only kill bacteria containing the AMR plasmid. Furthermore, the

development of phage resistant bacteria is desirable; since these resistant bacteria do not have the plasmids (antibiotic sensitive); or the plasmids are no longer self-transmissible.

Conjugative F plasmid mediated pili in Gram negative bacteria can be both thick and flexible that are attached to most donor cells (e.g. IncF, IncH); or rigid that are usually found free in the medium and rarely visualised attached to a donor cell (e.g. IncI, IncP). (Bradley et al., 1980). In the present study, we are focusing on the F plasmid-mediated sex pilus specific (SPS) phages. Previous studies revealed that these SPS phages are either spherical/icosahedral - single stranded RNA (ssRNA) or filamentous - ssDNA phages (Marvin and Hoffmann-Berling, 1963, Ackermann, 2005).

1.5.1 Single-stranded DNA (ssDNA) bacteriophages

The Family *Inoviridae* contains F pili specific ssDNA bacteriophages that are filamentous measuring >500 nm x 6–7 nm. The virion is composed of circular ssDNA packed in a two-stranded helix, surrounded by a tube made of thousands of helically arrayed major coat protein (pVIII) subunits. The tube is closed by two different proteins at each end (pVII/pIX and pIII/pVI) (Day, 2011) (Figure 1.7). The most known phages under this family are f1, M13 and fd; collectively known as filamentous phages, Ff. They are 98% identical to each other at the DNA sequence level and have been studied interchangeably (Russel et al., 2004, Rakonjac et al., 2017). The nine genes of Ff phage encode for 11 proteins in which five proteins form the phage coat whilst six are required for DNA replication and phage assembly (Russel et al., 2004, Mai-Prochnow et al., 2015) (Table 1.3).

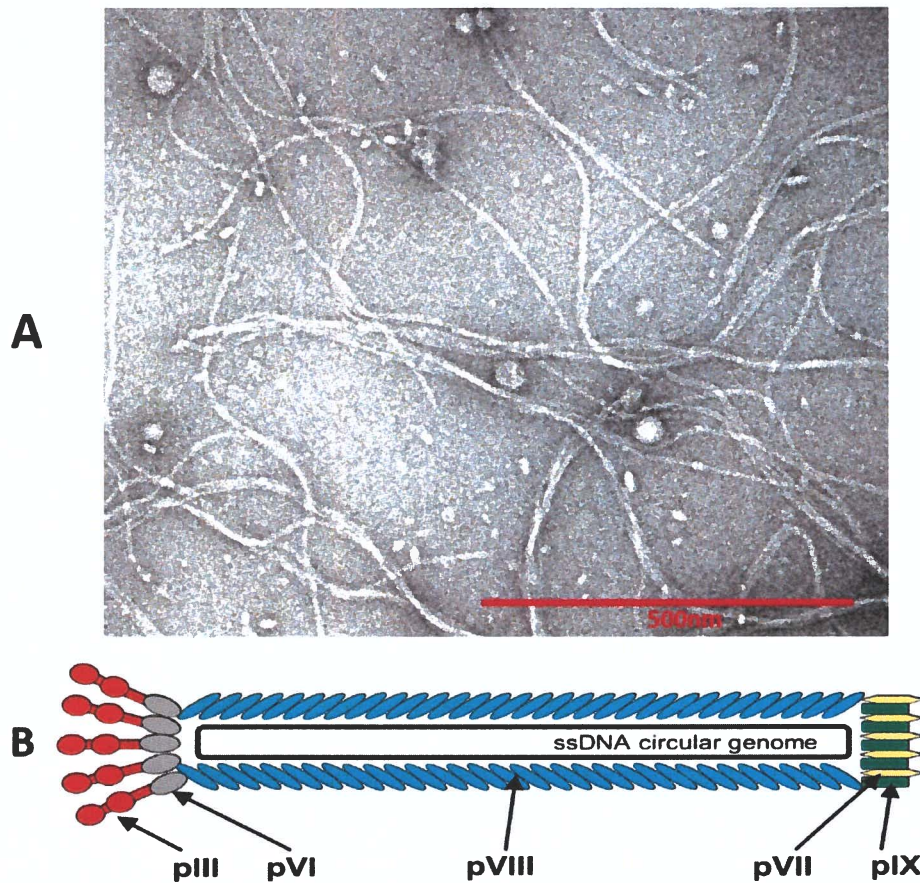


Figure 1.6. Electron micrograph & diagram of an ssDNA phage.

A: An electron micrograph of an ssDNA phage at 100,000 x magnification (image by this author). B: A schematic diagram of an M13 phage showing the location of each of the five proteins that constitute the phage coat containing the circular ssDNA genome. Adopted from (Russel et al., 2004).

Table 1.3. The genes and proteins of filamentous (Ff) phage.

Adopted from Russel et al. (2004) and Mai-Prochnow et al. (2015) with some modifications.

Gene	Protein name	Amino Acids	Mol. Wt. (kDa)	Function
Replication (R)				
gII	pII (G2P) Replication protein	410	46.12	Replication – Endonuclease <ul style="list-style-type: none"> Plays an essential role in viral DNA replication (the positive strand synthesis). Cleaves the dsDNA replicative form I (RFI) and after binding, generates the dsDNA replicative form II (RFII). Joins the ends of the displaced strand to generate a circular single-stranded molecule ready to be packed into a virion.
gV	pV (G5P) DNA binding protein	87	9.67	Replication – ssDNA binding <ul style="list-style-type: none"> Binds to ssDNA in a highly cooperative manner without pronounced sequence specificity. Prevents the conversion into the double-stranded replication form during synthesis of the ss (progeny) viral DNA. Displaced by the capsid protein pVIII (G8P) during phage assembly at the inner bacterial membrane.
gX	pX (G10P) Replication associated protein	111	12.67	Replication <ul style="list-style-type: none"> Translational product from an internal start codon within gene II; identical to the C-terminal domain of PII (G2P) Binds to double-stranded DNA and prevents hydrolysis by nucleases. Inhibitor of DNA replication
Structural (S)				
gIII	pIII (G3P) Attachment protein	424	42.68	Structural – Minor Virion Protein, Coat protein A – Adsorption <ul style="list-style-type: none"> Plays essential roles both in the entry of the viral genome into the bacterial host and in the release from the host membrane, as well as forming the pIII-pVI virion cap. Mediates adsorption of the phage to its primary receptor (F-pilus) during initiation and secondary receptor (domain III of TolA protein). Mediates the release of the membrane-anchored virion from the cell via its C-terminal domain. Interacts with pVI (G6P), pVIII (G8P) and host TolA.

Gene	Protein name	Amino Acids	Mol. Wt. (kDa)	Function
gVI	pVI (G6P) Minor virion protein	112	12.26	Structural – Minor Virion Protein, Coat Protein D <ul style="list-style-type: none"> Plays essential roles in the release of virions from the host membrane. Formation of the G3P-G6P complex is essential for correct termination of filamentous phage assembly and formation (structure) of the pIII-pVI virion cap.
gVII	pVII (G7P) Minor virion protein	33	3.59	Structural – Minor Virion Protein, Coat protein C <ul style="list-style-type: none"> Initiates with pIX (G9P) the virion concomitant assembly-export process by interacting with the packaging signal of the viral genome.
gVIII	pVIII (G8P) Major capsid protein	73	5.23	Structural Major Virion Protein – Coat protein B <ul style="list-style-type: none"> Assembles to form a helical filament-like capsid, wrapping up the viral genomic DNA.
gIX	pIX (G9P) Minor virion protein	32	3.65	Structural – Minor Virion Protein – Coat protein C <ul style="list-style-type: none"> Initiates with pVII (G7P) the virion assembly-export process, by interacting with the packaging signal of the viral genome.
	Assembly & Secretion (A-S)			
gI	pI (G1P) Virion assembly-export protein	348	39.50	Morphogenesis – Phage Assembly <ul style="list-style-type: none"> Inner membrane component of the trans-envelope assembly/secretion system. Interacts with pIV (G4P)
gIV	pIV (G4P) Virion assembly-export protein	426	45.79	Morphogenesis – Phage Assembly and Virion Export <ul style="list-style-type: none"> Acts in the assembly and export of the bacteriophage by forming a gated channel across the host outer membrane. Interacts with pI (G1P).
gI	pXI (G1P) Virion assembly-export protein	N/A	N/A	<ul style="list-style-type: none"> Translational product from an internal start codon within gene I. Required for phage assembly. Part of a trans-membrane complex with pI and pIV to protect pI from cleavage by endogenous proteases.

The filamentous ssDNA phages attach either to the tip (e.g. M13), or to the side (e.g. Pf3) of the pilus. The typical life cycle of a filamentous ssDNA (e.g., M13) is summarised in Figure 1.5. The absorption phase of replication begins upon the diffusion of an infective particle to the tip of the host's sex pilus. When viral DNA arrives in the cytoplasm, it synthesizes a complementary strand, creating a double-strand replicative form (RF). The resulting circular DNA molecule then replicates by a rolling circle replication, where a newly-synthesized DNA strand is used to displace an old strand. The old strand then serves as a template for the synthesis of a complementary strand or is packaged into a virion (Russel et al., 2004, Rakonjac, 2012, Rakonjac et al., 2017).

One unique characteristic of filamentous (Ff) phages is their ability not to lyse the host cells resulting in a chronic infection cycle. Instead, progeny virions are released by secretion, using a dedicated filamentous phage assembly secretion system (Rakonjac, 2012). Unlike most lytic phages, ssDNA filamentous phages require a live and healthy host for its assembly. Phage assembly requires a membrane-embedded assembly machinery, an inner- membrane-embedded, phage-encoded ATPase, and proton-motive force while inside the host (Feng et al., 1997).

1.5.2 Single-stranded RNA (ssRNA) bacteriophages

The Family *Leviviridae* contains the non-enveloped, small (about 26 nm in diameter), ssRNA phages that are spherical and exhibit icosahedral symmetry. Members are considered as the simplest and smallest phage (Olsthoorn and van Duin, 2001, Van Duin and Tsareva, 2006). The genome only contains three or four genes which encode four types of proteins namely maturation, coat, lysis and replicase (Olsthoorn and van Duin,

2001). The capsid contains 180 copies of 14 kDa coat protein (CP); the virions contain one molecule of positive (+) sense ssRNA of 3466–4276 nt in size and one copy of a 35-61 kDa A protein, which is required for virion maturation and pilus attachment (Figure 1.7). The ssRNA phages infect their host by attaching to the side of the F pili (Olsthoorn and van Duin, 2001, King, 2012). Aside from Enterobacteriaceae, they can also infect other species of the genera *Caulobacter*, *Pseudomonas* and *Acinetobacter* and other Gram negative bacteria, provided they express the appropriate sex pili on their surface (King, 2012).

Phages under the Family *Leviviridae* were originally classified into four subgroups. However, based on recent genomic and phylogenetic studies they are now been grouped into two genera: *Levivirus*, which include subgroups I and II; and *Allolevivirus*, which includes subgroups III and IV (Watanabe et al., 1967, Friedman et al., 2009, Murphy et al., 2012). Phage MS2 is the type species of the genus *Levivirus* and has a shorter genome of 3577 nt (3466-3577 nt). Phage Q β (Q β) is the type species for the genus *Allolevivirus* and has longer genome of 4217 nt (4217-42716 nt), with its extra RNA encoding a C-terminal extension of CP (King, 2012). Figure 1.8 shows a comparative general genetic map of a representative *Levivirus* (MS2) and an *Allolevivirus* (Q β) phage.

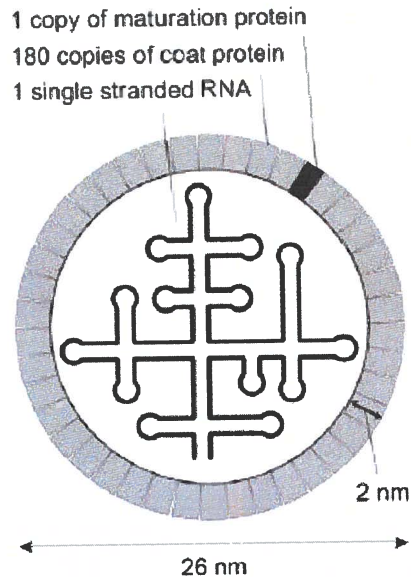
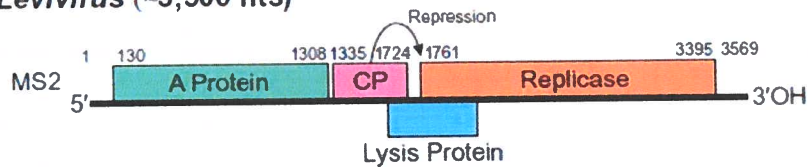


Figure 1.7. Schematic representation of *Leviviridae* virion.
Adopted from (King, 2012).

A. *Levivirus* (~3,500 nts)



B. *Allolevivirus* (~4,000 nts)

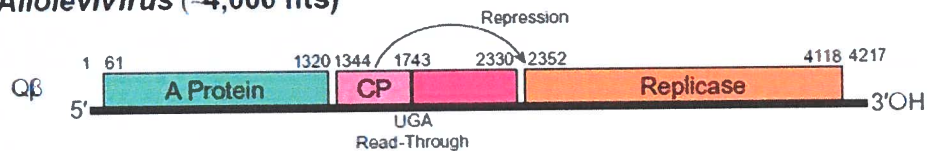


Figure 1.8. Genetic map of a (A) *Levivirus* and (B) *Allolevivirus*.

Enterobacteria phage (A) MS2 and (B) Qβ (Qβ). The maturation protein is also called A-protein. The lysis gene overlaps the replicase gene in a +1 frameshift. Arrows indicate repression of replicase translation by capsid protein binding to an RNA hairpin structure (the operator) present at the start of the gene. The UGA nonsense codon (nt 1743) is occasionally (ca. 6%) misread as tryptophan to produce the read-through protein (A2).
Adopted from (King, 2012).

Bacteriophages of the family *Leviviridae* infection proceeds via adsorption, penetration, replication, assembly, and release. The infection cycle of MS2, a type species for this family is presented in Figure 1.5. The infection cycle starts when MS2 attaches to the side of the pilus via its single maturation protein (Tars, 2020). The precise mechanism by which phage RNA enters the bacterium is still not completely understood. However, it is believed that phages use various mechanisms to breach the cell wall of bacteria and inject their genomes into the cytoplasm of the host. Once the viral RNA has entered the cell, it begins to function as a messenger RNA for the production of phage proteins. The relative synthesis of the four phage proteins is altered by elaborate translational control, via differential access of ribosome binding sites (RBS). For instance, the coat protein (most abundant protein) is immediately translated as it has the most readily accessible RBS on the phage RNA molecule, while the A (maturation) gene can only be translated during the replication of viral positive (+) strands. The MS2 replicase protein associates/assembles with three host proteins (ribosomal protein S1 and translation elongation factors EF-Tu and EF-Ts) to form a viral RNA-specific RNA polymerase. A fourth protein, called host factor is needed for synthesis of the minus (-) strand. This protein is not associated with the polymerase complex but acts directly on the RNA. The MS2 replicase is an RNA-templated RNA polymerase and makes both positive and negative strands of viral RNA. There is no DNA intermediate during MS2 replication. Late in infection, coat-protein dimers act as translational repressors of the replicase gene by binding to a RNA hairpin, the operator that contains the start site of this gene. This protein-RNA complex is considered to be the nucleation site for encapsidation (the

enclosure of viral nucleic acid within a capsid). Virions assemble in the cytoplasm around phage RNA and results in cell lysis releasing phage progenies per cell (King, 2012, Tars, 2020).

1.6 Bacteriophage (phage) therapy

The idea of Felix d'Hérelle that phages can be used to treat bacterial diseases was explored as early as 1917 (D'Herelle, 2007). The first human phage therapy was recorded in France in 1919, when d'Hérelle successfully treated several children suffering from severe dysentery (Sulakvelidze et al., 2001). The first use of phage therapy in veterinary medicine is believed to be carried out by Felix d'Hérelle (date unknown) against chicken typhus and bull haemorrhagic septicaemia (Kvesitadze, 1957). A declining interest was observed after World War II (especially in the West), due to excessive and often unrealistic claims, but with little understanding of the nature of bacteriophages and their strengths and limitations (early 1920s into the 1930s). The idea was eventually side lined in the West with the advent of antibiotic therapy.

The increasing incidence of antibiotic resistant bacterial infections coupled with a very slow antibiotic development has led to the revival of interest in bacteriophage therapy. Phage therapy was "rediscovered" in the English-language literature, starting with the work of Smith and Huggins in the 1980s (Smith and Huggins, 1982, Smith and Huggins, 1983, Smith et al., 1987a, Smith et al., 1987b).

1.7 Inhibition of conjugation and plasmid DNA transfer

Bacterial conjugation is the main mode of horizontal gene transfer whereby bacteria become resistant to antibiotics due transfer of resistant plasmids from F⁺ cells to F⁻ cells, as previously described (Ippen-Ihler and Minkley Jr, 1986, Waters, 1999). The worldwide spread of ESBLs, particularly the widely distributed CTX-M-15 enzyme, is due to mobile genetic elements including conjugative plasmids from the IncF families (that encode F-like plasmids) (Pitout, 2010). Strategies for inhibiting conjugation and plasmid DNA transfer may be useful for preserving the effectiveness of antibiotics and preventing the emergence of multi drug resistant bacterial strains. Therefore, the search for conjugation inhibitors has become a priority in the fight against the spread of antibiotic resistance genes (Baquero et al., 2011, Baym et al., 2016).

1.7.1 Pilus specific phage as inhibitor of conjugation

The F - conjugative sex pili are targeted by a variety of phages such as the filamentous ssDNA and ssRNA phages. Several decades ago, ssDNA and ssRNA phages were observed to inhibit bacterial conjugation, however its mechanism was not fully understood (Novotny et al., 1968, Ou, 1973). It is now known that lytic phages such as ssRNA actively destroy the bacterial cell wall and cell membrane; and kill bacteria by making many holes from the inside out. This mechanism is different to antibiotics' mode of action of inhibiting bacteria from doing a specific cellular process, such as cell wall synthesis. Since the above two studies, no research has been published yet investigating the use of lytic ssRNA phage to target actively conjugating bacteria.

Treatment with lytic pilus specific bacteriophage may select for phage resistant bacteria. However, this event is desirable since phage resistant bacteria are antibiotic sensitive and the plasmids are no longer self-transmissible (Leon and Bastias, 2015). This is because phage use structures present on the bacterial surface, such as lipopolysaccharide and outer membrane proteins, which can be virulence factors in different Gram-negative bacterial species (Koebnik et al., 2000, Raetz and Whitfield, 2002).

The chronic infection cycle by the filamentous ssDNA phages (M13, fd, and f1) can have a range of effects. These include reduction of the fitness of host cells resulting in decrease of F⁺ cells in the population over time. It was also observed that infection appears to cause pilus retraction, so the F⁺ cells might not be competent as donors. Furthermore, infection reduced the average number of pili per cell, but infected cells still possess pili from an average of 3.4 to 0.73 pili per cell (Jacobson, 1972).

A recent study on the inhibition of bacterial conjugation by phage M13 has revealed that the N-terminal domains of g3p (or pIII) may block contact with a recipient cell through physical occlusion of the F pilus or TolA (Lin et al., 2011). The occlusion of the conjugative pilus is mediated primarily by phage coat protein, g3p. The study revealed that overexpression of the N-terminal domains of g3p has led to the periplasmic localization of this protein, consequently inhibiting conjugation (Lin et al., 2011). It was also shown that exogenous addition of the soluble fragment of g3p inhibited conjugation at low nano molar concentrations. Furthermore, association between the pili and g3p has prevented transmission of an F plasmid encoding tetracycline resistance (Lin et al., 2011).

1.7.2 Other strategies to inhibit conjugation and plasmid DNA transfer

The use of heterocyclic compounds, intercalators, and acridine dyes to inhibit conjugation was investigated (Hahn and Ciak, 1976, Molnar et al., 1992, Nash et al., 2012). However, it was shown that these molecules were unspecific, mainly affecting bacterial growth and DNA synthesis rather than conjugation itself. Recently, two new drugs: rottlerin and the red compound were shown to inhibit conjugal transfer of plasmids pKM101, TP114, pUB307, and R6K (Oyedemi et al., 2016). Another strategy has looked at compounds that target proteins, such as relaxase, which initiates conjugation upon nicking plasmid DNA at the origin of transfer. One study has investigated the potential of relaxase-specific inhibitors etidronate (Didronel) and clodronate (Bonefos) (Lujan et al., 2007). Another study has investigated a specific single chain Fv antibodies (intrabodies) against the conjugative plasmid R388 relaxase's - TrwC (Garcillan-Barcia et al., 2007).

Other research has investigated a genetically modified M13 phage encoding a restriction endonuclease BglII gene and a modified phage lambda S holin genes as bactericidal agents against *E. coli* (Hagens and Blasi, 2003). Results showed that genetically engineered phage exerted a high killing efficiency while leaving the cells structurally intact; and release of endotoxin was minimized after infection.

1.8 Other published reports on phage therapy

Most phage therapy utilizes lytic phages to kill their respective bacterial hosts, while leaving the human/animal cells intact and reducing the broader impact on commensal bacteria that often results from antibiotic

use (Furfaro et al., 2018). Aside from the pili, the location and nature of the host cell receptors recognised by phages varies greatly. Examples include peptide sequences and polysaccharide moieties in the cell wall of both Gram-positive and negative bacteria; capsules; and flagella (Fehmel et al., 1975, Xia et al., 2011, Shin et al., 2012, Marti et al., 2013). The list below summarises several phage therapy investigations done in humans and animals models targeting the different surface receptors enumerated above. The different routes for phage therapy are also listed with corresponding key results (Lin et al., 2017) (Table 1.4).

Table 1.4. Phage therapy reports in humans and animal models.
Table adopted from Lin et al. (2017) with some modifications.

Causative Agent	Model	Route ¹	Condition	Result summary ²	Reference
<i>Shigella dysenteriae</i>	Human	Oral	Dysentery	All four treated individuals recovered after 24 h	(Chanishvili, 2012b)
<i>Vibrio cholerae</i>	Human	Oral	Cholera	68 of 73 survived in treatment group and only 44 of 118 in control group	(Chanishvili, 2012b)
<i>Pseudomonas aeruginosa</i>	Murine	Oral	Sepsis	66.7% reduced mortality	(Watanabe et al., 2007)
<i>Clostridium difficile</i>	Hamster	Oral	Ileocectitis	Co-administration with <i>C. difficile</i> prevented infection	(Ramesh et al., 1999)
<i>C. difficile</i>	Hamster	Oral	Ileocectitis	92% reduced mortality	(Ramesh et al., 1999)
Vancomycin-resistant <i>E. faecium</i>	Murine	i.p.	Bacteraemia	100% reduced mortality	(Biswas et al., 2002)
B-lactamase producing <i>E. coli</i>	Murine	i.p.	Bacteraemia	100% reduced mortality	(Wang et al., 2006b)
Imipenem-resistant <i>P. aeruginosa</i>	Murine	i.p.	Bacteraemia	100% reduced mortality	(Wang et al., 2006a)
<i>E. coli</i>	Murine	i.p. or s.c.	Meningitis & sepsis	100% and 50% reduced mortality for meningitis and sepsis, respectively	(Pouillot et al., 2012)
MDR <i>Vibrio parahaemolyticus</i>	Murine	i.p. & oral	Sepsis	92% and 84% reduced mortality for i.p. and oral routes, respectively	(Jun et al., 2014)
<i>S. aureus</i>	Rabbit	s.c.	Wound	Co-administration with <i>S. aureus</i> prevented infection	(Wills et al., 2005)
MDR <i>S. aureus</i>	Human	Topical	Foot ulcer	All 6 treated patients recovered	(Fish et al., 2016)
Unclassified bacterial dysentery	Human	Oral	Dysentery	Phage cocktail improved symptoms of 74% of 219 patients	(Chanishvili and Sharp, 2008)
<i>Salmonella typhi</i>	Human	Oral	Typhoid	In cohort of 18577 children, phage treatment associated with 5-fold decrease in typhoid incidence compared to placebo	(Kutateladze and Adamia, 2008)
Antibiotic resistant <i>P. aeruginosa</i>	Human	Oral	Otitis	Phage treatment safe and symptoms improved in double-blind, placebo-controlled Phase I/II trial	(Wright et al., 2009)

¹i.p.: intraperitoneal injection; s.c.: subcutaneous injection. ²Reduced mortality is for phage-treated groups and are relative to 100% mortality in control animals, unless otherwise specified.

In vivo studies have demonstrated that phage can be effective in treating bacterial infections in chickens, mice, calves, pigs, lambs and fish (Smith and Huggins, 1982, Smith and Huggins, 1983, Berchieri et al., 1991, Barrow et al., 1998, Park et al., 2000, Sklar and Joerger, 2001, Huff et al., 2002, Huff et al., 2003). The efficacy of a phage (HP3), against *E. coli* ST131 strains in reducing bacteraemia in an immunocompromised mouse was also demonstrated (Green et al., 2017). While the use of phage therapy is not still being used in human clinical practice in the European Union (EU), an EU project called PHAGOBURN (<https://cordis.europa.eu/project/id/601857/reporting>) were completed evaluating phage therapy for the treatment of *E. coli* and *P. aeruginosa* burn wound infections (Jault et al., 2018). Finally, phages are increasingly being recognized as a potential solution to the detection and biocontrol of bacteria, which cause food spoilage and decreased microbiological safety of foods (O'Sullivan et al., 2019).

1.9 Advantages and disadvantages of phage therapy

Phage therapy is rapidly evolving and has resulted in cases of life-saving therapeutic use and multiple clinical trials. Despite its many advantages there are several disadvantages that need to be addressed (Loc-Carrillo and Abedon, 2011) (Table 1.5). One of the biggest challenges phage therapy has to hurdle relates to regulations and policy surrounding clinical use and implementation beyond compassionate cases (Furfaro et al., 2018).

Table 1.5. The advantages and disadvantages of phage therapy.

Advantages	Reference	Disadvantages	Reference
Bactericidal	(Carlton, 1999)	Not all phages make for good therapeutics	(Hyman and Abedon, 2010)
Can increase in number over the course of treatment where hosts are located (auto dosing)	(Abedon and Thomas-Abedon, 2010)	Narrow host range	(Hyman and Abedon, 2010)
Non-toxic	(Kutter et al., 2010)	Phages are not unique pharmaceuticals	(Loc-Carrillo and Abedon, 2011)
Tend to only minimally disrupt normal flora	(Gupta and Prasad, 2011)	Unfamiliarity with phages	(Kutter et al., 2010)
Narrower potential for inducing resistance	(Hyman and Abedon, 2010)		
Lack of cross-resistance with antibiotics	(Gupta and Prasad, 2011)		
Easily discovered	(Hyman and Abedon, 2010)		
Formulation and application versatility	(Kutter et al., 2010)		
Disrupting bacterial biofilms	(May et al., 2011)		

1.10 Objectives of the study

The main objective of this research is to isolate and characterise sex pilus specific (SPS) bacteriophages, associated with transmissible/conjugative Incompatibility group F plasmids. The aim is to investigate the potential of these phages to interfere with AMR transfer and maintenance.

Specific objectives of this project were:

1. To isolate SPS bacteriophages and test them against selected field strains of *E. coli* isolated from chickens;
2. To analyse the morphological, genomic, and growth features of the SPS bacteriophages;
3. To describe the kinetics of AMR plasmid loss in bacterial strains harbouring derepressed and repressed F plasmids after interaction with SPS phages *in vitro*.

Chapter 2. Materials and Methods

2.1 Bacterial strains and culture condition

The bacteria used for isolation and characterisation of sex pilus specific (SPS) bacteriophage are listed in Table 2.1. This included the F plasmid negative strain (F⁻) *E. coli* J62 (711), which is a non-lactose fermenting *E. coli* mutant (Clowes and Rowley, 1954, Barrow and Hill, 1989). Two strains of *Salmonella* from which the large 54 kb virulence plasmid (pVP) had been previously eliminated, namely *S. Enteritidis* 125109 ΔpVP and *S. Typhimurium* F98 ΔpVP were also included as F⁻ strains (Smith and Tucker, 1975, Barrow, 1991, Halavatkar and Barrow, 1993). A derepressed F plasmid, p*Flac*::Tn3 (Amp^R) was introduced to these F⁻ strains generating the corresponding F plasmid positive strains (F⁺): *E. coli* J62 p*Flac*::Tn3, *S. Enteritidis* 125109 ΔpVP p*Flac*::Tn3 and *S. Typhimurium* F98 ΔpVP p*Flac*::Tn3 (Smith and Tucker, 1975, Barrow, 1991, Halavatkar and Barrow, 1993).

Several *E. coli* field strains containing repressed AMR F plasmid (from Prof. Paul Barrow's bacterial collection). isolated from poultry in the U.K. were selected for determining the host range, phage sensitivity and plasmid loss experiments (Smith, 1969). These repressed F-like plasmid were designated as pF16, pF18, pF21, pF23, pF26 and pF27. An F-like plasmid from *P. aeruginosa* was also included and was designated as p80610. The presence of the repressor gene *finO* of the correct size was previously detected by PCR for all these strains (Colom et al., 2019). *E. coli* J62 Rif^R was used as recipient strain for the effect of ssDNA phage R4 on plasmid

transfer rate during conjugation. Other wild-type F-like AMR plasmid from *E. coli*: pP13 and pP31; and *Pseudomonas aeruginosa*: p80610 were included for determining the host range of phage R4. The presence of *traA* gene in the F plasmid was also determined by PCR using the following primers: *traA* FW: AGTGTTTCAGGGTGCTTCTGC and *traA* RV: CCCGACATCGTTTTATTTCC giving an amplicon size of 373 bp.

Bacteria were revived and purified by routine inoculation in Luria-Bertani (LB), Miller broth (L3152, Sigma-Aldrich, St. Louis, Missouri, US) and LB agar (L2897, Sigma-Aldrich, St. Louis, Missouri, US), and incubated at 37°C for 18 hours. All isolates were confirmed as *E. coli* by test oxidase (PL.390, Pro-Lab, Merseyside, UK) and spot indole (PL.391, Pro-Lab, Merseyside, UK) tests; API® 20E (20100, BioMerieux, Marcy l'Etoile, France); and by 16S rRNA PCR using published primers ECO-1:GACCTCGGTTTAGTTCACAGA & ECO-2:CACACGCTGACGCTGACCA (Mamun et al., 2016). The plasmid Incompatibility group of the wild-type *E. coli* strains was previously determined as belonging to Incompatibility group F by PCR-based replicon typing using primers FIA, FIB, FIC and F_{repB} (Carattoli et al., 2005a, Colom et al., 2019).

The ssRNA phage MS2 (Overby et al., 1966); ssDNA phage M13 MP7 (Dr. Janis Rumnieks Collection, BMC, Riga, Latvia) and tailed dsDNA phage vB_EcoP_R (Smith and Huggins, 1980, 1982) served as control phages.

Table 2.1. Bacterial strains used for SPS phage isolation.

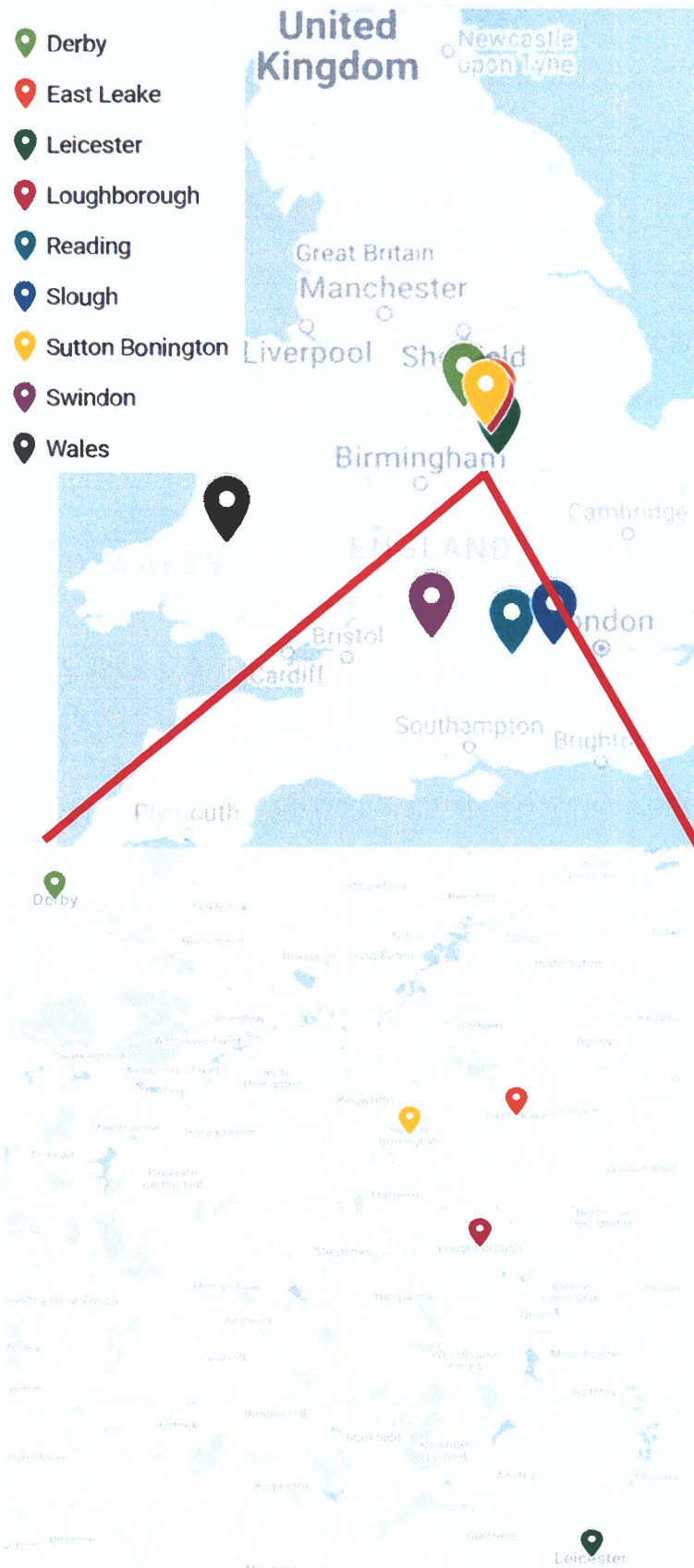
Bacterial strains	Phenotypes
<i>E. coli</i> J62/711	F ⁻ non-lactose fermenter
<i>E. coli</i> J62 p <i>Flac</i> ::Tn3	F ⁺ , lactose fermenter, Amp ^R
<i>Salmonella</i> Enteritidis 125109	F ⁻ , non-lactose fermenter
<i>S. Enteritidis</i> 125109 p <i>Flac</i> ::Tn3	F ⁺ , lactose fermenter, Amp ^R
<i>S. Typhimurium</i> F98	F ⁻ , non-lactose fermenter
<i>S. Typhimurium</i> F98 p <i>Flac</i> ::Tn3	F ⁺ , lactose fermenter, Amp ^R

2.2 Source and samples for phage isolation

Crude and mixed human sewage effluent were collected mainly from Severn Trent Water (STW) and other sewage treatment plants around England; and water river samples from around Wales. The table and figure below summarise the site and sample type used for phage isolation (Table 2.2 and Figure 2.1).

Table 2.2. Source and sample type for phage isolation.

Code	Sample Type	Site/Source	Date of Collection
CSD	Crude Sewage	Derby STW	24/04/2017
MSD	Mixed Fluid Sewage	Derby STW	24/04/2017
CSL	Crude Sewage	Leicester STW	04/05/2017
MSL	Mixed Fluid Sewage	Leicester STW	04/05/2017
CSLo	Crude Sewage	Loughborough STW	18/05/2017
MSLo	Mixed Fluid Sewage	Loughborough STW	18/05/2017
CSEL	Crude Sewage	East Leake	17/05/2017
CSSB	Crude Sewage	Sutton Bonnington	16/05/2017
CSR	Crude Sewage	Reading STW	23/05/2017
CSS	Crude Sewage	Slough STW	23/05/2017
CSSw	Crude Sewage	Swindon STW	22/05/2017
CSJLo	Crude Sewage	Loughborough STW	12/12/2016
Taff	River	Wales	01/04/2017
USK	River	Wales	01/04/2017
WYE	River	Wales	01/04/2017
Priv	River	Wales	01/04/2017



2.3 Phage Isolation

The isolation of sex (F) pilus specific bacteriophage was carried out according to previously described methods (Bradley and Pitt, 1974, Carey-Smith et al., 2006), with several modifications. Ten mL of samples were collected from different sources (Table 2.2), centrifuged at $6,100 \times g$ for 10 minutes and the supernatant filtered through a $0.45 \mu\text{m}$ pore size syringe filter (FIL6588, Minisarts Syringe Filters, Sartorius, Göttingen, Germany). A total of 0.2 g of LB broth powder and 100 μL of an overnight culture of *E. coli* J62 p*Flac*::Tn3 were added to ca. 10 mL filtered samples and were incubated overnight without shaking at 37°C. After incubation the samples were centrifuged for 10 min at $6,100 \times g$. To prepare a phage lysate, the supernatant was filtered through a $0.45 \mu\text{m}$ syringe filter (FIL6588, Minisarts Syringe Filters, Sartorius, Göttingen, Germany) and kept at 4°C until further use.

2.4 Confirmation of sex (F) pilus specificity

A phage lysate spot test was performed to determine the F pilus specificity of the phage isolates. If the lysate is pilus specific, the lysates should form plaques on plates seeded with F⁺ strains but not on the F⁻ strains. Serial 10-fold dilutions of the phage lysates in SM buffer were prepared in 96-well plates (from 10^{-1} to 10^{-8} dilutions). Volumes (10 μL) of each of the phage lysate dilutions were spotted onto LB agar plate overlaid with 3 mL of molten top agar seeded with 100 μL of the bacterial strains with (F⁺) and without (F⁻) F plasmid. The F⁻ strains include *E. coli* J62, *S. enteritidis* 125109 and *S. typhimurium* F98. The F⁺ strains include *E. coli* J62 p*Flac*::Tn3, *S. enteritidis* 125109 p*Flac*::Tn3, and *S. typhimurium* F98

p*Flac*::Tn3. After spotting, the plates were allowed to dry and incubated at 37°C for 18-24 hours. The phages that demonstrated plaques on plates seeded with F⁺ strains but not on the F⁻ strains were identified to be F pilus specific and were further propagated and purified.

2.5 Production of phage lysate

Individual plaques showing distinctive morphology were picked and suspended into 100 µL of SM buffer. SM buffer was prepared by adding 6 g of 1M of Tris base (Thermo Fisher Scientific), 5.8 g of NaCl, 2 g of MgSO₄·7H₂O and 5mL of 2% w/v gelatin to 1 L (final volume) of RO water. The pH of the solution was adjusted to 7.5 with concentrated HCl and sterilised by autoclaving. Twenty (20) µL of this preparation was again spotted onto lawns of F⁺ and F⁻ bacterial strains to further verify its pilus specificity. Individual plaques from phage that only demonstrated plaques on F⁺ strains were picked and further purified by streaking isolated plaques on LB agar and left to dry. The plates were then overlaid with 3 mL of soft top agar seeded with 100 µL of an F⁺ strain (*E. coli* J62 p*Flac*::Tn3). Individual plaques were picked and suspended in 100 µL of SM buffer and re plaque purified for three times.

To produce phage lysate, this purified phage suspension was propagated in *E. coli* J62 p*Flac*::Tn3 as the host strain. Briefly, 10 mL of pre warmed LB broth was inoculated with an overnight culture of the host strain to achieve an optical density (OD) of 0.01 (OD_{600 nm}). The culture was incubated at 37°C, shaking (150 rpm) for 2 h or until the cells reached mid-exponential growth phase at OD_{600 nm} = 0.5 (ca 10⁸ CFU/mL). The culture was then infected with the purified phage suspension at a

multiplicity of infection (MOI) of 0.1. The culture was further incubated with gentle agitation (150 rpm) overnight at 37°C and then centrifuged at 6,100 × *g* for 10 min. The supernatant containing the phage was filtered using a 0.45 µm pore size syringe filter (FIL6588, Minisarts Syringe Filters, Sartorius, Göttingen, Germany). The phage titre was determined by performing a plaque assay, described below. Briefly, the purified phage lysate was serially diluted in SM buffer and selected dilutions were plated out on LB agar plates using the double agar overlay method as previously described (Baig et al., 2017). All phage lysates were stored at 4°C.

2.6 High titre phage propagation

To produce high titre phage lysate (*ca* 10¹¹ CFU/mL), 500 µL of an overnight culture of the host strain, *E. coli* J62 *pFlac::Tn3* and 10 µL of phage lysate was inoculated on LB agar plates, overlaid with 15-20 mL of molten top agar cooled to 45°C, mixed by swirling and incubated overnight at 37°C. For each phage isolate, two to three LB agar plates were prepared. After incubation the top agar layers from several plates were scraped off, transferred to 50 mL conical centrifuge tubes (11347201, Thermo Fisher Scientific) and centrifuged for 20 min at 6,100 × *g*. The supernatant (lysate), containing the phage was filtered using a 0.45 µm pore size syringe filter (FIL6588, Minisarts Filters, Sartorius, Göttingen, Germany) and the titre was determined by plaque assay as described below.

2.7 Plaque assay and morphology

The phage titre was determined by a plaque assay as described previously, with modifications (Ploss and Kuhn, 2010). Filtered phage lysate was serially diluted in SM buffer and selected dilutions were plated

out on LB agar plates using the double agar overlay method as previously described (Kropinski et al., 2009), with modifications. Briefly, five mL melted LB top agar was mixed with 100 μ L of diluted phages and 500 μ L of overnight culture of the host strain, *E. coli* J62 p*Flac*::Tn3. and plated on LB-agar plates. Each dilution was plated at least in duplicate and were incubated at 37°C overnight. Formed plaques on the bacterial lawn were morphologically characterised, mean count determined and phage titre reported as PFU/mL.

2.8 Polyethylene Glycol (PEG) precipitation

A 200 mL pre-warmed LB broth (L3022, Sigma-Aldrich, St. Louis, Missouri, US) was inoculated with 10 mL of host bacteria, incubated at 37°C, shaking (150 rpm) until $OD_{600\text{ nm}} = 0.5$ (ca. 1-2 h) and then 200 μ L of 1 M $MgSO_4$ (M7506, Sigma-Aldrich, St. Louis, Missouri, US) was added. The suspension was inoculated with 5 μ L of high titre phage lysate at an MOI of 0.05 and were incubated shaking (150-200 rpm) at 37°C for 4 h. The suspension was then centrifuged at $6,100 \times g$ for 10 min and the supernatant was filtered using a 0.45 μ m pore size syringe filter (FIL6588, Minisarts Syringe Filters, Sartorius, Göttingen, Germany) and the titre was determined.

The supernatant (ca. 200 mL) containing phage particles was precipitated by addition of 6.15 g sodium chloride (S9625, Sigma, Sfeinheim, Germany) and PEG 8000 (V3011, Promega, Madison, WI, USA) to concentrations of 0.5 M and 10% (w/v), respectively, and was incubated for 24 to 48 hours at 4°C. The suspension was centrifuged at $6,100 \times g$ for 30 mins at 4°C. The supernatant was decanted, and the PEG-phage pellet

was resuspended with 2 mL of 20 mM Tris-HCl, pH 7.5 (Sigma, UK). The PEG precipitated suspension was treated with DNase I (EN0521, Thermo Fisher Scientific) to a final concentration of 10 µg/mL and incubated at 37°C for 15 mins.

2.9 Phage purification by Caesium chloride centrifugation

The PEG-precipitated phage lysate was layered on top of a preformed five-step caesium chloride (CsCl) (C4036, Sigma-Aldrich, St. Louis, Missouri, US) gradient (equal volumes of CsCl solutions in 20 mM Tris-HCl pH 7.5 (Sigma, UK) with densities (ρ) of 1.7, 1.6, 1.5, 1.4 and 1.3 g/mL) and ultracentrifuged (Hitachi Ultracentrifuge CP80 NX) at 141,000 $\times g$ at 4°C for 18 hours as previously described (Rumnieks and Tars, 2012, Nasukawa et al., 2017). The gradient was fractionated by carefully withdrawing 16 - 500 µL fractions from the top of the tube with a micropipette, trying not to stir up the contents of the tube. The fraction with the phage is indicated by the presence of a sharp band. This is further verified by measuring the optical density (OD) at 260 and 280 nm using a NanoDrop™ (ND-2000, Thermo Fisher Scientific, Waltham, Massachusetts, US). The corresponding fraction containing the band with the highest absorbance peak at both 260 and 280 nm in the gradients was dialysed against one litre of 20 mM Tris-HCl (Sigma, UK) pH 7.5 overnight at 4°C. The preparation was concentrated to 500 µL of the purified phage lysate preparation using Amicon Ultra - 0.5 mL 30K MW cut-off spin unit (UFC503008, Millipore, UK) following the manufacturer's instructions and was treated with DNase I (EN0521, Thermo Fisher, Scientific, UK) to remove any remaining bacterial DNA. To verify the recovery of the purified

phage from the dialysed phage lysate, 10 μ L of this preparation was loaded onto a 1% Agarose gel (BP1356, Fisher bioreagents, UK), run at 140 volts for 45 mins and stained with ethidium bromide (EtBr) and Coomassie Blue (LC6060, Thermo Fisher Scientific, UK).

2.10 Transmission Electron Microscopy

Transmission Electron Microscopy (TEM) of high titre phage lysates and selected phage infecting the host strain (*E. coli* J62 p*Flac*::Tn3) was performed. For TEM phage infection sample preparation, 50 μ L of overnight culture of the host strain was mixed with 150 μ L of high titre phage lysate and diluted with 700 μ L of SM buffer. The mixture was incubated for 5 mins at 37°C. The sample was fixed with 37% formaldehyde adjusting the final concentration to 3%. For negative staining, 3 μ L of the sample was applied to a hydrophilic (freshly glow discharged) carbon coated 300 square mesh copper EM grid (Agar Scientific Ltd., UK); and left to stand for 2 minutes to adsorb. Excess sample was removed by touching (at 90° to) the edge of the grid with a small piece of Whatman No. 1 filter paper just leaving a thin film of sample on the grid surface. The grid was immediately rinsed twice by adding 5 μ L distilled deionised water. One drop of uranyl acetate (1% and 0.22 μ m filtered) was applied to the grid and the excess removed immediately. The grids were then allowed to dry and were observed on a JEOL JEM-1400 TEM with an accelerating voltage of 100 kV. Digital images were recorded using a SIS Megaview III digital camera with iTEM software.

2.11 Sodium dodecyl sulphate polyacrylamide gel electrophoresis (SDS-PAGE)

The structural proteins of phage were analysed by SDS-PAGE. All reagents for this analysis came from Thermo Fischer Scientific, Waltham, Massachusetts, US, unless mentioned otherwise. Dialysed and CsCl purified phage lysate were mixed with NuPAGE™ LDS Sample Buffer (NP0007) and then heated at 95°C in a heat block for 10 mins. To demonstrate the separation of proteins, the samples were run in a NuPAGE™ 12% Bis-Tris protein gel (NP0342BOX) with NuPAGE™ MOPS SDS (NP0001) as running buffer and Pierce™ Unstained Protein Molecular Weight Marker (SM0431/26610). The samples were also run in a low molecular weight NuPAGE™ 4-12% Bis-Tris (NP0322BOX) gradient protein gel with NuPAGE™ MES SDS (NP0002) as running buffer and Mark12™ Unstained Molecular Weight Marker (LC5677, Invitrogen, UK). Both types of gels were run at 150 V (25 mA) for 90 to 120 mins in a XCell SureLock™ Mini-Cell Electrophoresis System (EI0001, Invitrogen, UK). The gels were stained with SimplyBlue™ Coomassie Blue (LC6060) and Pierce™ Silver Stain Kit (4612). Protein bands were visualized in ChemiDoc™ MP Imaging System (Bio-Rad, UK).

Biological Characterisation

2.12 Ribonuclease (RNAse) sensitivity

To determine the type of nucleic acid composition of the phage isolates, a plate ribonuclease sensitivity assay was performed as previously described (Bradley et al., 1981). Briefly, 10 µL of phage lysate (1×10^8 PFU/mL) were spotted on LB agar plates overlaid with *E. coli* J62

pF/ac::Tn3 containing pancreatic RNAase at a final concentration of 25 µg/mL. Another LB plate without RNAase was also spotted. Phage MS2 was included as a control RNA phage. The experiment was repeated twice.

2.13 Chloroform sensitivity

Sensitivity to chloroform was performed based on previously described methods with some modifications (Ackermann, 1987, Basdew and Laing, 2014). Bacteriophages with titre ranging from 10^7 to 10^{10} PFU/mL were used, including MS2 as control. Overnight culture of *E. coli* J62 pF/ac::Tn3 was used as the host strain. Briefly, 1,000 µL each of each phage were treated with 10 µL (ca 1 drop) of chloroform and was gently mixed at room temperature. The aqueous phase was withdrawn after 2 minutes, 1 and 2 hours contact time. Phage titre (PFU/mL) was determined by serially diluting the lysate in SM buffer at time 0 (T0) and after treating with chloroform (T2min, T1h and T2h). The lysates were spotted on LB plates overlaid with the host strain as previously described. The experiment was independently repeated three times.

2.14 Thermal stability

To determine the thermal stability of phage at different temperatures, a stability assay was developed based on previously described methods with some modifications (Zhang et al., 2015, Jurczak-Kurek et al., 2016). To strictly maintain the correct temperature throughout the experiment, a Bioer Gene Touch 2™ (Alpha Laboratories, Hampshire, UK) gradient thermocycler was used. Two sets of a 50 µL of high titre (ca 10^{11} PFU/mL) dialysed phage lysate were incubated at room temperature (RT) at 20°C, 37°C, 75°C, 86.3°C and 95.1°C. One set is incubated for 30 mins and the

other one for 60 mins. After incubation, phage titre was determined by preparing a serial 10-fold dilution in SM buffer and selected dilutions were plated out on LB agar plates using the double agar overlay method as previously described. Phage titre was also determined after long term storage at 3°C after three months.

2.15 pH stability

The pH stability testing was performed according to previously described methods with some modifications (Zhang et al., 2015, Jurczak-Kurek et al., 2016). High titre dialysed phage lysate was added at 1:9 into a solution containing 50 mM Tris, 10 mM MgSO₄ adjusted to pH 2, pH 4, pH 7.5, pH 10, pH 12 by either adding NaOH or HCl and then incubated at 37°C for 60 min. After incubation the phage lysate were serially 10-fold diluted in SM buffer pH 7.5. The phage titre was determined by plating selected dilutions on LB agar plates using the double agar overlay method as previously described.

2.16 SDS stability

Sodium dodecyl sulphate (SDS) (L4509, Sigma-Aldrich, St. Louis, Missouri, US), a common surfactant in cleaning and hygiene products can be found both in natural and clinical environments. To determine its effect, phages were tested on 0.1% and 0.5% SDS according to a procedure described previously, with some modifications (Jurczak-Kurek et al., 2016). The phage lysate was added to 0.1% and 0.5% SDS solution (1:9) and was incubated at 45°C for 30 min. After incubation, the phage titre was determined by plating selected dilutions on LB agar plates using the double agar overlay method as previously described.

Genomic Characterisation and Sequencing

Figure 2.2 is a flow diagram summarising the methods used for genomic characterisation and sequencing.

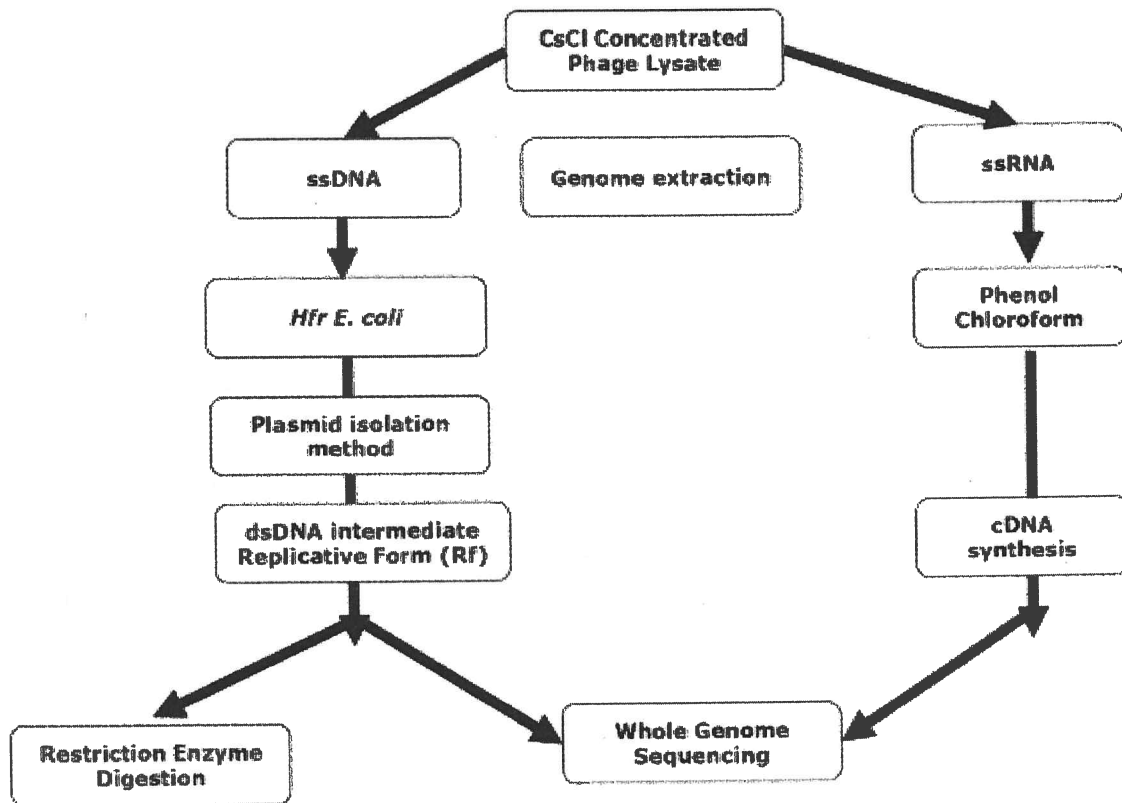


Figure 2.2. Diagram showing genomic and sequencing methods.

2.17 Genomic DNA and RNA extraction

Phage genomic DNA and RNA extraction was performed using the phenol-chloroform extraction technique with modifications (Rumnieks and Tars, 2012). Briefly, 500 μL of high titre purified phage lysate was mixed with 500 μL of phenol, 10% SDS (added to a final concentration of 0.5%) and 5 μL 1 M dithiothreitol (DTT). Basic phenol, pH 8 (P4557, Sigma, UK) was used for DNA phage while acid phenol, pH 4.5 (P4682, Sigma, UK) was used for RNA phage. The mixture was vigorously vortexed for 60 seconds and centrifuged at $15000 \times g$ for 5 minutes. The aqueous phase was extracted two more times with a 1:1 (basic or acid) phenol - chloroform mixture and once with chloroform. The DNA or RNA in the final aqueous phase was precipitated by adding 2.5 volumes of ice-cold 96% ethanol and 0.1 volume of 3 M sodium acetate; vortexed to mix and incubated at -20°C overnight. The precipitated DNA or RNA was centrifuged for 15 min at $15000 \times g$, then the supernatant was discarded, and the remaining pellet was collected. To this, 1 mL of ice-cold 70% ethanol was added and vortexed, then centrifuged for 15 min at $15000 \times g$ and pellet collected. This washing step was repeated twice; making sure that any remaining ethanol was removed from the bottom of the tube. The pellet was air-dried for 10-15 minutes then re-dissolved with 50 μL of diethyl pyrocarbonate (DEPC) treated water. The DNA and RNA concentration was determined using a Nanodrop. The quality of the extracted nucleic acids was analysed in a 1% agarose gel electrophoresis (BP1356, Fisher, UK), stained with EtBr and visualized in ChemiDoc™ MP Imaging System (Bio-Rad, UK). The

GeneRuler 1 kb Plus (SM1333, Thermo Fisher Scientific, UK) served as molecular weight ladder.

2.18 Preparation of replicative form (RF) of ssDNA phage

To prepare the replicative form (RF) of the ssDNA phage, a high frequency (Hfr) strain - *E. coli* K37 Hfr (Farber and Ray, 1980) was infected with the isolated ssDNA phage. An Hfr strain has incorporated an F factor into its chromosome and when infected with pilus specific ssDNA phage will produce double-stranded (ds), closed-circular, RF of the phage in high copy numbers. These RF in infected cells are essentially identical to those of double-stranded, closed-circular plasmid DNAs in their physical characteristics (Green and Sambrook, 2017).

A method was developed to isolate the double stranded – replicative form (RF) of the isolated ssDNA phages. Briefly, 10 mL of pre warmed LB broth was inoculated with an overnight culture of *E. coli* K37 to achieve an optical density (OD) of 0.01 (OD_{600 nm}). The culture was incubated at 37°C, shaking (200 rpm) for 3 h or until the cells reached mid-exponential growth phase at OD_{600 nm} = 0.5 (ca 10⁸ CFU/mL). The culture was then infected with the purified phage suspension at a multiplicity of infection (MOI) of 0.1. and non-infected culture served as a negative control. The culture was further incubated with gentle agitation (150 rpm) overnight at 37°C and then centrifuged at 6,100 × *g* for 10 min at 15°C. The supernatant was discarded and the pellet containing the phage RF was collected. As the RF is similar to double-stranded, closed-circular plasmid DNA; any of the methods commonly used to isolate and purify plasmid DNA can therefore be utilised. To do this, the QIAprep Spin Miniprep Kit (27106X4, Qiagen,

Germany) was used following the manufacturer's instructions. The RF concentration was determined at 260 nm using a Nanodrop. The quality of the isolated RF was analysed in a 1% agarose gel electrophoresis (BP1356, Fisher, UK), stained with EtBr and visualized in ChemiDoc™ MP Imaging System (Bio-Rad, UK). The GeneRuler 1 kb Plus (SM1331, Thermo Fisher Scientific, UK) served as molecular weight ladder.

2.19 Restriction digestion

Restriction digestion of the double stranded RF was carried out by several restriction enzymes (RE). Initially, 1 µg of dsDNA RF of phage R1 was digested by individual RE, which includes *Bam*HI, *Eco*RI, *Eco*RV, *Hinc*II, *Hind*III and *Not*I (New England Biolabs, USA), following the manufacturer's instructions. Restriction digestion with two RE (double RE digestion) were performed using RE that was able to demonstrate RE activity on single RE digestion. After incubation at 37°C for 60 mins, electrophoresis of the samples in 1% agarose gel (BP1356, Fisher, UK) stained with EtBr was performed. The RE digested samples were visualized in ChemiDoc™ MP Imaging System (Bio-Rad, UK) with GeneRuler 1 kb Plus (SM1331, Thermo Fisher Scientific, UK) as molecular weight ladder.

2.20 cDNA synthesis of ssRNA phage genome

Synthesis of double-stranded cDNA from 3.5 µg of extracted RNA was carried out using Maxima™ H Minus Double-Stranded cDNA Synthesis Kit (K2561, Thermo Fisher Scientific, UK), following the manufacturer's instructions. Random hexamer was used as primer to generate the first strand cDNA while the second strand cDNA is generated using the first strand cDNA as a template. Purification of ds cDNA was carried using

GeneJET PCR Purification Kit (K0701, Thermo Fisher Scientific, Waltham, Massachusetts, US) and eluted in 50 µL Elution Buffer (EB). Concentration of ds cDNA was determined using a NanoDrop and reaction products were visualized in ChemiDoc™ MP Imaging System (Bio-Rad, UK).

2.21 Phage genome sequencing

Whole genome sequencing (WGS) of the isolated phages was provided by MicrobesNG (<https://microbesng.com/>). Upon receipt of the samples, genomic DNA libraries were prepared using Nextera XT Library Prep Kit (Illumina, San Diego, USA) and libraries were sequenced on the Illumina HiSeq using a 2x250 bp paired-end reads protocol at a minimum coverage of 30x. MicrobesNG also provided standard bioinformatics, including de novo assembly of the reads using SPAdes and automated annotation using Prokka (Bankevich et al., 2012, Seemann, 2014). The closest available reference genome was identified using Kraken version 2 software (Wood and Salzberg, 2014).

2.22 Genome sequence analysis

The sequencing results, in FASTA format, were further analysed for any errors in contigs assembly using BLAST (<http://blast.ncbi.nlm.nih.gov/Blast.cgi>). Complementary strands were generated using on-line reverse complement tool (https://www.bioinformatics.org/sms/rev_comp.html). Since the genomes of ssDNA phage are circular, they “start” at arbitrary positions in the FASTA files. To circularise it, the start and the end of the genome was determined based on a reference sequence and re-arranged. To identify the species of each phage and how related they are to each other; further *in silico*

analyses, including annotation, genomic illustrations, genomic sequence alignments, and phylogenetic tree assembly were generated using Geneious Prime 2021.1.1 (<https://www.geneious.com>) (Kearse et al., 2012). Nucleotide sequence alignments were performed using Clustal Omega run from within Geneious Prime and percent similarity and number of non-identical bases were determined (Thompson et al., 1994). The genome phylogenetic trees were constructed based on genetic distance model Tamura-Nei evolution model (Tamura and Nei, 1993). Neighbor-Joining (NJ) algorithm was used as tree build method (Saitou and Nei, 1987, Tamura et al., 2004).

Species identification was based on the guidelines of the Bacterial and Archaeal Viruses Subcommittee (BAVS) of the International Committee on the Taxonomy of Viruses (ICTV) (<https://talk.ictvonline.org/taxonomy/>) and according to 2019 Master Species List 35 (MSL35), v1 taxonomy release of the ICTV (ICTV, 2020). Enterobacteria phages NC_003287.2 M13, NC_025824.1 fd, and V00606.1 f1; *Pseudomonas* phage M19377.1 Pf3; and *Vibrio* phage NC_001956.1 fs2 served as reference strains for ssDNA phages. Enterobacteria phages NC_001417.2 MS2 and AB971354.1 Q β ; other distantly related *Leviviridae* Enterobacteria phages AF059243.1_NL95, NC_019922.1_Hgal1, AF227250.1_KU1, NC_001426.1_GA and X15031.1_fr; *Pseudomonas* phage NC_001628_PP7; and *Acinetobacter* phage NC_002700.2_AP205 served as reference strains for ssRNA phages.

2.23 Protein and amino acid sequence analysis

Nucleotide sequences were translated into protein using a computer-generated DNA-to-protein translation tool within Geneious Prime 2021.1.1 (<https://www.geneious.com>) (Kearse et al., 2012). Translation alignments were performed on selected protein sequence using Clustal Omega in Geneious Prime (Thompson et al., 1994). The length and percent similarity of each protein and number of non-identical amino acids with the corresponding proteins of the reference strain were determined. Phylogenetic trees were constructed based on genetic distance model Jukes-Cantor evolution model and Neighbor-Joining (NJ) algorithm was used as tree build method (Saitou and Nei, 1987, Tamura et al., 2004, Som, 2006).

2.24 Naming and classification of phage isolates

The isolated phages were named and classified based on a “bottom-up” approach following the latest guidelines set by the Bacterial and Archaeal Viruses Subcommittee (BAVS) of the International Committee on the Taxonomy of Viruses (ICTV) (Krupovic and Dutilh, 2016, Adriaenssens and Brister, 2017, Adriaenssens et al., 2017).

Host range and growth dynamics

2.25 Phage host range in wild-type *E. coli* strains

A single step replication assay was performed to determine the ability of the isolated phages to infect wild-type *E. coli* strains containing repressed AMR F-like plasmids, as previously described (Colom et al., 2019). Preparation of the host wild-type *E. coli* strains was made by diluting

(1/100) an overnight culture of the strain in LB broth pre-warmed at 37°C, incubated for 2–3 h with shaking until the mid-exponential phase is reached. One millilitre (1 mL) of the host strain preparation was then aliquoted in individual Eppendorf tubes in pairs and was infected with a low concentration of phage (*ca* 10³ PFU/mL). One set of samples were taken at 0 h (T0) to determine initial phage titre. The remaining tubes were incubated at 37°C for 24 h without shaking after which phage titre was determined at 24 h (T24). To determine phage titre, samples from T0 and T24 were serially diluted 10-fold in SM buffer and spotted on LB agar plates in duplicate overlaid with 3 mL of soft top agar seeded with 100 µL of *E. coli* J62 p*Flac*::Tn3. Plaques were counted to determine phage titre (PFU/mL) and percent titre increase was calculated. An increase between initial (T0) and final (T24) phage titre indicated phage replication in the host strain. Phage MS2 was included as control. The experiment was independently repeated three times.

2.26 Phage adsorption assay

Adsorption of selected phage was performed based on previously published methods of Ploss and Kuhn 2001 and Baig *et al.*, 2017 , with modifications (Ploss and Kuhn, 2010, Baig *et al.*, 2017). *E. coli* 711 p*Flac* (with F⁺ plasmid) served as the bacterial host strain for this assay.

A 50 mL volume of LB-broth was inoculated with 500 µL of overnight culture of the host strain and incubated at 37°C for 2 to 2.5 hours, shaking at 200 rpm or until an OD₆₀₀ = 0.5 is reached. The titre of the phage lysate master stock was determined before the experiment and was adjusted to at least x 10¹⁰ PFU/mL. The exponentially growing culture (37°C) were

shifted to 4°C and was infected with the phage lysate at an MOI of 0.1 (for those containing derepressed plasmids) and MOI of 0.01 (for those containing repressed plasmids). The phage adsorption was performed at 4°C to allow virus binding to the F-pili and to avoid the entry of the phage DNA into the host (Jacobson, 1972). Briefly, a 1 mL sample was taken out at time 0 in an Eppendorf tube and subsequent 1 mL samples were taken at every two minutes time interval for 16 minutes. The samples were centrifuged at $17,000 \times g$ for 1 minute. The supernatant containing the unbound phage was collected in fresh Eppendorf tubes and kept at 4°C. Each sample was serially diluted and selected dilutions were plated out on the LB agar plates using the double agar overlay method. The adsorption period was considered as the time taken to achieve a 90% reduction in free, unbound phage (i.e., a one log reduction in PFU/mL). The plating was performed in duplicate and the experiment was independently performed three times.

2.27 One – step growth curve

One-step growth curve was performed for selected phage based on previously described method of Ploss and Kuhn 2001, with modifications (Ploss and Kuhn, 2010). *E. coli* 711 p*Flac* (with F⁺ plasmid) served as the host strain for this assay. Briefly, the host bacterial strain were grown in 50 mL LB medium to a cell density of $OD_{600} = ca. 0.5$. These mid-exponentially growing cells were cooled to 4°C and infected with phage at MOI of 0.1 and MOI of 0.01 for those containing derepressed and repressed plasmids, respectively. The phages were allowed to adsorb to the time of 90% adsorption as calculated in the adsorption assay. Unbound phage particles were separated from cells by centrifugation at $6100 \times g$ for 5 min

at 4°C. The supernatant containing the unbound phage particles was discarded and the cell pellet was gently resuspended in 2 mL ice-cold LB medium. Resuspended cells were transferred in 48 mL prewarmed LB medium at time zero ($t = 0$). The resuspended cells were then shaken (100 rpm) at 37°C and 1 mL samples were drawn at various time points at 5, 10, 20, 30, 60, 90 and 120 minutes. An aliquot was taken from the sample for bacterial titre determination and the rest was centrifuged immediately at $16000 \times g$ for 1 min at 4°C. The supernatant containing the extracellular phage particles was withdrawn and titre was determined by plating selected dilutions on LB agar plates using the double agar overlay method. The plating was performed in duplicate and the experiment was independently performed three times.

2.28 Burst size determination

The burst size was calculated as the difference in the PFU between the end of rise period and the latent period (Bolger-Munro et al., 2013).

2.29 Plasmid population kinetics model with derepressed plasmid

Plasmid population kinetics experiments were carried out following the protocol from a previous study, with several modifications (Colom et al., 2019). For the derepressed plasmid model, two 10 mL tubes of prewarmed LB broth were inoculated (1/100) with an overnight LB broth culture of *E. coli* J62 containing the derepressed p*Flac*::Tn3 plasmid. Both tubes were incubated at 37°C with shaking until an exponential growth phase of $OD_{600} = 0.500$ is reached (*ca* 2 hours). After incubation, one of the tubes was inoculated with selected ssDNA (R1, R4, R10) and ssRNA

(R13, R15) phages at a final MOI of 10 (treatment group). Both cultures were then incubated at 37°C for 24 h with moderate shaking at 150 rpm. The following day, aliquots from these cultures were used to inoculate (1/100) another two fresh prewarmed LB broth, incubated at 37°C with shaking until an exponential growth phase is reached; and then corresponding phages were added to treatment group at MOI of 10 as before. This process was repeated at 48 and 72 h. Aliquots were taken at each time points, then serially diluted in LB broth and were plated on LB agar to determine bacterial count (CFU/mL). For plasmid loss, a total of 100 colonies were randomly selected on LB agar and were replicate plated on MacConkey agar (CM0007, Oxoid, Basingstoke, Hants, UK) with and without ampicillin (100 µg/mL) and then incubated at 37°C for 24 h. The percentage of plasmid loss was then calculated as:

$$\text{(Ampicillin sensitive colonies/Total number of colonies)} \times 100$$

The plating was performed in duplicate and the experiment was independently repeated three times.

2.30 Plasmid population kinetics model with repressed plasmid

For the repressed plasmid model against selected ssDNA phages, two 10 mL tubes of prewarmed LB broth were inoculated (1/100) with an overnight culture of an *E. coli* strain carrying an F-like repressed pF26 plasmid (Sm^R). Both tubes were incubated at 37°C with shaking until an exponential growth phase of OD₆₀₀ = 0.500 is reached (ca 2 hours). After incubation, one of the tubes was inoculated with selected ssDNA (R1, R4, R10) phages at a final MOI of 10 (treatment group). Both cultures were

then incubated at 37°C for 24 h with moderate shaking at 150 rpm. For the repressed plasmid model against selected ssRNA phages, similar protocol was followed but this time overnight culture of an *E. coli* strain carrying an F-like repressed pF21 plasmid (Sm^R) served as the host strain. Treatment group was inoculated with selected ssRNA (R13, R15) phages at a final MOI of 10. The next day, aliquots from these cultures were used to inoculate (1/100) another two fresh prewarmed LB broth, incubated at 37°C with shaking until an exponential growth phase is reached; and then corresponding phages were added to treatment group at MOI of 10 as before. This process was repeated daily for 14 days. Aliquots were taken at day 1, 7, 10 and 14, then serially diluted in LB broth and were plated on LB agar to determine bacterial count (CFU/mL). To determine the plasmid loss, a total of 100 colonies were randomly selected on LB agar and were replicate plated on MacConkey agar (CM0007, Oxoid, Basingstoke, Hants, UK) with and without streptomycin (100 µg/mL) and then incubated at 37°C for 24 h. The percentage of plasmid loss was then calculated as:

$$\text{(Streptomycin sensitive colonies/Total number of colonies)} \times 100$$

The plating was performed in duplicate and the experiment was independently repeated three times.

2.31 Effect of R4 phage during conjugation

The conjugation experiment was performed based on a previously described method with modifications (Colom et al., 2019). Overnight LB broth cultures of donor *E. coli* J62 p*Flac*::Tn3 (derepressed) and wild-type *E. coli* pF21 (repressed) and recipient *E. coli* J62 Rif^R strains were prepared. For the conjugation, 5 µL of the overnight culture of both donor and

recipient strains were mixed together in the same fresh 5 mL LB broth with or without ssDNA phage at a final MOI of 10. The mixture was then incubated overnight at 37°C without shaking. After incubation, dilutions were plated on MacConkey agar (CM0007, Oxoid, Basingstoke, Hants, UK) supplemented with rifampicin (100 µg/mL) to enumerate the recipient strain. Similarly, for the trans-conjugant counts dilutions were plated on MacConkey agar (CM0007, Oxoid, Basingstoke, Hants, UK) with rifampicin and ampicillin (100 µg/mL) for the donor plasmid. The plasmid transfer rate was calculated as:

$$\frac{\text{Trans-conjugant (CFU/mL)}}{\text{Recipient (CFU/mL)}}$$

The plating was performed in duplicate and the experiment was independently repeated three times.

2.32 Statistical analysis

To evaluate the effect of ssDNA and ssRNA phages on plasmid loss and total bacterial count on derepressed and repressed plasmid the mean of two samples per strain in one experiment was determined. The experiment was repeated three times and the mean of each strain from three independent experiments were analysed. The distribution of data was tested for normality according to Shapiro-Wilk normality test (SPSS statistics 26 software, IBM). The data were analysed by two-way ANOVA with Tukey's multiple comparisons post hoc test using GraphPad Prism version 9.3.1 for Windows (GraphPad Software, San Diego, California USA). Correlations where $P < 0.05$ were considered statistically significant.

Chapter 3. Isolation and Characterisation of SPS Phages

3.1 Introduction

Phages are the most abundant and diverse biological entities on the planet that can outnumber bacteria by approximately tenfold in some ecosystems. (Suttle, 2005). They are found in every explored environment, from the human gastrointestinal tract to sewage; to rivers and lakes down to the oceanic basement (Nigro et al., 2017). Given their abundance in the environment, phages exhibit a variety of structural morphologies with impressive genomic diversity and lifestyle. Phage genomes are composed of either DNA or RNA, which may be double-stranded or single-stranded. This genetic material is packaged into a capsid that can be polyhedral/icosahedral, filamentous or pleomorphic collectively referred to as PFP; or connected to a tail (Ackermann, 2009).

Conjugation is the main mode of horizontal gene transfer that spreads antibiotic resistance carried in plasmids among bacteria. These plasmids are transferred from one bacterium to another during conjugation through plasmid encoded sex pilus that is expressed from the donor cell and binds to the recipient cell, mediating DNA transfer. However, the presence of this conjugative pilus can also confer a substantial disadvantage to the host cell, since the pilus is used as the site of attachment for certain DNA and RNA phages. Therefore, these sex pilus specific (SPS) phages constitute an attractive therapeutic candidate that could be used either to prevent bacterial conjugation or to inflict an evolutionary cost against bacteria-harboring resistance conferring conjugative plasmid (Ojala et al., 2016). Among these SPS phages include ssDNA filamentous phages belonging to

Family *Inoviridae* and the polyhedral ssRNA phages of the Family *Leviviridae*. The majority of known phages are tailed (over 95%), which may be a reflection of the ease of isolation and identification as compared to SPS phages which are more difficult to isolate and are less reported (Dion et al., 2020). The aim of this chapter is to attempt to isolate these SPS phages employing our own developed protocol and to determine its physical, morphological, structural, and biochemical characteristics.

3.2 Results

3.2.1 Phage isolation

A total of 15 sex pilus specific (SPS) phages were confirmed from around 50 isolated suspected SPS phages isolated from crude and mixed human sewage effluent obtained around East Midlands and Slough but none were isolated from river samples (Table 3.1). All these phages were confirmed to be F pilus specific as demonstrated by the presence of plaques on plates seeded with strains containing F plasmid (p*Flac*::Tn3), but absent on plates seeded with bacterial strains not containing the F plasmid (Figure 3.1).

Table 3.1. List of isolated SPS phages and their sources.

Phage ID	Sample type	Site
R1	Crude Sewage	Derby STW
R2	Crude Sewage	Leicester STW
R3	Crude Sewage	Leicester STW
R4	Mixed Fluid Sewage	Leicester STW
R5	Crude Sewage	Leicester STW
R6	Crude Sewage	Leicester STW
R7	Mixed Fluid Sewage	Leicester STW
R8	Crude Sewage	East Leake
R9	Crude Sewage	East Leake
R10	Crude Sewage	Sutton Bonington
R11	Crude Sewage	Sutton Bonington
R12	Crude Sewage	East Leake
R13	Crude Sewage	Slough STW
R14	Crude Sewage	Slough STW
R15	Crude Sewage	Loughborough STW

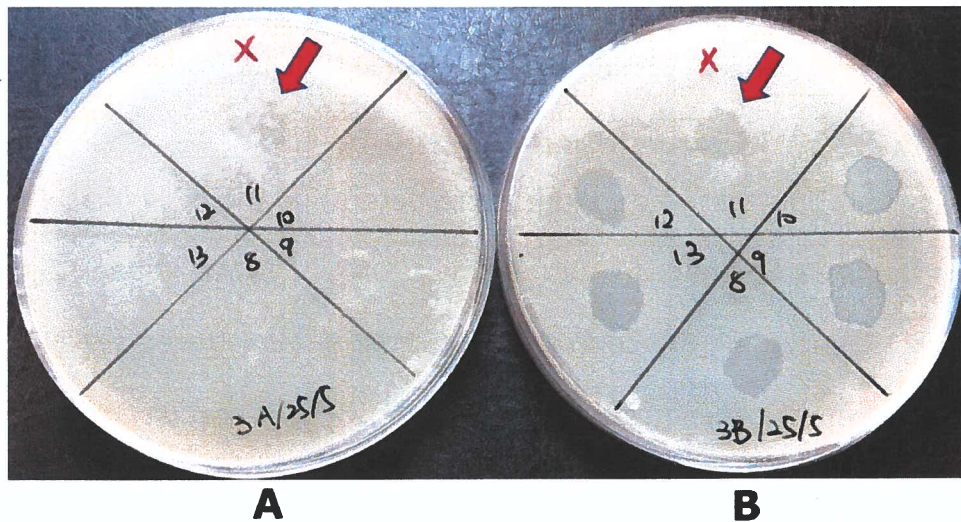


Figure 3.1. Spot test to demonstrate pilus specificity of phage. Plate A is seeded with a bacterial strain lacking the F plasmid; while plate B is seeded with a bacterial strain containing the F plasmid. In this figure, phage 11 (pointed by an arrow) is not a pilus specific phage as plaque could be seen in both plates.

3.2.2 Plaque morphology

Two types of plaque morphology were observed. The first type, which is demonstrated by four phages (R5, R13, R14 and R15), were characterised as being clear with varying diameter averaging at around 5mm. The second type, which was demonstrated by the remaining phages were turbid, smaller (average 3mm) and uniform in sizes (

Figure 3.2).

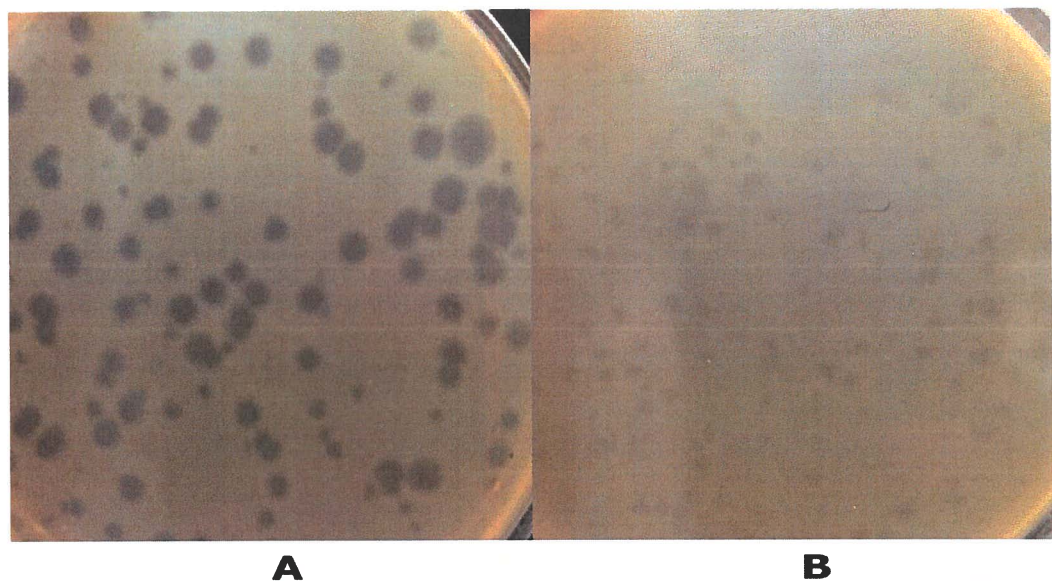


Figure 3.2. Plaque morphology demonstrated by isolated phages.
A - clear with varying sizes; B - turbid with fairly uniform sizes.

3.2.3 Ribonuclease sensitivity

This test was conducted to determine the nucleic acid composition of the isolated phages whether it is a DNA or RNA. Phage R5, R13, R14 and R15; including the control phage, MS2 demonstrated sensitivity to RNAase at a final concentration of 25 µg/mL in LB agar seeded with *E. coli* J62 pF/lac::Tn3. This was indicated by absence or significant reduction of plaque formation compared to LB agar without RNAse. The remaining phages were not sensitive to RNAse as indicated by formation of plaque (

Figure 3.3). Based on these results, four phages (R5, R13, R14 and R15), could be putative RNA phages while the remaining 11 phages (R1, R2, R3, R4, R6, R7, R8, R9, R10, R11 and R12) are most likely to be DNA phages.

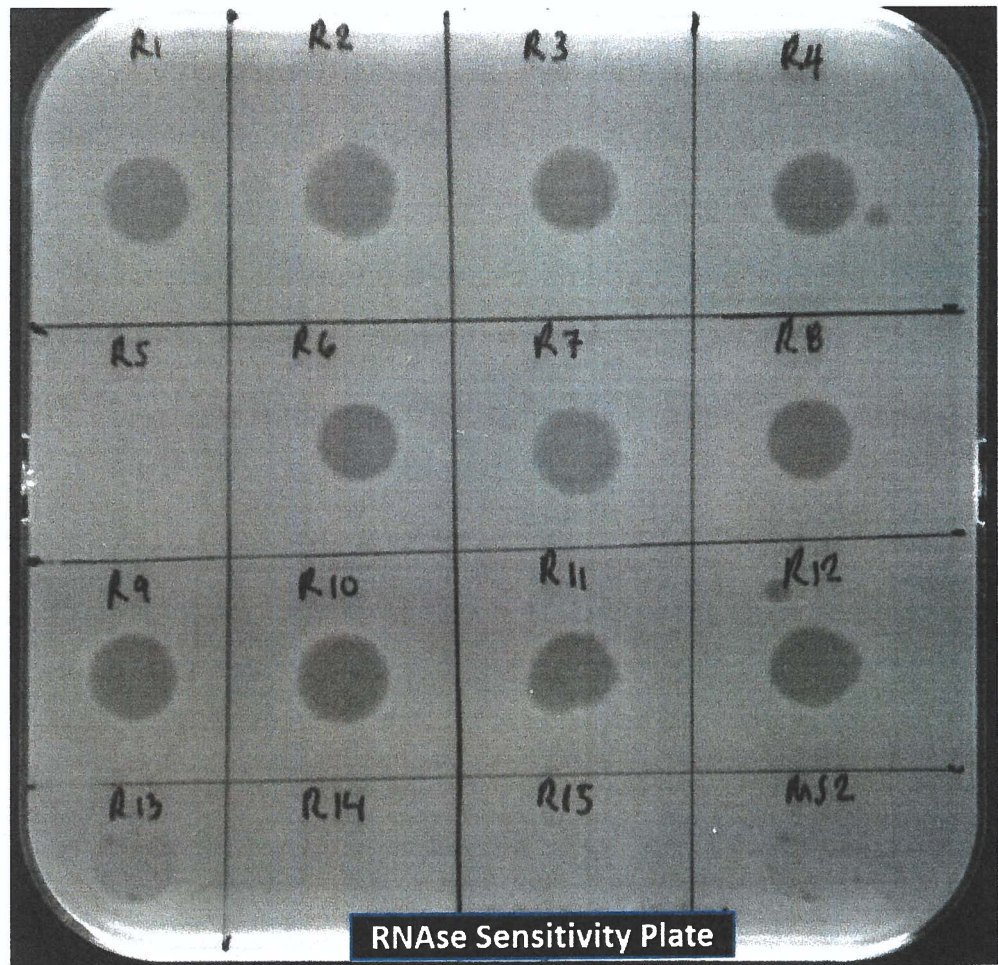


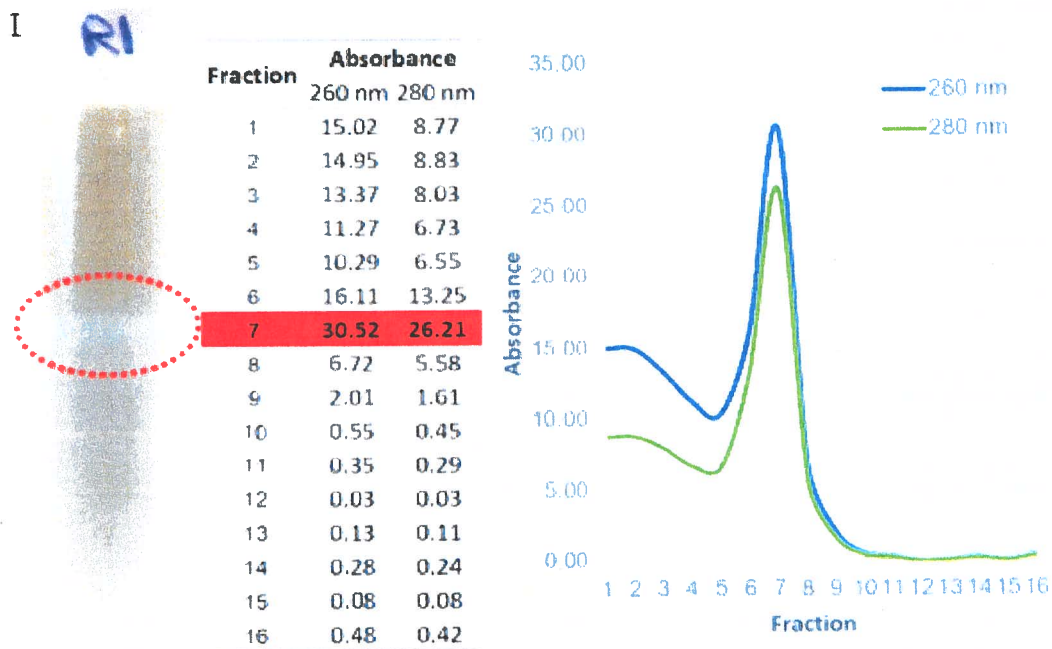
Figure 3.3. Ribonuclease sensitivity of the phage isolates.

Pancreatic RNAse was added on the plate at a final concentration of 25µg/mL. Representative from two identical experiments. RNAse sensitivity is indicated by the inability to produce plaque or substantial reduction of plaque formation.

3.2.4 Phage lysate characterisation CsCl purification

All the isolated phages were purified using density gradient centrifugation with CsCl. A band which mainly contain the concentrated phage was demonstrated after CsCl density gradient centrifugation of the phage lysate. The absorbance of ca 16 aliquots from along the CsCl

gradient were determined at 260 nm and 280 nm, where the highest absorbance peak in the gradients corresponds to the location of the phage band (Figure 3.4). Phages were divided in two groups based on the location of the band in the density gradient of the phage lysate preparation. Group I, consisting of phage isolates R1, R2, R3, R4, R6, R7, R8, R9, R10, R11 and R12 have bands that are located higher in the density gradient, as compared to group II, which consists of phages R5, R13, R14 and R15.]



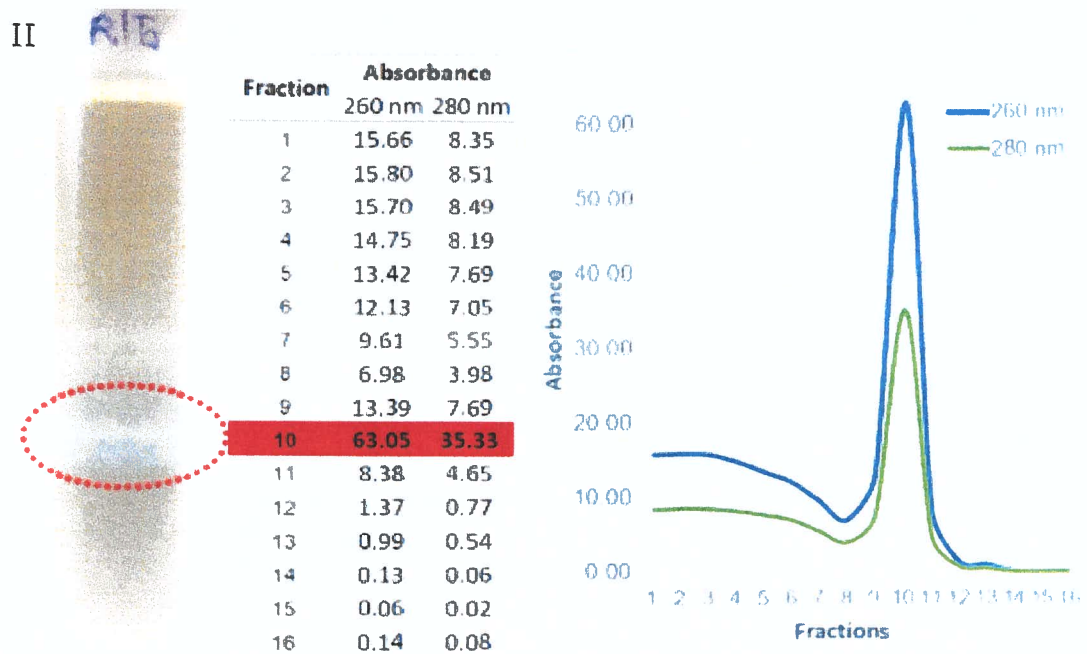


Figure 3.4. CsCl density gradient centrifugation of the phage lysate. The location of the band, which contains the concentrated phage is encircled, and corresponds to the highest absorbance peak at 260 nm and 280 nm. Based on these results, phages can be divided in two groups: **group I** represented here by R1, has phage band that is located higher in the density gradient; as compared to **group II**, represented here by R15.

3.2.5 Purified phage staining in agarose gel

The recovery of the purified phage after dialysis were visualised in agarose gel that was stained with EtBr and then re-stained with Coomassie Blue. This strategy of employing both stains has resulted in classifying the isolated phages into two groups and has provided evidence that they have different genomic composition. Phages R1, R2, R3, R4, R6, R7, R8, R9, R10, R11 and R12 were only stained by Coomassie Blue, whereas phages R5, R13, R14 and R15 were stained both with EtBr and Coomassie Blue.

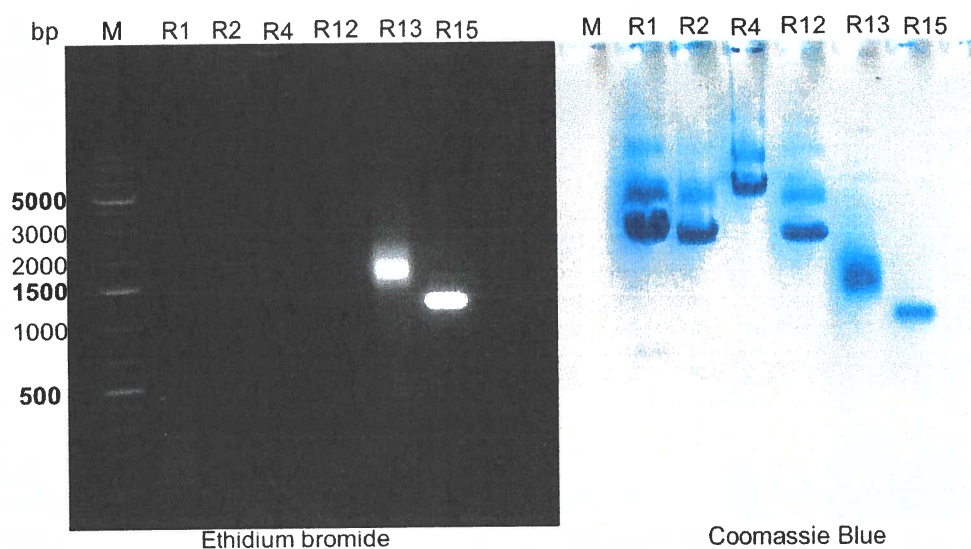


Figure 3.5. Selected dialysed phage visualised on an agarose gel. Purified phage lysate was loaded onto the agarose gel after dialysis and were stained with EtBr (left) and Coomassie blue (right). Results showed that phages R1, R2, R4 and R12 were only stained with Coomassie Blue, whereas phages R13 and R15 were stained both with EtBr and Coomassie Blue. M, 1 kb Plus DNA Ladder.

3.2.6 Virion morphology

Transmission electron microscopy revealed two types of morphology. Phages R1, R2, R3, R4, R6, R7, R8, R9, R10, R11 and R12 appeared as circular filamentous phages. Measuring 20 virions revealed a mean length of 940 nm and thickness of 8 ± 2 nm (Figure 3.6, Appendix A). However, because of its highly circular morphology, there was a difficulty in locating

the ends of each virion. The remaining phages R5, R13, R14 and R15, appeared as icosahedral and non-tailed phages. The measurement of 20 virions per phage gave an average diameter of 20 ± 3 nm (R5), 19 ± 5 nm (R13), 21 ± 4 nm (R14) and 22 ± 2 nm (Figure 3.6, Appendix A). All four phages attached to the side of the F pilus (

Figure 3.7).

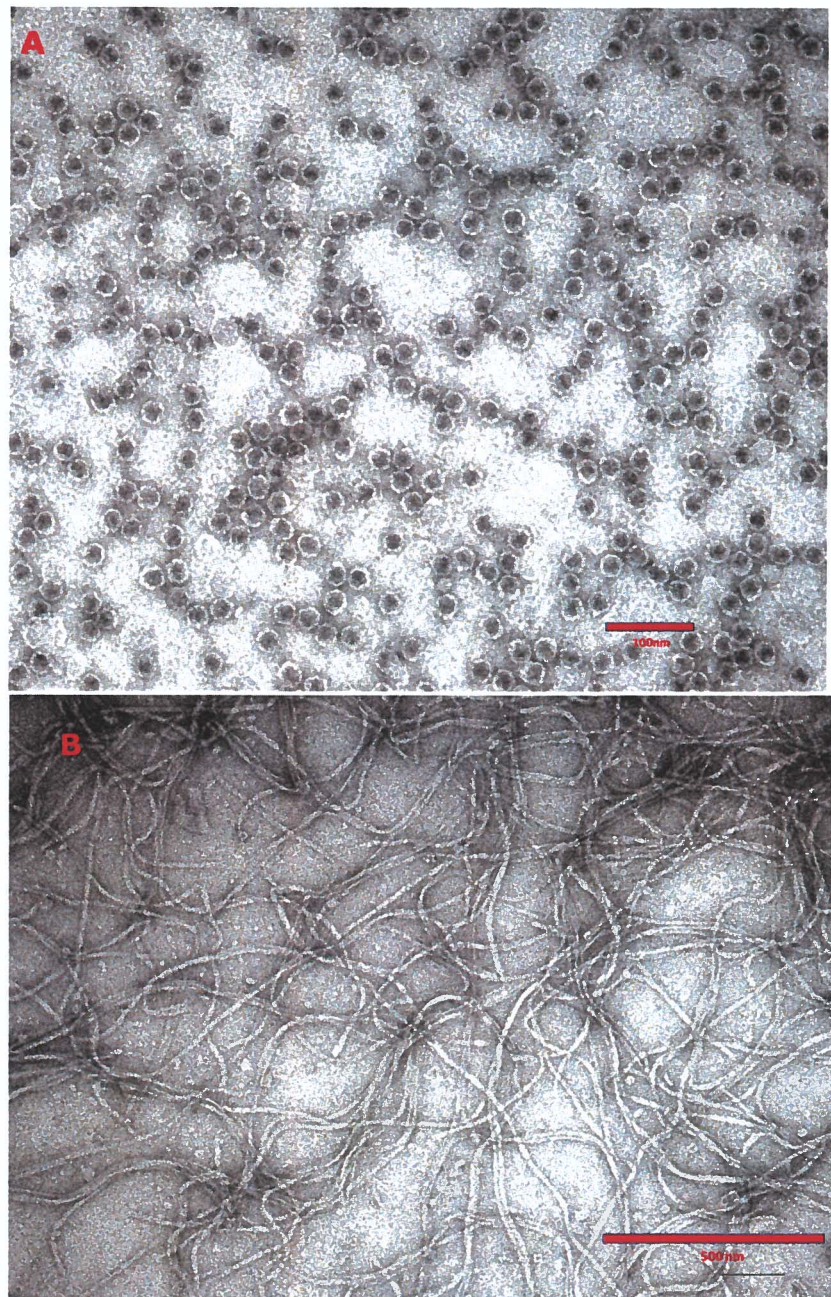


Figure 3.6. TEM – negative staining images of phage.

A: icosahedral, non-tailed phage and B: circular, filamentous phage. The bar represents 100 & 500 nm, respectively. All electron micrographs were taken at 100,000 x magnification by a JEOL JEM-1400 transmission electron microscope.



Figure 3.7. ssRNA R13 phage attaching to the side of the F pilus.
The bar represents 100 nm. All electron micrographs were taken at 100,000 x magnification by a JEOL JEM-1400 transmission electron microscope. Image by this author.

3.2.7 Chloroform sensitivity

Chloroform sensitivity was determined, as chloroform sensitivity could indicate that a phage contains an envelope. Phage titres (PFU/mL) were compared before and after contact with chloroform from 10 seconds up to two hours (Figure 3.8). There was no difference observed which indicated that all 15 phages were chloroform insensitive.

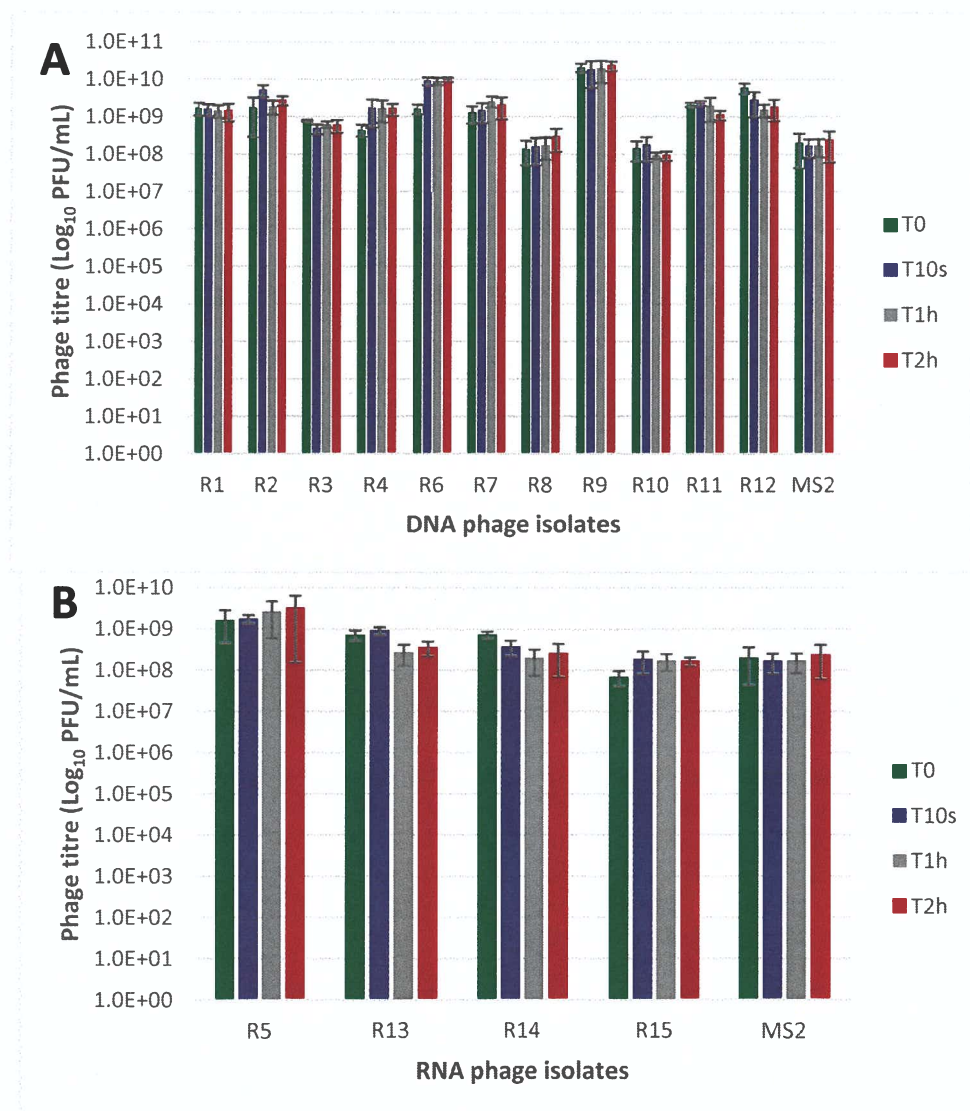


Figure 3.8. Effect of chloroform on phage titres.

An F^+ *E. coli* J62 $pFlac::Tn3$ strain served as the host bacterial strain for ssDNA (A) and ssRNA (B) phage propagation. Phage titres (PFU/mL) were compared before and after contact with chloroform at different times. Values represent the mean of three independent experiments ($n=3$) \pm standard deviation (SD).

3.2.8 Restriction digestion

Among the restriction enzymes (RE) that were tested, *Bam*HI and *Hinc*II were able to cleave the double stranded RF of the ssDNA phages showing a digestion product of around 6.4 kb (Figure 3.9). This also confirmed the successful generation of the double stranded replicative form (RF) of the ssDNA phages, as these RE can only cleave DNA that is double-stranded.

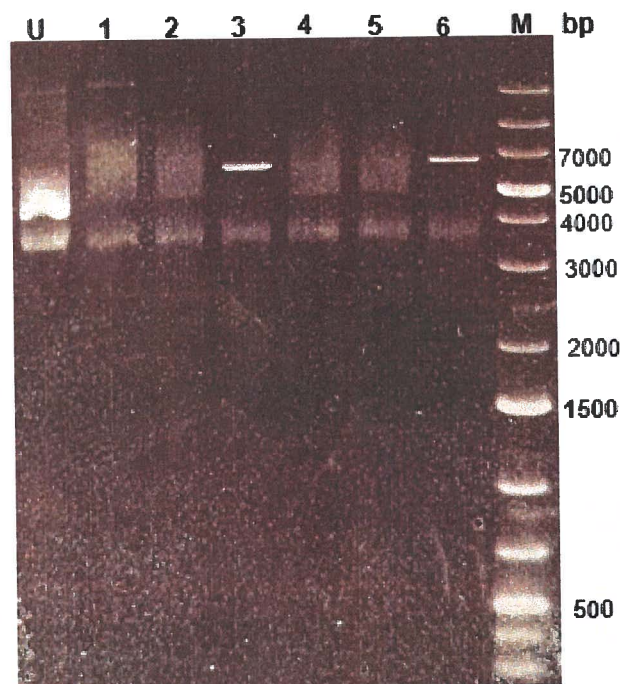


Figure 3.9. Restriction analysis of the RF of phage R1.

The RF of phage R1 was digested by several RE (NEB) individually to determine specific restriction sites present in the double stranded RF. Lanes U: undigested RF of phage R1, 1: *Eco*RI, 2: *Eco*RV, 3: *Bam*HI, 4: *Hind*III, 5: *Not*I, 6: *Hinc*II, M: 1 kb Plus DNA Ladder. *Bam*HI and *Hinc*II were able to digest the RF resulting to around 6.4 kb RE digestion product.

Using both enzymes for a double RE digestion, two bands of around 4.1 kb and 2.3 kb in size were generated (

Figure 3.10). These results have confirmed that the restriction sites G/GATCC and GTY/RAC (where Y = C or T and R = A or G) for *Bam*HI and *Hinc*II, respectively are present in the DNA sequence of the dsDNA RF of all the isolated ssDNA phages.

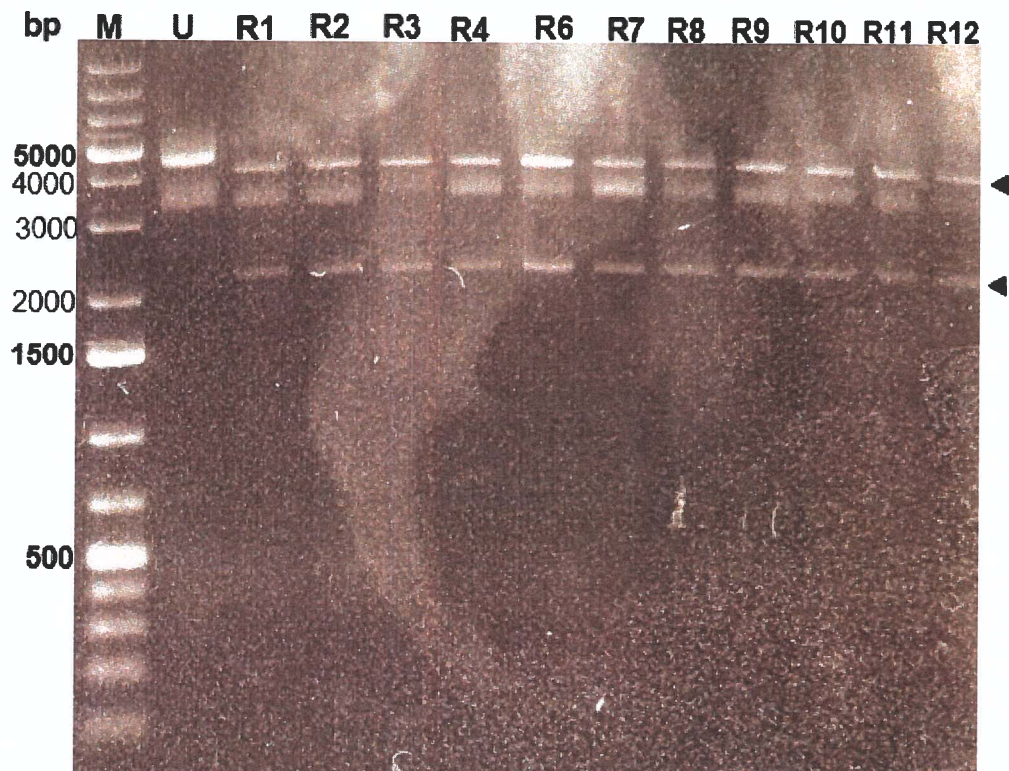


Figure 3.10. Restriction pattern of the RF of ssDNA phages. Lane M: 1 kb Plus DNA Ladder; U: undigested RF; R1 to R12: RF of ssDNA phages. Two bands of around 4.1 kb and 2.3 kb (marked with arrows) were generated after *Bam*HI and *Hinc*II double RE digestion.

3.2.9 Structural proteins analysis by SDS-PAGE

The phage structural proteins were analysed by SDS-PAGE to further characterise and differentiate the isolated phages. Phages that were identified as ssDNA phages based on initial characterisations, demonstrated a structural proteins profile typical of Family *Inoviridae*, Genus *Inovirus*, which include phages M13, fd and f1; collectively known as filamentous phages, Ff. Initially, the samples were run in a 12% Bis-Tris protein gel with MOPS as running buffer and stained with Coomassie Blue. In this set-up, the major CP, pVIII were clearly visualised, together with the attachment protein, pIII (Figure 3.11). The protein profiles of the isolated phages were highly similar to each other, which is expected as majority of

the known filamentous ssDNA phages are highly related. Interestingly, phages R4 and R7 appear to have a smaller pIII protein as compared to the remaining phages. The extra bands on the gel are highly likely not phage proteins but might be some impurities, such as bacterial proteins or some degradation products of the phage proteins.

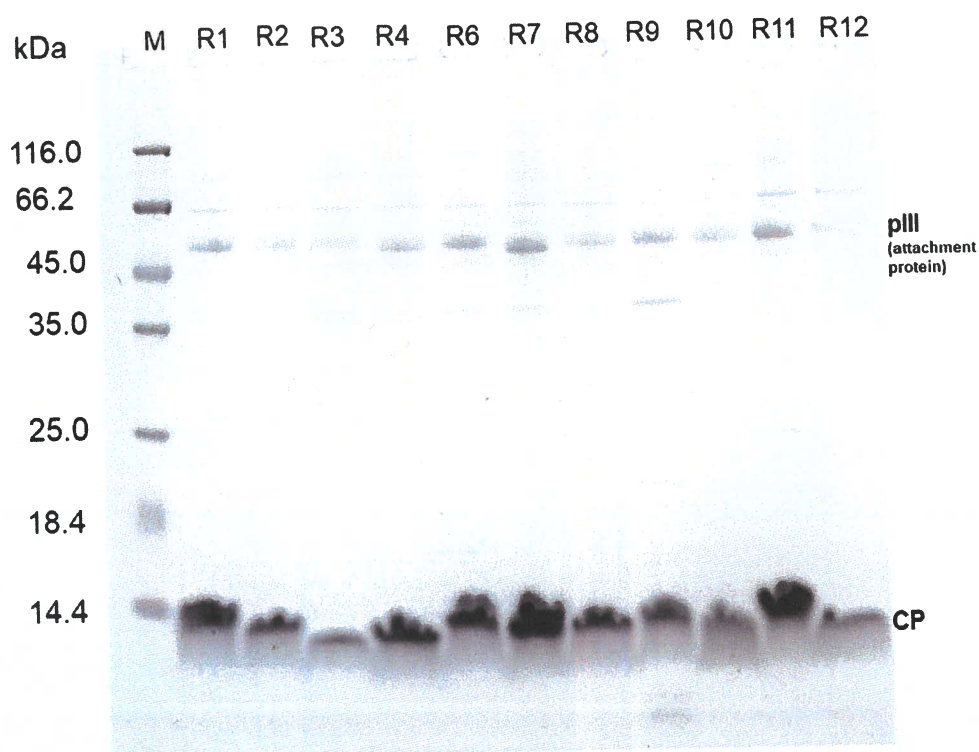


Figure 3.11. SDS-PAGE analysis of ssDNA phages.

Lane M, Pierce™ Unstained Protein Molecular Weight Marker; R1 to R12, ssDNA phages. The samples were run in a NuPAGE™ 12% Bis-Tris protein gel with NuPAGE™ MOPS SDS as running buffer stained with Coomassie Blue SimplyBlue™. The major coat protein (CP), pVIII together with the attachment protein, pIII were demonstrated.

In order to better visualise the major and minor coat proteins, the samples were also run in a low molecular weight 4-12% Bis-Tris gradient protein gel with MES SDS as running buffer and stained with silver stain (Figure 3.12). In this set-up, the 5.2 kDa major CP, pVIII was visualised and possibly the 12 kDa minor CP, pVI. A fainter 3.6 kDa band that matches the size of minor coat proteins, pVII and pIX was also visualised.

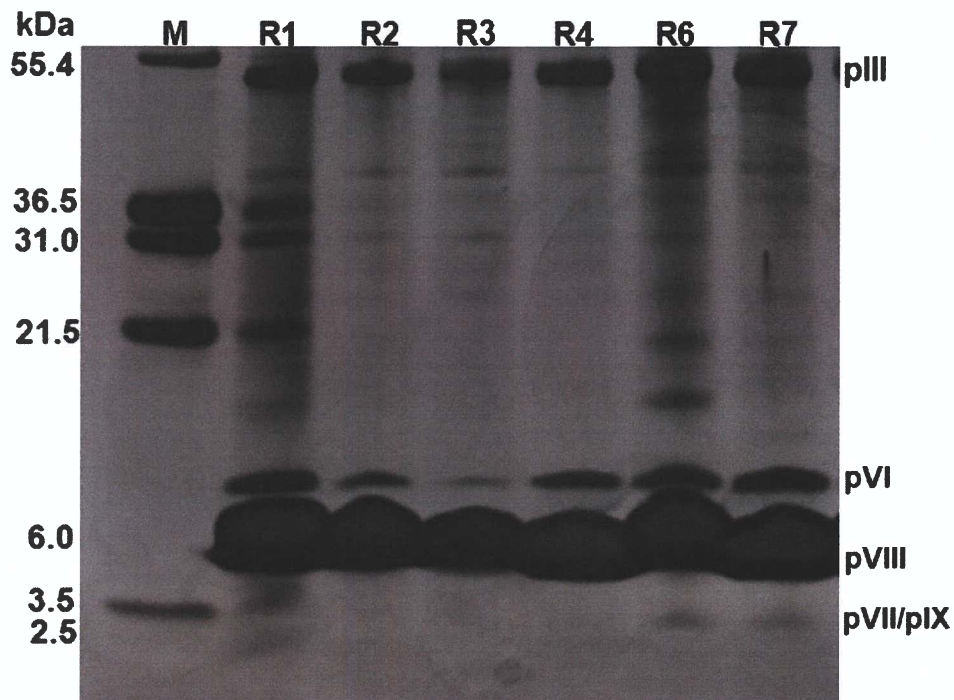


Figure 3.12. SDS-PAGE analysis of ssDNA phages.

Lane M, Mark12™ Unstained Molecular Weight Marker; R1 to R7, selected ssDNA phages. The samples were run in a low molecular weight NuPAGE™ 4-12% Bis-Tris gradient protein gel with NuPAGE™ MES SDS as running buffer and stained with Pierce™ Silver stain. The 5.2 kDa major CP, pVIII; and possibly the 12 kDa minor CP, pVI and a fainter 3.6 kDa minor coat proteins, pVII and pIX were visualised.

Phages R5, R13, R14 and R15 that were identified initially as ssRNA phages demonstrated structural proteins profile typical of the Family *Leviviridae* (

Figure 3.13). These four phages belong to two different families. Phages R5, R14 and R15 all demonstrated the ~13.9 kDa coat protein (CP) and the ~44 kDa maturation protein (A), which matches of those of Family *Levivirus*. A faint band between 66.2 and 116.0 kDa was also observed in phage R14. As these phages have small genomes that encode just a few well-known structural proteins, this extra band that does not match any of the known structural proteins is most probably a bacterial protein or some impurities. Phage R13 demonstrated a slightly bigger CP and a ~48 kDa

maturation protein (A2); and an extra ~36 kDa minor coat protein (A1), which is a characteristic of the Family *Allolevivirus*. The structural proteins of these phages were demonstrated in 12% Bis-Tris protein gel with MOPS as running buffer and stained with Coomassie Blue.

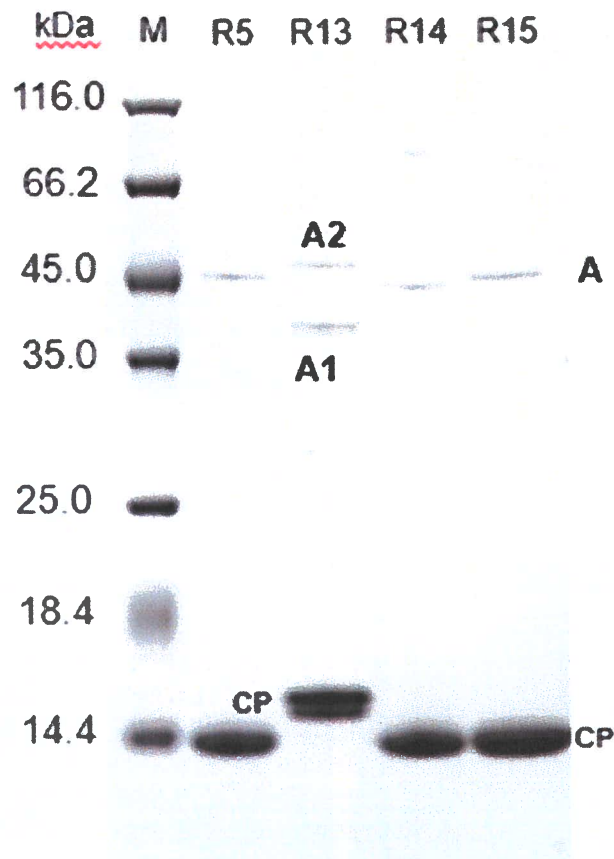


Figure 3.13. SDS-PAGE analysis of ssRNA phages.

Lane M, Pierce™ Unstained Protein Molecular Weight Marker; R5, R13 to R15, ssRNA phages. The samples were run in a NuPAGE™ 12% Bis-Tris protein gel with NuPAGE™ MOPS SDS as running buffer stained with Coomassie Blue SimplyBlue™. The coat protein (CP) and the maturation protein (A) was demonstrated by phages R5, R14 and R15. A slightly bigger CP and maturation protein (A2); and minor coat protein (A1), was demonstrated by phages R13.

3.2.10 Thermal stability

Stability of isolated phages was tested against a wide temperature (3°C to 95°C) range to determine their survival during storage or shipment. Representative phages from the isolated ssDNA (R1, R4, R10) and ssRNA (R13, R15) phages were tested for thermal stability. All ssDNA phages demonstrated better stability at higher temperatures as compared to ssRNA phages (

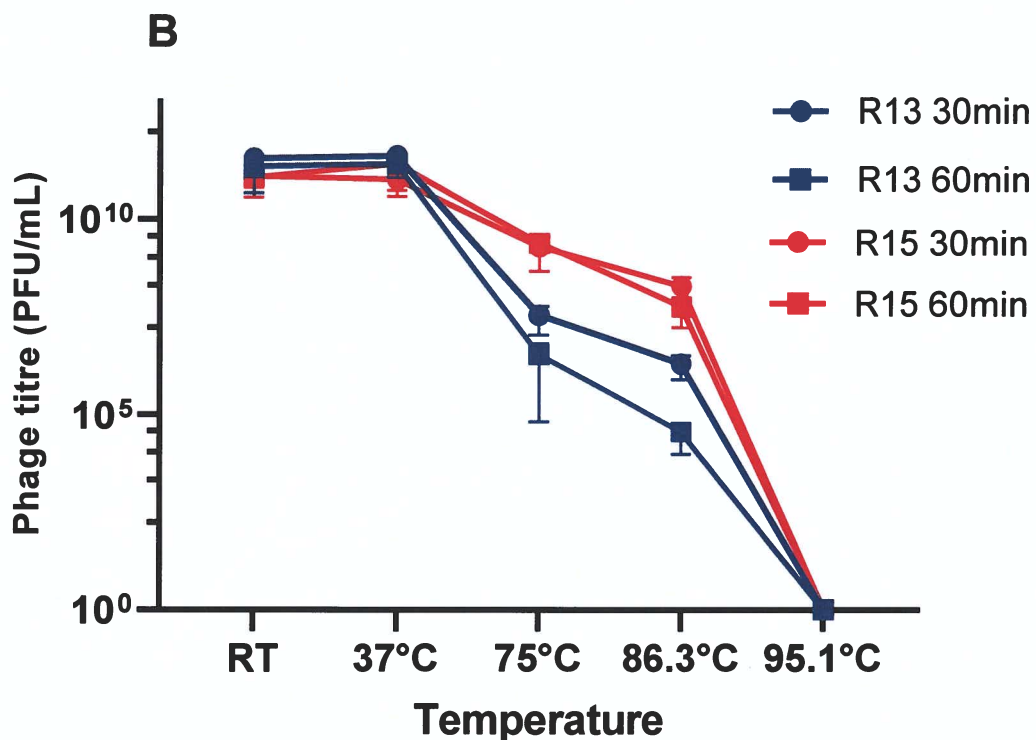
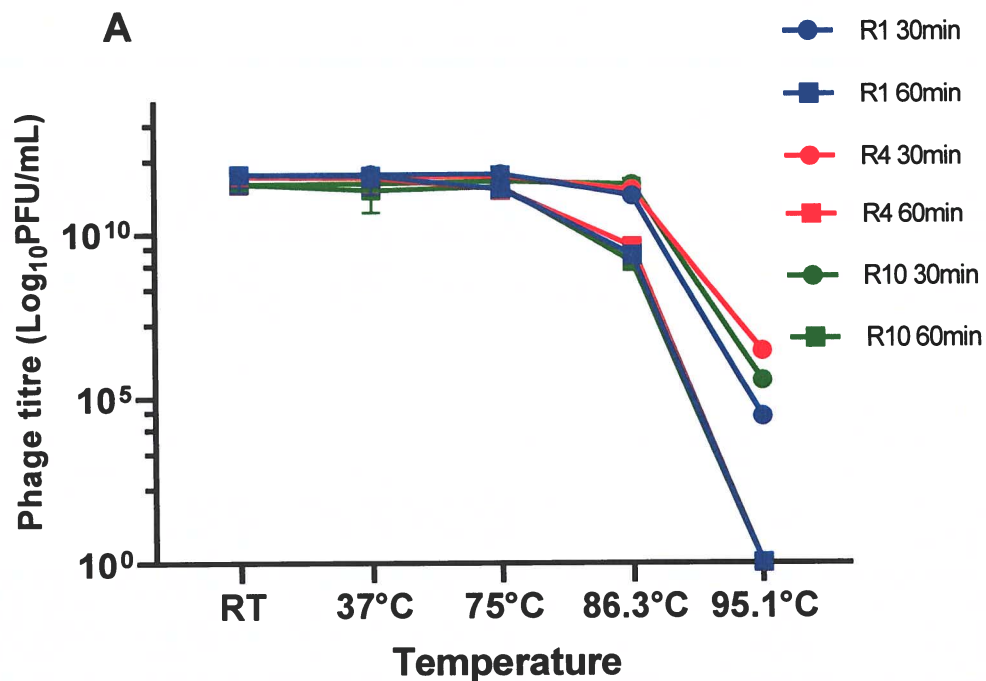


Figure 3.14). All ssDNA phages maintained a high titre level of 10¹¹ PFU/mL at 20°C (RT) and 37°C for up to 60 min, with only a minimal decrease (<1 log₁₀) in titre when heated at 75°C for up to 60 min and at 86.3°C for 30 min. A decrease in titre (*ca* 2 logs) was only observed when exposed to 86.3°C for 60 min and continued to drop (5 to 7 logs) when heated at 95.1°C for 30 min. Full inactivation of all ssDNA phages was observed at 95.1°C for a longer exposure time of 60 min.

Both representative ssRNA phages were only able to maintain a high titre level at RT and 37°C for up to 60 min. A decrease in titre was first observed at 75°C for 30 min and a further drop of up to *ca* 6 logs at 86.3°C for 60 min. Full inactivation of both phages was observed starting at 95.1°C for 30 min. Comparing the two ssRNA phages, R15 appeared slightly more stable than R13. The phages stability at refrigerated (3°C) temperature after 90 days was also determined (data not shown) to ensure their survivability during prolonged storage. All ssDNA phages maintained a high titre level of 10¹¹ PFU/mL at period of 90 days at 3°C. All ssRNA phages are less stable showing a decrease in titre (*ca* 2 logs) after 90 days of storage at 3°C.



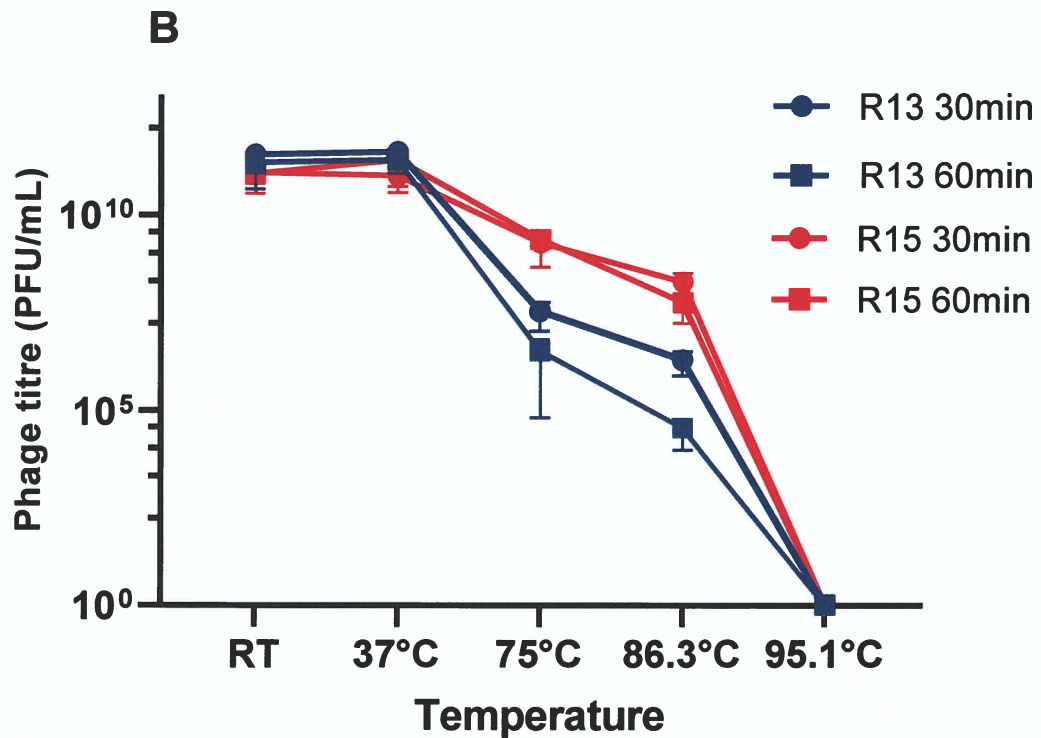


Figure 3.14. Thermostability of (A) ssDNA and (B) ssRNA phages.

The phage titres (PFU/mL) of representative isolated phages were determined at five temperatures for 30 and 60 min. An F⁺ *E. coli* J62 p*Flac*::Tn3 strain served as the host bacterial strain for phage propagation. Values represent the mean of three independent experiments (n=3) ± standard deviation (SD).

3.2.11 pH stability

The stability experiments of the isolated phages at different pH was carried out in order to determine its suitability as possible biocontrol agent and for phage therapy. For instance, if it can survive at low pH such as in GI tract (pH 1–5) through oral administration or if it can be stable in multiple-hurdle approach in processing facilities or on food-contact surfaces if used as a biocontrol agent.

The effect of an acidic and an alkaline pH on the titre of representative ssDNA (R1, R4, R10) and ssRNA (R13, R15) phages is shown in Figure 3.15. All ssDNA phages showed a good stability on a wide range of pH, with optimum pH recorded at 7.5. Both ssRNA phages also maintained high titre

at pH 7.5. Comparing the two ssRNA phages, R13 showed better viability at an alkaline pH, while R15 survived better in an acidic pH. When compared to pH 7, there was a 3 log difference in titre when R13 was exposed to pH 2 and only 2 log difference when grown at pH 12. The opposite pattern was observed for R15.

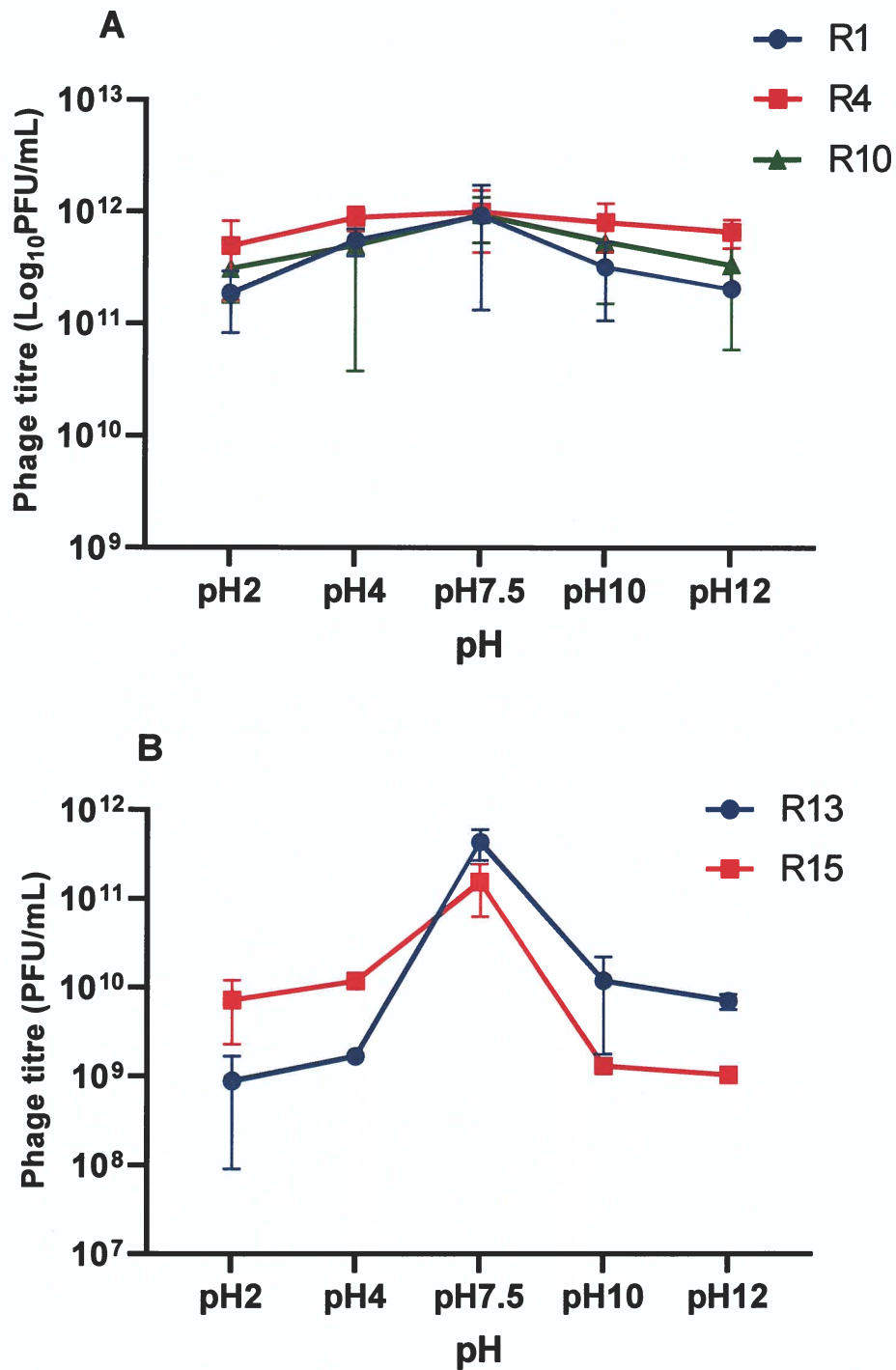


Figure 3.15. pH stability of (A) ssDNA and (B) ssRNA phages.

The phage titres (PFU/mL) were determined after exposure to several pH for 60 min. An F⁺ *E. coli* J62 p*Flac*::Tn3 strain served as the host bacterial strain for phage propagation. Values represent the mean of three independent experiments (n=3) ± standard deviation (SD).

3.2.12 Detergent stability

It was shown that the present of detergents such as SDS, in the environment can affect phage stability. The SDS was chosen because it is a common surfactant in most cleaning products and has been reported to be present in environment (Scanlan et al., 2017). The stability of the selected ssDNA and ssRNA phages to 0.10% and 0.50% SDS is shown in Figure 3.16. The ssDNA phages are more stable than ssRNA phages at both concentrations. All ssDNA phages maintained a high titre level of 10^{11} CFU/mL at both SDS concentrations after being exposed for 60 min. Both ssRNA phages showed decreased in titre after exposure to SDS, with R13 being less stable when compared to R15. A *ca* 3 and 4 log decrease in titre was demonstrated by R13 after exposure to 0.10% and 0.50% SDS, respectively. A *ca* 2 log decrease in titre was demonstrated by R15 after exposure to 0.10% and 0.50% SDS.

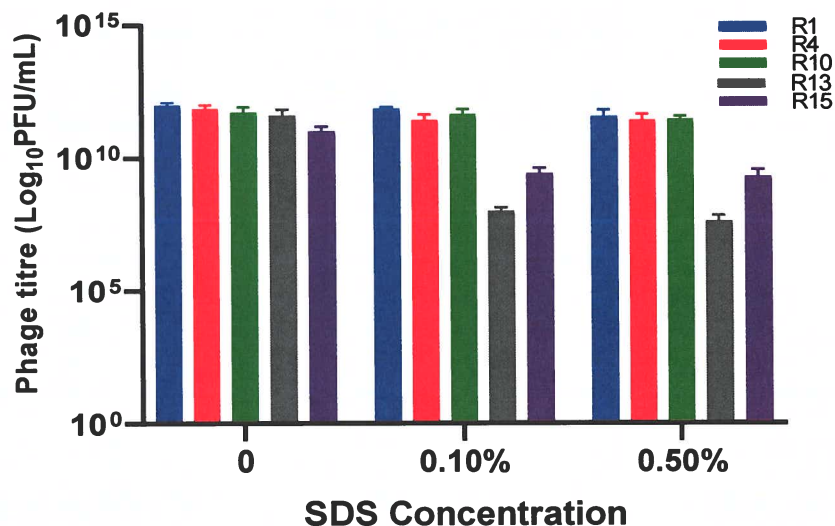


Figure 3.16. SDS stability of selected ssDNA and ssRNA phages.

The phage titres (PFU/mL) of representative isolated ssDNA (R1, R4, R10) and ssRNA (R13, R14) phages were determined after exposure to 0.1% and 0.5% SDS for 30 min. An F^+ *E. coli* J62 p*Flac*::Tn3 strain served as the host bacterial strain for phage propagation. Values represent the mean of three independent experiments ($n=3$) \pm standard deviation (SD).

Table 3.2. Summary of the characteristics of the isolated phages.

Phage ID	Plaque Morphology ^a	TEM Morphology ^b	RNAse sensitivity ^c	Chloroform sensitivity	Optimum temperature	Optimum pH	Detergent stability
Putative DNA Phage							
R1	T	F	R	-	20 to 37°C	7.5	+++
R2	T	F	R	-	20 to 37°C	7.5	+++
R4	T	F	R	-	20 to 37°C	7.5	+++
R6	T	F	R	-	20 to 37°C	7.5	+++
R7	T	F	R	-	20 to 37°C	7.5	++
R8	T	F	R	-	20 to 37°C	7.5	+++
R9	T	F	R	-	20 to 37°C	7.5	+++
R10	T	F	R	-	20 to 37°C	7.5	+++
R11	T	F	R	-	20 to 37°C	7.5	+++
R12	T	F	R	-	20 to 37°C	7.5	+++
Putative RNA Phage							
R5	C	I	S	-	20 to 37°C	7.5	++
R13	C	I	S	-	20 to 37°C	7.5	+
R14	C	I	S	-	20 to 37°C	7.5	+
R15	C	I	S	-	20 to 37°C	7.5	++

^aT=Turbid, C=Clear; ^bF=Filamentous, I=Icosahedral; ^cR=Resistant, S=Sensitive

3.3 Discussion

In this study, sex pilus specific (SPS) phages isolated from human sewage effluent can be divided into two groups. Group-I, which includes phages R1, R2, R3, R4, R6, R7, R8, R9, R10, R11 and R12, formed hazy plaques suggestive of either intermittent bacterial resistance or incomplete lysis during infection. Group-II, which includes R5, R13, R14 and R15, demonstrated clear plaques, suggestive of lytic infection. This group distinction was maintained when comparing RNAase sensitivity with the Group-II phages being sensitive to RNAase in media. This result is an indication that Group-II phages are RNA phages, as RNAase sensitivity was found to be a characteristic common to all ssRNA phages (Kannoly et al., 2012). The group-I isolates were long flexible filamentous phages under TEM. As such they resemble those belonging to Family *Inoviridae* similar to that of Ff filamentous phages (M13, fd and f1) (Rakonjac et al., 2017). Group-II phages appeared as icosahedral, non-tailed phages under electron microscope and resemble to those phages belonging to the family *Leviviridae* (Tars, 2020). This is the same family as the control phage used in this study and by Colom et al. (2019) in their studies on SPS phage.

The presumptive groupings based on similarity to previously described phages suggest we have ssDNA and ssRNA genomes. Further evidence of this come from the EtBr and Coomassie Blue staining. This staining can be a useful method in determining the phage genome composition (Plevka et al., 2009) and will help direct how further isolation for sequencing should proceed. Ethidium bromide is a DNA interchelator, inserting itself into the spaces between the base pairs of the double stranded helix, which strongly enhanced its staining of the double stranded structure of DNA. Staining of

single stranded DNA (ssDNA) or RNA is relatively insensitive, requiring some 10-fold more nucleic acid for equivalent detection. However, phages containing a single stranded RNA (ssRNA) genome such as those belonging to Family *Leviviridae* can be stained with EtBr because they contain numerous self-complementary sequences which form both double-helical "hairpins" or long-distance base pairing (Friedman et al., 2009, Tars, 2020). In other studies, most of the bases in ssRNA genomes (some 75%) form base-pairs, thus EtBr stains this group well (Fiers et al., 1976, Beekwilder et al., 1995). Therefore, based on the differences in staining, Group I are those phages that can only be stained with Coomassie Blue, while Group II are those that can be stained both by EtBr and Coomassie Blue stains. Based on these staining results, we were able to presumptively identify Group-I as having a single stranded DNA (ssDNA) genome and group II as having a single stranded RNA (ssRNA) genome. These findings also agree with the results of ribonuclease sensitivity.

To further verify these results and to assess similarity of these phages, their structural protein profile was assessed by SDS-PAGE. The structural proteins of the ssDNA filamentous phages (Group-1) consist of the major coat protein (CP), pVIII and minor coat proteins pIII, pVI, pVII, and pIX. The phage coat protein is composed of about 2,800 copies of the major coat protein, pVIII, for every five copies of the minor coat proteins, pIII/pVI and pVII/pIX (Russel et al., 2004, Mai-Prochnow et al., 2015). Therefore, a prominent band of major CP, pVIII was clearly visible on the SDS gel whereas the other minor structural proteins such as pIII appeared fainter. The major coat protein, pVIII is a small protein with a molecular weight of around 5.2 kDa. As this protein is smaller than the lower limit of the SDS

gel, the protein has the tendency to congregate at the base of the gel, hence the “smudge” appearance of the CP. The other structural proteins, such as pVII and pIX, are even smaller and similar in weight (~3.5 kDa), that they were difficult to visualise and separate on a 12% SDS gel. Therefore, low molecular weight 4-12% gradient SDS gel was used and was able to visualise these smaller proteins. As with the ssRNA phages isolates (Group II), the results of the SDS-PAGE analysis were useful as it was able to divide the isolates into two groups based on the structural protein profile. Phages R5, R13 and R15 appeared to be similar to *Levivirus* having shown similar sized coat protein (CP) and maturation protein (A), Phage R13 on the hand demonstrated a slightly bigger CP and a *ca* 48 kDa maturation protein (A2); and an extra *ca* 36 kDa minor coat protein (A1), which is a characteristic of the Family *Allolevivirus* (Singleton et al., 2018). Our results showed that analysis of structural protein profiles by SDS-PAGE of these SPS phages is of benefit in further differentiating them.

Based on the presumptive categorisation from the protein profiles, results of chloroform sensitivity were as expected with resistance reflecting a lack of envelope. This was also observed for the ssDNA phages and although, they have been described as chloroform sensitive, chloroform-resistant isolates of fd and M13 have also been reported (Oh et al., 1999). All reported SPS ssRNA phages are chloroform resistant (Kannoly et al., 2012). The effects of various external physical and chemical factors on phage survival were investigated. Factors, such as temperature, pH, and detergent stability can determine the robustness of phages under different physical and chemical environment. Our results showed that group-I representative ssDNA phages were stable even at higher temperature and

across a wide range of pH. However, no variation between isolates was observed. Our results are consistent with previous findings for ssDNA M13 phage, where optimal temperature and pH were reported to be at 37°C and pH 6 to 9, respectively. They were also able to survive at pH 2 for 1 h (Jończyk et al., 2011). Results from this study also showed that significant decrease in phage titre only starts at 86°C for 60 min. The group-II representative ssRNA phages are less stable at higher temperature and not as stable to wide pH ranges as compared to ssDNA phages. The optimum stability was observed between room temperature (ca. 20°C) and 37°C; and a significant decrease in phage titre started at 75°C for 30 min exposure. In terms of pH stability, differences were observed between the two representative ssRNA phages. The phage R13 which was presumptively identified as *Allolevivirus* were more stable at a higher pH. In contrast, phage R15 presumptively identified as *Levivirus* were more stable at a lower pH. These results agreed with previous report, where MS2 (*Levivirus*) survived better in acidic environment while Q β (*Allolevivirus*) showed a better survival rate under alkaline condition (Feng et al., 2003). It has also been reported that the inactivation rates of both genera increase when the pH was decreased to below 6 or increased to above 8 coupled with increasing temperature (Feng et al., 2003). We also investigated how exposure to compounds present in the environment can alter phage stability by affecting its replication. Sodium dodecyl sulphate (SDS) was chosen because it is a common surfactant in cleaning and hygiene products and is present in the environment. A previous study by Scanlan et al. (2017) demonstrated that exposure to SDS has a detrimental effect on the stability of phages. Our results showed that exposure to 0.10% and 0.50% SDS did

not affect the stability of the ssDNA phages but has some effects on the stability of the ssRNA phages.

In this chapter we were able to characterise and presumptively identify our phage isolates based on its morphological and biochemical characteristics. We were also able to investigate the effect of external physical and chemical factors on phage survivability. It was suggested that there are possible relationships between a phage's morphology and its survival abilities. For instance, a relationship between TSP4 phage's thermal stability and the presence of an extremely long and flexible tail (785 nm in length and 10 nm in width) was suggested (Lin et al., 2010). Lasobras et al. (1997) suggested there may be some relationships between phage structure and their survivability. It was suggested that phages with *Siphoviridae* morphology are the most resistant to adverse conditions (Lasobras et al., 1997). More in depth characterisations based on genomic analysis using next generation sequencing will be carried out in the next chapter.

Chapter 4. Genomic and Phylogenetic Analysis

4.1 Introduction

The advancements in next generation sequencing methods and the increasing availability of whole genome phage sequences have led to an increase in the use of phylogenetics to classify both culturable and uncultured phages given the (Callanan and Stockdale, 2020, Dion et al., 2020, Cook et al., 2021). Among the phages reported, the ssDNA and ssRNA phages may well be under reported because much of the approaches are focused mainly towards tailed dsDNA phages. The physical characterisations of isolates suggest that ssDNA filamentous (*Inoviridae*) and ssRNA icosahedral (*Leviviridae*) phages were isolated. Sequence analysis of these phages will be useful to support studies on host range and infection. The main objective for this chapter is to determine and analyse the whole genome sequences of the 15 isolated SPS phages and to determine their similarity to previously reported phages.

4.2 Results

4.2.1 ssDNA phage

4.2.1.1 *Species identification and comparison to reference strains*

The phages R1, R2, R3, R4, R6, R7, R8, R9, R10, R11 and R12 were assigned to the family *Inoviridae* and genus *Inovirus* using Kraken v2. Further characterisations were performed using Geneious Prime 2021.1.1 software package (<https://www.geneious.com>). The genome sizes of these 11 phages ranged from 6,407 to 6,411 nucleotides long and were consistent with the circular ssDNA *Inoviridae* genome (Table 4.1). The full-length

A phylogenetic tree was constructed using Tamura-Nei evolution model and Neighbour-Joining (NJ) algorithm and tested using the bootstrap method with 100 replicates (Figure 4.1). Nine of the isolated phages and the three reference Ff phage genomes clustered together and can be further sub divided into two clusters. The first cluster which comprises R1, R2, R6, R8, R9, R11 and R12 are clustered with M13 and f1 with > 98% similarity at the nucleotide level. Among them, R8 and R9, are 100% similar to each other. Cluster 2, which includes R3 and R10 are more closely related to fd, with a similarity of > 98% at the nucleotide level. R3 and R10 are 98.5% similar to each other. R4 and R7 which are 98.8% similar to each other comprises cluster 3, which has a similarity of only 92-93% to either M13, f1 and fd. As both phage genomes are different by more than 5% from any of the Ff reference strains, they can be considered as new species of *Escherichia virus M13* based on species definition set by the BAVS-ICTV (Adriaenssens and Brister, 2017). The phylogenetic analysis also confirmed that all 11 isolates are different from other filamentous phages including *Pseudomonas* phage Pf3 and *Vibrio* phage fs2, with 30% and 37% similarity at the nucleotide level, respectively.

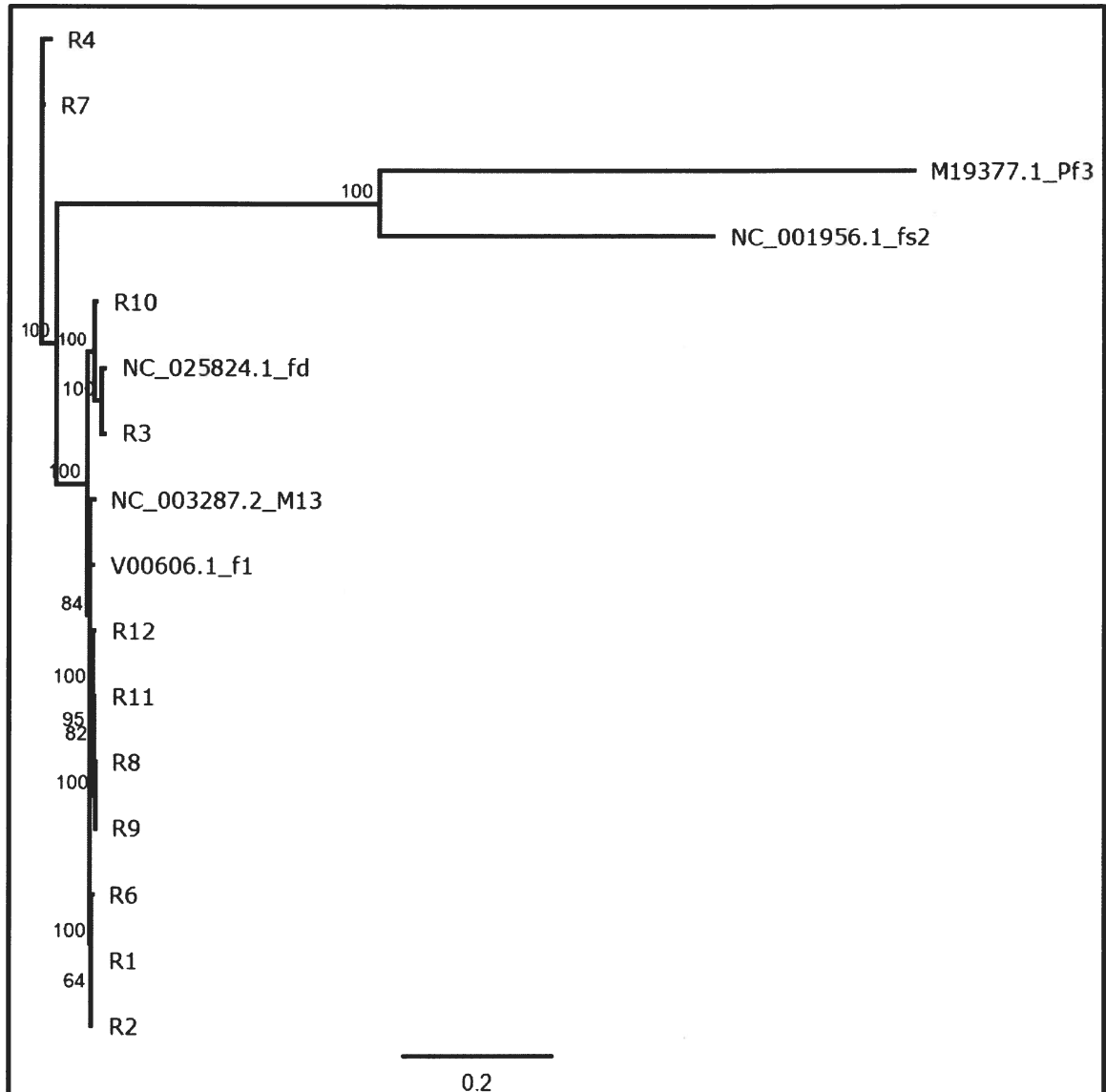


Figure 4.1. Phylogeny of ssDNA phage genome.

The phylogenetic analysis was based on whole genome sequences. The tree was constructed by Tamura-Nei evolution model with Neighbour-Joining (NJ) algorithm and tested using the bootstrap method with 100 replicates. The bootstrap values are expressed as percentages next to the nodes. Genome sequences were aligned using Clustal Omega and the phylogenetic tree was constructed in Geneious 2021.1.1 program. Enterobacteria phages M13, fd and f1; Pseudomonas phage Pf3; and Vibrio phage fs2 were included as reference strains.

4.2.1.2 Genome structure and organisation

The sequences of the isolates were compared to the model sequence, M13 and then individual reading frames were confirmed and annotated to create genetic maps of the phages (Figure 4.2 to Figure 4.7, Appendix B). All phages were shown to have a circular single-stranded DNA coding for about 10 genes with similar canonical *Inoviridae* genome organisation

following each other in the 5'-3' direction. Each individual gene was also compared against the genes of the M13 reference strain, and the percent similarity was determined. Results showed that except for the length of gVIII of R1 and R2, the length of the remaining nine genes of all the phages in cluster 1 were similar to M13 reference strain. All the 10 genes were highly similar (>97%) to the genes of reference strain. Genes gX, gVII and gIX were highly conserved for all the isolated phages with 100% similarity to M13 reference phage. The annotated genetic map of representative phages in cluster 1, including the location and percentage similarity of each gene to M13 reference strain are shown below (Figure 4.2 and Figure 4.3). R1 represents the genetic map of those phages with a genome similarity of $\geq 99\%$ (R1, R2, R6), while R8 represents those phages with a genome similarity of $\geq 98\%$ (R8, R9, R11, R12). From 5'-3' direction the 10 genes are arranged as follows: gII, gX, gV, gVII, gIX, gVIII, gIII, gVI, gI, and gIV.

Table 4.4. Phage gene length and percent similarity to M13.

Gene*	Individual gene length (nt) and percent (%) similarity to NC_003287.2 M13																		
	M13	R1	%	R2	%	R3	%	R6	%	R8	%	R9	%	R10	%	R11	%	R12	%
R																			
gII	1233	1233	99.84	1233	99.84	1233	97.32	1233	99.84	1233	99.92	1233	99.92	1233	97.24	1233	99.92	1233	99.92
gX	336	336	100	336	100	336	96.43	336	100	336	100	336	100	336	96.73	336	100	336	100
gV	264	264	98.11	264	98.11	264	95.45	264	98.11	264	98.11	264	98.11	264	96.59	264	98.11	264	98.11
S																			
gVII	102	102	100	102	100	102	100	102	100	102	100	102	100	102	100	102	100	102	100
gIX	99	99	100	99	100	99	100	99	100	99	100	99	100	99	100	99	100	99	100
gVIII	222	225	97.78	225	97.78	222	98.20	222	99.10	222	99.55	222	99.55	222	98.65	222	99.55	222	98.65
gIII	1275	1275	99.22	1275	99.22	1275	98.12	1275	99.22	1275	96.86	1275	96.86	1275	98.43	1275	97.57	1275	96.94
gVI	339	339	99.71	339	99.71	339	98.82	339	99.71	339	99.41	339	99.41	339	99.12	339	99.41	339	99.41
A-S																			
gI	1047	1047	99.43	1047	99.43	1047	97.13	1047	99.43	1047	99.52	1047	99.52	1047	98.19	1047	99.52	1047	99.62
gIV	1281	1281	97.50	1281	97.50	1281	94.93	1281	97.50	1281	97.35	1281	97.35	1281	97.74	1281	97.35	1281	97.66

* The genes are listed in groups which is based on functions: replication (R), structural (S), and assembly-secretion (A-S) modules.

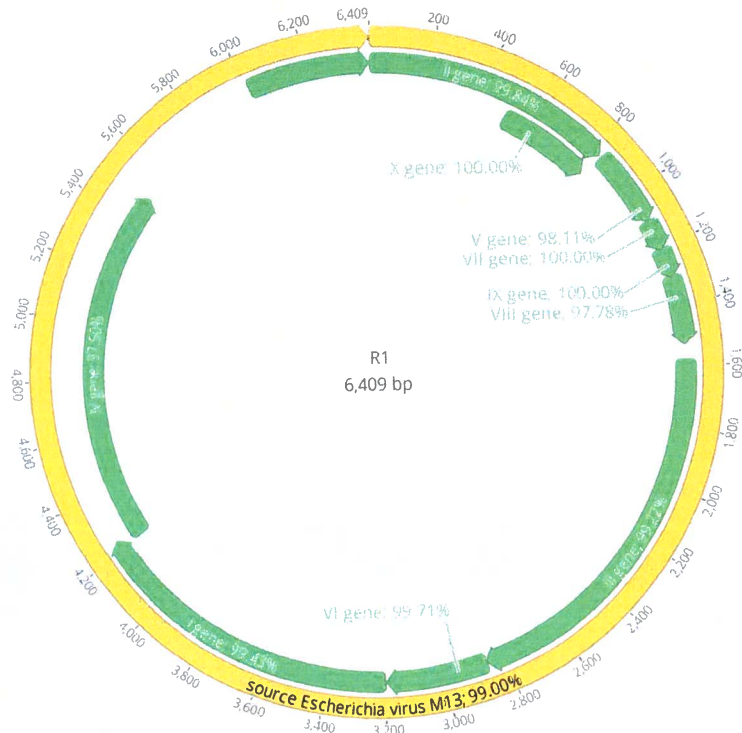


Figure 4.2. Genome organisation of phage R1.
The location of phage genes and % similarity to M13 are indicated.

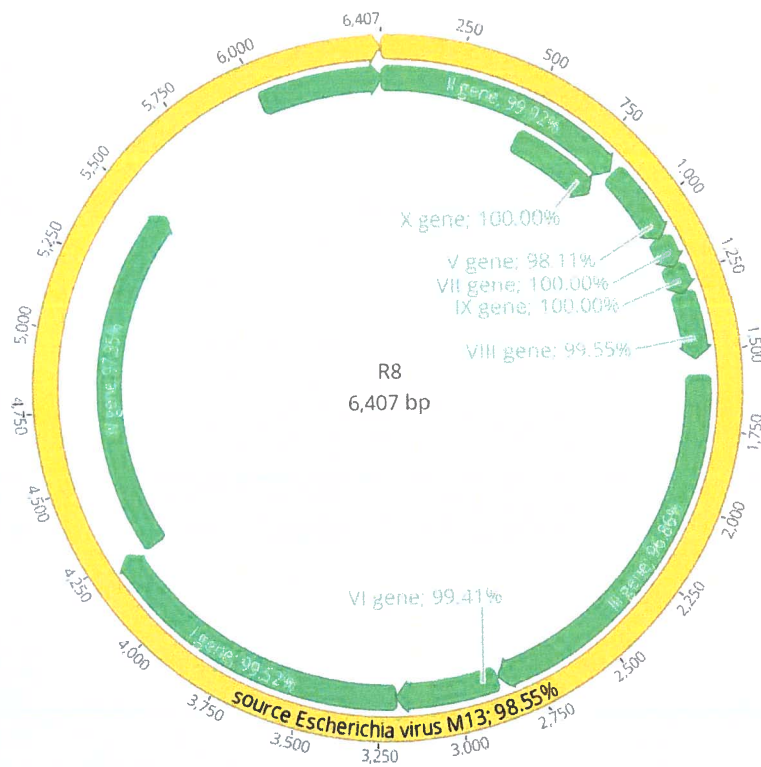


Figure 4.3. Genome organisation of phage R8.
The location of phage genes and % similarity to M13 are indicated.

Phages R3 and R10, which are in cluster 2 also have 10 genes. The genes have the same length and are highly similar (>98%) at the nucleotide level, apart from gIV gene of R10 (94.61%) when compared with the fd reference strain (Table 4.5). Among the ten genes, gVII and gIX were highly conserved with 100% similarity. Figure 4.4 and Figure 4.5 show the annotated genetic map of R3 and R10, respectively, including gene location and percentage similarity with the reference strain. The genes are also organised following the canonical genome organisation of most Ff phages. As seen in the genetic map, the order of the genes are as follows: gII, gX, gV, gVII, gIX, gVIII, gIII, gVI, gI, and gIV in the 5'-3' direction.

Table 4.5. Phage gene length and percent similarity to fd.
Phage individual gene length (nt) and percent (%) similarity to NC_025824.1 fd

Gene	fd	R3	%	R10	%
R					
gII	1233	1233	99.51	1233	99.68
gX	336	336	99.40	336	99.70
gV	264	264	98.48	264	99.62
S					
gVII	102	102	100	102	100
gIX	99	99	100	99	100
gVIII	222	222	99.10	222	99.55
gIII	1275	1275	98.82	1275	99.76
gVI	339	339	100	339	99.71
A-S					
gI	1047	1047	99.81	1047	98.95
gIV	1281	1281	98.13	1281	94.61

* The genes are listed in groups which is based on functions: replication (R), structural (S) and assembly/ secretion (A-S) modules.

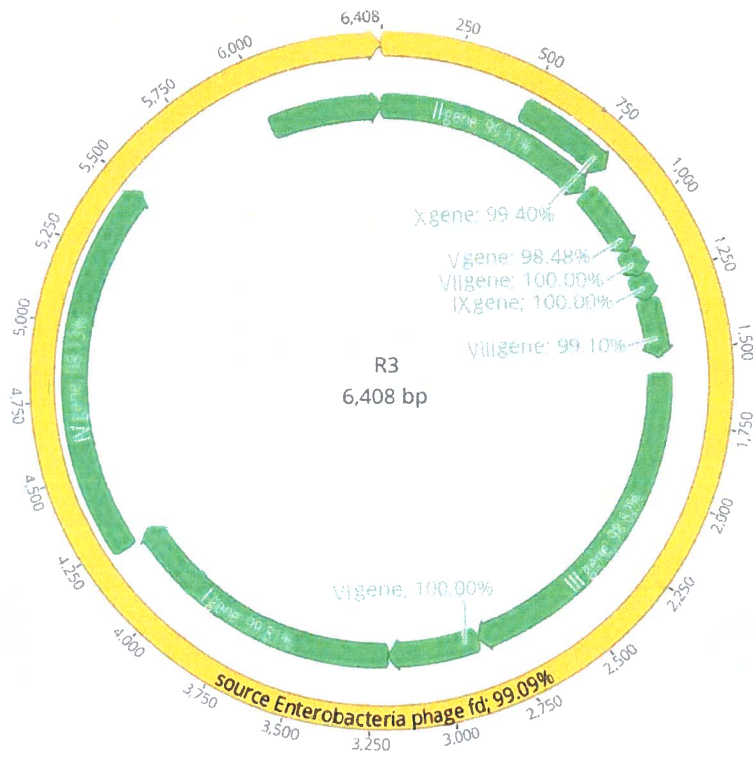


Figure 4.4. Genome organisation of phage R3.
The location of phage genes and % similarity to fd are indicated.

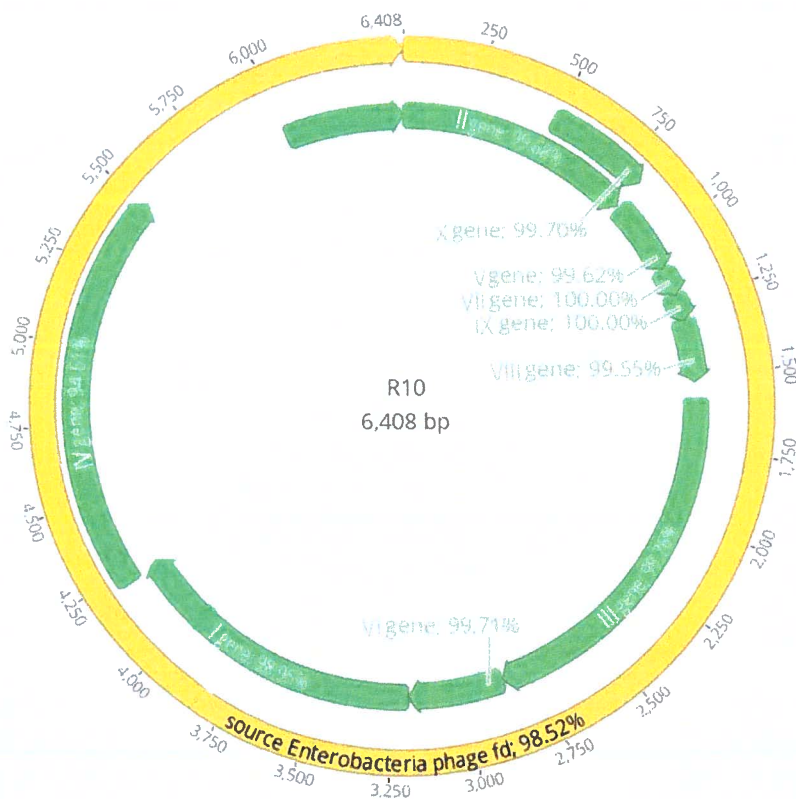


Figure 4.5. Genome organisation of phage R10.
The location of phage genes and % similarity to fd are indicated.

Each gene of phage R4 and R7, with their full-length genome sequences similarity of <95% to either M13, f1 or fd, were compared against the genes of the M13 reference strain. The results showed that except for gene gIII of both R4 and R7, the length of the remaining nine genes are all the same size as the M13 reference strain. However, there is no single gene that is 100% identical to its counterpart gene in M13 reference strain. Genes gVIII, gIII, gVI, gI and gIV have a similarity between 88% and 94%. Figure 4.6 and Figure 4.7 show the annotated genetic map of R4 and R7, including the location and percentage similarity of each gene to M13 reference strain. Similar to other isolated phages, the 10 genes of R4 and R7 are also organised following the canonical genome organisation of most Ff phages. The genome organisation starts with the replication (R) module containing genes gII, gX and gV. This is followed by five genes: gVII, gIX, gVIII, gIII, gVI, which comprise the structural (S) module, and lastly by gI, gIV of the assembly and secretion (A-S) module. All of these genes follow the 5'-3' direction.

Table 4.6. Novel phage gene length and percent similarity to M13.

Gene*	Phage individual gene length (nt) and percent (%) similarity to NC_003287.2 M13				
	M13	R4	%	R7	%
R					
gII	1233	1233	97.97	1233	98.05
gX	336	336	93.75	336	93.75
gV	264	264	93.18	264	92.80
S					
gVII	102	102	97.06	102	97.06
gIX	99	99	96.97	99	96.97
gVIII	222	222	94.59	222	94.59
gIII	1275	1278	89.20	1278	89.28
gVI	339	339	89.38	339	89.38
A-S					
gI	1047	1047	91.40	1047	91.21
gIV	1281	1281	88.13	1281	92.12

*The genes are listed in groups which is based on functions: replication (R), structural (S) and assembly/ secretion (A-S) modules.

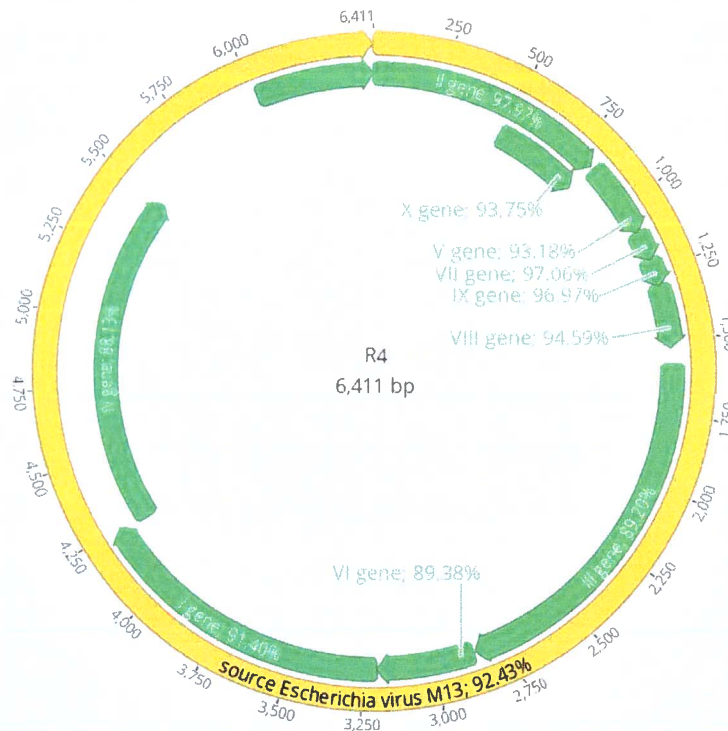


Figure 4.6. Genome organisation of phage R4.
The location of phage genes and % similarity to M13 are indicated.

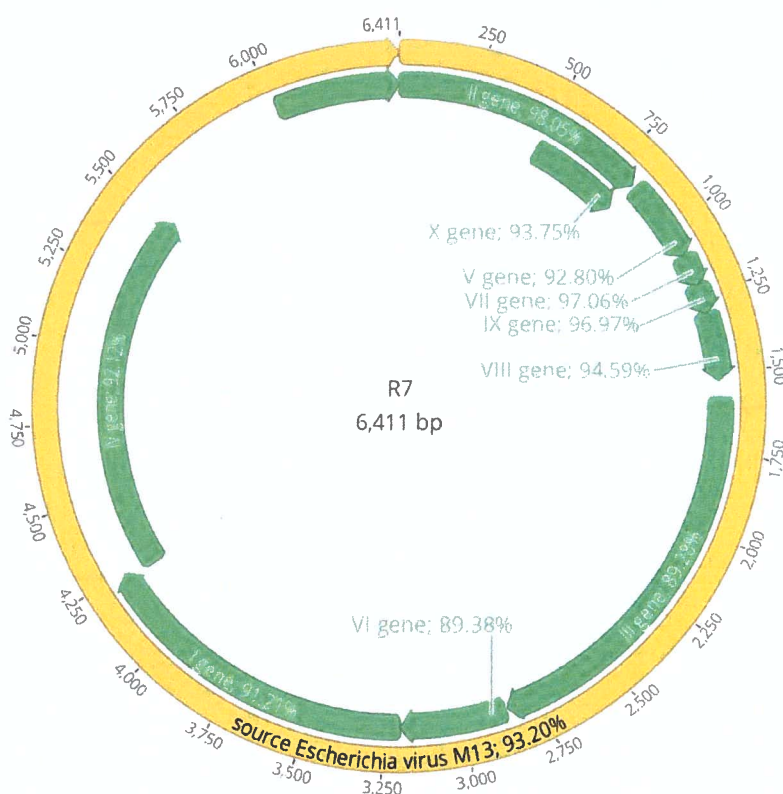


Figure 4.7. Genome organisation of phage R7.
The location of phage genes and % similarity to M13 are indicated.

4.2.1.3 Amino Acid and Protein Analysis

Individual genes were translated into proteins and deduced amino acid sequences corresponding to each gene were analysed. Because of its vital role in the initiation of infection of host cells, further analysis of the attachment pIII protein was performed. The resulting amino acid sequence of pIII was analysed, and corresponding phylogenetic tree was generated (Figure 4.8). The resulting phylogeny showed that phages R1, R2, R6, R8, R9, R11, R12, R3 and R10 clustered together with M13 and fd. It also demonstrated that R4 and R7 clustered separately from the rest of the isolated phages and Ff reference strains.

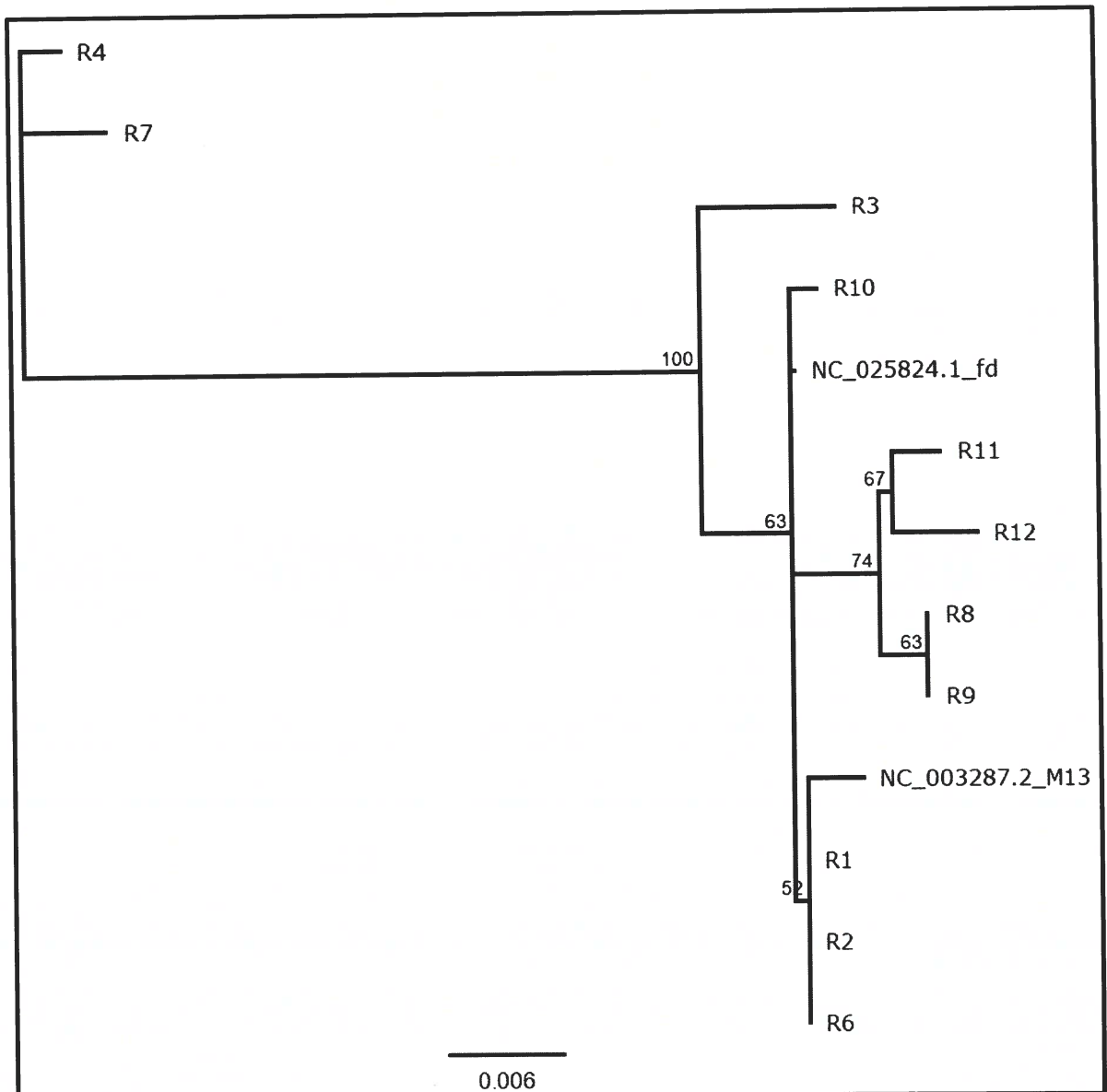


Figure 4.8. Phylogeny of ssDNA phage protein pIII.

The phylogenetic analysis was based on the amino acid sequences of the pIII protein. The tree was constructed by Jukes-Cantor evolution model with Neighbour-Joining (NJ) algorithm and tested using the bootstrap method with 100 replicates. The bootstrap values are expressed as percentages next to the nodes. Amino acid sequences were aligned using Clustal Omega and tree was constructed in Geneious Prime 2021.1.1. program. Enterobacteria phages M13 and fd served as reference strains.

In addition to the phylogenetic analysis of the full genomes, further analysis was carried to assess variation of the attachment protein, pIII using Clustal Omega. When compared to M13, there were only a total of seven amino acid replacements observed in R1, R2, R6, R8, R9, R11 and R12. These include five replacements in R12, with 98.82% similarity, and four each in R8, R9 and R11 accounting to 99.05% similarity. R1, R2 and R6 pIII are 99.76% similar to M13, with only one replacement at amino acid number 378 (Figure 4.9).

NC_003287.2_M13	VVCTGDETQCYGTWVPIGLAIPENEGGGSEGGGSEGGGSEGGGTRPPEYGDTPIPGYTY	120
R1	VVCTGDETQCYGTWVPIGLAIPENEGGGSEGGGSEGGGSEGGGTRPPEYGDTPIPGYTY	120
R2	VVCTGDETQCYGTWVPIGLAIPENEGGGSEGGGSEGGGSEGGGTRPPEYGDTPIPGYTY	120
R6	VVCTGDETQCYGTWVPIGLAIPENEGGGSEGGGSEGGGSEGGGTRPPEYGDTPIPGYTY	120
R8	VVCTGDETQCYGTWVPIGLAIPENEGGGSEGGGSEGGGSEGGGTRPPEYGDTPIPGYTY	120
R9	VVCTGDETQCYGTWVPIGLAIPENEGGGSEGGGSEGGGSEGGGTRPPEYGDTPIPGYTY	120
R11	VVCTGDETQCYGTWVPIGLAIPENEGGGSEGGGSEGGGSEGGGTRPPEYGDTPIPGYTY	120
R12	VVCTGDETQCYGTWVPIGLAIPENEGGGSEGGGSEGGGSEGGGTRPPEYGDTPIPGYTY	120
NC_025824.1_fd	VVCTGDETQCYGTWVPIGLAIPENEGGGSEGGGSEGGGSEGGGTRPPEYGDTPIPGYTY	120
NC_003287.2_M13	INPLDGTYPGTEQNPNANPNPSLEESQPLNTFMPQNNRFRNRQOGALTYVTGTVTQGTDPV	180
R1	INPLDGTYPGTEQNPNANPNPSLEESQPLNTFMPQNNRFRNRQOGALTYVTGTVTQGTDPV	180
R2	INPLDGTYPGTEQNPNANPNPSLEESQPLNTFMPQNNRFRNRQOGALTYVTGTVTQGTDPV	180
R6	INPLDGTYPGTEQNPNANPNPSLEESQPLNTFMPQNNRFRNRQOGALTYVTGTVTQGTDPV	180
R8	INPLDGTYPGTEQNPNANPNPSLEESQPLNTFMPQNNRFRNRQOGALTYVTGTVTQGTDPV	180
R9	INPLDGTYPGTEQNPNANPNPSLEESQPLNTFMPQNNRFRNRQOGALTYVTGTVTQGTDPV	180
R11	INPLDGTYPGTEQNPNANPNPSLEESQPLNTFMPQNNRFRNRQOGALTYVTGTVTQGTDPV	180
R12	INPLDGTYPGTEQNPNANPNPSLEESQPLNTFMPQNNRFRNRQOGALTYVTGTVTQGTDPV	180
NC_025824.1_fd	INPLDGTYPGTEQNPNANPNPSLEESQPLNTFMPQNNRFRNRQOGALTYVTGTVTQGTDPV	180
NC_003287.2_M13	KTYYYQYTPVSSKAMYDAYWNGKFRDCAFHSGFNEDPFVCEYQGQSSDLPOPPVNAAGGSG	240
R1	KTYYYQYTPVSSKAMYDAYWNGKFRDCAFHSGFNEDPFVCEYQGQSSDLPOPPVNAAGGSG	240
R2	KTYYYQYTPVSSKAMYDAYWNGKFRDCAFHSGFNEDPFVCEYQGQSSDLPOPPVNAAGGSG	240
R6	KTYYYQYTPVSSKAMYDAYWNGKFRDCAFHSGFNEDPFVCEYQGQSSDLPOPPVNAAGGSG	240
R8	KTYYYQYTPVSSKAMYDAYWNGKFRDCAFHSGFNEDPFVCEYQGQSSDLPOPPVNAAGGSG	240
R9	KTYYYQYTPVSSKAMYDAYWNGKFRDCAFHSGFNEDPFVCEYQGQSSDLPOPPVNAAGGSG	240
R11	KTYYYQYTPVSSKAMYDAYWNGKFRDCAFHSGFNEDPFVCEYQGQSSDLPOPPVNAAGGSG	240
R12	KTYYYQYTPVSSKAMYDAYWNGKFRDCAFHSGFNEDPFVCEYQGQSSDLPOPPVNAAGGSG	240
NC_025824.1_fd	KTYYYQYTPVSSKAMYDAYWNGKFRDCAFHSGFNEDPFVCEYQGQSSDLPOPPVNAAGGSG	240
NC_003287.2_M13	RQYLPSLPQSVECRPFVFCAGKPYEFSIDCDKINLFRGVFAFLLYVATFMYVSTFANIL	419
R1	RQYLPSLPQSVECRPFVFCAGKPYEFSIDCDKINLFRGVFAFLLYVATFMYVSTFANIL	419
R2	RQYLPSLPQSVECRPFVFCAGKPYEFSIDCDKINLFRGVFAFLLYVATFMYVSTFANIL	419
R6	RQYLPSLPQSVECRPFVFCAGKPYEFSIDCDKINLFRGVFAFLLYVATFMYVSTFANIL	419
R8	RQYLPSLPQSVECRPFVFCAGKPYEFSIDCDKINLFRGVFAFLLYVATFMYVSTFANIL	419
R9	RQYLPSLPQSVECRPFVFCAGKPYEFSIDCDKINLFRGVFAFLLYVATFMYVSTFANIL	419
R11	RQYLPSLPQSVECRPFVFCAGKPYEFSIDCDKINLFRGVFAFLLYVATFMYVSTFANIL	419
R12	RQYLPSLPQSVECRPFVFCAGKPYEFSIDCDKINLFRGVFAFLLYVATFMYVSTFANIL	419
NC_025824.1_fd	RQYLPSLPQSVECRPFVFCAGKPYEFSIDCDKINLFRGVFAFLLYVATFMYVSTFANIL	419

Figure 4.9. Alignment of attachment protein (pIII) against M13.

The translated amino acid sequence is compared to Enterobacteria phage NC_003287.2 M13. The location of amino acid mutation is shaded in grey. Enterobacteria NC_025824.1 fd reference sequence was also included.

Four amino acid replacements at position 42, 67, 233 and 411 were detected when pIII protein of R3 was compared to fd, giving a 99.05% similarity. In the case of R10, only one amino acid replacement at position 144 was detected, giving a 99.76% similarity. R3 has six amino acid replacements at positions 42, 67, 233, 375, 378 and 411, while R10 has three at amino acid positions 144, 375 and 378 (Figure 4.10). For phages R4 and R7, there were a total of 39 amino acid replacements in pIII when compared to M13. R4 has 19 amino acid replacements, with 95.51% similarity while R7 has 20 replacements accounting for 95.28% similarity (Figure 4.11).

NC_025824.1_fd	MKKLLFAIPLVVPFYSHSAETVESCLAKPHTENSFTNVWKDDKTLDRYANYEGCLWNATG	60
R3	MKKLLFAIPLVVPFYSHSAETVESCLAKPHTENSFTNVWKDEKTLDRYANYEGCLWNATG	60
R10	MKKLLFAIPLVVPFYSHSAETVESCLAKPHTENSFTNVWKDDKTLDRYANYEGCLWNATG	60
NC_003287.2_M13	MKKLLFAIPLVVPFYSHSAETVESCLAKPHTENSFTNVWKDDKTLDRYANYEGCLWNATG	60
NC_025824.1_fd	VVVCTGDETQCYGTWVPIGLAIPENEGGGSEGGGSEGGGSEGGGTPPEYGDTPIPGYTY	120
R3	VVVCTGDETQCYGTWVPIGLAIPENEGGGSEGGGSEGGGSEGGGTPPEYGDTPIPGYTY	120
R10	VVVCTGDETQCYGTWVPIGLAIPENEGGGSEGGGSEGGGSEGGGTPPEYGDTPIPGYTY	120
NC_003287.2_M13	VVVCTGDETQCYGTWVPIGLAIPENEGGGSEGGGSEGGGSEGGGTPPEYGDTPIPGYTY	120
NC_025824.1_fd	INPLDGYPPGTEQNPNPNPSLEESQPLNTFMFQNNRFRNRQALTVYTGTVTQGTDPV	180
R3	INPLDGYPPGTEQNPNPNPSLEESQPLNTFMFQNNRFRNRQALTVYTGTVTQGTDPV	180
R10	INPLDGYPPGTEQNPNPNPSLEESQPLNTFMFQNNRFRNRQALTVYTGTVTQGTDPV	180
NC_003287.2_M13	INPLDGYPPGTEQNPNPNPSLEESQPLNTFMFQNNRFRNRQALTVYTGTVTQGTDPV	180
NC_025824.1_fd	KTYIQYTPVSSKAMYDAYWNGKFRDCAFHSGFNEDPFVCEYQGQSSDLPQPPVNAGGGSG	240
R3	KTYIQYTPVSSKAMYDAYWNGKFRDCAFHSGFNEDPFVCEYQGQSSDLPQPPVNAGGGSG	240
R10	KTYIQYTPVSSKAMYDAYWNGKFRDCAFHSGFNEDPFVCEYQGQSSDLPQPPVNAGGGSG	240
NC_003287.2_M13	KTYIQYTPVSSKAMYDAYWNGKFRDCAFHSGFNEDPFVCEYQGQSSDLPQPPVNAGGGSG	240
NC_025824.1_fd	GGG-GGGSEGGGSEGGGSEGGGSEGGGSGGGSGGDFDYEKMANANKGAMTENADENALQ	299
R3	GGG-GGGSEGGGSEGGGSEGGGSEGGGSGGGSGGDFDYEKMANANKGAMTENADENALQ	299
R10	GGG-GGGSEGGGSEGGGSEGGGSEGGGSGGGSGGDFDYEKMANANKGAMTENADENALQ	299
NC_003287.2_M13	GGG-GGGSEGGGSEGGGSEGGGSEGGGSGGGSGGDFDYEKMANANKGAMTENADENALQ	299
NC_025824.1_fd	SDAKGKLDVATDYGAAIDGFIGDVSLANGNGATGDFAGSNSQMAQVGDGDN SPLMNNF	359
R3	SDAKGKLDVATDYGAAIDGFIGDVSLANGNGATGDFAGSNSQMAQVGDGDN SPLMNNF	359
R10	SDAKGKLDVATDYGAAIDGFIGDVSLANGNGATGDFAGSNSQMAQVGDGDN SPLMNNF	359
NC_003287.2_M13	SDAKGKLDVATDYGAAIDGFIGDVSLANGNGATGDFAGSNSQMAQVGDGDN SPLMNNF	359
NC_025824.1_fd	RQYLPSLPQSVECRPYVFGAGKPYEFSIDCDKINLFRGVFAFLLYVATFMYVVFSTFANIL	419
R3	RQYLPSLPQSVECRPYVFGAGKPYEFSIDCDKINLFRGVFAFLLYVATFMYVVFSTFANIL	419
R10	RQYLPSLPQSVECRPYVFGAGKPYEFSIDCDKINLFRGVFAFLLYVATFMYVVFSTFANIL	419
NC_003287.2_M13	RQYLPSLPQSVECRPYVFGAGKPYEFSIDCDKINLFRGVFAFLLYVATFMYVVFSTFANIL	419
NC_025824.1_fd	RNKES	424
R3	RNKES	424
R10	RNKES	424
NC_003287.2_M13	RNKES	424

Figure 4.10. Alignment of attachment protein (pIII) against fd.

The translated amino acid sequence is compared to Enterobacteria phage NC_025824.1 fd. The location of amino acid mutation is shaded in grey. Enterobacteria phage NC_003287.2 M13 reference sequence was also included.

NC_003287.2_M13	MKKLLFAIPLVVPFYSHSAETVESCLAKPHTENSFTNVWKKDKTLDRYANYEGCLWNATG	60
R4	MKKLLFAIPLVIIPFYSHSAETVESCLAKPHTENSFTNVWKKDKTLDRYANYEGCLWNATG	60
R7	MKKLLFAIPLVIIPFYSHSAETVESCLAKPHTENSFTNVWKKDKTLDRYANYEGCLWNATG	60
NC_025824.1_fd	MKKLLFAIPLVVPFYSHSAETVESCLAKPHTENSFTNVWKKDKTLDRYANYEGCLWNATG	60
NC_003287.2_M13	VVVTGDETCQCYGTWVPIGLAIPENEGGGSEGGGSEGGGSEGGGTPPEYGDTPPIPGYTY	120
R4	VVVTGDETCQCYGTWVPIGVAIENEGGGSEGGGSEGGGSEGGGTPPEYGDTPPIPGYTY	120
R7	VVVTGDETCQCYGTWVPIGVAIENEGGGSEGGGSEGGGSEGGGTPPEYGDTPPIPGYTY	120
NC_025824.1_fd	VVVTGDETCQCYGTWVPIGLAIPENEGGGSEGGGSEGGGSEGGGTPPEYGDTPPIPGYTY	120
NC_003287.2_M13	INPLDGTYPGTEONPANPNPSLEESQPLNTFMFQNNRFRNRQGALTVYTGTVTQGTDPV	180
R4	INPLDGTYPGTEONPANPNPDLLESQPLNTFMFQNNRFRNRQGALTVYTGTVTQGTDPV	180
R7	INPLDGTYPGTEONPANPNPDLLESQPLNTFMFQNNRFRNRQGALTVYTGTVTQGTDPV	180
NC_025824.1_fd	INPLDGTYPGTEONPANPNPSLEESQPLNTFMFQNNRFRNRQGALTVYTGTVTQGTDPV	180
NC_003287.2_M13	KTTYQYTPVSSKAMYDAYWNGKFRDCAFHSGFNEDPFVCEYQGQSSDLQPPVFNAGGGSG	240
R4	KTTYQYTPVSSKAMYDAEWNGKFRDCAFHSGFNEDPFVCEYQGQSSDLQPPFINAGGGSG	240
R7	KTTYQYTPVSSKAMYDAEWNGKFRDCAFHSGFNEDPFVCEYQGQSSDLQPPFINAGGGSG	240
NC_025824.1_fd	KTTYQYTPVSSKAMYDAYWNGKFRDCAFHSGFNEDPFVCEYQGQSSDLQPPVFNAGGGSG	240
NC_003287.2_M13	GGGSGGGSEGGGSEGGGSEGGGSEGGGSGGGSGGDFDYKMANANKGAMTENADENALQ	299
R4	GGSGGGSEGGGSEGGGSEGGGSEGGGSGGGSGGDFDYKMANANKGAMTENADENALQ	300
R7	GGSGGGSEGGGSEGGGSEGGGSEGGGSGGGSGGDFDYKMANANKGAMTENADENALQ	300
NC_025824.1_fd	GGSGGGSEGGGSEGGGSEGGGSEGGGSGGGSGGDFDYKMANANKGAMTENADENALQ	299
NC_003287.2_M13	SDAKGLDSVATDYGAAIDGFIGDVSGLANGNGATGDFAGSNSQMAQVGDGDN SPLMNNF	359
R4	SDAKGLDSVANDYGVVADGFIGDVSGLANGNGATGDFAGSNSQMAQVGDGDN SPLMNNF	360
R7	SDAKGLDSVANDYGVVADGFIGDVSGLANGNGATGDFAGSNSQMAQVGDGDN SPLMNNF	360
NC_025824.1_fd	SDAKGLDSVATDYGAAIDGFIGDVSGLANGNGATGDFAGSNSQMAQVGDGDN SPLMNNF	359
NC_003287.2_M13	RQYLPSLPQSVECRPFVFCAGKPYEFSIDCDKINLFRGVFAFLLYVATFMYVFSTFANIL	419
R4	RQYLPSLPQSVECRPFVFCAGKPYEFSIDCDKINLFRGVFAFLLYVATFMYVFSTFANIL	420
R7	RQYLPSLPQSVECRPFVFCAGKPYEFSIDCDKINLFRGVFAFLLYVATFMYVFSTFANIL	420
NC_025824.1_fd	RQYLPSLPQSVECRPFVFCAGKPYEFSIDCDKINLFRGVFAFLLYVATFMYVFSTFANIL	419
NC_003287.2_M13	RNKES	424
R4	RNKES	425
R7	RNKES	425
NC_025824.1_fd	RNKES	424

Figure 4.11. Alignment of pIII of novel R4 & R7 phages against M13.

The translated amino acid sequence is compared to Enterobacteria phage NC_003287.2 M13. The location of amino acid mutation is shaded in grey. Enterobacteria NC_025824.1 fd reference sequence was also included.

4.2.2 ssRNA phage

4.2.2.1 Species identification and comparison to reference strains

The ssRNA phages aligned with the family *Leviviridae* and were split into two genera namely *Levivirus* (R5, R14, R15) and *Allolevivirus* (R13) using Kraken v2. The Geneious Prime 2021.1.1 software package (<https://www.geneious.com>) was used for more specific comparisons. The genome size ranges from 3,521 to 3,529 (R5, R14, R15) and 4, 220 (R13) at the nucleotide level and consistent with the linear ssRNA *Leviviridae* genome (Table 4.7).

Table 4.7. The ssRNA phages sequence characteristics.

Phage	Sequence length	% GC	Topology
R5	3521	52.1	linear
R13	4220	47.6	linear
R14	3569	52.1	linear
R15	3526	52.2	linear

The full-length phage genome sequences were annotated against reference Enterobacteria MS2 (Accession No.: NC_001417.2) and Q β (Accession No: AB971354.1) phage genomes. The species of each isolated phage was identified and similarity or difference to reference strains, MS2 and Q β , were determined (Table 4.8). A phylogenetic tree was constructed using Tamura-Nei evolution model and Neighbour-Joining (NJ) algorithm and tested using the bootstrap method with 100 replicates (Figure 4.12).

Aside from MS2 and Q β reference strains, other distantly related *Leviviridae* Enterobacteria phages NL95, Hgal1, KU1, GA, fr; *Pseudomonas* phage PP7, and *Acinetobacter* phage AP205 were included (Figure 4.12). Based on these analyses, it was shown that R5, R14, R15 are homologous to MS2 with > 97% similarity and are clustered together, while R13 is clustered with Q β with a 93.55% similarity, at the nucleotide level. The phylogenetic tree also demonstrated the low similarity of R5, R14 and R15 with other *Levivirus* Enterobacteria phages Hgal1 (39%), KU1 (49%), GA (50%), fr (76%); and unclassified *Leviviridae* phages *Acinetobacter* phage AP205 (31%) and *Pseudomonas* phage PP7 (34%). R13 has the closest similarity with Q β but is different to another *Allolevivirus* Enterobacteria phage NL95 (54%). However, R13 has a similarity of only 93.55% to Q β and may represent a new species of *Allolevivirus* based on the species definition set by BAVS-ICTV.

Table 4.8. ssRNA phages identified based on nucleotide similarity.

Strain*	% Nucleotide sequence similarity with the indicated strain			
	R5	R13	R14	R15
MS2	97.98	-	99.44	98.12
Q β	-	93.55	-	-

*Enterobacteria phages NC_001417.2 MS2 and AB971354.1 Q β serve as reference strains.

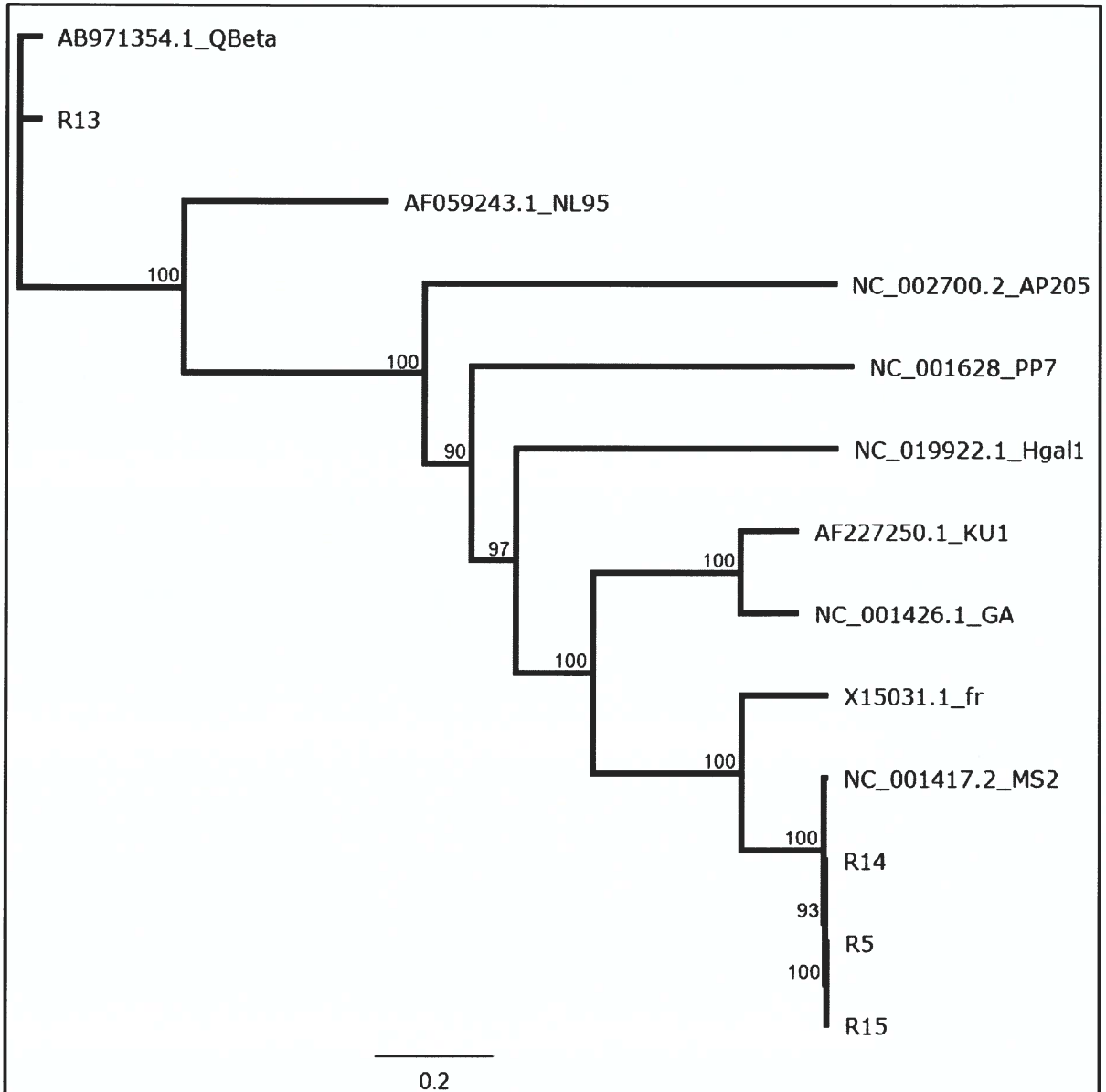


Figure 4.12. Phylogeny of ssRNA phage genome.

The phylogenetic analysis was based on whole genome sequences. The tree was constructed by Tamura-Nei evolution model with Neighbour-Joining (NJ) algorithm and tested using the bootstrap method with 100 replicates. The bootstrap values are expressed as percentages next to the nodes. Genome sequences were aligned using Clustal Omega and the phylogenetic tree was constructed in Geneious 2021.1.1 program. Enterobacteria phages MS2, Q β , NL95, Hgal1, KU1, GA, fr; *Pseudomonas* phage PP7, and *Acinetobacter* phage AP205 were included as reference strains.

4.2.2.2 Genome structure and organisation

The linear genome of phages R5, R14 and R15 follows a typical MS2 genome organisation with maturation, coat, lysis and replicase genes following each other in the 5'-3' direction (Figure 4.13). These four genes have the same length when compared to phage MS2, with each gene having a similarity of >99% (Table 4.9).

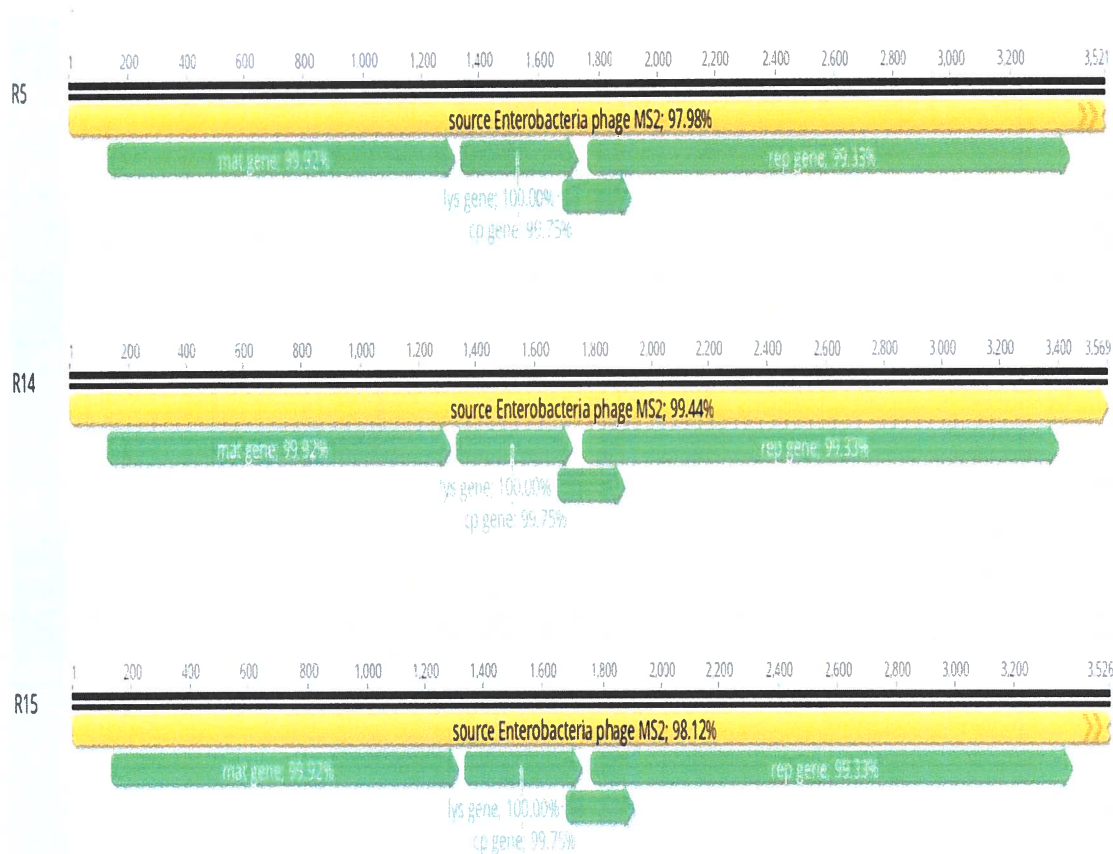


Figure 4.13. Genome organisation of phages R5, R14 and R15. The location of phage genes and % similarity to M13 are indicated.

Table 4.9. Individual gene length and percent similarity to MS2.

Gene	Individual gene length (nt) and percent (%) similarity to NC_001417.2_MS2						
	MS2	R5	%	R14	%	R15	%
maturation (<i>mat</i>)	1182	1182	99.92	1182	99.92	1182	99.92
coat protein (CP)	393	393	99.75	393	99.75	393	99.75
lysis (<i>lys</i>)	228	228	100	228	100	228	100
replicase (<i>rep</i>)	1638	1638	99.33	1638	99.33	1638	99.33

The linear genome of phage R13 follows the canonical Q β genome organisation with maturation protein (A2), coat protein (CP), minor CP (A1) – an extended read-through of the CP and replicase protein cistrons following each other in the 5'-3' direction (Figure 4.14). Except for minor CP (A1), the remaining three genes have the same length when compared to phage Q β . However, each gene has a similarity ranging from >91% to 96.27% (Table 4.10). Unlike R5, R14 and R15; R13 does not contain a separate lysis gene.

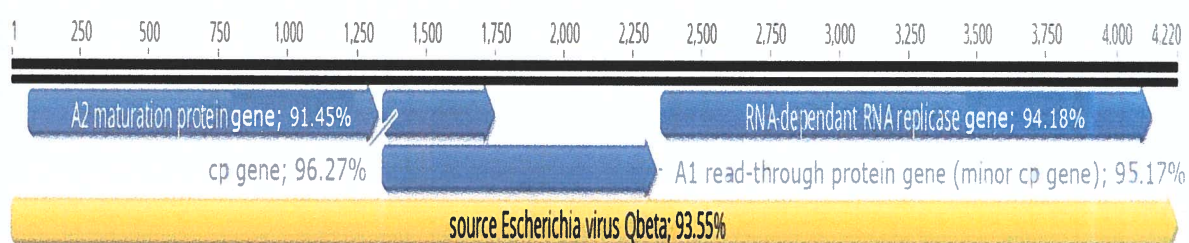


Figure 4.14. Genome organisation of phage R13.
The location of phage genes and % similarity to Q β are indicated.

Table 4.10. Individual gene length and percent similarity to Q β .

Gene	Q β	R13	%
maturation (A2)	1263	1263	91.45
coat protein (CP)	402	402	96.27
minor CP (A1)	990	993	95.17
replicase (rep)	1770	1770	94.18

4.2.2.3 Amino Acid and Protein Analysis

Reading frames were translated into their amino acid sequences. Four proteins, namely maturation (mat), coat protein (CP), lysis (lys) and replicase (rep) were identified in R5, R14 and R15. Each of these proteins contain similar number of amino acids, and except for replicase protein, the remaining proteins have 100% amino acid sequence similarity when compared to MS2 (Table 4.11). The replicase protein has four amino acid differences or 99.27% similarity as compared to MS2. Four proteins,

namely maturation (A2), coat protein (CP), replicase (rep) and a read-through protein or minor CP (A1) were translated in R13 and does not contain an independent lysis protein. Except for A1, which has an extra amino acid; there were similar number of amino acids in the remaining three proteins as compared to Q β reference strain. Amino acid sequence similarity ranges from 93% to 97% (

Table 4.12).

Table 4.11. Individual protein length and percent similarity to MS2.

Protein	Individual protein length (aa) & percent (%) similarity to MS2						
	MS2	R5	%	R14	%	R15	%
maturation (mat)	393	393	100	393	100	393	100
coat protein (CP)	130	130	100	130	100	130	100
lysis (lys)	75	75	100	75	100	75	100
replicase (rep)	545	545	99.27	545	99.27	545	99.27

Table 4.12. Individual protein length and percent similarity to Q β .

Protein	Individual protein length (aa) & percent (%) similarity to Q β		
	Q β	R13	%
maturation (A2)	420	420	93.81
coat protein (CP)	134	134	96.25
minor CP (A1)	329	330	96.36
replicase (rep)	589	589	97.45

The amino acid sequences of maturation, coat and replicase proteins from all isolated ssRNA phages were aligned and phylogenetic trees were constructed for each protein (Figure 4.15, Figure 4.16, and Figure 4.17). As with the results of the whole genome sequencing analysis, phylogenetic analysis of the amino acid sequence of each protein showed the clustering of R5, R14 and R15 together with MS2, while R13 is clustered with Q β . The

phylogenetic trees also confirmed that all four isolates are distantly related to *Pseudomonas* phage PP7.

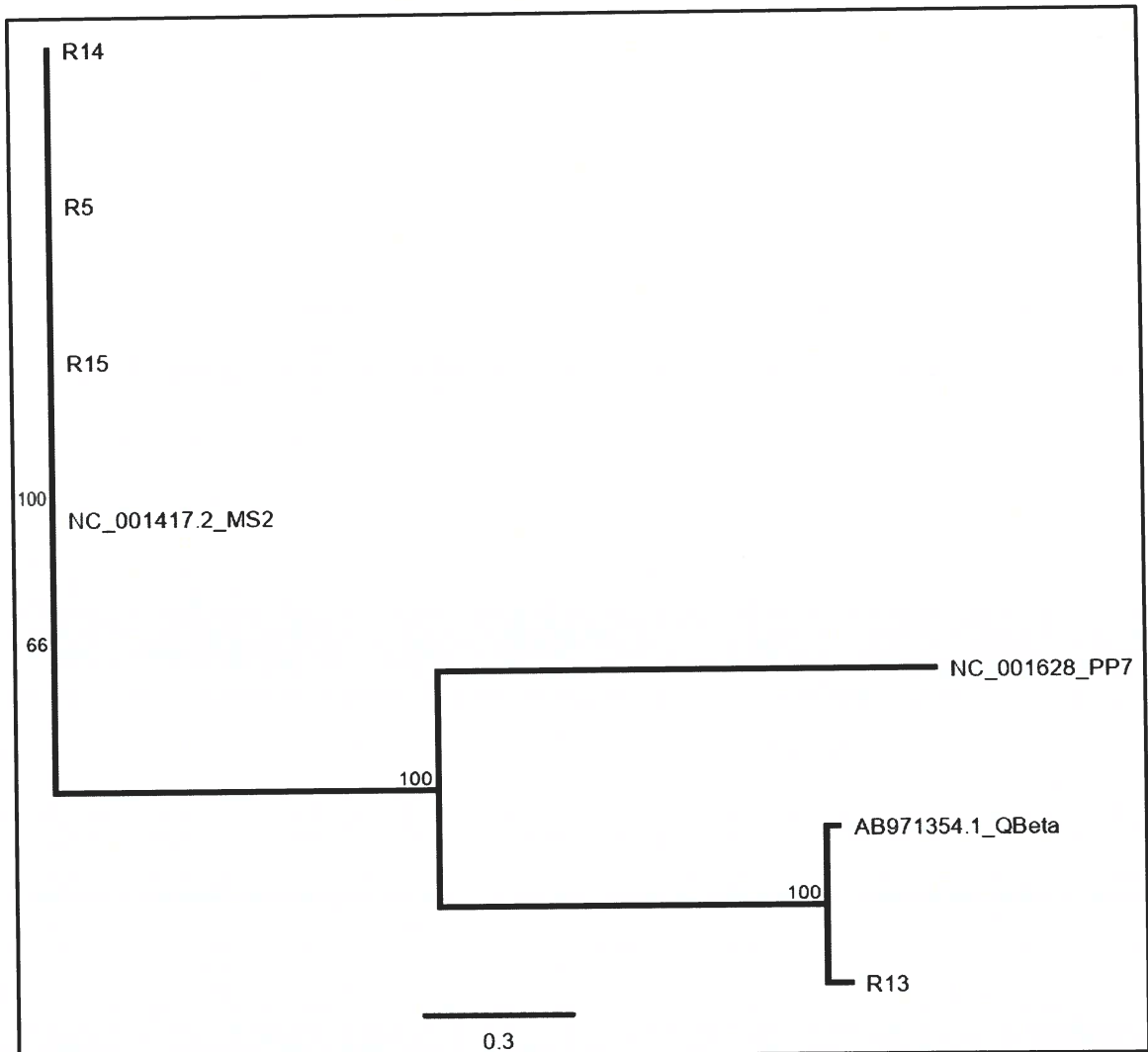


Figure 4.15. Phylogeny of ssRNA phage maturation protein.

The phylogenetic analysis was based on the amino acid sequences of the maturation protein. The tree was constructed by Jukes-Cantor evolution model with Neighbour-Joining (NJ) algorithm and tested using the bootstrap method with 100 replicates. The bootstrap values are expressed as percentages next to the nodes. Amino acid sequences were aligned using Clustal Omega and tree was constructed in Geneious 2021.1.1 program. Enterobacteria phages MS2, Q β , and *Pseudomonas* phage PP7 were included as reference strains.

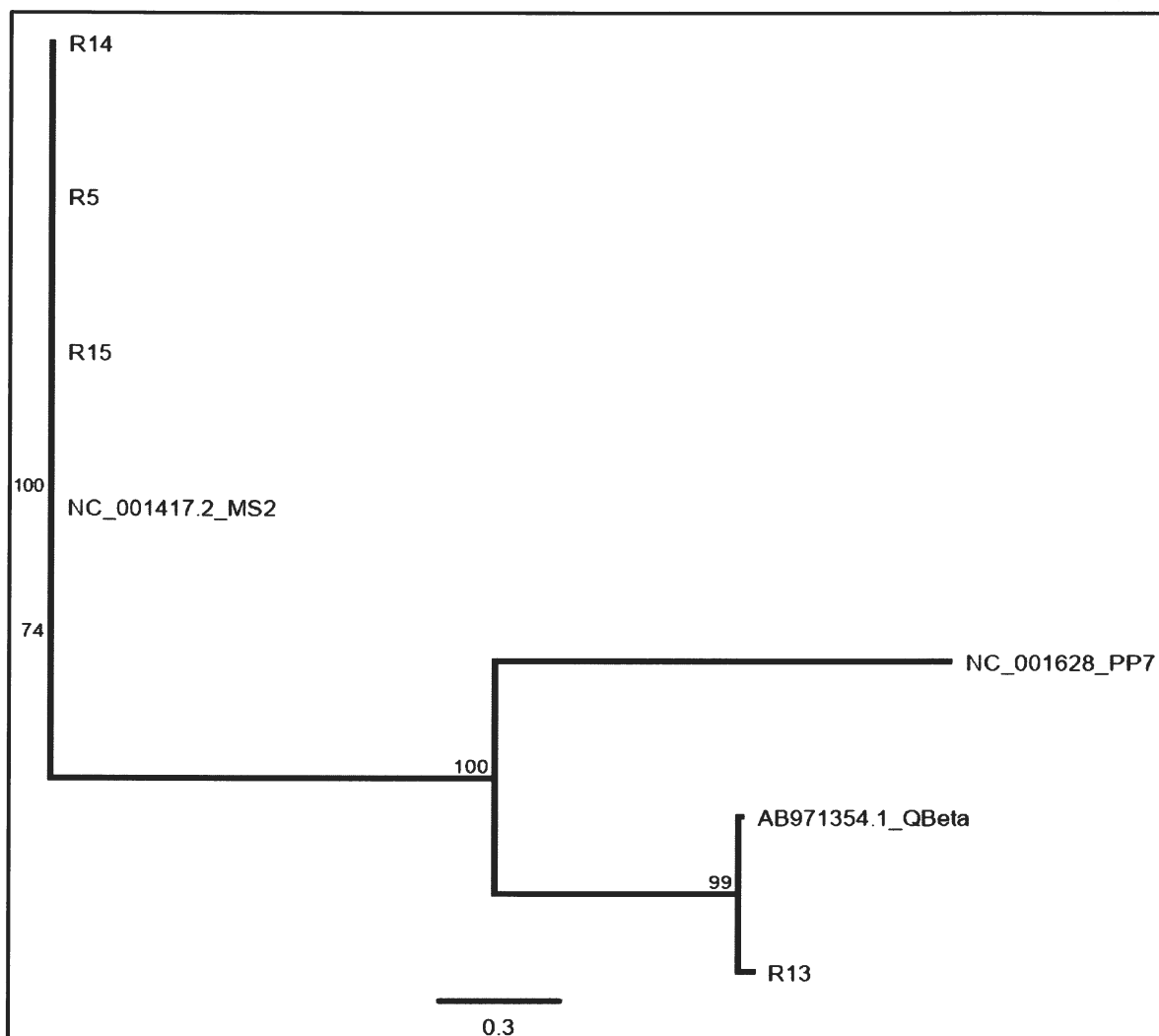


Figure 4.16. Phylogeny of ssRNA phage coat protein.

The phylogenetic analysis was based on the amino acid sequences of the coat protein. The tree was constructed by Jukes-Cantor evolution model with Neighbour-Joining (NJ) algorithm and tested using the bootstrap method with 100 replicates. The bootstrap values are expressed as percentages next to the nodes. Amino acid sequences were aligned using Clustal Omega and tree was constructed in Geneious 2021.1.1 program. Enterobacteria phages MS2, Q β , and *Pseudomonas* phage PP7 were included as reference strains.

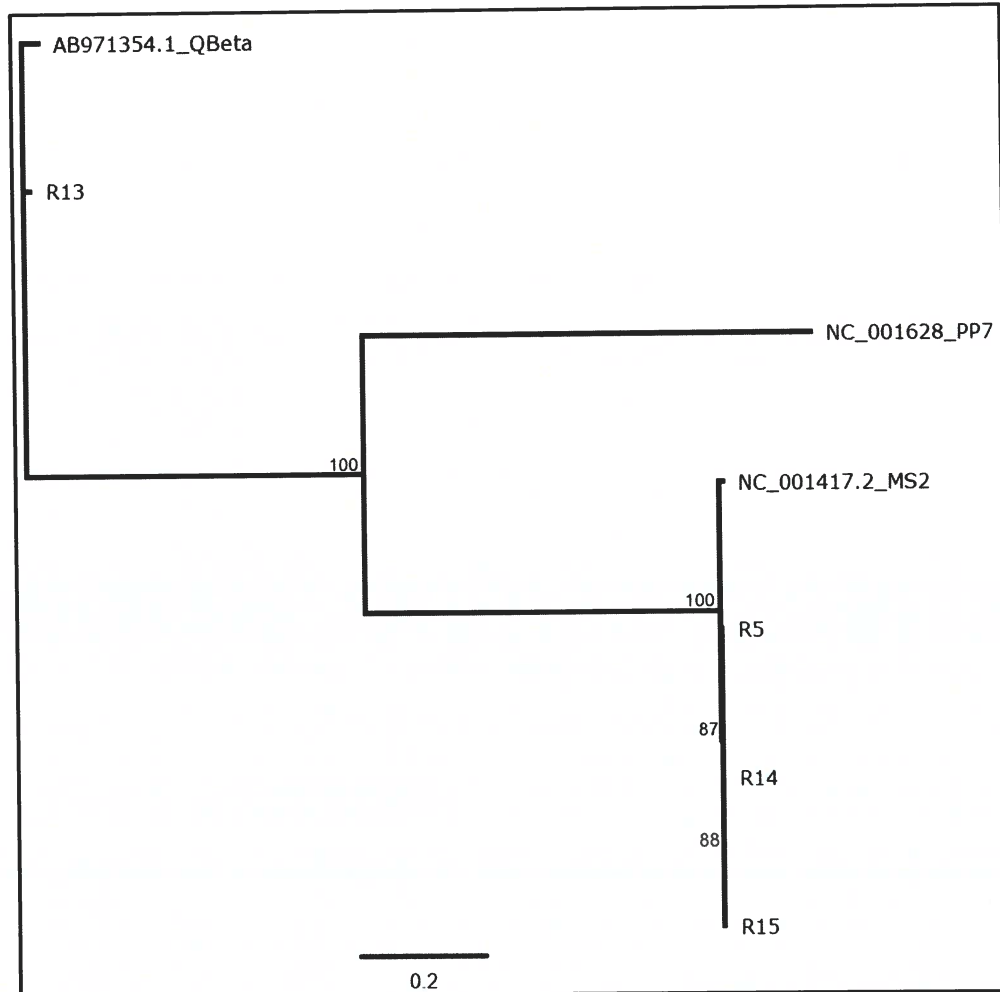


Figure 4.17. Phylogeny of ssRNA phage replicase protein.

The phylogenetic analysis was based on the amino acid sequences of the replicase protein. The tree was constructed by Jukes-Cantor evolution model with Neighbour-Joining (NJ) algorithm and tested using the bootstrap method with 100 replicates. The bootstrap values are expressed as percentages next to the nodes. Amino acid sequences were aligned using Clustal Omega and tree was constructed in Geneious 2021.1.1 program. Enterobacteria phages MS2, Q β , and *Pseudomonas* phage PP7 were included as reference strains.

4.2.3 Naming and classification of phage isolates

Isolated phages were classified following the ICTV International Code of Virus Classification and Nomenclature (ICVCN) “bottom-up” (species, genera, families) approach (Table 4.13). Phage isolates were named based on a tripartite construct consisting of the host genus name (non-italicised), the word “phage”, and a unique identifier, for example “*Escherichia* phage T4”. The latter part of the name (T4) will be the phage’s common name, which will be referred in BAVS reports and scientific publications (Krupovic

and Dutilh, 2016, Adriaenssens and Brister, 2017, Adriaenssens et al., 2017). The current ICVN main species demarcation criterion for bacterial and archaeal viruses is currently set at a genome sequence identity of 95%. Following this criterion, Escherichia phage RPM4, RPM7, and RPM13 may represent novel species.

Table 4.13. Characteristics of the isolated phages.

Code	Isolate Name	Family	Genus	Species	Genome
R1	Escherichia phage RPM1	<i>Inoviridae</i>	<i>Inovirus</i>	<i>Escherichia virus M13</i>	ssDNA
R2	Escherichia phage RPM2	<i>Inoviridae</i>	<i>Inovirus</i>	<i>Escherichia virus M13</i>	ssDNA
R3	Escherichia phage RPM3	<i>Inoviridae</i>	<i>Inovirus</i>	<i>Escherichia virus M13</i>	ssDNA
R4	Escherichia phage RPM4	<i>Inoviridae</i>	<i>Inovirus</i>	<i>Escherichia virus M13</i>	ssDNA
R6	Escherichia phage RPM6	<i>Inoviridae</i>	<i>Inovirus</i>	<i>Escherichia virus M13</i>	ssDNA
R7	Escherichia phage RPM7	<i>Inoviridae</i>	<i>Inovirus</i>	<i>Escherichia virus M13</i>	ssDNA
R8	Escherichia phage RPM8	<i>Inoviridae</i>	<i>Inovirus</i>	<i>Escherichia virus M13</i>	ssDNA
R9	Escherichia phage RPM9	<i>Inoviridae</i>	<i>Inovirus</i>	<i>Escherichia virus M13</i>	ssDNA
R10	Escherichia phage RPM10	<i>Inoviridae</i>	<i>Inovirus</i>	<i>Escherichia virus M13</i>	ssDNA
R11	Escherichia phage RPM11	<i>Inoviridae</i>	<i>Inovirus</i>	<i>Escherichia virus M13</i>	ssDNA
R12	Escherichia phage RPM12	<i>Inoviridae</i>	<i>Inovirus</i>	<i>Escherichia virus M13</i>	ssDNA
R5	Escherichia phage RPM5	<i>Leviviridae</i>	<i>Levivirus</i>	<i>Escherichia virus MS2</i>	ssRNA
R13	Escherichia phage RPM13	<i>Leviviridae</i>	<i>Allolevivirus</i>	<i>Escherichia virus Qβ</i>	ssRNA
R14	Escherichia phage RPM14	<i>Leviviridae</i>	<i>Levivirus</i>	<i>Escherichia virus MS2</i>	ssRNA
R15	Escherichia phage RPM15	<i>Leviviridae</i>	<i>Levivirus</i>	<i>Escherichia virus MS2</i>	ssRNA

4.3 Discussion

4.3.1 ssDNA phage discussion

Genome and phylogenetic analyses of the 11 ssDNA phage genomes confirmed that they belong to family *Inoviridae*, genus *Inovirus* and are related to the filamentous (Ff) phage group that comprises M13, f1 and fd. A high level of similarity of >98% to reference Ff phage genomes was demonstrated by nine of the phage isolates. The phage phylogenetic segregation did not correlate with their site of isolation. The Ff phages (M13, fd and f1) are known to resemble each other so closely that generally no distinction could be made among them (Rasched and Oberer, 1986). Except for a small number of base differences, DNA sequences showed similarity of $\geq 97\%$ at the nucleotide level. Hence, phages M13, fd and f1 are currently considered strains of the species *Escherichia virus M13* (Knezevic and Andriansen, 2021). The analyses also confirmed that all 11 phage genomes are different to *Inovirus* phage genomes *Pseudomonas* phage Pf3 and *Vibrio* phage fs2. The genomes of R4 and R7 demonstrated a similarity of <95% to M13. The current ICVCN guidelines of the BAVS-ICTV indicate that phages belonging to the same species should not differ from each other by more than 5% at the nucleotide level (Krupovic and Dutilh, 2016, Adriaenssens and Brister, 2017, Adriaenssens et al., 2017). Thus, R4 and R7 may represent a new species of *Inovirus*.

The gene organisation of the 11 isolated phages follows the established genome organisation of other filamentous phages. This includes three DNA replication genes (R: gII, gX, gV), followed by the five main structural genes (S: gVII, gIX, gVIII, gIII, gVI) and lastly by the assembly and secretion genes (A-S: gI, gIV) from 5'-3' direction (Rakonjac et al.,

2017). The sequences of the nine phages showed great uniformity in terms of predicted protein length and ORF positions. The attachment or minor coat protein (pIII) was further analysed because of its vital role in the initiation of infection of host cells by binding to the tip of F-pili and then interacting with the TolA protein (Lin et al., 2011). It has previously been demonstrated that M13 inhibited conjugation through occlusion of the conjugative pilus mediated primarily by phage coat protein pIII. Furthermore, exogenous addition of the soluble fragment of pIII inhibited conjugation at low nanomolar concentrations (Lin et al., 2011). Our results showed that the number of amino acids in the pIII is constant among all the isolated phages, ranging from 419 to 424 amino acids.

Both genome and amino acid sequence analyses of R4 and R7 have indicated that these phages may represent a new species of *Inovirus*. There are 19-20 amino acid differences in the predicted amino acid sequences. However, these replacements appear to be conservative mutations and did not affect the resulting proteins.

4.3.2 ssRNA phage

Genomic and phylogenetic analyses confirmed that the four isolates belong to family *Leviviridae* from two genera *Levivirus* and *Allolevivirus*.

Phages R5, R14, and R15 belong to genus *Levivirus* with > 97% genome similarity to MS2, but are different to other *Levivirus* Enterobacteria phages Hgal1, KU1, GA, fr; and *Pseudomonas* phage PP7. Although these three phages were isolated from different sites, they demonstrated a high genetic similarity of greater than 95%, which suggests that location does not play an important role in sequence variability. The

three isolated phages all showed uniformity in both gene and protein length when compared to MS2. The genomes with maturation, coat, lysis and replicase cistrons follow each other in the 5'-3' direction, which is typical of *Levivirus* genome (Friedman et al., 2009, Friedman et al., 2012). The protein coding regions of phages R5, R14 and R15 are of similar length to those of MS2, with all four genes having similar number of nucleotides as compared to MS2. The amino acids in maturation, coat and lysis proteins are highly conserved with similarity of 100%. There were only four amino acid differences in the replicase protein between the isolates. The amino acid groups involved in the changes are conserved. Therefore, they may be predicted to have limited impact on function of the protein, although this can not be ruled out if these are critical residues. However, our analysis shows that these mutations have no effect on the translated proteins.

Phage R13 belongs to genus *Allolevivirus* with a 93.55% similarity to Q β and was confirmed to be different to Acinetobacter phage AP205 with only 31% similarity at the nucleotide level. A similarity of <95% to Q β is an indication that R13 may represent a new species of *Allolevivirus* based on species definition set by BAVS-ICTV (Krupovic and Dutilh, 2016, Adriaenssens and Brister, 2017, Adriaenssens et al., 2017). However, R13 showed uniformity in both gene and protein length when compared to Q β . For instance, the coding regions for maturation, coat and replicase proteins are of similar length, with all three genes having similar number of nucleotides. The minor coat protein cistron is three nucleotides longer and when translated to protein contain one extra amino acid as compared to Q β . The genome with maturation protein (A2), coat protein (CP), minor CP

(A1) and replicase protein cistrons follow each other in the 5'-3' direction, which is typical of *Allolevivirus* genome (Singleton et al., 2018).

The amino acid similarity for the four proteins was not 100%; but despite these dissimilarities the translated proteins are conserved (93 to 97% amino acid similarity). Unlike MS2 and other *Levivirus* genome, *Allolevivirus* genome is unique in the sense that it contains a minor coat protein (A1) (Figure 4.18). This feature was demonstrated as R13's A1 protein shares the same initiation codon with the major coat protein (CP) gene but was separately translated when the leaky stop codon (UGA) of the major CP cistron is misread as a tryptophan codon (UGG), hence A1 is termed the read-through protein (Weiner and Weber, 1973, Singleton et al., 2018).

MAKLETVTLGNIGKDGKQTLVLNPRGVNPTNGVASLSOAGAVPALEKRVTVSVSQ
PSRNRKNYKVQVKIONPTACTANGSCDPSVTRQAYADVTFSTQYSTDEERAFVR
TELAALLASPLLIDAIDQLNPAYWTLIIAGGGSGSKPDPVIPDPPIDPPPGTGKYTCP
FAIWSLEEVYEPPTKNRPWPIYNAVELQPREFDVALKDLLGNTKWRDWD SRLSYTT
FRGCRGNGYIDL DATYLATDQAMRDQKYDIREGKKPGAFGNIERFIYLKSINAYCS
LSDIAAYHADGVIVGFWRDPSSGGAIPDFTKFDKTKCPIQAVIVVPR

Figure 4.18. Amino acid sequence of the minor coat protein (A1).

The A1 protein is produced by translational read-through of the leaky stop codon (UGA) of the major CP cistron (underline); the stop codon is read as tryptophan (W).

Another unique feature of *Levivirus* genome, which was also demonstrated by R13 is the absence of an independent lysis gene. Instead, the lysis function is performed by the maturation protein (A2) as overexpression of A2 was shown to mediate cell lysis (Bernhardt et al., 2002). All four isolated ssRNA phages contain the YGDD motif which is required for replicase activity and is universally conserved among all positive-sense ssRNA viruses (Kamer and Argos, 1984, Koonin and Dolja, 1993, Inokuchi et al., 1994, Rūmnieks and Tārs, 2018).

In conclusion, the genomic and phylogenetic analysis of the isolated ssDNA and ssRNA phages have confirmed the nucleotide and gene sequence diversity of these isolated phages. However, despite these variations, it was demonstrated that predicted translated proteins are highly conserved despite the differences in the nucleotide and amino acid sequences. The phylogenetic analysis was also able to confirm the groupings based on the results from previous chapter. Phages representing these groups have been selected for growth analysis and plasmid loss kinetics, which will be carried out in the next chapter.

Chapter 5. Host range, growth, and plasmid loss kinetics

5.1 Introduction

The phages isolated in the early part of this study can be split into three genera: *Inovirus* (all the ssDNA isolates), *Levivirus* (ssRNA R5, R14 and R15) and *Allolevivirus* (ssRNA R13). All these were isolated using the *E. coli* J62 p*Flac*::Tn3 as a host. Although isolated on the same pilus there is potential that they have different target sequences associated with that pilus and this may be reflected in the host range. While other polymorphisms may impact on their growth kinetics and replication efficiency, both host range and replication efficiency may affect the suitability for use of these phages in therapy. This chapter focuses on host range, adsorption, and replication efficiency impact on plasmid carriage and to understand if these factors are reflected in subsequent plasmid stability and carriage in derepressed and repressed strains.

5.2 Results

5.2.1 Phage host range on field strains of *E. coli*

The ability of the isolated phages to infect field isolates of *E. coli* containing variably repressed AMR F-like plasmids was assessed. Due to repression of pili in these strains, plaques do not form on lawns of the field isolates as repressed strains are refractive to phage infection and mask the developing plaques (data not shown). To demonstrate infectivity on these field strains, a single step replication assay was conducted, assessing the increase of phage by counting pre and post field strain infection phage numbers by enumeration on derepressed *E. coli* J62 p*Flac*::Tn3. Replication on *E. coli* wild-type strains represented by PFU/mL increase between T0 and

T24 hours. The phages demonstrated different replication ability depending on the exact phage host strain combination (Table 5.1, Table 5.2, and Figure 5.2).

An increase in the final phage titre of more than two logs from the initial (T0) to final (T24) titre was demonstrated by all ssDNA phages but varied by host bacteria/plasmid (Figure 5.1). Replication was observed against all six field isolates (Figure 5.1 and Table 5.1), including pF26 which would not support replication of the control ssRNA phage MS2. The ssRNA phages demonstrated varying replication ability on five of the six different *E. coli* field isolates (Figure 5.2 and Table 5.2). No replication was observed on *E. coli* pF26 and only phage R15 replicated in *E. coli* pF18 (Table 5.2). All four ssRNA phages demonstrated a high level ($7 \log_{10}$ PFU/mL) replication step on *E. coli* harbouring pF16 and pF21. A consistently lower level of replication (*ca.* $2 \log_{10}$ PFU/mL and below) of ssRNA phage was observed against strains harbouring pF23 and pF27 (Table 5.2 and Figure 5.3).

Table 5.1. Replication of ssDNA phages on field isolates

phage	<i>E. coli</i> field strains plasmids					
	pF16	pF18	pF21	pF23	pF26	pF27
R1	+	-	-	-	+	-
R2	+	+	-	+	+	-
R3	-	-	+	+	+	-
R4	-	+	+	-	+	-
R6	+	-	+	-	-	-
R7	+	-	+	+	+	+
R8	-	-	+	+	-	-
R9	+	-	+	-	+	-
R10	-	+	+	-	+	+
R11	-	-	+	+	+	+
R12	+	-	-	+	+	+
MS2	+	-	+	+	-	+

+ replication observed; - replication not observed

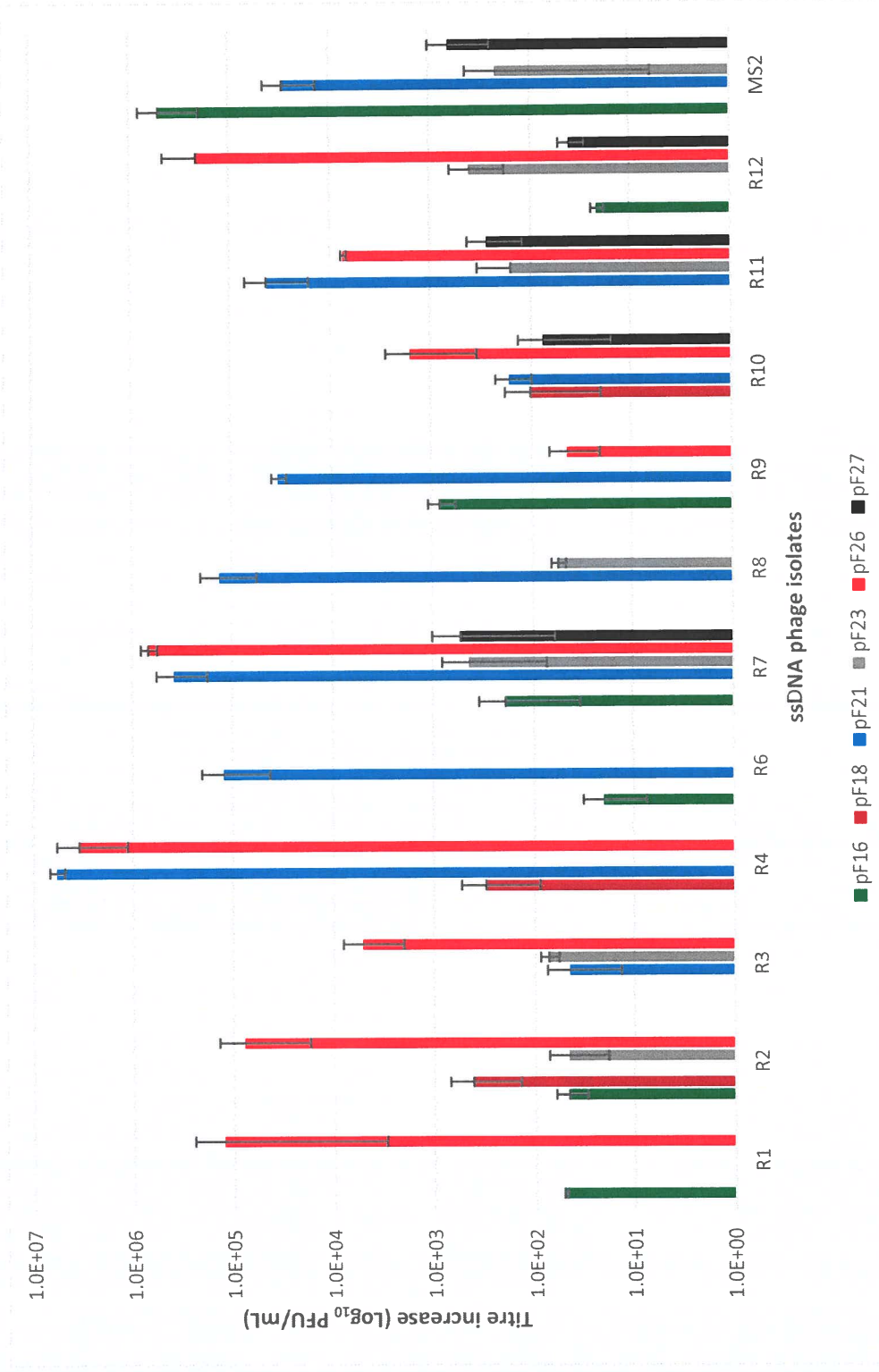


Figure 5.1. ssDNA phages replication against *E. coli* field strains. Bars represent phage titre increase in wild-type *E. coli* field strains containing repressed AMR F-like plasmids after 24 h incubation. Blank area indicates no phage replication. The ssRNA phage MS2 served as a control phage. Values represent the mean of three independent experiments (n=3) ± standard deviation (SD).

Table 5.2. Replication of ssRNA phages on field isolates
E. coli field strains plasmids

phage	<i>E. coli</i> field strains plasmids					
	pF16	pF18	pF21	pF23	pF26	pF27
R5	+	-	+	+	-	-
R13	+	-	+	+	-	-
R14	+	-	+	+	-	-
R15	+	+	+	+	-	+
MS2	+	-	+	+	-	+

+ replication observed; - replication not observed

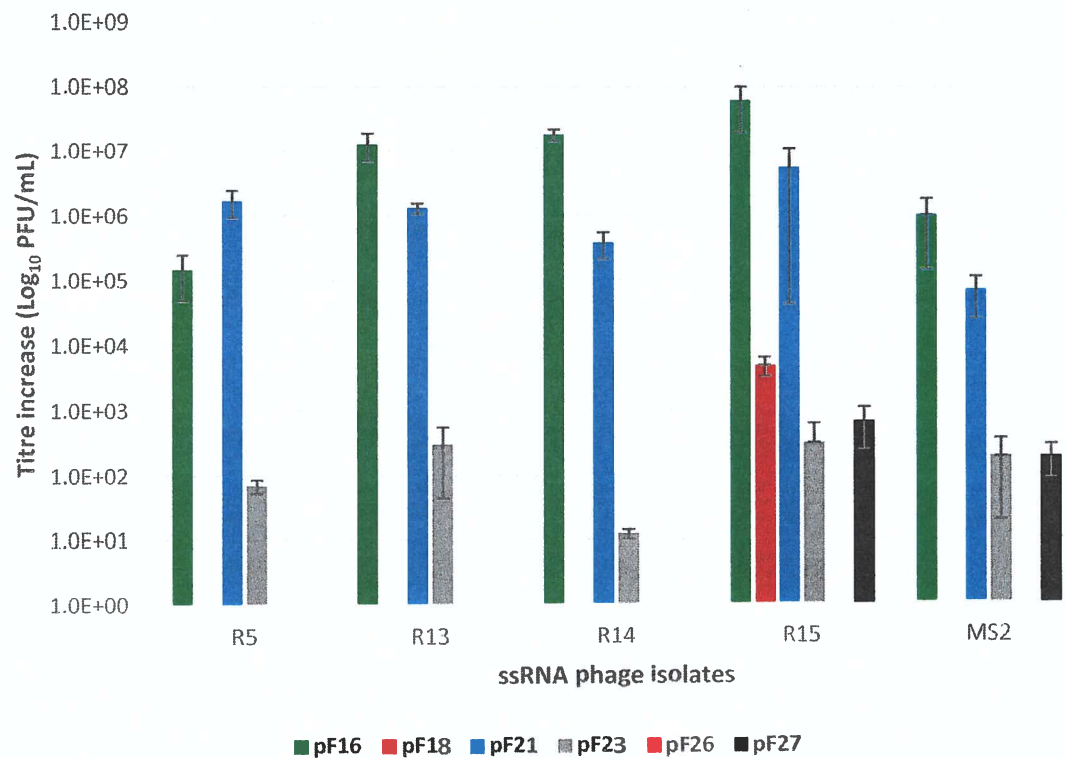


Figure 5.2. ssRNA phages replication against *E. coli* strains.

Bars represent phage titre increase in wild-type *E. coli* strains containing repressed AMR F-like plasmids after 24 h incubation. Blank area indicates no phage replication. The ssRNA phage MS2 served as a control phage. Values represent the mean of three independent experiments (n=3) + standard deviation (SD).

5.2.2 Phage Adsorption and one-step growth curve

The growth characteristics of representative ssDNA and ssRNA phages, which were selected based on their phylogenetic distinction were determined in both derepressed and repressed plasmids.

Growth characteristics on derepressed plasmid p*Flac*::Tn3.

The time taken for the ssDNA phages (R1, R4 and R10) to adsorb to host *E. coli* harbouring the derepressed plasmid p*Flac*::Tn3 varied between 8 and 10 min. Phages R1 and R10 have the same latent period of 5 min and a duration of rise period of 25 min (Table 5.3). Phage R4 had a slightly longer latent period of 10 min with a shorter duration of rise period of 20 min (Table 5.3). The three ssDNA phages have a duration of growth cycle ranging from 38 to 40 min. In terms of burst size, R4 was the best performing ssDNA phage with 398 PFU/cell followed by R1 and R10 with burst sizes of 249 and 254 PFU/cell, respectively (Table 5.3). The ssRNA phages R13 and R15 had an adsorption time of 8 and 12 min, respectively (Table 5.3). Both R13 and R15 had a latency of 5 min and a rise period of 25 min. Phage R13 has a longer duration of growth cycle of 42 min, with a bigger burst size of 85 PFU/cell as compared to R15's duration of growth cycle of 38 min and a burst size of 68 PFU/cell (Table 5.3).

Table 5.3. Growth characteristics of SPS phages on *E. coli* with derepressed plasmid.

Phage ID	Genus	Species	Adsorption time (min)	Latent period (min)	Duration of rise period (min)	Duration of growth cycle (min)	Mean burst size (PFU per infected cell \pm SEM)**
ssDNA phages*							
R1	<i>Inovirus</i>	<i>Escherichia virus M13</i>	8	5	25	38	249.0 \pm 7.9
R4	<i>Inovirus</i>	<i>Escherichia virus M13</i>	8	10	20	38	398.3 \pm 34.7
R10	<i>Inovirus</i>	<i>Escherichia virus M13</i>	10	5	25	40	254.7 \pm 14.1
ssRNA phages*							
R13	<i>Allolevivirus</i>	<i>Escherichia virus Qβ</i>	12	5	25	42	85.2 \pm 3.4
R15	<i>Levivirus</i>	<i>Escherichia virus MS2</i>	8	5	25	38	68.1 \pm 9.0

* An F⁺ *E. coli* J62 with derepressed plasmid pFlac::Tn3 served as the host strain. **Values represent the mean of three independent experiments (n=3) \pm standard error of the mean (SEM).

The number of phages secreted per unit time after the end of the rise period when culture is on a non-synchronous state *in vitro* (secondary infection) was also estimated. Linear regression was used to calculate the gradient, by drawing a trend line between 30 min (end of rise period) to 120 min to compute the number of phages secreted per unit time using the generated formula (Table 5.4 and Figure 5.3).

Table 5.4. Estimated number of phages secreted per unit time.

Phage ID	R ² *	Gradient Formula**	No. of phage secreted (PFU/mL)	
			1 min	60 min
R1	0.9936	y=0.0305x + 5.6511	1.07	64.20
R4	0.9812	y=0.0635x + 6.865	1.16	69.60
R10	0.9968	y=0.0308x + 5.6519	1.07	64.20

*Coefficient of determination = measures how well the regression line fits the data; value should be 1 or nearest to 1; y = the number of phages secreted per unit time after the end of rise period; and x = time.

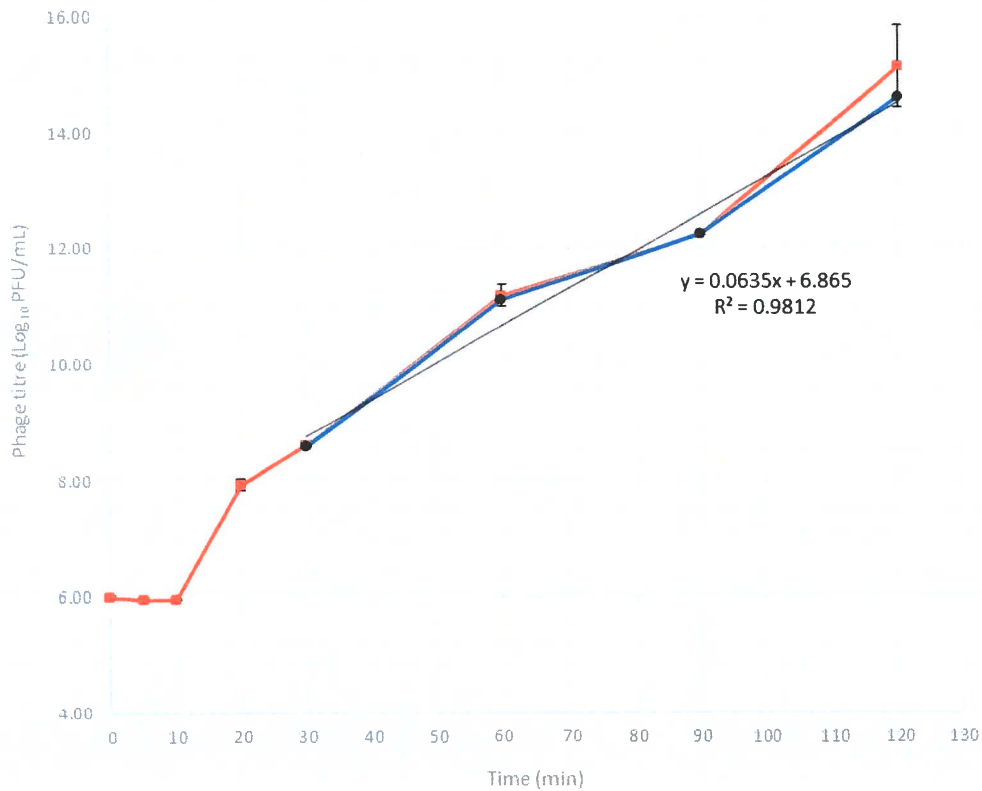


Figure 5.3. One step growth curve of R4 in derepressed plasmid.

One step growth curve of the filamentous ssDNA phage R4 in *E. coli* J62 with derepressed plasmid pF/ac::Tn3 demonstrating the latent and rise period after an adsorption time of 8 min at 4 °C (data not shown). The graph shows that as the incubation time progressed, the plaque number increased due to the release of free phage particles from infected cells until levelling off, identified as the end of rise period (30 min). To estimate the number of phages secreted per unit time on a non-synchronous culture, a trend line between 30 to 120 min was drawn. Values represent the mean of three independent experiments (n=3) ± standard error of the mean (SEM).

Growth characteristics on field isolates harbouring repressed plasmids.

The growth characteristics of the ssDNA and ssRNA phages were also determined on different wild-type *E. coli* strains harbouring repressed AMR F-like plasmids. The ssDNA phages were assessed using *E. coli* pF26 and ssRNA phages against *E. coli* pF21 (Table 5.5).

The ssDNA phages R1 and R4 took 8 min to adsorb to host cell, while in line with the results of pF/ac::Tn3, R10 has a slightly longer adsorption time of 12min. The three ssDNA phages have an increased latent period of 20 min compared to that for depressed plasmid growth of 5 and 10 min (Table 5.3 and Table 5.5). Conversely, they showed a reduced rise period of 10 min, but duration of growth cycle (38-42 min) was similar to that found on *E. coli* harbouring derepressed plasmid. The burst size on the repressed strain pF26 was small compared to the derepressed strain ranging from 3.2 to 3.8 PFU/cell (Table 5.5).

E. coli containing the repressed plasmid designated as pF21 served as host strain for ssRNA phages R13 and R15. The adsorption time and latent period for these phages were the same on *E. coli* pF21 as they were for the derepressed control strain (Table 5.3 & Table 5.5). Phage R13 have an adsorption time and latent period of 12 min and 5 min, respectively, while R15 has 8 min and 5 min, respectively (Table 5.5). The duration of rise and growth cycle times were both reduced compared to derepressed plasmids host. The mean burst size was drastically reduced for both ssRNA phages being less than one PFU/cell compared to the bust size observed on the derepressed control strain (Table 5.3 and Table 5.5).

Table 5.5. Growth characteristics of SPS phages on *E. coli* with repressed plasmid.

Phage ID	Host plasmid	Genus	Species	Adsorption time (min)	Latent period (min)	Duration of rise period (min)	Duration of growth cycle (min)	Mean burst size (PFU per infected cell \pm SEM)*
ssDNA phages								
R1	pF26	<i>Inovirus</i>	<i>Escherichia virus M13</i>	8	20	10	38	3.6 \pm 1.5
R4	pF26	<i>Inovirus</i>	<i>Escherichia virus M13</i>	8	20	10	38	3.8 \pm 0.6
R10	pF26	<i>Inovirus</i>	<i>Escherichia virus M13</i>	12	20	10	42	3.2 \pm 0.9
ssRNA phages								
R13	pF21	<i>Allolevivirus</i>	<i>Escherichia virus Qβ</i>	12	5	10	27	0.47 \pm 0.08
R15	pF21	<i>Levivirus</i>	<i>Escherichia virus MS2</i>	8	5	10	23	0.49 \pm 0.05

*Values represent the mean of three independent experiments ($n=3$) \pm standard error of the mean (SEM).

5.2.3 Plasmid loss kinetics with derepressed plasmid

The effect of three selected ssDNA phages (R1, R4 and R10), on plasmid loss against the depressed control strain, *E. coli* J62 p*Flac*::Tn3 was assessed. After 24 hours (Day 1) incubation 37%, 47% and 40%, of the bacterial population had lost the plasmid after treating with phages R1, R4 and R10, respectively (Figure 5.4A). There was no plasmid loss to the bacterial culture incubated without phage. After 2 and 3 days, further plasmid loss was observed from 45%, 51% and 48% on Day 2 to 59%, 66% and 62% on Day 3 under the selective pressure of phages (R1, R4 and R10, respectively). There was no plasmid loss observed on Day 2 and only a 4% reduction in carriage after Day 3 of incubation in the control phage free cultures. Statistical analysis revealed that there is a significant difference between the untreated control group and phage treated group from Day 1 to Day 3 ($P < 0.05$). Among the three ssDNA phages, R4 performed the best in reducing plasmid carriage (Figure 5.4A). Significant difference ($P < 0.05$) among the three phages was only observed at Day 1.

The total bacterial count was also determined over three days showing a subtle *ca.* 1 \log_{10} (CFU/mL) increase in total bacterial count in stationary phase bacteria between control and infected group (Figure 5.4B). At Day 1, the number of bacteria in the control group is significant higher ($P < 0.05$) than the treated group. However, on Day 2 the number of bacteria on treated group was significantly higher ($P < 0.05$) than the control untreated group. There was no significant difference between the control and infected group at Day 3.

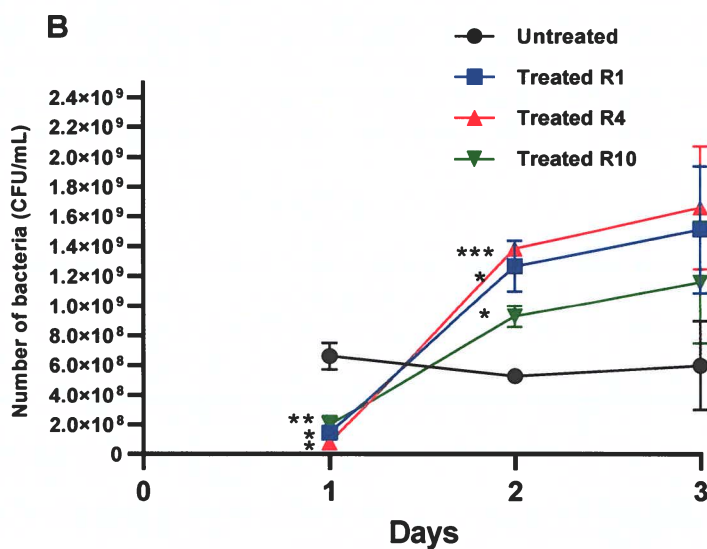
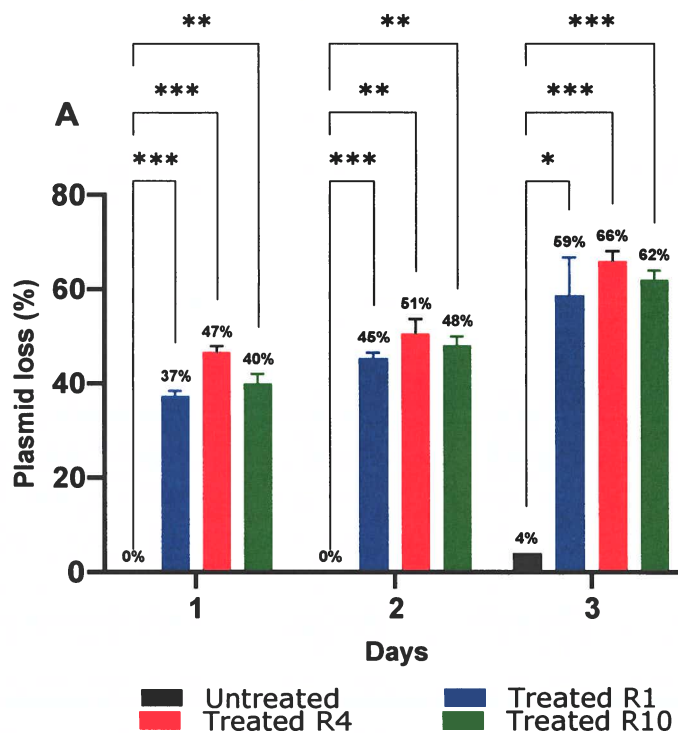


Figure 5.4. Effect of ssDNA phages on derepressed plasmid.

The effect of ssDNA phages on plasmid loss (A) and total bacterial count (B). Treatment group was infected with selected phages at a final MOI of 10. Values represent the mean of three independent experiments ($n=3$) \pm standard deviation (SD). Significance was calculated using two-way ANOVA with Tukey's multiple comparisons post hoc test. *** $P<0.001$, ** $P<0.01$, * $P<0.05$.

The effects of two selected ssRNA phages, R13 and R15, on plasmid loss were also assessed against the derepressed *E. coli* J62 p*Flac*::Tn3. Phage R13 reduced plasmid carriage by 33%, 47% and 61%; while R15 reduced plasmid carriage by 32, 45 and 62% over days one to three (Figure 5.5A). In untreated bacteria there was a *ca.* 2% reduction plasmid carriage after three days. There is a significant difference between the untreated control group and phage treated group from Day 1 to Day 3 ($P < 0.05$), however there is no significant difference ($P < 0.05$) between R13 and R15.

As with the DNA phages treatments with the ssRNA phage led to a *ca.* 1 Log_{10} (CFU/mL) increase in bacterial numbers at stationary phase in phage treated cultures compared to untreated cultures (Figure 5.5B). At Day 1, the number of bacteria in the control group is significant higher ($P < 0.05$) than the treated group. However, there is no significance difference ($P < 0.05$) between control and treated group at Day 2 and Day 3 and between the two ssRNA phages for the entire 3 day duration.

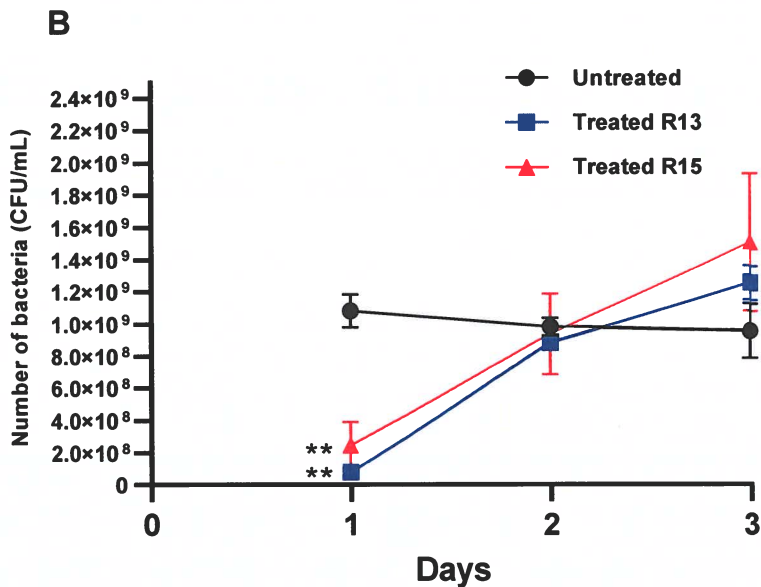
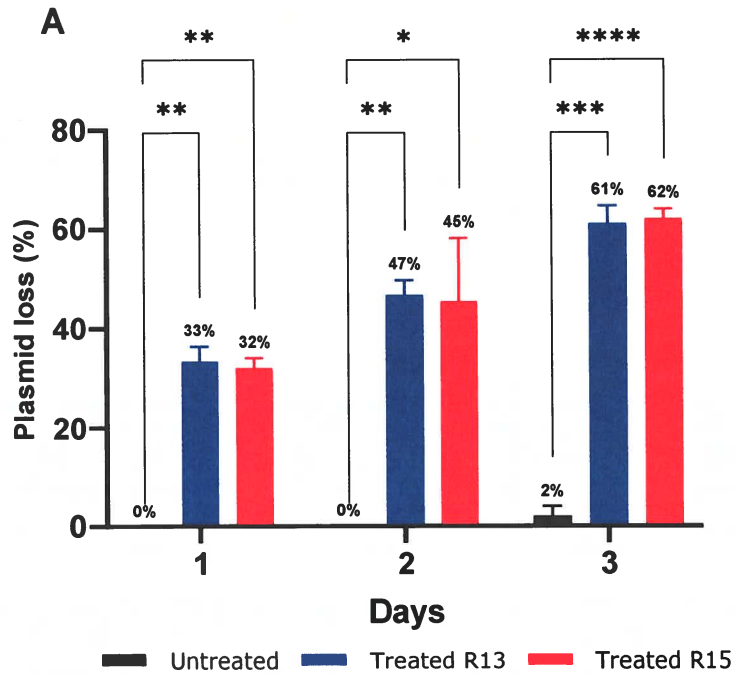


Figure 5.5. Effect of ssRNA phages on derepressed plasmid.

The effect of ssRNA phages on plasmid loss (A) and total bacterial count (B) on derepressed plasmid pF/ac::Tn3. Treatment group was infected with selected phages at a final MOI of 10. Values represent the mean of three independent experiments (n=3) ± standard deviation (SD). Significance was calculated using two-way ANOVA with Tukey's multiple comparisons post hoc test. ****P<0.0001, ***P<0.001, **P<0.01, *P<0.05.

5.2.4 Plasmid loss kinetics with repressed plasmid

The same panel of phages which were assessed against the derepressed *E. coli* were assessed for impact on the repressed field isolates *E. coli* pF26 and *E. coli* pF21.

The ssDNA phages (R1, R4 and R10) did not affect plasmid carriage in *E. coli* pF26 on days 1, 7, 10, 14 and 21 post infection. There was no significant difference $P < 0.05$ in the total bacterial count between the untreated and phage treated groups and between strains over the 21 day period.

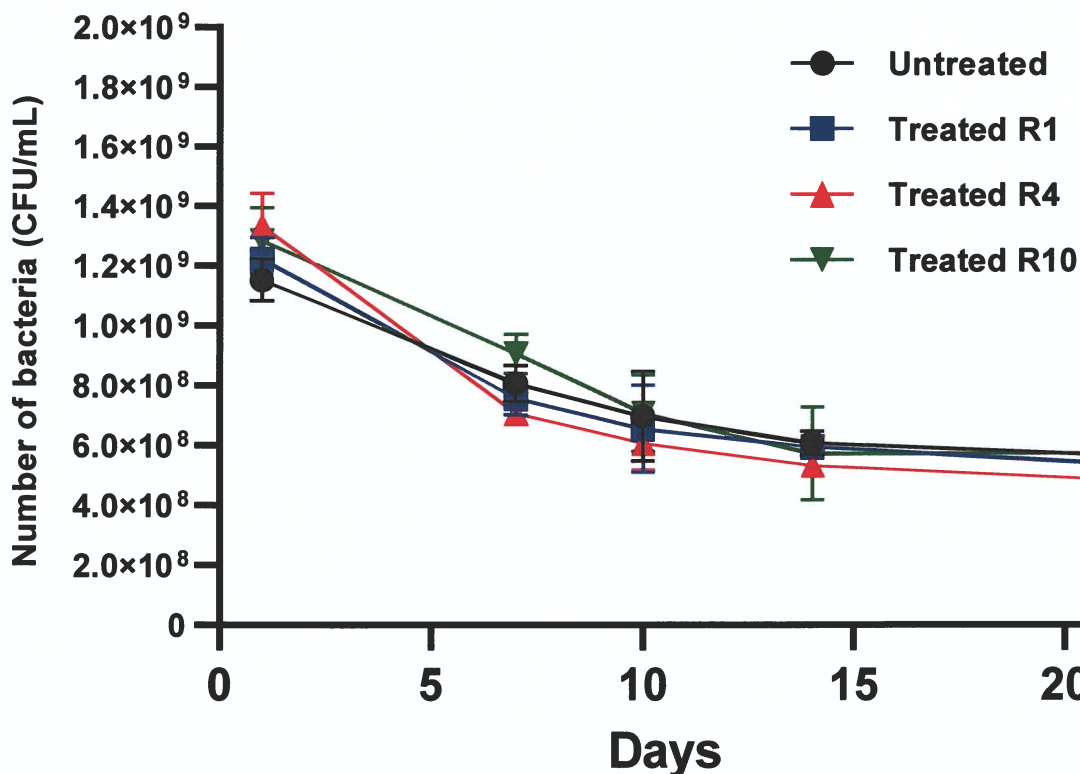


Figure 5.6. Effect of ssDNA phages on repressed plasmid pF26.

The effect of ssDNA phages on repressed plasmid pF26. Treatment group was infected with selected phages at a final MOI of 10. Values represent the mean of three independent experiments ($n=3$) \pm standard deviation (SD). Significance was calculated using two-way ANOVA with Tukey's multiple comparisons post hoc test.

The ssRNA phages R13 and R15 led to a significant reduction ($P < 0.05$) in pF21 carriage from day 7 to 14 (Figure 5.7A). At day 1, there was no observable plasmid loss for either phage. At day 7, 10 and 14 plasmid loss rates of 11%, 12% and 14%, respectively were observed for R13 treated bacteria, while a lower plasmid loss rate of 5%, 5% and 13% was observed for R15. There is a significant difference ($P < 0.05$) between R13 and R15 at Day 7 and 10, however no significant difference between them was observed at Day 14. There was no plasmid loss observed in the untreated culture for the entire 14 days of passage. There was no significant difference ($P < 0.05$) in the bacterial count for the untreated and treated culture from day 1 to day 14, with untreated group showing a *ca.* 1 log₁₀ higher total count than either of the treated groups (Figure 5.7B).

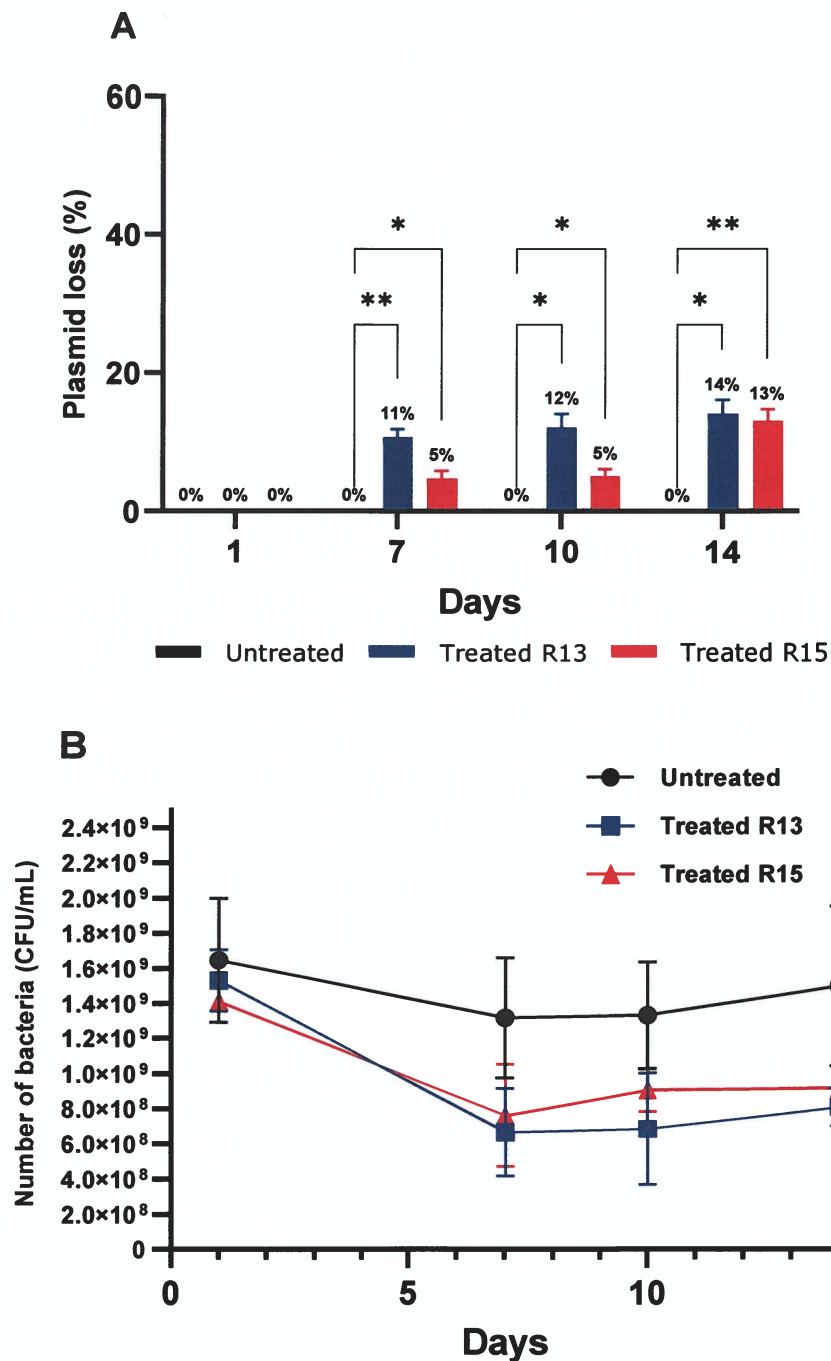


Figure 5.7. Effect of ssRNA phages on repressed plasmid pF21.

The effect of ssRNA phages on plasmid loss (A) and total bacterial count (B) on repressed plasmid pF21. Treatment group was infected with selected phages at a final MOI of 10. Values represent the mean of three independent experiments (n=3) ± standard deviation(SD). Significance was calculated using two-way ANOVA with Tukey's multiple comparisons post hoc test. **P<0.01, *P<0.05.

5.2.5 Effect of R4 phage during conjugation

The ssDNA phages such as M13 have been shown to block bacterial conjugation (Lin et al., 2011). To verify this previous finding, phage R4 was selected and its effect on conjugation was investigated in a conjugation assay *in vitro*. The results showed that R4 was able to block transmission of the derepressed plasmid p*Flac*::Tn3, reducing the transfer rate by 65.5%. For the repressed plasmids pF26, the effect of the phage was lower reducing the transfer rate by 33.3% (Table 5.6).

Table 5.6. Plasmid transfer rate after conjugation with *E. coli* J62 Rif^R with and without phage R4.

Plasmid	Phage R4	Transfer rate (%) [*]	Reduction in transfer rate (%)
Flac::Tn3	-	100 ± 0.0	0
	MOI 10	34.5 ± 1.2	65.5
pF26	-	94.7 ± 3.5	0
	MOI 10	66.7 ± 3.5	33.3

*Values represent the mean of three independent experiments ($n=3$) ± standard error.

5.2.6 Replication of phage R4 on different bacterial species

The ability of phage R4 to replicate in different species of bacteria carrying both derepressed and repressed F plasmids was also assessed. Results showed that replication was depended on the presence of the specific plasmid rather than the species of bacteria. Maximum replication was observed on *S. Enteritidis*, *S. Typhimurium* and *E. coli* (control) carrying the derepressed p*Flac*::Tn3 plasmid. Varying replication was observed on field strains harbouring repressed F like plasmids. Highest replication was observed in *E. coli* pF26 (control) followed by *E. coli* pP13, *P. aeruginosa* pPA80610 and *E. coli* pP31 (Figure 5.8).

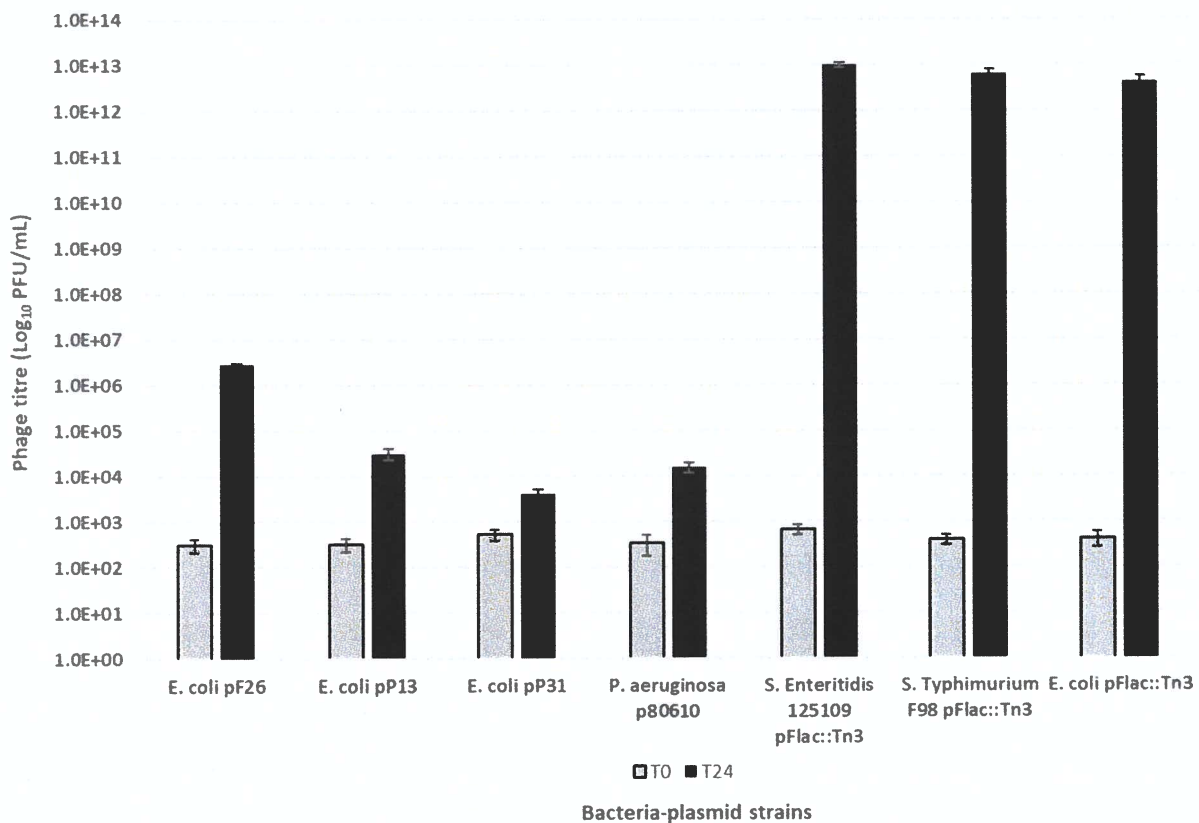


Figure 5.8. Replication of phage R4 on different bacterial species.

Gray bars represent titre at time 0 h, while black bars show the titre after 24 h incubation at 37 °C. *E. coli* J62 *Flac*::Tn3 was set as a positive control for derepressed plasmid while *E. coli* pF26 served as control for repressed plasmid. Values represent the mean of three independent experiments (n=3) ± standard deviation (SD).

5.3 Discussion

Several studies have shown that sex pilus specific (SPS) phages have the potential to kill bacteria containing conjugative plasmids, select for plasmid loss or block conjugation (Jalasvuori et al., 2011, Ojala et al., 2013, Colom et al., 2019). However, these studies focused on well characterised ssRNA phages reference strains. In this chapter we isolated new field strains of both ssDNA and ssRNA SPS phages; assessed their growth characteristics and impact in infecting both derepressed and repressed F and F-like plasmid.

We observed a mixed host susceptibility of field bacterial isolates of varied repression; and all *E. coli* field strains were susceptible to at least one of the isolated phages. As indicated, the ssDNA phages showed a mixed pattern of replication but all F-like plasmid strains were susceptible to at least one ssDNA phage. The alignment of the attachment protein, pIII (Figure 4.9 to Figure 4.11) of the ssDNA phages shows polymorphism but these do not match to the infection profiles (Figure 5.1). Individual ssDNA phage showed a slightly more restricted host range as compared to the ssRNA phage. However, no ssRNA phage assessed in this study could infect *E. coli* pF26. Three of the ssRNA strains only infected three of the bacterial isolates and one phage (R15) infected the same four *E. coli* strains as MS2.

The pattern of host susceptibility to ssRNA phages was not directly related to Genera, with the *Levivirus* isolates R5 and R14 having the same pattern of host susceptibility as the *Allolevivirus* R13. This study has confirmed previous finding by Colom et al. (2019) that *E. coli* pF26 appears not to be susceptible to infection by ssRNA phage, however it was shown that *E. coli* pF26 was susceptible to some of the

isolated ssDNA SPS phages. Plasmid pF26 is highly self-transmissible and while the rate we observed was lower than that indicated by Colom et al. (2019), it is still substantial and suggestive of strong pilus expression. The resistance to infection of *E. coli* pF26 to ssRNA phages could reflect a fundamental difference in binding site between the ssDNA and ssRNA phages. However, it would still be interesting to assess the impact of phage on its transfer rate to confirm that no binding or interference occurs.

We observed differences in the replication steps of our phages when infecting the different *E. coli* strains. All four ssRNA phages demonstrated the highest replication rate in *E. coli* containing plasmids pF16 and pF21, with R15 being the best performing ssRNA phage. However, the ssRNA phage showed similar general trends in phage increase suggesting that replication efficiency is similar for all bacteria/phage combinations including between the different genera of ssRNA phage. The replication of ssDNA phage is less clear cut, but replication efficiency once infected appears to be host strain specific. For instance, phages R4 and R7 being suggested as different species at nucleotide level showed the highest replication rate on field strains containing pF21 and pF26 plasmids.

One step growth analysis of selected ssDNA (*Inovirus*: R1, R4, R10) and ssRNA (*Allolevirus*: R13; *Levivirus*: R15) phages on *E. coli* harbouring derepressed plasmid demonstrated efficient growth characteristics. The ssDNA phages demonstrated shorter latent periods of between 5 to 10 min and larger burst sizes (>245 PFU per infected cell), compared to tailed phages (*Myoviridae*) latent periods of between 21 and 120 min and burst sizes between 50 and 100 PFU per infected host cell (Foschino

et al., 1995, Petty et al., 2006, Raya et al., 2011). The short latent period and large burst size of these SPS phages is an indication of high lytic activity and robust propagation of the phage. We observed a burst size of around 250 PFU per cell for R1 and R10 which is in line with that observed for M13 (250 PFU per cell)(Ploss and Kuhn, 2010). Phage R4 had a greater burst size compared to the other ssDNA phage assessed. This may reflect that this phage is not completely similar based on its phylogenetic analysis and alignment of its attachment protein.

Both ssRNA phages (R13, R15) demonstrated similar latent and duration of rise periods. Phage R13 has a slightly longer adsorption time (12 vs. 8 min), but a larger burst size (85 vs. 68 PFU per cell) as compared to R15. The burst size of 85 PFU per cell for R13 was almost similar to previously reported 90 PFU per cell (Tsukada et al., 2009). The average burst size of around 70 PFU per cell for R15 is also within the previously reported values, however results from the literature are quite variable with burst sizes ranging from 10 to 400 PFU per cell (De Paepe and Taddei, 2006, Jain et al., 2006).

The filamentous ssDNA phages have a unique life cycle that they are neither lytic nor lysogenic. Instead, they release their progeny by a secretory process through budding or extrusion without lysing the host bacteria, causing a chronic infection of the host cells. The burst size is the best estimate of how many progenies were secreted per infected cell. However, this is not the most ideal measure for this type of phage, as the progeny is continuously being secreted by infected host cell. Therefore, the estimated number of phages secreted per unit time was also determined after the end of the rise period until 60 minutes. The results showed that

this approach could be used to estimate the number of phages secreted during the chronic infection *in vitro*.

The growth characteristics of the SPS phages have never been investigated on field strains harbouring repressed plasmids. An attempt was made to determine the effect of repression on the growth of these phages. The present results have confirmed that repression has a great effect on the growth of these phages. Growth of all ssDNA phages showed a longer latent period with shorter rise period and a burst size of only less than four (<4) PFU per cell. A similar pattern was also observed among the ssRNA phages, with even smaller burst size of less than one (<1) PFU per cell. These results may reflect a functional role for pilus repression in reducing impact of phage infection.

The effect of these SPS phages on plasmid loss was also investigated on derepressed and repressed plasmid hosts. Around 60% plasmid loss was demonstrated by *E. coli* containing derepressed plasmid infected by ssDNA and ssRNA phages compared to less than 5% loss for uninfected control. These results match the loss observed for derepressed plasmids in two previous studies where plasmid loss was demonstrated by phage MS2, which attaches to the sex-pilus of IncF plasmid; and by phage PRD1, which attaches to the sex-pilus of IncP, N and W plasmids (Jalasvuori et al., 2011, Colom et al., 2019).

Phage R4 led to an increased loss of derepressed plasmid compared to R1 and R10. This may reflect that R4 is less than 95% similar to any of the other Ff phages and so could be considered a different species. Both ssRNA phages R13 and R15 showed almost similar levels of derepressed plasmid loss to that observed with the

ssDNA phages. It was interesting to note that derepressed cultures infected with ssDNA and ssRNA phages overall OD₆₀₀ increased suggesting a physiological impact leading to either change in cell volume and therefore OD, or increased number of bacteria in what will be stationary phase. It has been shown that the absence of large transmissible plasmids can lead to an increase in the growth rate of bacteria in the absence of the environmental conditions that select for the plasmid maintenance (Johnson et al., 2015). One could hypothesize that a competitive exclusion advantage may come into place over time against the plasmid containing strains. This correlates with the idea that there are suicide systems in plasmids to maintain them in populations against this effect (Unterholzner et al., 2013).

While previous studies by Colom et al. (2019) and this study on derepressed strains were limited in duration and may not observe a significant impact of this growth advantage. The work with ssDNA and ssRNA phages on the repressed strains did continue longer for 21 and 14 days, respectively. On this extended period there was no obvious overtake or exclusion of strains. We did however see an increase on plasmid loss of around 14% on day 14 compared to previous studies with MS2 (Colom et al., 2019).

We also assessed the impact of selected ssDNA (R1, R4, R10) and ssRNA (R13, R15) phages on plasmid loss during infection of the field strains of *E. coli* harbouring repressed plasmids pF26 and pF2. When infecting pF26 with the selected ssDNA phages we observed no plasmid loss whereas we observed around 60% plasmid loss over three days against derepressed control strains. This is interesting as pF26 has a transfer rate of 66% in our hands and 99% in other studies (Colom et al., 2019).

Unlike Colom et al. (2019), we can clearly observe replication on pF26 and reduction of plasmid transfer rate to *ca.* 33%, which is an indication of infection. So why do we not see loss at all? This is a conundrum and may reflect unknown growth dynamics due to chronic life cycle of ssDNA phages and the way the progenies are being released through extrusion. To compensate for this we extended the time of infection up to 21 days, but still observed no loss of plasmids.

The lower rate of repressed pF21 plasmid loss as compared to the derepressed plasmid may be explained by its more repressed nature. In such repressed systems, where fewer bacterial population express sex-pili the effective MOI may be greater than for a completely derepressed plasmid. However, plasmid transfer to a recipient population is widespread with new recipients showing a burst of sex-pilus production resulting from momentary derepression following low intracellularly concentrations of FinO and FinP (Zatyka and Thomas, 1998). The presence of a SPS phages in the environment at the time of conjugation activity could prevent plasmid transmission even if these are highly repressed (Colom et al., 2019). Our results showed a 33% plasmid reduction rate on repressed plasmid pF26 infected with phage R4.

We also determined the replication of ssDNA phage R4 on several field strains of *E. coli* and a *P. aeruginosa* containing repressed F plasmid and against *S. Enteritidis*, *S. Typhimurium* and *E. coli* harbouring the derepressed F plasmid p*Flac::Tn3* (Figure 5.8). As expected, R4 demonstrated similar replication in *Salmonella* and *E. coli* strains containing the depressed plasmid. The phage R4 was also able to replicate on other species of bacteria containing repressed plasmid at varying degrees as exhibited by R4 replicating on *P. aeruginosa* containing the

repressed plasmid pP80610. These results have demonstrated that host range is determined foremost by the presence of the conjugative plasmid rather than by the bacterial species or strains (Frost and Koraimann, 2010). Since conjugative plasmids often spread in taxonomically diverse groups of bacteria, the host range of these plasmid dependent SPS phages is broader as compared to other groups of phages (Loeb, 1960).

Chapter 6. General Discussion

According to the World Health Organization AMR has become a serious global threat to public health and livestock industry. It is estimated that a continued rise in resistance by 2050, would lead to 10 million people dying every year and a reduction of 2% to 3.5% in Gross Domestic Product (GDP) costing the world up to 100 trillion USD (O'Neill, 2014). A major risk for spread of AMR is due to transfer and acquisition of resistance genes on self-transmissible resistance plasmids. A major group of plasmids involved in AMR are the F plasmids which can self-transmit at a high rate through plasmid encoded sex-pili which attach to other bacterial cells and mediates the initial stage of the conjugation process. These pili which are central to plasmid transfer can also be an attachment sites for a variety of bacteriophages referred here as sex pilus specific (SPS) phages. The ability of SPS phage to control bacterial strains harbouring derepressed plasmids has been explored but with only previously characterised reference phages (Ojala et al., 2016, Colom et al., 2019).

In this study 15 field strains of SPS phages were isolated and assessed for their potential to interfere with F-plasmid maintenance and transfer for both derepressed and repressed plasmids. Phenotypic, morphological, biological and genetic characterisation coupled with analysis of their structural proteins by SDS-PAGE confirmed the 11 isolated phages to be ssDNA phages belonging to Family *Inoviridae* and the remaining four (4) belonging to Family *Leviviridae*. Phylogenetic analyses of the 11 ssDNA phage genomes confirmed that they belong to genus *Inovirus* and are mostly related to the highly similar filamentous (Ff) phages (M13, fd, f1). However, two ssDNA phages R4 and R7, only demonstrated a similarity of

<95% to any of the Ff reference strains at the nucleotide level. Following the ICVCN guidelines for speciation based on whole genome sequence they may be considered to represent a new species of *Inovirus*. There are 19-20 predicted amino acid differences across the whole of R4 and R7 compared to the reference strain. These polymorphisms appear to be conservative amino acid substitutions and not predicted to have major effect on function of the affected proteins or phage phenotype. Nevertheless, phylogenetic analysis of this protein put R4 and R7 in a separate cluster from the remaining ssDNA phages suggestive of genetic divergence.

Phylogenetic analyses of the four ssRNA phage genomes confirmed three of the four phages (R5, R14, R15) to be highly similar to genus *Levivirus* and the remaining phage (R13) defined as *Allolevivirus* at the nucleotide level. As with ssDNA phages, the predicted proteins of these ssRNA phages were determined and their amino acid sequence compared with those of key reference strains. The amino acids sequence of maturation, coat, and lysis proteins of three isolated ssRNA were 100% similar to MS2. There were only four amino acid differences in the replicase protein. However, given the central role of this protein in replication is it hard to see how these mutations have a significant functional impact on the replicase function. The ssRNA phage, R13 only showed a 93.55% similarity to *Allolevivirus* type species Q β at the nucleotide level. Again, following the ICVCN guidelines this may represent a new species of *Allolevivirus*. Despite these nucleotide differences, R13 showed uniformity in predicted protein length and these differences have no effect on the translated proteins.

One-step growth analysis of selected SPS phages (typical of each genus we isolated) were determined against bacterial strains harbouring either derepressed or repressed plasmids. Replication on derepressed plasmid hosts generated a shorter latent period and a larger burst size compared to equivalent reported periods for tailed phages. This is an indication of high lytic activity and robust growth of these phages, suggesting they would be useful in control of bacteria. The phages resulting in around 60% plasmid loss of the derepressed plasmid may suggest that the remaining 40% had either lost the plasmid or were no longer expressing their pilus. Previous studies by Colom et al. (2019), observed similar phage resistant bacteria which were either plasmid efficient or had mutations leading to lack of sex pili expression. We did not have time to determine this in this study.

Longer latent periods with shorter rise periods and much smaller burst sizes were observed against repressed plasmid hosts. There was limited loss of plasmids observed, with the most effective being 14% plasmid loss which seemed to reflect a relatively lower levels of pilus repression, as suggested by transfer data for repressed plasmids. Taken together these data suggest that repression of pili is playing a protective role to reduce the impact of environmentally present SPS phages on plasmid stability in field environments.

So can SPS phages be used successfully to control AMR bacteria? The use of SPS phages could be used to reduce conjugation and transfer. They could also put enough selective pressure on some isolates which can also make antibiotic treatment more effective. It is interesting to note the slight bacterial numbers increase in population where plasmids are lost. While *in vitro* we did not observe a competitive

selection leading to progressively plasmid free cultures, this may occur *in vivo* where host selective pressures may play an additional role in selection. The data from Colom et al. (2019) is suggestive that use of SPS phages on derepressed plasmids *in vivo* can work. However, studies on the effects of these SPS phages on repressed plasmid *in vivo* has yet to be carried out. There is an alternate hypothesis indicating that pilus expression is increased *in vivo* during transitory derepression, which may render SPS phage treatment more effective. Both these hypotheses would require further data to fully understand if this approach could work. It would be interesting to test the isolated phages against a panel of field strains which are naturally repressed *in vivo* to determine if pilus expression alters and if selection would play a major role in its effectiveness *in vivo*.

Investigations could also look for approaches to trigger transitory derepression to increase the effectiveness of SPS phages on otherwise repressed hosts. In addition, this study has focused on a single phage selection host, and it would help to create more derepressed plasmids not only on IncF plasmid but other incompatibility groups to see if more effective SPS phages exist. Stability tests of our phages for temperature, pH and detergent suggest they are as robust as could be expected for field application.

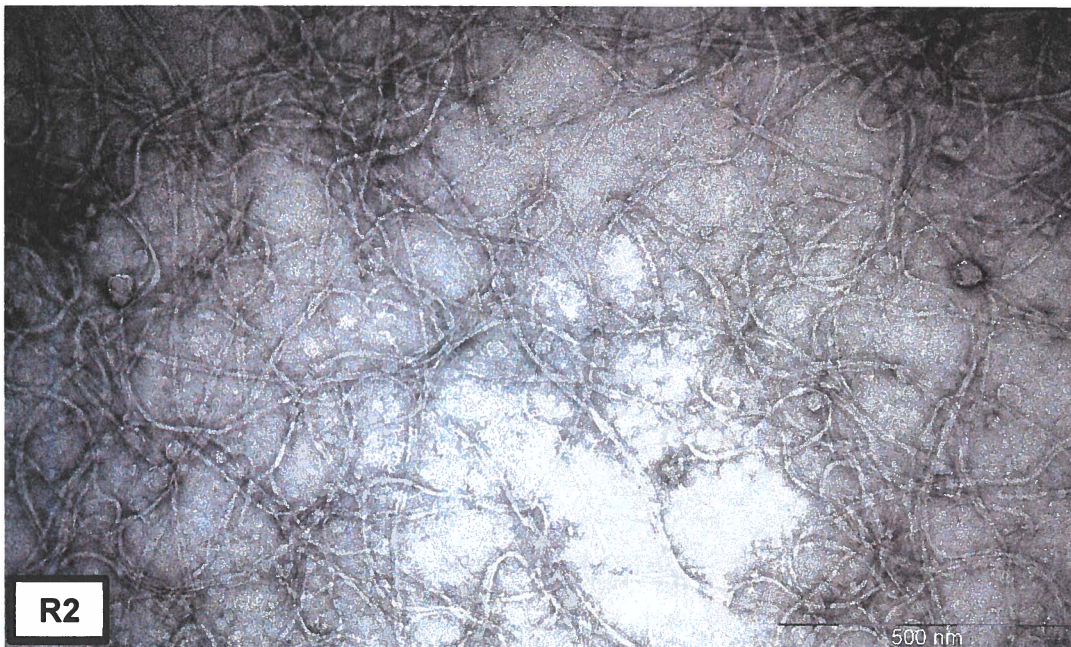
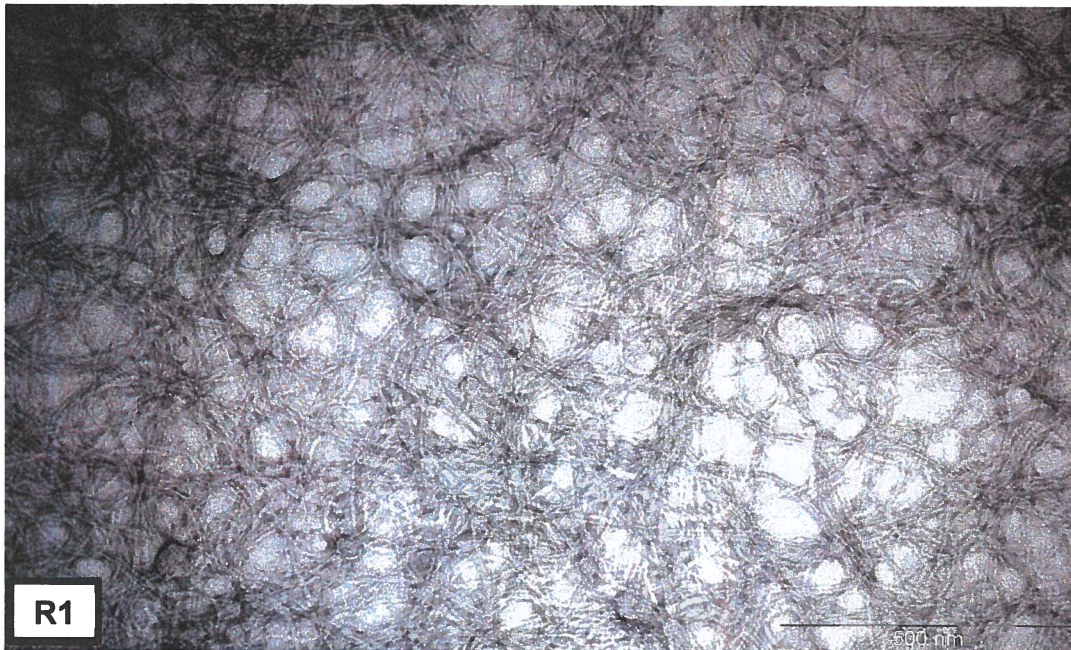
Based on the current results, it was shown the variation for ssDNA phages host range. Taking this into consideration, will creating a cocktail of several of these phages an effective approach *in vivo*? Additional targeting of pili will focus on a single binding structure and so may be susceptible to resistance. Simply targeting pilus will mean any route to pilus loss will make the bacteria resistant. So, consideration

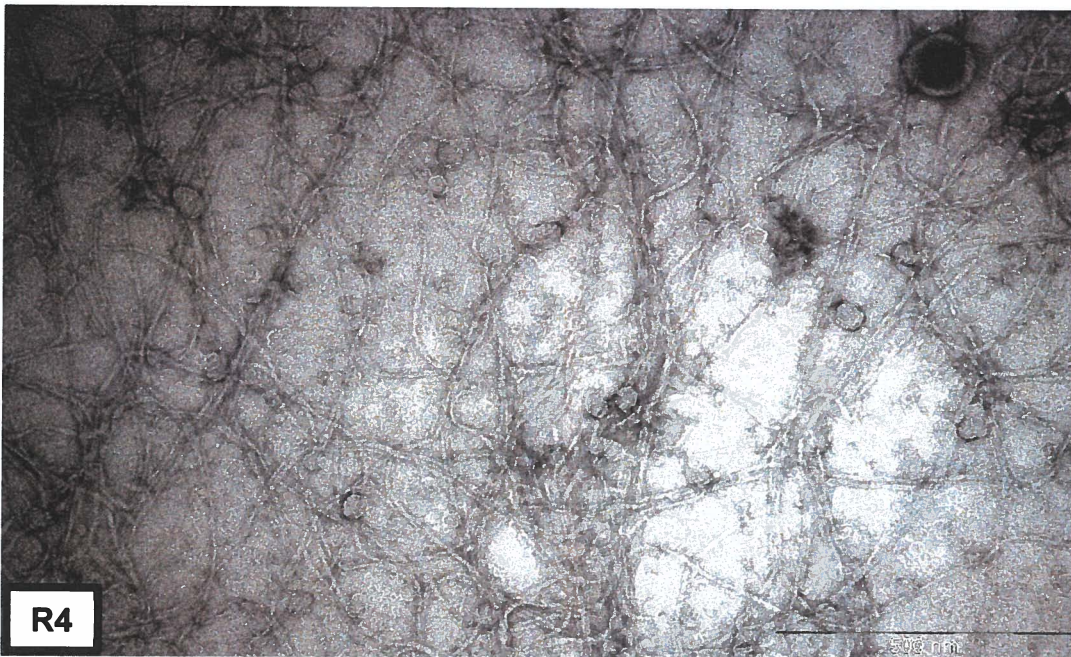
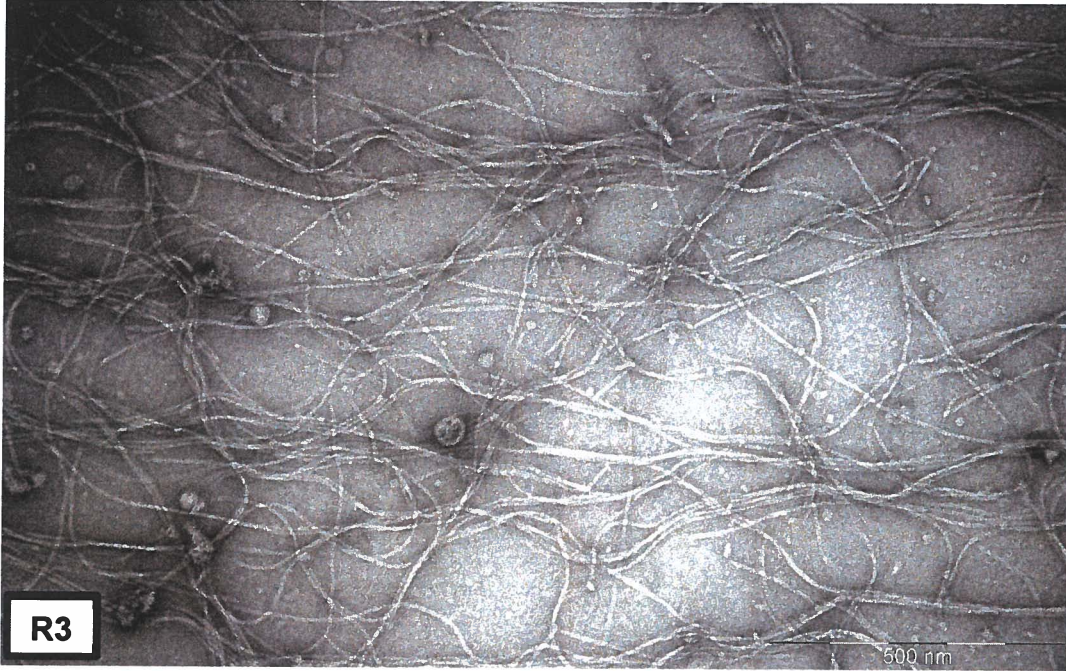
should be given to cocktail of phages which target not just the pilus but also other phage binding sites to reduce remaining bacteria in the population. The combination of targets should reduce the frequency of resistance occurring to provide a more robust treatment regimen.

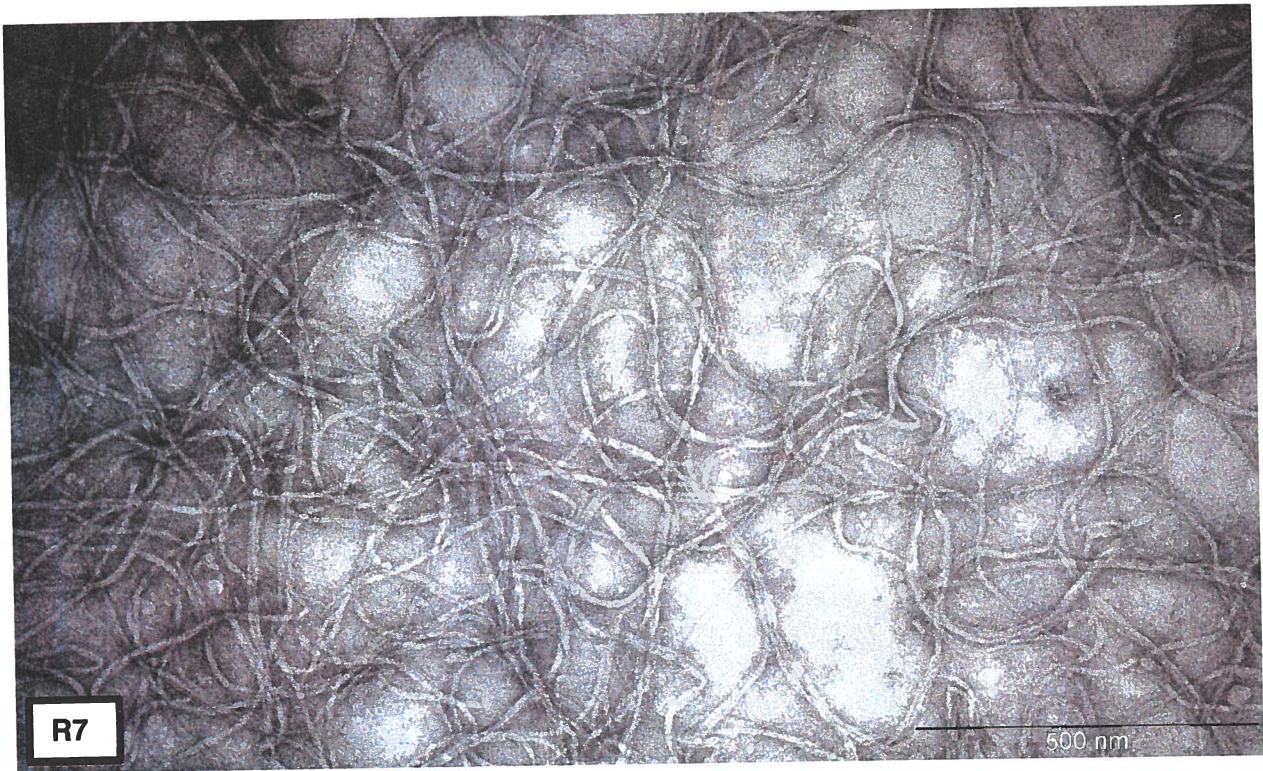
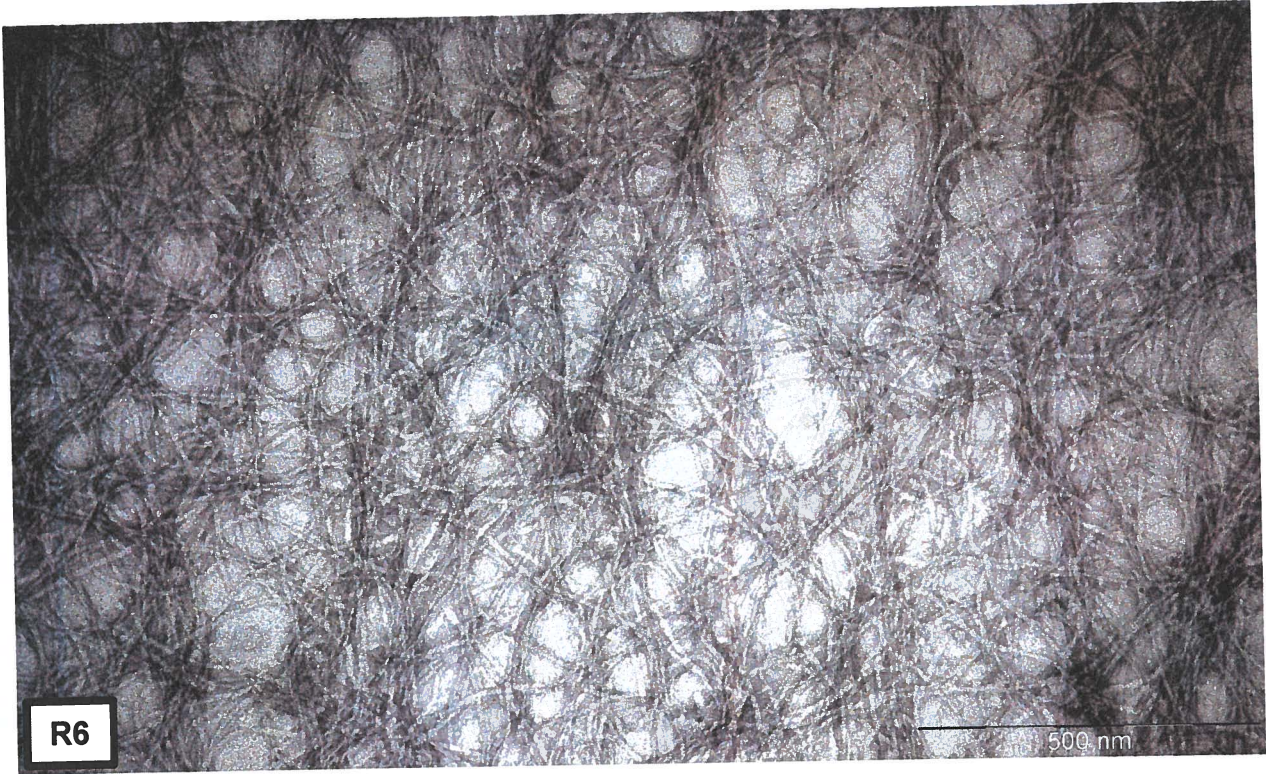
This study has looked at the growth of the alternate SPS phages to other studies but has shown similar limitations to those previously observed. The growth data suggests a role for repression to avoid rapid proliferation and impact of SPS phages in the environment. Although the isolation of SPS phage would suggest that pilus expression is sufficient for phage maintenance. The variable expression of pili from plasmids in the field may prove a hindrance to successful application of this approach. However, if a route to interfere with repression *in vivo* can be found then it may provide a window of opportunity to control plasmid mediated AMR infection.

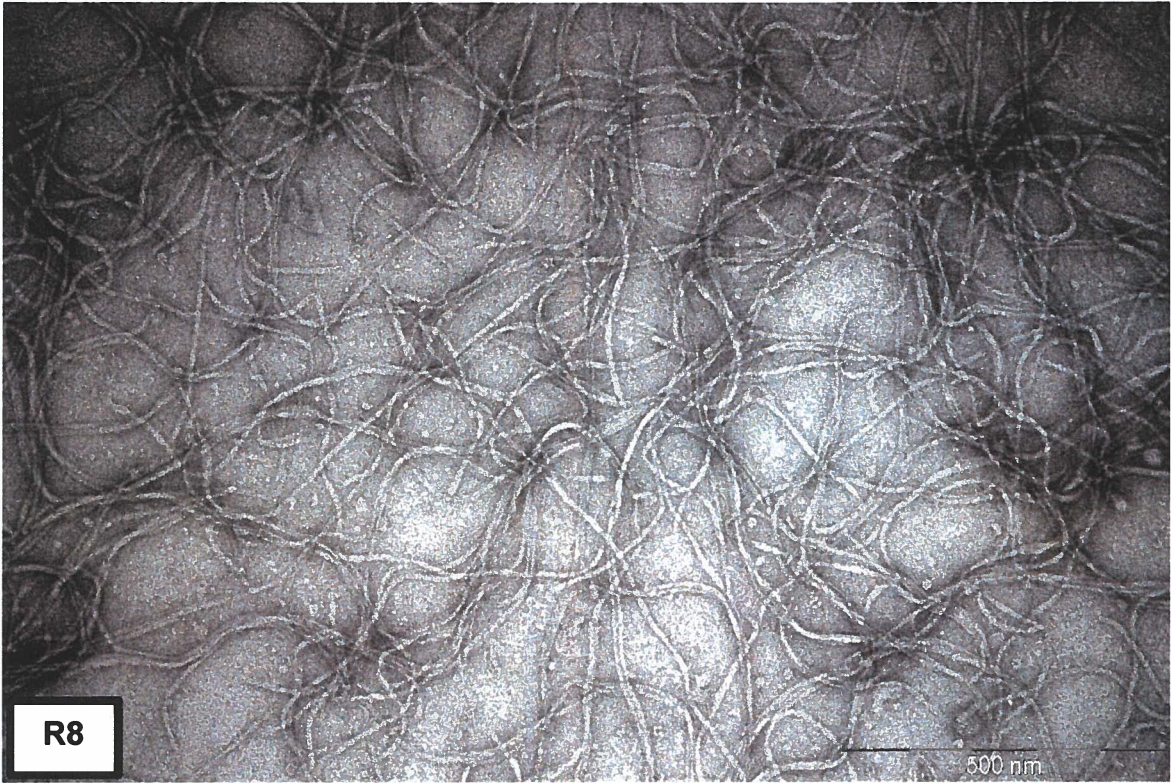
Appendix A.

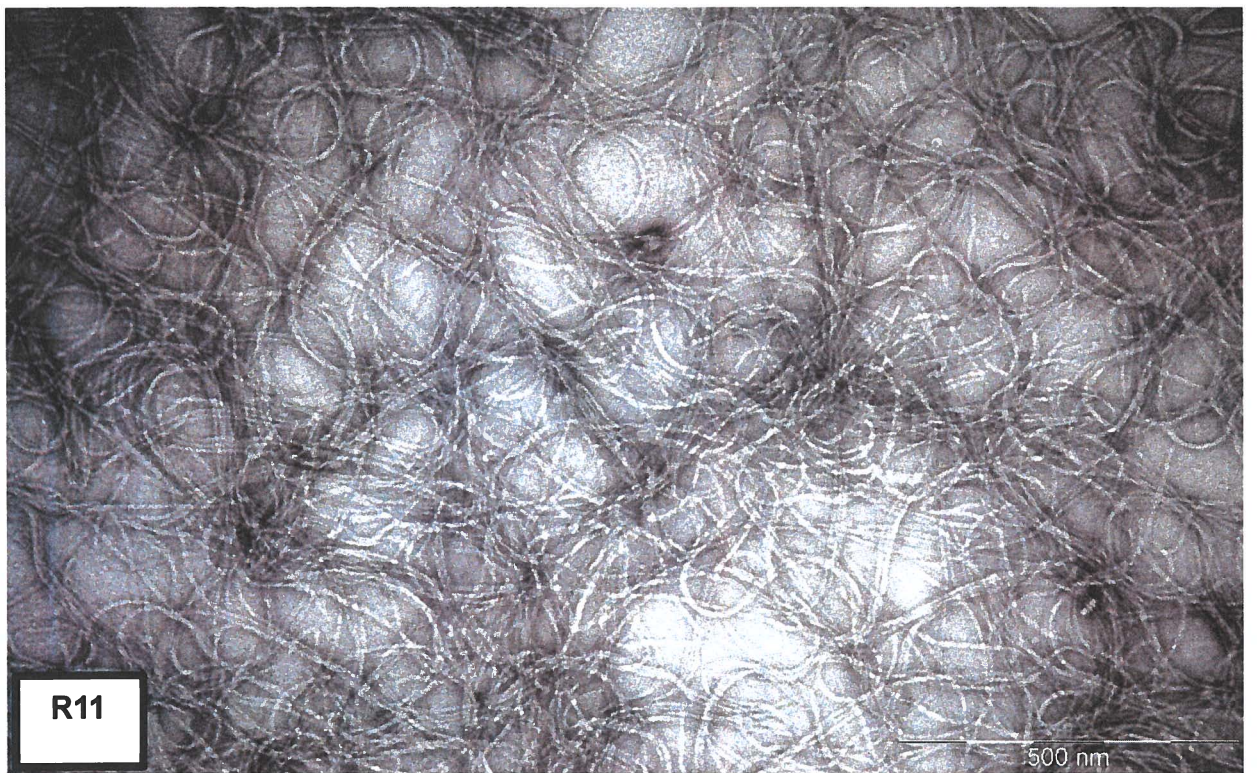
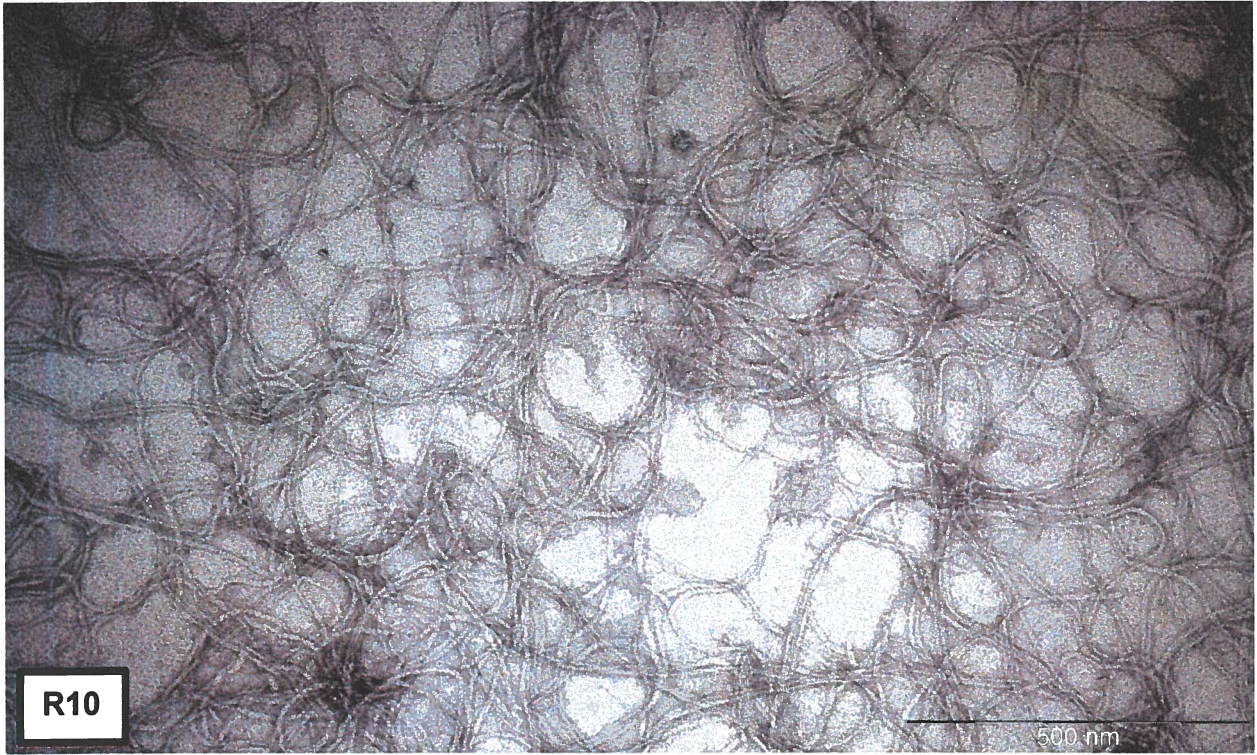
Transmission Electron Micrograph of isolated phages

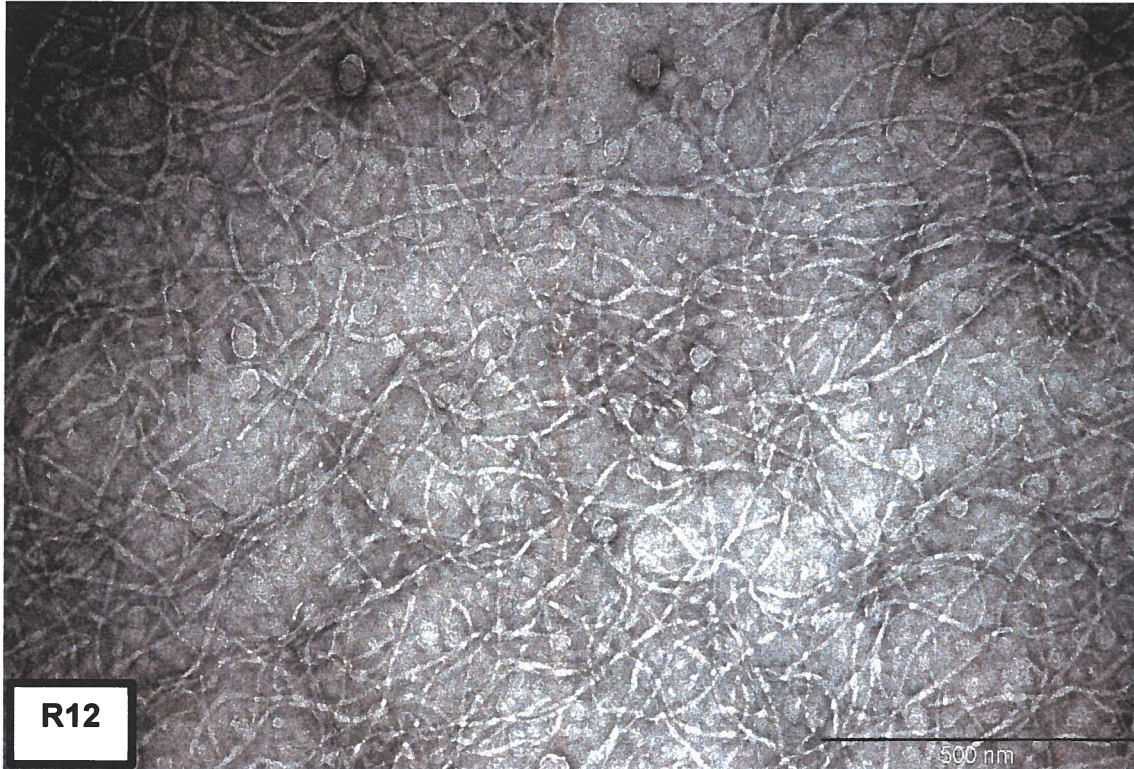




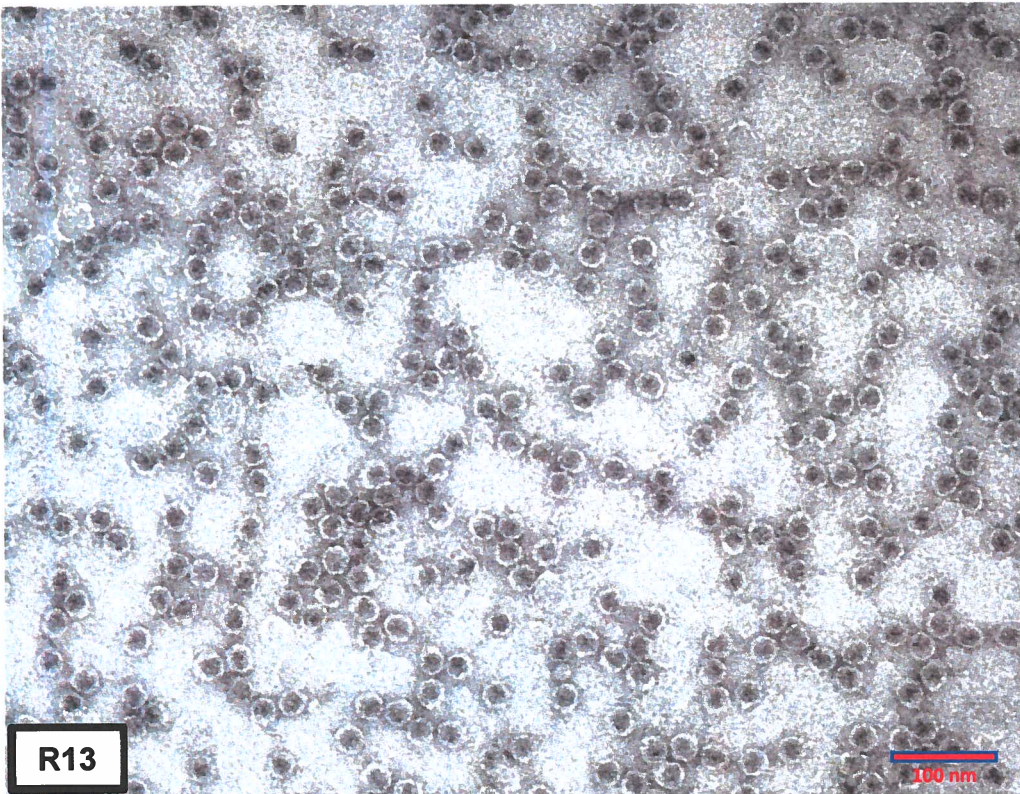
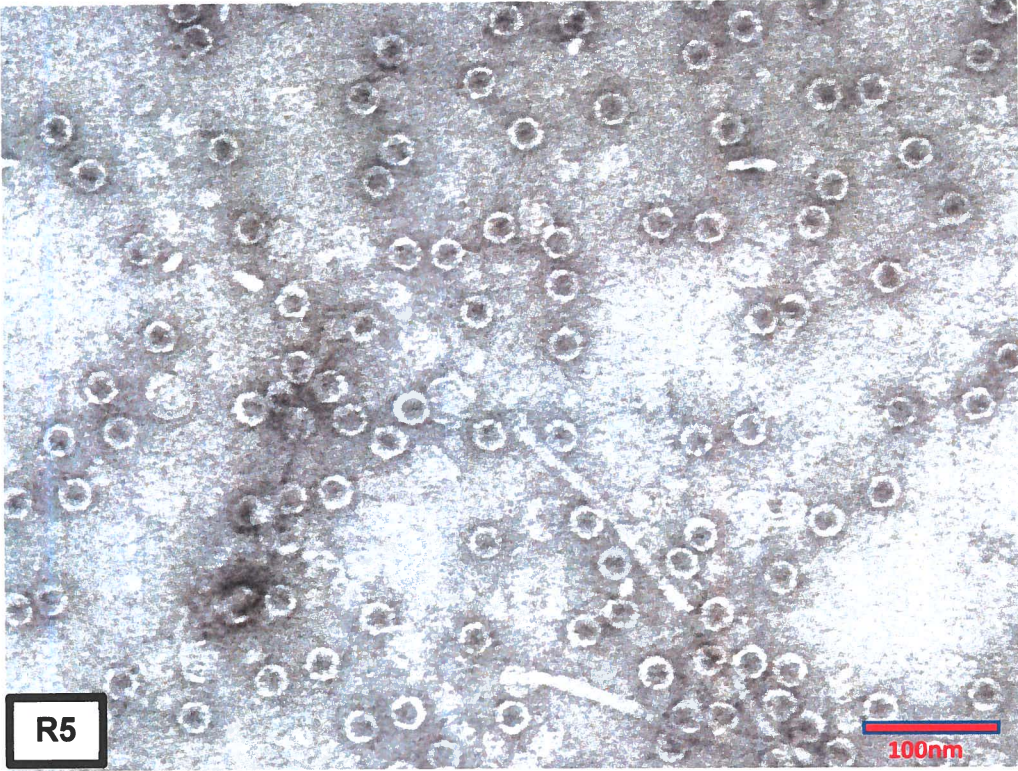


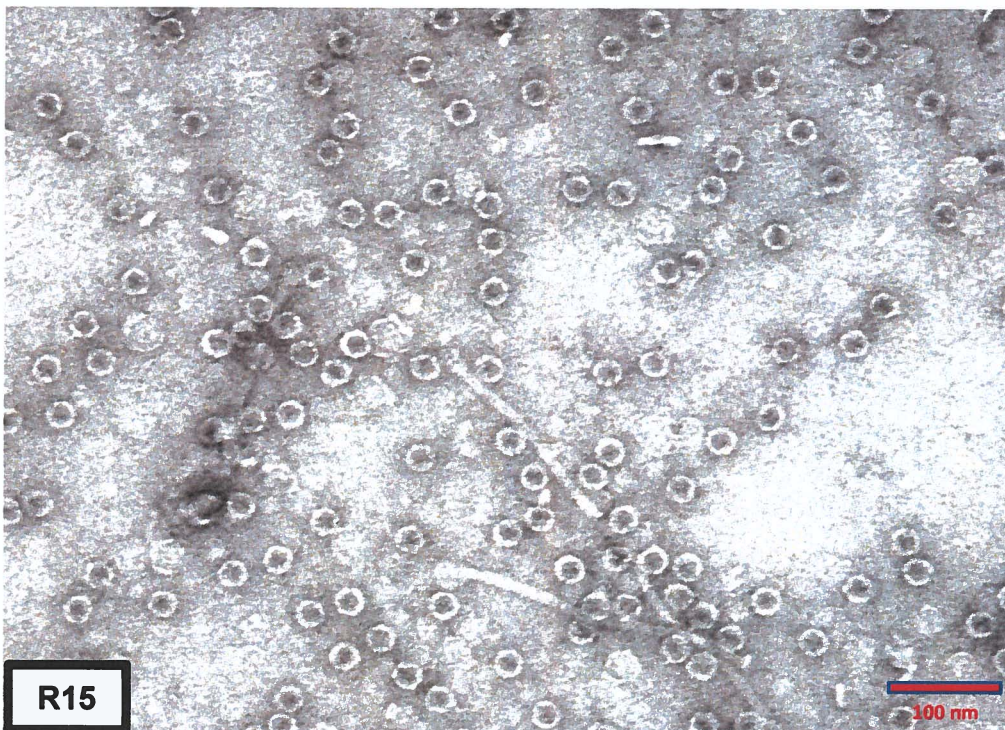
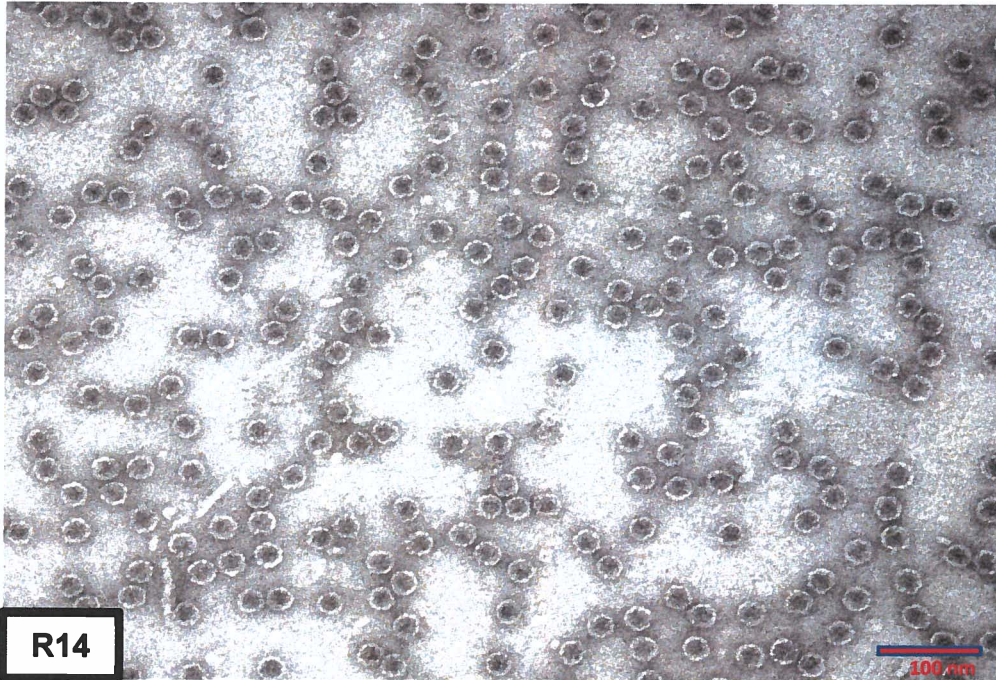






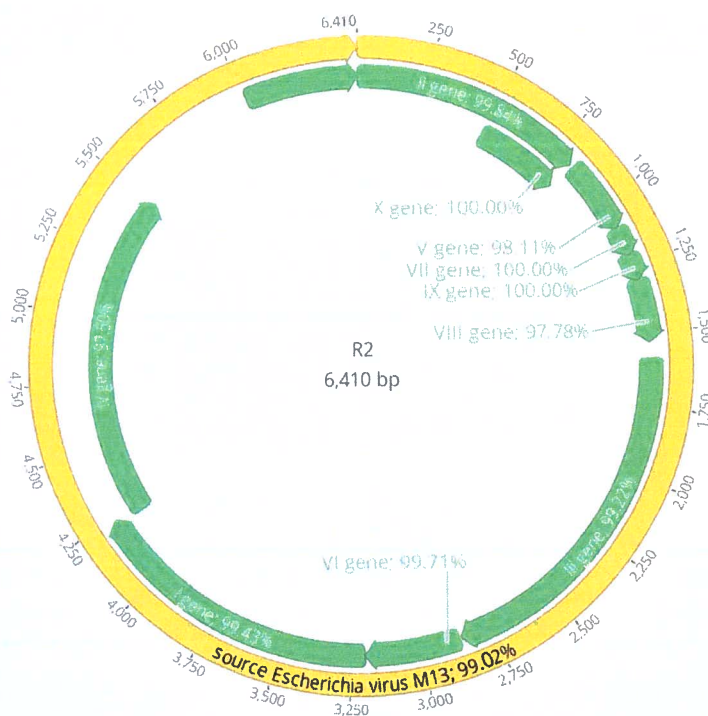
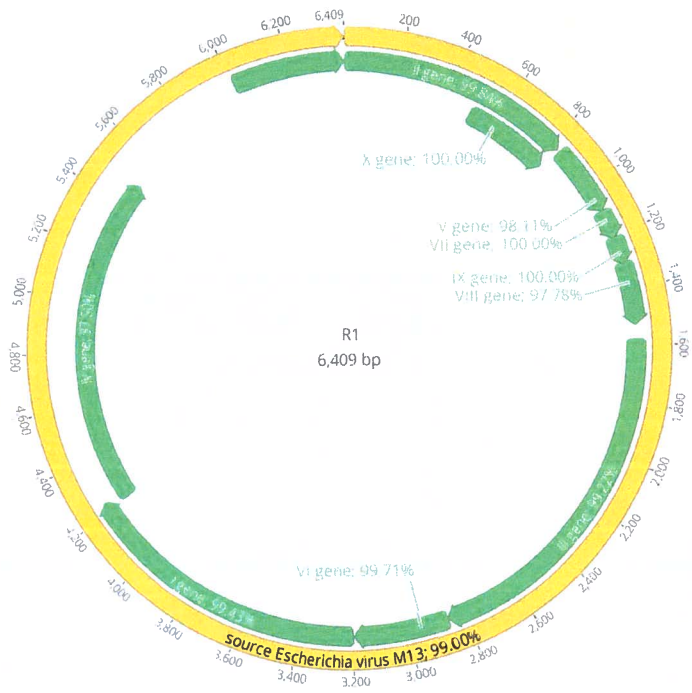
Transmission Electron Microscopy (TEM) of isolated ssDNA phages.
All electron micrographs were taken at 100,000 x magnification by a JEOL JEM-1400 transmission electron microscope. The bar represents 500 nm.

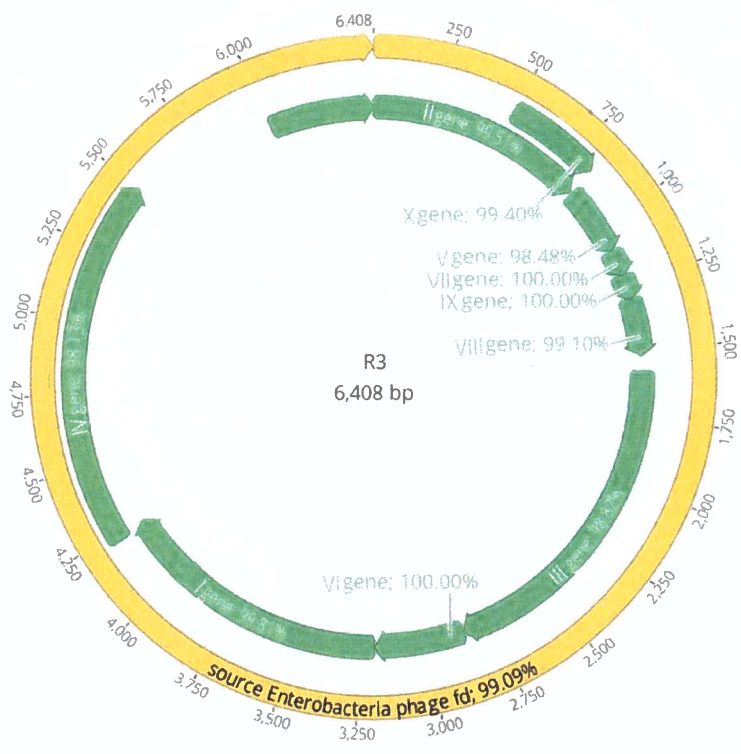
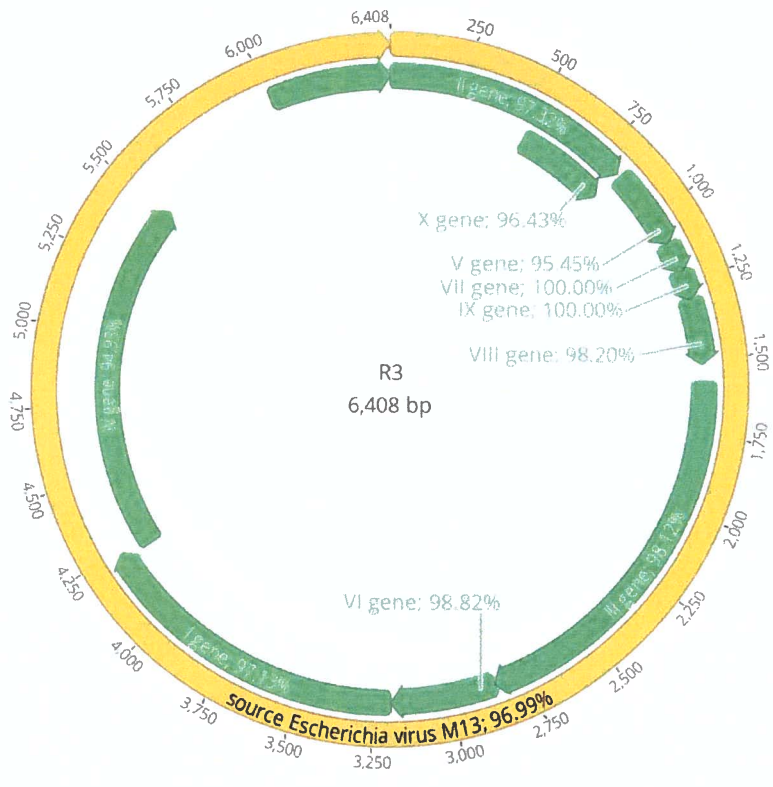


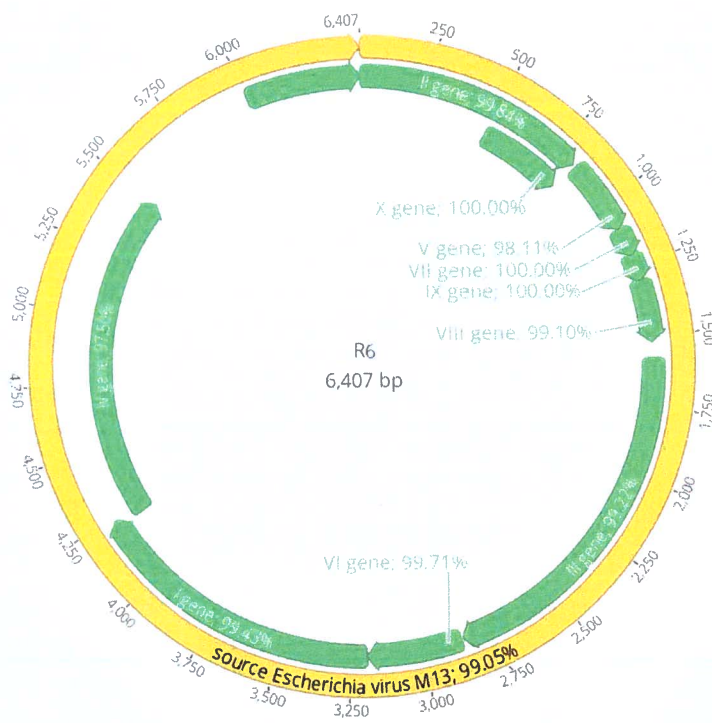
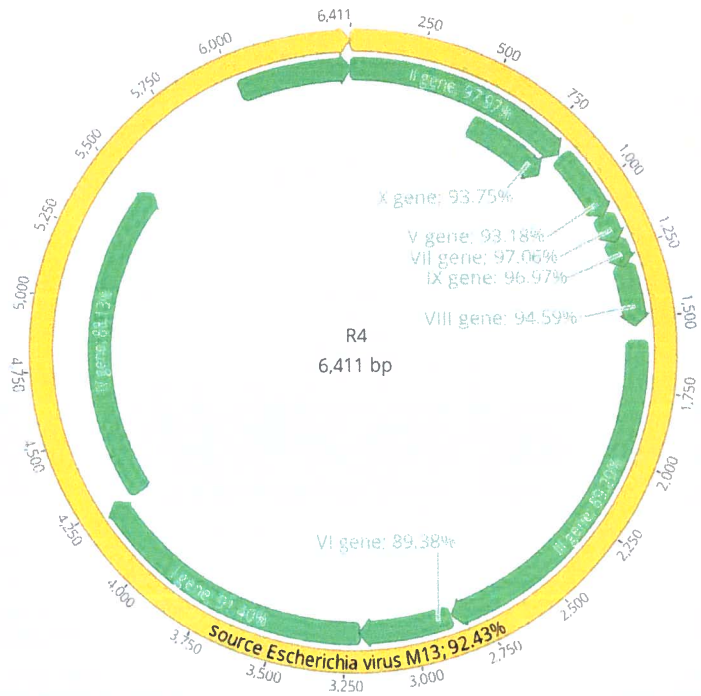


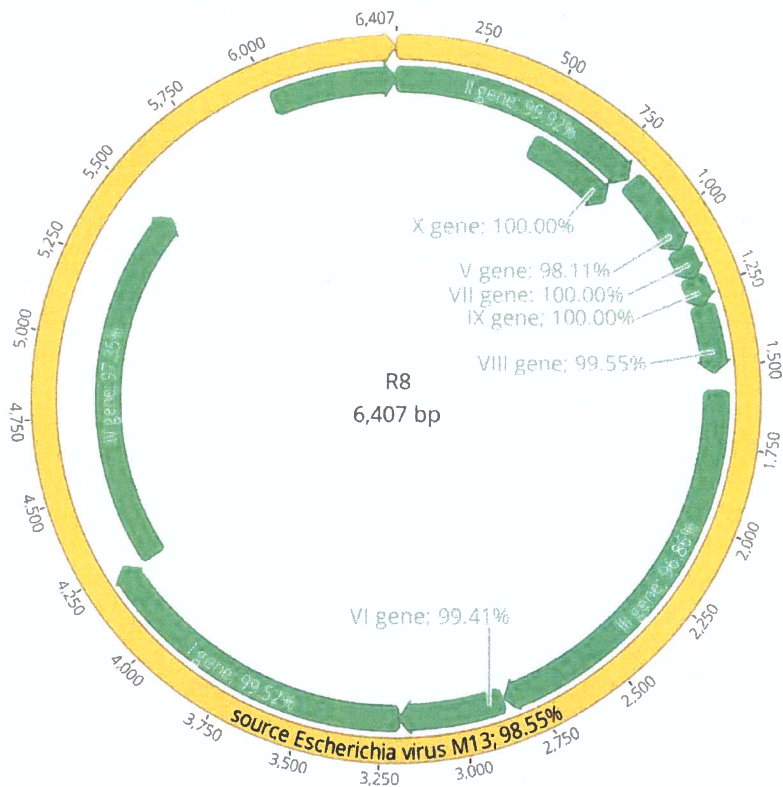
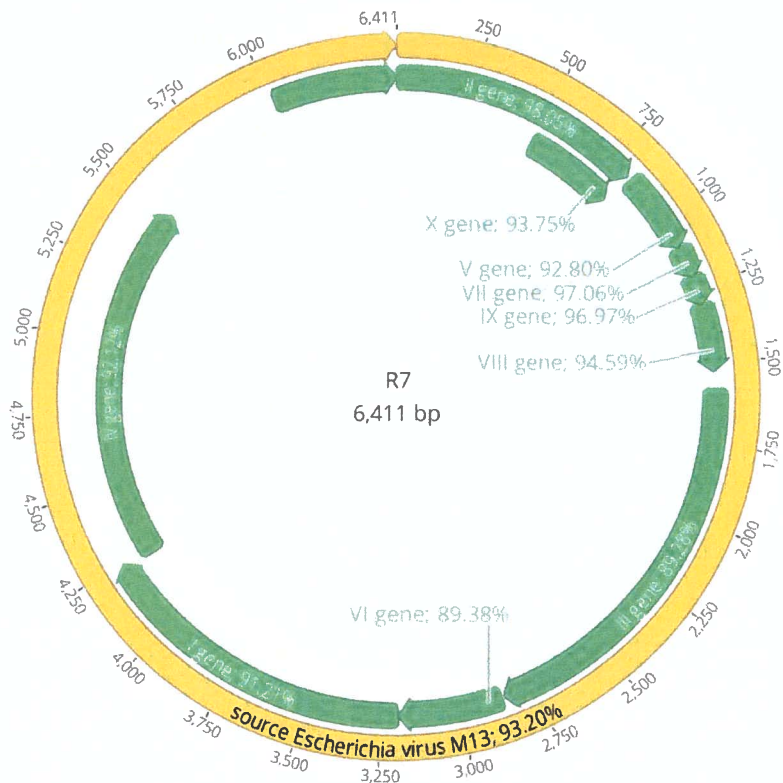
Transmission Electron Microscopy (TEM) of isolated ssRNA phages. All electron micrographs were taken at 100,000 x magnification by a JEOL JEM-1400 transmission electron microscope. The bar represents 500 nm.

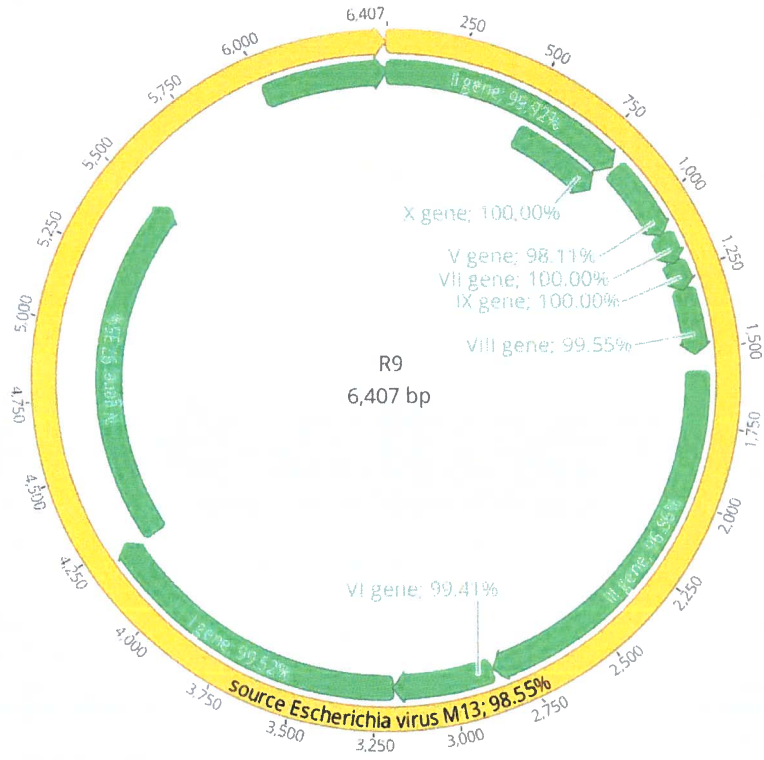
Appendix B.

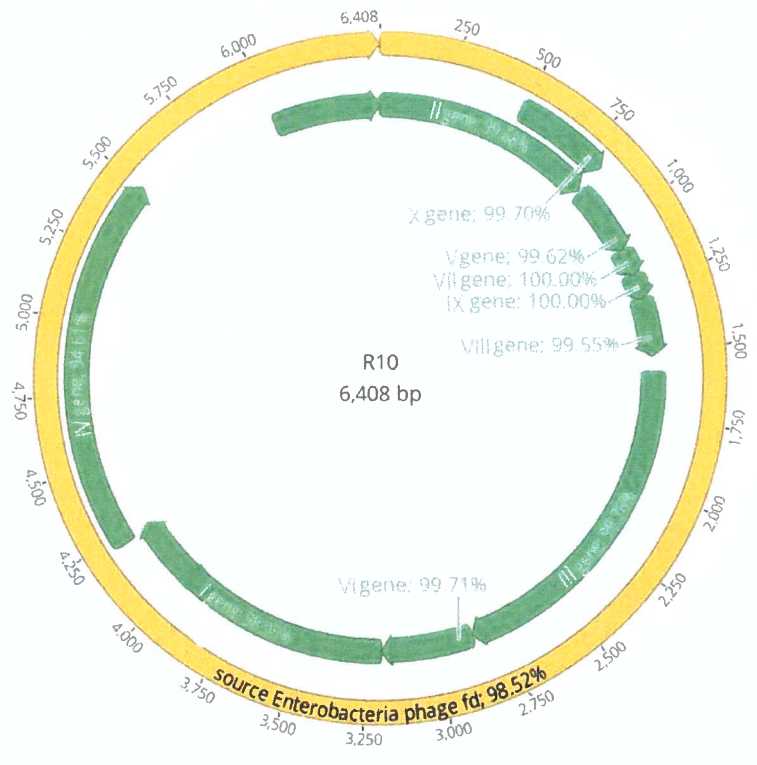
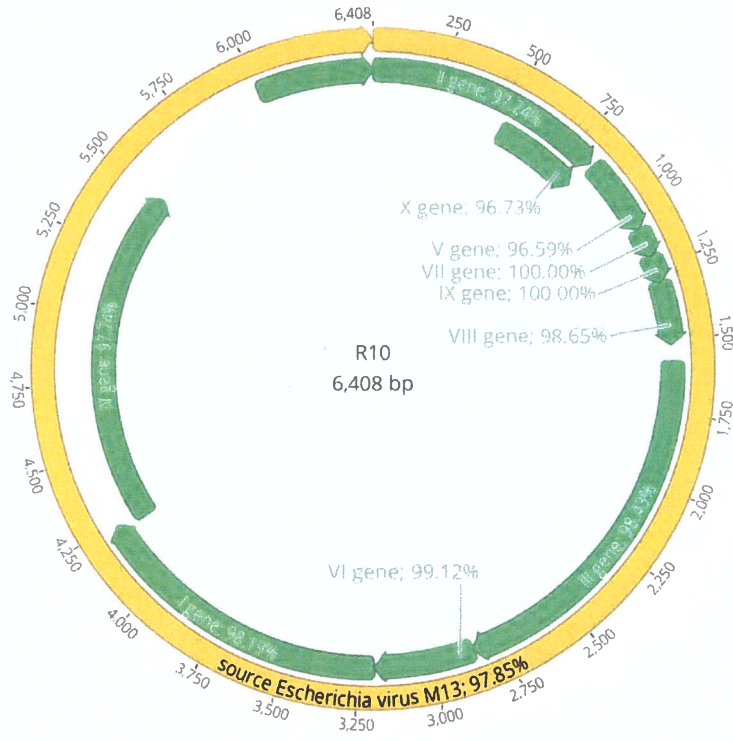


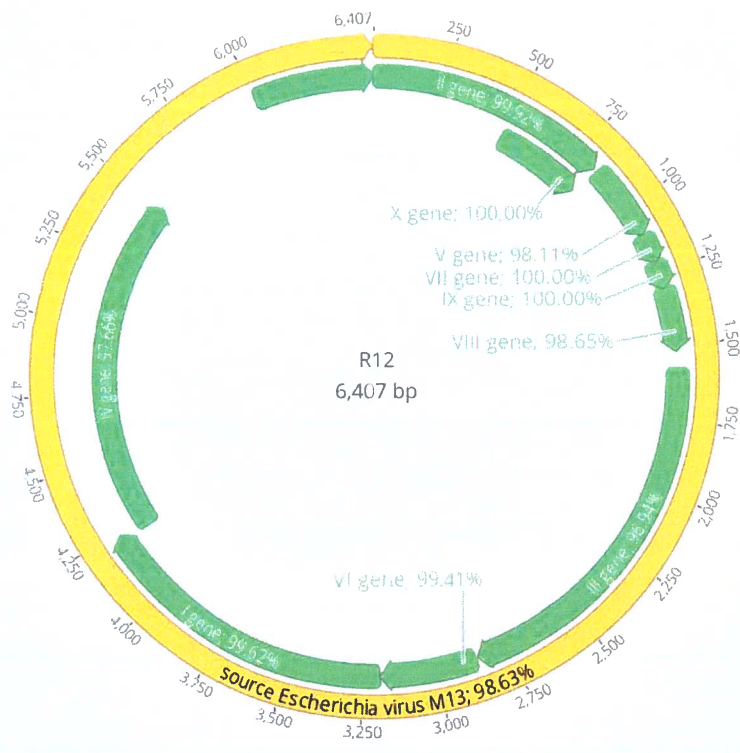
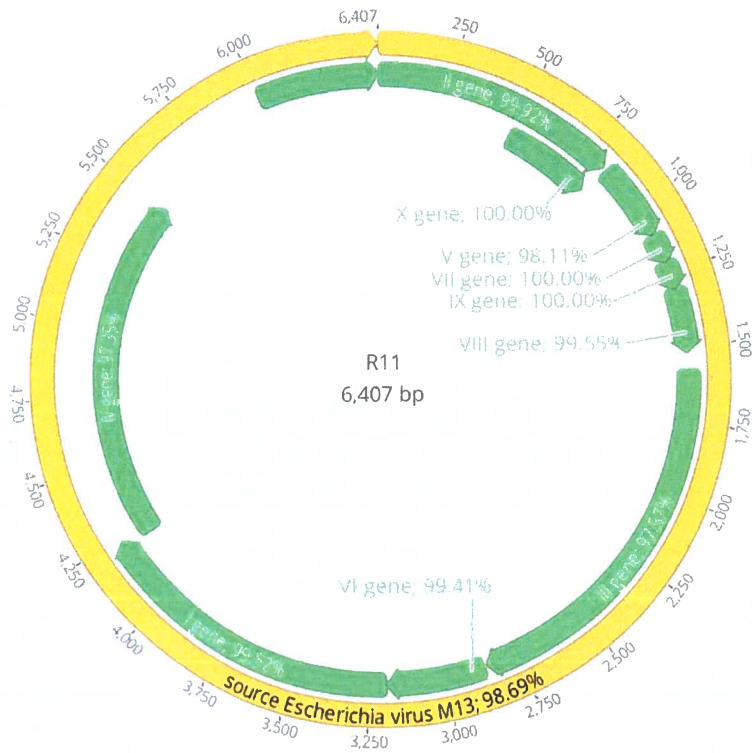




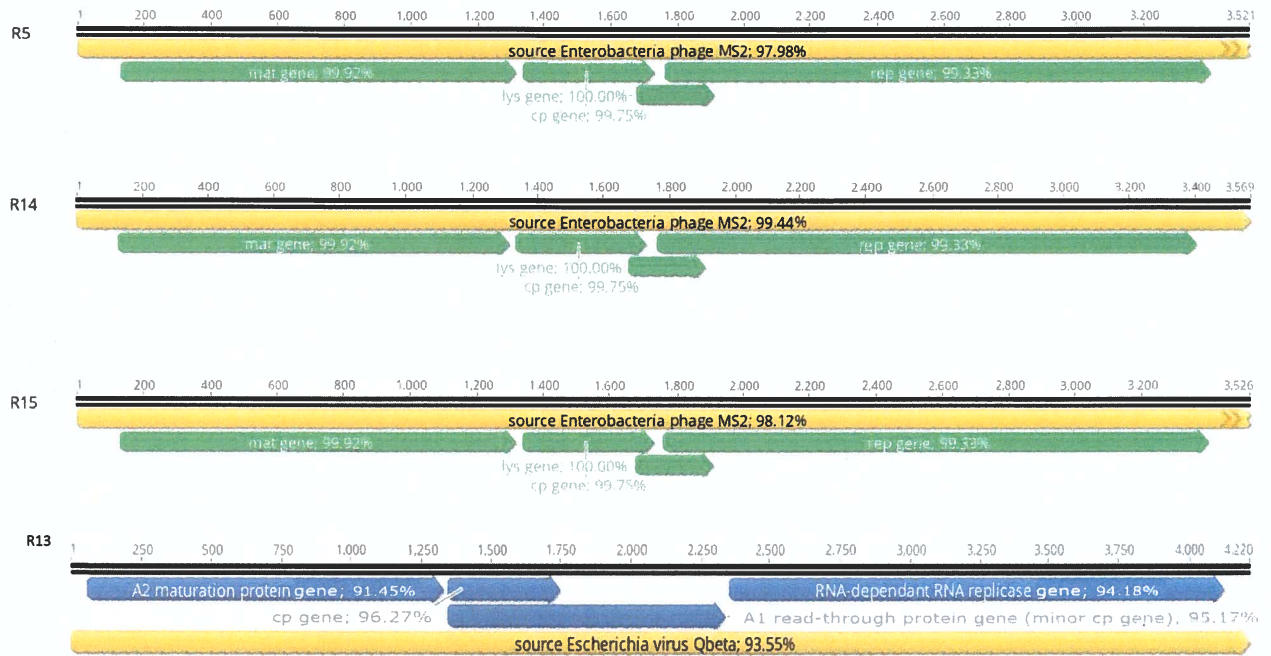








Genetic maps of isolated ssDNA phages.



Genetic maps of isolated ssRNA phages.

Appendix C.

Appendix C: Nottingham BBSRC DTP Stipulated PIPS Reflective Statement

Note to examiners:

This statement is included as an appendix to the thesis in order that the thesis accurately captures the PhD training experienced by the candidate as a BBSRC Doctoral Training Partnership student.

The Professional Internship for PhD Students is a compulsory 3-month placement which must be undertaken by DTP students. It is usually centred on a specific project and must not be related to the PhD project. This reflective statement is designed to capture the skills development which has taken place during the student's placement and the impact on their career plans it has had.

I already had a stable career in veterinary microbiology and diagnostics when I decided to go back to university, so it was a decision that I took very seriously. My goals in pursuing a PhD were not only to gain expertise in my chosen research topic, but also to develop a well-rounded set of skills that I can apply to a wide range of opportunities. It was primarily the inclusion of the PIPS internship in the BBSRC DTP PhD program that attracted me and made up my mind to apply.

Choosing where and what to do for my internship was a daunting task. Growing up from a poor background, I needed to work hard to overcome significant life challenges. One of my objectives for my internship was therefore to learn how my academic research could be utilised for policy-making for the betterment of society. DTP and Graduate School staff helped me set SMART goals

(Specific, Measurable, Attainable, Relevant and Timely) for my internship which enabled me to identify the work I wanted to do, and the right type of host organisation.

As a veterinary microbiologist, I am interested in antimicrobial resistance (AMR) because it is considered as one of the greatest threats to mankind and has a significant impact in poorer countries. Therefore, I decided to do my internship at the Food and Agriculture Organization (FAO) of the United Nations - Regional Office for Asia and the Pacific (FAO-RAP) in Bangkok, Thailand.

At FAO, I had the privilege to work with Dr. Katinka de Balogh, Senior Animal Production and Health Officer of the FAO-RAP and with the AMR team headed by Dr. Joy Gordoncillo. I was mainly involved in two AMR projects: mitigating the effects of antimicrobial resistance through creating awareness on the threat of AMR in the Asia Pacific region; enhancing surveillance on AMR and antimicrobial use (AMU) as well as providing policy guidance and good practices in line with AMR-Global Action Plan (GAP). I had independence and flexibility on what skills-sets that I wanted to develop and share with the team; such as on AMR, AMU, risk communications, and good practices. During my internship I was able to work closely with the AMR team on issues related to AMU, AMR, risk management, risk communications, and good practices. Through this, I also gained an excellent overview of the day to day work of the organization, how meetings are being conducted and I had the opportunity to work with other international collaborators and country officers in the Asia Pacific Region.

I had the opportunity to work with the One Health Tripartite Coordination Group FAO/WHO/OIE/UNEP, which provided me with the opportunity to learn how combating the problem of AMR is being addressed in a "One Health" approach. I was also highly involved in the FAO's GAP on AMR which focuses on Awareness, Surveillance, Governance and Stewardship on AMR. I was involved in the formulation of Surveillance Guideline in bacterial pathogens from diseased livestock and poultry and assisted in reviewing the AMR Regional Surveillance of antimicrobial resistance in bacteria from healthy food animals intended for consumption. I got also involved in organising two international AMR Technical Seminar: Introduction to essential basic concepts on AMR for future veterinarians and Practical actions and antimicrobial stewardship in veterinary practice during the World Antibiotic Awareness Week (WAAW). I was able to deliver a plenary presentation on alternatives to antibiotics during this seminar.

During my internship, I was involved in many projects, such as the formulation of surveillance guidelines and writing a background paper on alternatives to antibiotics utilising my PhD research knowledge. I was also able to attend conferences, webinars and transferrable skills workshops on creative and critical thinking, and resilience building.


My internship at FAO-RAP exceeded all my expectations. It helped me to build a network that will be useful for my future career, make friendships, allowed me to explore the country, and I developed new sets of skills outside of the laboratory. Most importantly though, the internship enriched my perspectives on the type of work that

I want to do upon the completion of my PhD; and cemented a desire to give back to society and help to improve the lives of others.


I would like to thank the BBSRC DTP and Graduate School teams headed by Prof. Zoe Wilson for guidance, financial support and my pre-internship orientation. I would also like to thank everyone at the FAO-RAP AMR team, headed by Dr. Joy Gordoncillo. Finally, I am very grateful and indebted to Dr. Katinka de Balogh, my supervisor at FAO for making my internship a very productive one and for all the opportunities for personal and professional development.

Appendix D.

Research Poster Presented at The 23rd Biennial Evergreen International Phage Biology Meeting, The Evergreen College, Olympia, WA 98505, USA, 2019.



The University of Nottingham
UNITED KINGDOM · CHINA · MALAYSIA



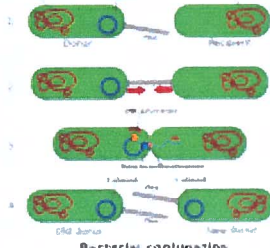
BBSRC Doctoral Training Partnerships

Isolation and characterisation of sex pilus-specific bacteriophage

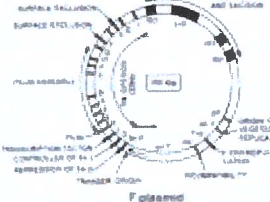
Ramon P. Maluping*, Robert Atterbury, Paul Barrow and Michael A. Jones
School of Veterinary Medicine and Science, University of Nottingham, Sutton Bonington Campus, Leicestershire, LE12 5RD, UK
*E-mail address: ramon.maluping@nottingham.ac.uk

Background

- Bacterial conjugation is a sexual mode of genetic transfer whereby bacteria become resistant to antibiotics due to transfer of antimicrobial resistance (AMR) plasmids.
- F plasmid is an example of a conjugative AMR plasmid that contains transfer (*tra*) genes that allow plasmids to be transferred from one bacterium to another through the F conjugative sex pilus.
- These pilus also serve as the binding site of a variety of phages that, upon attaching to them, either can inhibit conjugation or kill the host.
- The use of these sex pilus specific phages might have several advantages:
 - 1) bacteria containing the conjugative AMR plasmids are killed,
 - 2) phage selects for naturally occurring mutants which in this case have spontaneously lost their plasmid,
 - 3) these bacteria, which lost their AMR plasmid multiply faster and eventually predominate.

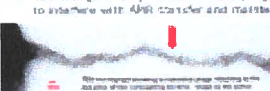



Bacterial conjugation



Aim:

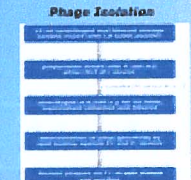
- To isolate and characterise sex pilus phages which are specific for fertility (*F₊*) cells.
- To investigate the potential of these phage to interfere with AMR transfer and maintenance.

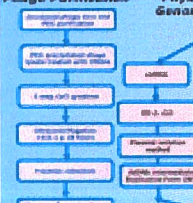
Evergreen Phage Lab

Methods


Phage Isolation



Phage Purification

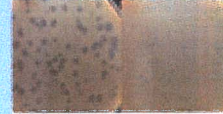


Physical, Biochemical & Genomic Characteristics



Results

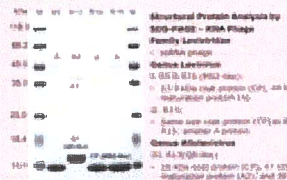
Phage	Host	Hydrophobicity	Stability	Characterisation	Thermal stability	pH stability	Conductivity
R1	F	+	+	+	+	+	+
R2	F	+	+	+	+	+	+
R3	F	+	+	+	+	+	+
R4	F	+	+	+	+	+	+
R5	F	+	+	+	+	+	+
R6	F	+	+	+	+	+	+
R7	F	+	+	+	+	+	+
R8	F	+	+	+	+	+	+
R9	F	+	+	+	+	+	+
R10	F	+	+	+	+	+	+
R11	F	+	+	+	+	+	+
R12	F	+	+	+	+	+	+
R13	F	+	+	+	+	+	+
R14	F	+	+	+	+	+	+
R15	F	+	+	+	+	+	+
R16	F	+	+	+	+	+	+
R17	F	+	+	+	+	+	+



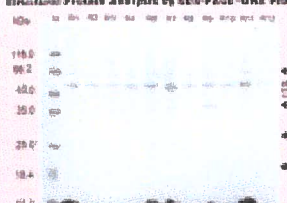
Phage R11, top panel measuring an average diameter of 26.5 nm. Phage R12, bottom panel measuring an average length of 166 nm.

Results

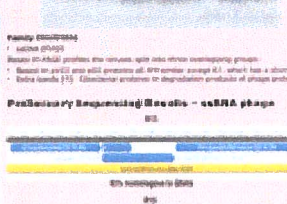
Structural Protein Analysis by SDS-PAGE - SRA Phage



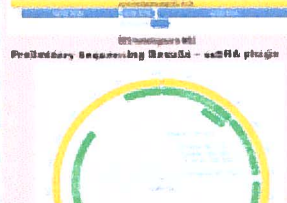
Structural Protein Analysis by SDS-PAGE - SRA Phage



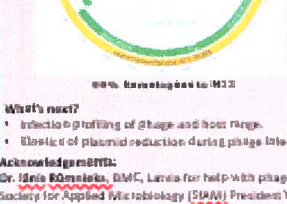
Proteomic Sequencing Results - SRA phage



Proteomic Sequencing Results - SRA phage



Proteomic Sequencing Results - SRA phage



What's next?

- Infectio-phage profiling of phage and host range.
- Effects of plasmid reduction during phage infection.

Acknowledgements:
Dr. Irena Komolova, DMC, Latvia for help with phage work; Society for Applied Microbiology (SfAM) President's Fund; Federation of European Microbiological Societies (FEMS) & Evergreen Phage Lab for the Meeting Grants received.

Appendix E.

I. Sample Raw Data: One Step Growth Curve of phage R4 on *E. coli* with derepressed plasmid

One Step Growth Curve of phage R4 on *E. coli* with derepressed plasmid

Time	Exp 1		Exp 2		Exp 3		Log ₁₀		Log ₁₀		Log ₁₀	
	Count 1	Count 2	Count 1	Count 2	Count 1	Count 2	Count 1	Count 2	Average	SEM	SD	Average
0	9.20E+05	8.80E+05	1.20E+06	1.10E+06	1.00E+06	1.00E+06	1.00E+06	1.00E+06	1.01E+06	6.96E+04	1.21E+05	6.00
5	8.50E+05	7.50E+05	9.80E+05	9.80E+05	9.80E+05	9.20E+05	9.50E+05	9.10E+05	9.10E+05	5.57E+04	9.64E+04	5.96
10	9.00E+05	1.10E+06	8.50E+05	9.50E+05	9.00E+05	8.40E+05	8.70E+05	9.23E+05	9.23E+05	3.93E+04	6.81E+04	5.96
20	1.20E+08	1.20E+08	5.00E+07	5.40E+07	9.00E+07	9.00E+07	9.00E+07	8.73E+07	8.73E+07	1.97E+07	3.41E+07	7.92
30	4.30E+08	4.10E+08	4.00E+08	4.00E+08	4.10E+08	3.50E+08	3.80E+08	4.00E+08	4.00E+08	1.15E+07	2.00E+07	8.60
60	5.80E+10	6.20E+10	2.80E+11	2.70E+11	1.30E+11	1.30E+11	1.30E+11	1.54E+11	1.54E+11	6.24E+10	1.08E+11	11.11
90	1.60E+12	1.60E+12	1.64E+12	1.60E+12	1.92E+12	1.84E+12	1.88E+12	1.70E+12	1.70E+12	9.02E+10	1.56E+11	12.23
120	1.60E+13	1.40E+13	1.94E+15	1.98E+15	1.80E+15	2.00E+15	1.90E+15	1.29E+15	1.29E+15	6.39E+14	1.11E+15	15.11
BS			465.56		350.09		379.13	398.26	398.26	34.68	60.06	2.60
												2.67
												2.54
												2.58
												2.60
												0.03
												0.03
												0.02
												0.11
												0.01
												0.19
												0.02
												0.70
												0.04

End of Latent Period **10 mins**

End of Rise Period **30 mins**

Duration of Rise Period **20 mins**

Burst Size (BS) = (PFU End of Rise - PFU End of Latent)/ number of Infected Bacteria at T0

II. Sample Raw Data: One Step Growth Curve of phage R4 on *E. coli* with repressed plasmid

One Step Growth Curve of phage R4 on *E. coli* with repressed plasmid

Time	Exp 1		Exp 2		Exp 3		Average		SEM	SD
	Count 1	Count 2	Count 1	Count 2	Count 1	Count 2	Exp 1 to 3	Exp 1 to 3		
0	7.20E+04	7.60E+04	7.40E+04	7.00E+04	7.20E+04	8.20E+04	8.00E+04	7.53E+04	1.66E+03	4.39E+03
5	9.80E+04	9.80E+04	9.20E+04	9.20E+04	9.20E+04	7.40E+04	8.00E+04	9.00E+04	3.13E+03	8.28E+03
10	1.60E+05	1.00E+05	1.00E+05	1.00E+05	1.00E+05	1.00E+05	1.00E+05	1.07E+05	2.86E+03	7.56E+03
20	1.00E+05	1.00E+05	1.00E+05	1.20E+05	1.10E+05	1.40E+05	1.20E+05	1.10E+05	5.65E+03	1.50E+04
30	2.80E+05	3.20E+05	4.00E+05	4.00E+05	4.00E+05	5.00E+05	5.00E+05	4.00E+05	2.86E+04	7.56E+04
60	3.00E+05	3.00E+05	5.20E+06	4.80E+06	5.00E+05	5.20E+05	5.00E+05	4.33E+05	8.39E+05	2.22E+06
90	5.40E+08	4.60E+08	7.20E+05	6.80E+05	7.00E+05	6.40E+05	6.00E+05	6.00E+05	3.02E+04	7.99E+04
120	6.00E+05	6.00E+05	7.00E+05	7.00E+05	7.00E+05	7.00E+05	7.00E+05	6.67E+05	1.43E+04	3.78E+04
BS			2.70		4.03		4.75	3.83	0.60	1.04

End of Latent Period **20 mins**

End of Rise Period **30 mins**

Duration of Rise Period **10 mins**

Burst Size (BS) = (PFU End of Rise - PFU End of Latent) / number of Infected Bacteria at T0

References

- Abedon, S. T. & Thomas-Abedon, C. 2010. Phage therapy pharmacology. *Curr Pharm Biotechnol*, 11, 28-47.
- Ackermann, H.-W. 1987. *Viruses Of Prokaryotes*, CRC Pres.
- Ackermann, H.-W. 2005. Bacteriophage classification. In: KUTTER, E., SULAKVELIDZE, A. (ed.) *Bacteriophages: Biology and Applications*. Boca Raton: CRC Press.
- Ackermann, H. W. 2007. 5500 Phages examined in the electron microscope. *Arch Virol*, 152, 227-43.
- Ackermann, H. W. 2009. Phage classification and characterization. *Methods Mol Biol*, 501, 127-40.
- Adriaenssens, E. & Brister, J. R. 2017. How to Name and Classify Your Phage: An Informal Guide. *Viruses*, 9.
- Adriaenssens, E. M., Krupovic, M., Knezevic, P., Ackermann, H.-W., Barylski, J., Brister, J. R., Clokie, M. R., Duffy, S., Dutilh, B. E. & Edwards, R. A. 2017. Taxonomy of prokaryotic viruses: 2016 update from the ICTV bacterial and archaeal viruses subcommittee. *Archives of virology*, 162, 1153-1157.
- Adriaenssens, E. M., Sullivan, M. B., Knezevic, P., Van Zyl, L. J., Sarkar, B., Dutilh, B. E., Alfenas-Zerbini, P., Łobocka, M., Tong, Y. & Brister, J. R. 2020. Taxonomy of prokaryotic viruses: 2018-2019 update from the ICTV Bacterial and Archaeal Viruses Subcommittee. *Archives of virology*, 1-8.
- Austin, D. J., Kristinsson, K. G. & Anderson, R. M. 1999. The relationship between the volume of antimicrobial consumption in human communities and the frequency of resistance. *Proc Natl Acad Sci U S A*, 96, 1152-6.
- Baig, A., Colom, J., Barrow, P., Schouler, C., Moodley, A., Lavigne, R. & Atterbury, R. 2017. Biology and Genomics of an Historic Therapeutic Escherichia coli Bacteriophage Collection. *Front Microbiol*, 8, 1652.
- Bankevich, A., Nurk, S., Antipov, D., Gurevich, A. A., Dvorkin, M., Kulikov, A. S., Lesin, V. M., Nikolenko, S. I., Pham, S., Prjibelski, A. D., Pyshkin, A. V., Sirotkin, A. V., Vyahhi, N., Tesler, G., Alekseyev, M. A. & Pevzner, P. A. 2012. SPAdes: a new genome assembly algorithm and its applications to single-cell sequencing. *J Comput Biol*, 19, 455-77.
- Baquero, F., Coque, T. M. & De La Cruz, F. 2011. Ecology and evolution as targets: the need for novel eco-evo drugs and strategies to fight antibiotic resistance. *Antimicrob Agents Chemother*, 55, 3649-60.
- Barrow, P., Lovell, M. & Berchieri, A., Jr. 1998. Use of lytic bacteriophage for control of experimental Escherichia coli septicemia and meningitis in chickens and calves. *Clin Diagn Lab Immunol*, 5, 294-8.
- Barrow, P. A. 1991. Experimental infection of chickens with Salmonella enteritidis. *Avian Pathol*, 20, 145-53.
- Barrow, P. A. & Hill, A. W. 1989. The virulence characteristics of strains of Escherichia coli isolated from cases of bovine mastitis in England and Wales. *Vet Microbiol*, 20, 35-48.

- Basdew, I. H. & Laing, M. D. 2014. Stress sensitivity assays of bacteriophages associated with *Staphylococcus aureus*, causal organism of bovine mastitis. *African Journal of Microbiology Research*, 8 (2), 200-210.
- Baym, M., Stone, L. K. & Kishony, R. 2016. Multidrug evolutionary strategies to reverse antibiotic resistance. *Science*, 351, aad3292.
- Beekwilder, M. J., Nieuwenhuizen, R. & Van Duin, J. 1995. Secondary structure model for the last two domains of single-stranded RNA phage Q beta. *J Mol Biol*, 247, 903-17.
- Berchieri, A., Jr., Lovell, M. A. & Barrow, P. A. 1991. The activity in the chicken alimentary tract of bacteriophages lytic for *Salmonella typhimurium*. *Res Microbiol*, 142, 541-9.
- Bergstrom, C. T., Lipsitch, M. & Levin, B. R. 2000. Natural selection, infectious transfer and the existence conditions for bacterial plasmids. *Genetics*, 155, 1505-1519.
- Bernhardt, T. G., Wang, I. N., Struck, D. K. & Young, R. 2002. Breaking free: "protein antibiotics" and phage lysis. *Res Microbiol*, 153, 493-501.
- Biswas, B., Adhya, S., Washart, P., Paul, B., Trostel, A. N., Powell, B., Carlton, R. & Merrill, C. R. 2002. Bacteriophage therapy rescues mice bacteremic from a clinical isolate of vancomycin-resistant *Enterococcus faecium*. *Infect Immun*, 70, 204-10.
- Bolger-Munro, M., Cheung, K., Fang, A. & Wang, L. 2013. T4 bacteriophage average burst size varies with *Escherichia coli* B23 cell culture age. *J Exp Microbiol Immunol*, 17, 115-119.
- Bonomo, R. A. 2017. beta-Lactamases: A Focus on Current Challenges. *Cold Spring Harb Perspect Med*, 7.
- Bradley, D. E., Coetsee, J. N., Bothma, T. & Hedges, R. W. 1981. Phage X: a plasmid-dependent, broad host range, filamentous bacterial virus. *J Gen Microbiol*, 126, 389-96.
- Bradley, D. E. & Pitt, T. L. 1974. Pilus-dependence of four *Pseudomonas aeruginosa* bacteriophages with non-contractile tails. *J Gen Virol*, 24, 1-15.
- Bradley, D. E., Taylor, D. E. & Cohen, D. R. 1980. Specification of surface mating systems among conjugative drug resistance plasmids in *Escherichia coli* K-12. *J Bacteriol*, 143, 1466-70.
- Bush, K. & Bradford, P. A. 2016. beta-Lactams and beta-Lactamase Inhibitors: An Overview. *Cold Spring Harb Perspect Med*, 6.
- Bush, K. & Jacoby, G. A. 2010. Updated functional classification of beta-lactamases. *Antimicrob Agents Chemother*, 54, 969-76.
- Callanan, J. & Stockdale, S. R. 2020. Expansion of known ssRNA phage genomes: From tens to over a thousand. 6, eaay5981.
- Callanan, J., Stockdale, S. R., Adriaenssens, E. M., Kuhn, J. H., Rumnieks, J., Pallen, M. J., Shkoporov, A. N., Draper, L. A., Ross, R. P. & Hill, C. 2021. Leviviricetes: expanding and restructuring the taxonomy of bacteria-infecting single-stranded RNA viruses. *Microbial Genomics*, 7.
- Cantón, R., Novais, A., Valverde, A., Machado, E., Peixe, L., Baquero, F. & Coque, T. M. 2008. Prevalence and spread of extended-spectrum β -lactamase-producing Enterobacteriaceae in Europe. *Clinical Microbiology and Infection*, 14, 144-153.

- Carattoli, A. 2009. Resistance plasmid families in Enterobacteriaceae. *Antimicrob Agents Chemother*, 53, 2227-38.
- Carattoli, A., Bertini, A., Villa, L., Falbo, V., Hopkins, K. L. & Threlfall, E. J. 2005a. Identification of plasmids by PCR-based replicon typing. *J Microbiol Methods*, 63, 219-28.
- Carattoli, A., Bertini, A., Villa, L., Falbo, V., Hopkins, K. L. & Threlfall, E. J. 2005b. Identification of plasmids by PCR-based replicon typing. *Journal of Microbiological Methods*, 63, 219-228.
- Card, R. M., Cawthraw, S. A., Nunez-Garcia, J., Ellis, R. J., Kay, G., Pallen, M. J., Woodward, M. J. & Anjum, M. F. 2017. An In Vitro Chicken Gut Model Demonstrates Transfer of a Multidrug Resistance Plasmid from Salmonella to Commensal Escherichia coli. *MBio*, 8.
- Carey-Smith, G. V., Billington, C., Cornelius, A. J., Hudson, J. A. & Heinemann, J. A. 2006. Isolation and characterization of bacteriophages infecting Salmonella spp. *FEMS Microbiol Lett*, 258, 182-6.
- Carlton, R. M. 1999. Phage therapy: past history and future prospects. *Arch Immunol Ther Exp (Warsz)*, 47, 267-74.
- Ceyssens, P. & Lavigne, R. 2010. Introduction to Bacteriophage Biology and Diversity. In: SABOUR, P. M. & GRIFFITHS, M. (eds.) *Bacteriophages in the control of food- and waterborne pathogens*. Washington, DC: Knovel: ASM Press.
- Chanishvili, N. 2012a. *A Literature Review of the Practical Application of Bacteriophages Research*, New York, NY, Nova Science Publishers
- Chanishvili, N. 2012b. Phage therapy--history from Twort and d'Herelle through Soviet experience to current approaches. *Adv Virus Res*, 83, 3-40.
- Chanishvili, N. & Sharp, R. 2008. Bacteriophage therapy: experience from the Eliava Institute, Georgia. *Microbiology Australia*, 29, 96-101.
- Cheah, K. C. & Skurray, R. 1986. The F plasmid carries an IS3 insertion within finO. *J Gen Microbiol*, 132, 3269-75.
- Clowes, R. C. & Rowley, D. 1954. Some observations on linkage effects in genetic recombination in Escherichia coli K-12. *J Gen Microbiol*, 11, 250-60.
- Cohen, M. L. 1992. Epidemiology of drug resistance: implications for a post-antimicrobial era. *Science*, 257, 1050-5.
- Colom, J., Batista, D., Baig, A., Tang, Y., Liu, S., Yuan, F., Belkhir, A., Marcelino, L., Barbosa, F., Rubio, M., Atterbury, R., Berchieri, A. & Barrow, P. 2019. Sex pilus specific bacteriophage to drive bacterial population towards antibiotic sensitivity. *Sci Rep*, 9, 12616.
- Cook, R., Brown, N., Redgwell, T., Rihtman, B., Barnes, M., Clokie, M., Stekel, D. J., Hobman, J., Jones, M. A. & Millard, A. 2021. INfrastructure for a PHAge REference Database: Identification of Large-Scale Biases in the Current Collection of Cultured Phage Genomes. *PHAGE*, 2, 214-223.
- Coque, T. M., Novais, Â., Carattoli, A., Poirel, L., Pitout, J., Peixe, L., Baquero, F., Cantón, R. & Nordmann, P. 2008. Dissemination of clonally related Escherichia coli strains expressing extended-spectrum β -lactamase CTX-M-15. *Emerging infectious diseases*, 14, 195.
- Cullum, J., Collins, J. & Broda, P. 1978. The spread of plasmids in model populations of Escherichia coli K12. *Plasmid*, 1, 545-556.

- D'herelle, F. 2007. On an invisible microbe antagonistic toward dysenteric bacilli: brief note by Mr. F. D'Herelle, presented by Mr. Roux. 1917. *Res Microbiol*, 158, 553-4.
- D'hérelle, F. L. 1926 *The bacteriophage and its behavior* Baltimore, MD, The Williams & Wilkins company.
- Day, L. A. 2011. Family Inoviridae. In: KING, A. M., LEFKOWITZ, E., ADAMS, M. J. & CARSTENS, E. B. (eds.) *Virus taxonomy: Ninth Report of the International Committee on Taxonomy of Viruses: Elsevier Academic Press*
- De Paepe, M. & Taddei, F. 2006. Viruses' life history: towards a mechanistic basis of a trade-off between survival and reproduction among phages. *PLoS Biol*, 4, e193.
- Dion, M. B., Oechslin, F. & Moineau, S. 2020. Phage diversity, genomics and phylogeny. 18, 125-138.
- ECDC. 2014. *Antimicrobial resistance in Europe* [Online]. European Centre for Disease Prevention and Control. Available: <https://ecdc.europa.eu/en/publications-data/antimicrobial-resistance-europe> [Accessed August 8, 2017].
- Eiamphungporn, W., Schaduangrat, N., Malik, A. A. & Nantasenamat, C. 2018. Tackling the Antibiotic Resistance Caused by Class A beta-Lactamases through the Use of beta-Lactamase Inhibitory Protein. 19.
- Farber, M. B. & Ray, D. S. 1980. A clear-plaque mutation of bacteriophage M13 affects the regulation of viral DNA synthesis. *J Virol*, 33, 1106-10.
- Fauquet, C. M., Mayo, M., Maniloff, J. & Desselberger, U. 2005. *Virus taxonomy: The eighth report of the international committee on taxonomy of viruses*. Elsevier Académie Press, San Diego.
- Fehmel, F., Feige, U., Niemann, H. & Stirm, S. 1975. Escherichia coli capsule bacteriophages. VII. Bacteriophage 29-host capsular polysaccharide interactions. *Journal of virology*, 16, 591-601.
- Feng, J. N., Russel, M. & Model, P. 1997. A permeabilized cell system that assembles filamentous bacteriophage. *Proc Natl Acad Sci U S A*, 94, 4068-73.
- Feng, Y. Y., Ong, S. L., Hu, J. Y., Tan, X. L. & Ng, W. J. 2003. Effects of pH and temperature on the survival of coliphages MS2 and Qbeta. *J Ind Microbiol Biotechnol*, 30, 549-52.
- Fernandes, M. R., Mcculloch, J. A., Vianello, M. A., Moura, Q., Perez-Chaparro, P. J., Esposito, F., Sartori, L., Dropa, M., Matte, M. H., Lira, D. P., Mamizuka, E. M. & Lincopan, N. 2016. First Report of the Globally Disseminated IncX4 Plasmid Carrying the mcr-1 Gene in a Colistin-Resistant Escherichia coli Sequence Type 101 Isolate from a Human Infection in Brazil. *Antimicrob Agents Chemother*, 60, 6415-7.
- Fiers, W., Contreras, R., Duerinck, F., Haegeman, G., Iserentant, D., Merregaert, J., Jou, W. M., Molemans, F., Raeymaekers, A. & Van Den Berghe, A. 1976. Complete nucleotide sequence of bacteriophage MS2 RNA: primary and secondary structure of the replicase gene. *Nature*, 260, 500-507.
- Fish, R., Kutter, E., Wheat, G., Blasdel, B., Kutateladze, M. & Kuhl, S. 2016. Bacteriophage treatment of intrasigent diabetic toe ulcers: a case series. *Journal of wound care*, 25, S27-S33.

- Foschino, R., Perrone, F. & Galli, A. 1995. Characterization of two virulent *Lactobacillus fermentum* bacteriophages isolated from sour dough. *Journal of applied bacteriology*, 79, 677-683.
- Founou, L. L., Founou, R. C. & Essack, S. Y. 2016. Antibiotic Resistance in the Food Chain: A Developing Country-Perspective. *Frontiers in Microbiology*, 7.
- Friedman, S. D., Genthner, F. J., Gentry, J., Sobsey, M. D. & Vinje, J. 2009. Gene mapping and phylogenetic analysis of the complete genome from 30 single-stranded RNA male-specific coliphages (family Leviviridae). *J Virol*, 83, 11233-43.
- Friedman, S. D., Snellgrove, W. C. & Genthner, F. J. 2012. Genomic sequences of two novel levivirus single-stranded RNA coliphages (family Leviviridae): evidence for recombination in environmental strains. *Viruses*, 4, 1548-68.
- Frost, L. S. & Koraimann, G. 2010. Regulation of bacterial conjugation: balancing opportunity with adversity. *Future Microbiol*, 5, 1057-71.
- Furfaro, L. L., Payne, M. S. & Chang, B. J. 2018. Bacteriophage Therapy: Clinical Trials and Regulatory Hurdles. *Frontiers in Cellular and Infection Microbiology*, 8.
- Garcillan-Barcia, M. P., Francia, M. V. & De La Cruz, F. 2009. The diversity of conjugative relaxases and its application in plasmid classification. *FEMS Microbiol Rev*, 33, 657-87.
- Garcillan-Barcia, M. P., Jurado, P., Gonzalez-Perez, B., Moncalian, G., Fernandez, L. A. & De La Cruz, F. 2007. Conjugative transfer can be inhibited by blocking relaxase activity within recipient cells with intrabodies. *Mol Microbiol*, 63, 404-16.
- Ghuysen, J. M. 1991. Serine beta-lactamases and penicillin-binding proteins. *Annu Rev Microbiol*, 45, 37-67.
- Green, M. R. & Sambrook, J. 2017. Preparation of Double-Stranded (Replicative Form) Bacteriophage M13 DNA. *Cold Spring Harb Protoc*, 2017, pdb.prot093443.
- Green, S. I., Kaelber, J. T., Ma, L., Trautner, B. W., Ramig, R. F. & Maresso, A. W. 2017. Bacteriophages from ExPEC Reservoirs Kill Pandemic Multidrug-Resistant Strains of Clonal Group ST131 in Animal Models of Bacteremia. *Sci Rep*, 7, 46151.
- Gupta, R. & Prasad, Y. 2011. Efficacy of polyvalent bacteriophage P-27/HP to control multidrug resistant *Staphylococcus aureus* associated with human infections. *Curr Microbiol*, 62, 255-60.
- Hagens, S. & Blasi, U. 2003. Genetically modified filamentous phage as bactericidal agents: a pilot study. *Lett Appl Microbiol*, 37, 318-23.
- Hahn, F. E. & Ciak, J. 1976. Elimination of resistance determinants from R-factor R1 by intercalative compounds. *Antimicrob Agents Chemother*, 9, 77-80.
- Halavatkar, H. & Barrow, P. A. 1993. The role of a 54-kb plasmid in the virulence of strains of *Salmonella enteritidis* of phage type 4 for chickens and mice. *J Med Microbiol*, 38, 171-6.
- Hall, B. G. & Barlow, M. 2005. Revised Ambler classification of {beta}-lactamases. *J Antimicrob Chemother*, 55, 1050-1.
- Hanon, J. B., Jaspers, S., Butaye, P., Wattiau, P., Meroc, E., Aerts, M., Imberechts, H., Vermeersch, K. & Van Der Stede, Y. 2015. A trend analysis of antimicrobial

- resistance in commensal *Escherichia coli* from several livestock species in Belgium (2011-2014). *Prev Vet Med*, 122, 443-52.
- Hawkey, P. 2008. Molecular epidemiology of clinically significant antibiotic resistance genes. *British journal of pharmacology*, 153, S406-S413.
- Helinski, D. R., Aresa, T.E., Novick, R.P. 1996. Replication Control and Other Stable Maintenance Mechanisms of Plasmids. *In: NEIDHARDT, F., CURTISS, R. (ed.) Escherichia coli and Salmonella : cellular and molecular biolog.* 2nd ed. ed. Washington, D.C: Washington, D.C : ASM Press.
- Huff, W. E., Huff, G. R., Rath, N. C., Balog, J. M. & Donoghue, A. M. 2002. Prevention of *Escherichia coli* infection in broiler chickens with a bacteriophage aerosol spray. *Poult Sci*, 81, 1486-91.
- Huff, W. E., Huff, G. R., Rath, N. C., Balog, J. M. & Donoghue, A. M. 2003. Evaluation of aerosol spray and intramuscular injection of bacteriophage to treat an *Escherichia coli* respiratory infection. *Poult Sci*, 82, 1108-12.
- Hyman, P. & Abedon, S. T. 2010. Bacteriophage host range and bacterial resistance. *Adv Appl Microbiol*, 70, 217-48.
- Ictv 2020. Bacterial and Archaeal Viruses Subcommittee (BAVS) of the International Committee on the Taxonomy of Viruses (ICTV) 2019 Master Species List (MSL35), v1. April 23, 2020 ed. Berlin, Germany.
- Inokuchi, Y., Kajitani, M. & Hirashima, A. 1994. A study on the function of the glycine residue in the YGDD motif of the RNA-dependent RNA polymerase β -subunit from RNA coliphage Q β . *The Journal of Biochemistry*, 116, 1275-1280.
- Ippen-Ihler, K. & Minkley Jr, E. 1986. The conjugation system of F, the fertility factor of *Escherichia coli*. *Annual review of genetics*, 20, 593-624.
- Jacobson, A. 1972. Role of F pili in the penetration of bacteriophage fl. *J Virol*, 10, 835-43.
- Jacoby, G. A. & Munoz-Price, L. S. 2005. The new beta-lactamases. *N Engl J Med*, 352, 380-91.
- Jain, R., Knorr, A. L., Bernacki, J. & Srivastava, R. 2006. Investigation of bacteriophage MS2 viral dynamics using model discrimination analysis and the implications for phage therapy. *Biotechnol Prog*, 22, 1650-8.
- Jalasvuori, M., Friman, V. P., Nieminen, A., Bamford, J. K. & Buckling, A. 2011. Bacteriophage selection against a plasmid-encoded sex apparatus leads to the loss of antibiotic-resistance plasmids. *Biol Lett*, 7, 902-5.
- Jault, P., Leclerc, T., Jennes, S., Pirnay, J. P., Que, Y. A., Resch, G., Rousseau, A. F., Ravat, F., Carsin, H., Le Floch, R., Schaal, J. V., Soler, C., Fevre, C., Arnaud, I., Bretaudeau, L. & Gabard, J. 2018. Efficacy and tolerability of a cocktail of bacteriophages to treat burn wounds infected by *Pseudomonas aeruginosa* (PhagoBurn): a randomised, controlled, double-blind phase 1/2 trial. *Lancet Infect Dis*.
- Jerome, L. J. 1999. Mechanism of FinOP fertility inhibition of F-like plasmids.
- Johnson, T. J., Singer, R. S., Isaacson, R. E., Danzeisen, J. L., Lang, K., Kobluk, K., Rivet, B., Borewicz, K., Frye, J. G. & Englen, M. 2015. In vivo transmission of an IncA/C plasmid in *Escherichia coli* depends on tetracycline concentration, and acquisition of the plasmid results in a variable cost of fitness. *Applied and environmental microbiology*, 81, 3561-3570.

- Jończyk, E., Kłak, M., Międzybrodzki, R. & Górski, A. 2011. The influence of external factors on bacteriophages--review. *Folia microbiologica*, 56, 191-200.
- Jun, J. W., Shin, T. H., Kim, J. H., Shin, S. P., Han, J. E., Heo, G. J., De Zoysa, M., Shin, G. W., Chai, J. Y. & Park, S. C. 2014. Bacteriophage therapy of a *Vibrio parahaemolyticus* infection caused by a multiple-antibiotic-resistant O3:K6 pandemic clinical strain. *J Infect Dis*, 210, 72-8.
- Jurczak-Kurek, A., Gasiór, T., Nejman-Falencyk, B., Bloch, S., Dydecka, A., Topka, G., Necel, A., Jakubowska-Deredas, M., Narajczyk, M., Richert, M., Mieszkowska, A., Wrobel, B., Wegrzyn, G. & Wegrzyn, A. 2016. Biodiversity of bacteriophages: morphological and biological properties of a large group of phages isolated from urban sewage. *Sci Rep*, 6, 34338.
- Kaiser, G. & Suchman, E. 2013. Transfer of Conjugative Plasmids and Mobilizable Plasmids in Gram-Negative Bacteria.
- Kamer, G. & Argos, P. 1984. Primary structural comparison of RNA-dependent polymerases from plant, animal and bacterial viruses. *Nucleic Acids Res*, 12, 7269-82.
- Kannoly, S., Shao, Y. & Wang, I. N. 2012. Rethinking the evolution of single-stranded RNA (ssRNA) bacteriophages based on genomic sequences and characterizations of two R-plasmid-dependent ssRNA phages, C-1 and Hgal1. *J Bacteriol*, 194, 5073-9.
- Kearse, M., Moir, R., Wilson, A., Stones-Havas, S., Cheung, M., Sturrock, S., Buxton, S., Cooper, A., Markowitz, S., Duran, C., Thierer, T., Ashton, B., Meintjes, P. & Drummond, A. 2012. Geneious Basic: an integrated and extendable desktop software platform for the organization and analysis of sequence data. *Bioinformatics*, 28, 1647-9.
- King, A. M. 2012. *Virus Taxonomy: Classification and Nomenclature of Viruses: Ninth Report of the International Committee on Taxonomy of Viruses*, Elsevier.
- Knezevic, P., Adriaenssens, E. M. & Consortium, I. R. 2021. ICTV Virus Taxonomy Profile: Inoviridae. *The Journal of General Virology*, 102.
- Knezevic, P. & Andriansen, E. 2021. Inoviridae, ICTV Report. https://talk.ictvonline.org/ictv-reports/ictv_online_report/ssdna-viruses/w/inoviridae.
- Koebnik, R., Locher, K. P. & Van Gelder, P. 2000. Structure and function of bacterial outer membrane proteins: barrels in a nutshell. *Mol Microbiol*, 37, 239-53.
- Koonin, E. V. & Dolja, V. V. 1993. Evolution and taxonomy of positive-strand RNA viruses: implications of comparative analysis of amino acid sequences. *Crit Rev Biochem Mol Biol*, 28, 375-430.
- Koraimann, G., Koraimann, C., Koronakis, V., Schlager, S. & Högenauer, G. 1991. Repression and derepression of conjugation of plasmid R1 by wild-type and mutated finP antisense RNA. *Molecular microbiology*, 5, 77-87.
- Koraimann, G., Teferle, K., Markolin, G., Woger, W. & Hogenauer, G. 1996. The FinOP repressor system of plasmid R1: analysis of the antisense RNA control of traJ expression and conjugative DNA transfer. *Mol Microbiol*, 21, 811-21.
- Kropinski, A. M., Mazzocco, A., Waddell, T. E., Lingohr, E. & Johnson, R. P. 2009. Enumeration of bacteriophages by double agar overlay plaque assay. *Methods Mol Biol*, 501, 69-76.

- Krupovic, M. & Dutilh, B. E. 2016. Taxonomy of prokaryotic viruses: update from the ICTV bacterial and archaeal viruses subcommittee. *161*, 1095-9.
- Kutateladze, M. & Adamia, R. 2008. Phage therapy experience at the Eliava Institute. *Med Mal Infect*, *38*, 426-30.
- Kutter, E., De Vos, D., Gvasalia, G., Alavidze, Z., Gogokhia, L., Kuhl, S. & Abedon, S. T. 2010. Phage therapy in clinical practice: treatment of human infections. *Curr Pharm Biotechnol*, *11*, 69-86.
- Kvesitadze, I. F. Application of bacteriophages in veterinary practice. Bacteriophage Research, Inter-Institutional Conference, 1957 Tbilisi. 337-344.
- Lasobras, J., Muniesa, M., Frias, J., Lucena, F. & Jofre, J. 1997. Relationship between the morphology of bacteriophages and their persistence in the environment. *Water Science and Technology*, *35*, 129-132.
- Lee, S. H., Frost, L. S. & Paranchych, W. 1992. FinOP repression of the F plasmid involves extension of the half-life of FinP antisense RNA by FinO. *Mol Gen Genet*, *235*, 131-9.
- Leflon-Guibout, V., Blanco, J., Amaqdouf, K., Mora, A., Guize, L. & Nicolas-Chanoine, M. H. 2008. Absence of CTX-M enzymes but high prevalence of clones, including clone ST131, among fecal *Escherichia coli* isolates from healthy subjects living in the area of Paris, France. *J Clin Microbiol*, *46*, 3900-5.
- Leon, M. & Bastias, R. 2015. Virulence reduction in bacteriophage resistant bacteria. *Front Microbiol*, *6*, 343.
- Levy, S. B. & Marshall, B. 2004. Antibacterial resistance worldwide: causes, challenges and responses. *Nat Med*, *10*, S122-9.
- Lin, A., Jimenez, J., Derr, J., Vera, P., Manapat, M. L., Esvelt, K. M., Villanueva, L., Liu, D. R. & Chen, I. A. 2011. Inhibition of bacterial conjugation by phage M13 and its protein g3p: quantitative analysis and model. *PLoS One*, *6*, e19991.
- Lin, D. M., Koskella, B. & Lin, H. C. 2017. Phage therapy: an alternative to antibiotics in the age of multi-drug resistance. *World journal of gastrointestinal pharmacology and therapeutics*, *8*, 162.
- Lin, L., Hong, W., Ji, X., Han, J., Huang, L. & Wei, Y. 2010. Isolation and characterization of an extremely long tail *Thermus* bacteriophage from Tengchong hot springs in China. *Journal of basic microbiology*, *50*, 452-456.
- Liu, Y. Y., Wang, Y., Walsh, T. R., Yi, L. X., Zhang, R., Spencer, J., Doi, Y., Tian, G., Dong, B., Huang, X., Yu, L. F., Gu, D., Ren, H., Chen, X., Lv, L., He, D., Zhou, H., Liang, Z., Liu, J. H. & Shen, J. 2016. Emergence of plasmid-mediated colistin resistance mechanism MCR-1 in animals and human beings in China: a microbiological and molecular biological study. *Lancet Infect Dis*, *16*, 161-8.
- Llosa, M., Roy, C. & Dehio, C. 2009. Bacterial type IV secretion systems in human disease. *Molecular microbiology*, *73*, 141-151.
- Loc-Carrillo, C. & Abedon, S. T. 2011. Pros and cons of phage therapy. *Bacteriophage*, *1*, 111-114.
- Loeb, T. 1960. Isolation of a bacteriophage specific for the F+ and Hfr mating types of *Escherichia coli* K-12. *Science*, *131*, 932-933.
- Love, D. C., Davis, M. F., Bassett, A., Gunther, A. & Nachman, K. E. 2011. Dose imprecision and resistance: free-choice medicated feeds in industrial food animal production in the United States. *Environ Health Perspect*, *119*, 279-83.

- Lundquist, P. D. & Levin, B. R. 1986. Transitory derepression and the maintenance of conjugative plasmids. *Genetics*, 113, 483-497.
- Mai-Prochnow, A., Hui, J. G., Kjelleberg, S., Rakonjac, J., Mcdougald, D. & Rice, S. A. 2015. 'Big things in small packages: the genetics of filamentous phage and effects on fitness of their host'. *FEMS Microbiol Rev*, 39, 465-87.
- Mamun, M., Parvej, M., Ahamed, S., Hassan, J., Nazir, K., Nishikawa, Y. & Rahman, M. 2016. Prevalence and characterization of shigatoxigenic Escherichia coli in broiler birds in Mymensingh. *Bangladesh Journal of Veterinary Medicine*, 14, 5-8.
- Markovska, R., Schneider, I., Ivanova, D., Mitov, I. & Bauernfeind, A. 2014. Predominance of IncL/M and IncF plasmid types among CTX-M-ESBL-producing Escherichia coli and Klebsiella pneumoniae in Bulgarian hospitals. *Apmis*, 122, 608-15.
- Marti, R., Zurfluh, K., Hagens, S., Pianezzi, J., Klumpp, J. & Loessner, M. J. 2013. Long tail fibres of the novel broad-host-range T-even bacteriophage S 16 specifically recognize S almonella OmpC. *Molecular microbiology*, 87, 818-834.
- Marvin, D. & Hoffmann-Berling, H. 1963. Physical and chemical properties of two new small bacteriophages. *Nature*, 197, 517.
- May, T., Tsuruta, K. & Okabe, S. 2011. Exposure of conjugative plasmid carrying Escherichia coli biofilms to male-specific bacteriophages. *Isme j*, 5, 771-5.
- Medeiros, A. A. 1997. Evolution and dissemination of beta-lactamases accelerated by generations of beta-lactam antibiotics. *Clin Infect Dis*, 24 Suppl 1, S19-45.
- Mediavilla, J. R., Patrawalla, A., Chen, L., Chavda, K. D., Mathema, B., Vinnard, C., Dever, L. L. & Kreiswirth, B. N. 2016. Colistin- and Carbapenem-Resistant Escherichia coli Harboring mcr-1 and blaNDM-5, Causing a Complicated Urinary Tract Infection in a Patient from the United States. *MBio*, 7.
- Meynell, E., Meynell, G. G. & Datta, N. 1968. Phylogenetic relationships of drug-resistance factors and other transmissible bacterial plasmids. *Bacteriological reviews*, 32, 55.
- Miller, R. V. & Day, M. 2008. Contribution of lysogeny, pseudolysogeny and starvation to phage ecology. In: ABEDON, S. T. (ed.) *Bacteriophage ecology : population growth, evolution, and impact of bacterial viruses*. Cambridge: Cambridge : Cambridge University Press.
- Molnar, J., Fischer, J. & Nakamura, M. J. 1992. Mechanism of chlorpromazine binding by gram-positive and gram-negative bacteria. *Antonie Van Leeuwenhoek*, 62, 309-14.
- Mullineaux, P. & Willetts, N. 1985. Promoters in the transfer region of plasmid F. *Basic Life Sci*, 30, 605-14.
- Murphy, F. A., Fauquet, C. M., Bishop, D. H., Ghabrial, S. A., Jarvis, A. W., Martelli, G. P., Mayo, M. A. & Summers, M. D. 2012. *Virus taxonomy: classification and nomenclature of viruses*, Springer Science & Business Media.
- Nash, R. P., Mcnamara, D. E., Ballentine, W. K., 3rd, Matson, S. W. & Redinbo, M. R. 2012. Investigating the impact of bisphosphonates and structurally related compounds on bacteria containing conjugative plasmids. *Biochem Biophys Res Commun*, 424, 697-703.

- Nasukawa, T., Uchiyama, J., Taharaguchi, S., Ota, S., Ujihara, T., Matsuzaki, S., Murakami, H., Mizukami, K. & Sakaguchi, M. 2017. Virus purification by CsCl density gradient using general centrifugation. *Arch Virol*, 162, 3523-3528.
- Nicolas-Chanoine, M. H., Bertrand, X. & Madec, J. Y. 2014. Escherichia coli ST131, an intriguing clonal group. *Clin Microbiol Rev*, 27, 543-74.
- Nigro, O., Jungbluth, S., Lin, H., Hsieh, C., Miranda, J., Schvarcz, C., Rappé, M. & Steward, G. 2017. Viruses in the oceanic basement. *mBio* 8: e02129-16.
- Novick, R. P., Clowes, R. C., Cohen, S. N., Curtiss, R., 3rd, Datta, N. & Falkow, S. 1976. Uniform nomenclature for bacterial plasmids: a proposal. *Bacteriol Rev*, 40, 168-89.
- Novotny, C., Knight, W. S. & Brinton, C. C., Jr. 1968. Inhibition of bacterial conjugation by ribonucleic acid and deoxyribonucleic acid male-specific bacteriophages. *J Bacteriol*, 95, 314-26.
- O'sullivan, L., Bolton, D., Mcauliffe, O. & Coffey, A. 2019. Bacteriophages in Food Applications: From Foe to Friend. *Annu Rev Food Sci Technol*, 10, 151-172.
- O'neill, J. 2014. Review on Antimicrobial Resistance. Antimicrobial Resistance: Tackling a Crisis for the Health and Wealth of Nations. Wellcome Trust and UK Government.
- Oh, J. S., Davies, D. R., Lawson, J. D., Arnold, G. E. & Dunker, A. K. 1999. Isolation of chloroform-resistant mutants of filamentous phage: localization in models of phage structure. *J Mol Biol*, 287, 449-57.
- Ojala, V., Laitalainen, J. & Jalasvuori, M. 2013. Fight evolution with evolution: plasmid-dependent phages with a wide host range prevent the spread of antibiotic resistance. *Evol Appl*, 6, 925-32.
- Ojala, V., Mattila, S., Hoikkala, V., Bamford, J. K., Hiltunen, T. & Jalasvuori, M. 2016. Scoping the effectiveness and evolutionary obstacles in using plasmid-dependent phages to fight antibiotic resistance. *Future microbiology*, 11, 999-1009.
- Olsthoorn, R. & Van Duin, J. 2001. Bacteriophages with ss RNA. *e LS*.
- Ou, J. T. 1973. Inhibition of formation of Escherichia coli mating pairs by f1 and MS2 bacteriophages as determined with a Coulter counter. *Journal of Bacteriology*, 114, 1108-1115.
- Overby, L. R., Barlow, G. H., Doi, R. H., Jacob, M. & Spiegelman, S. 1966. Comparison of two serologically distinct ribonucleic acid bacteriophages. I. Properties of the viral particles. *J Bacteriol*, 91, 442-8.
- Owens, R. C., Jr., Johnson, J. R., Stogsdill, P., Yarmus, L., Lolans, K. & Quinn, J. 2011. Community transmission in the United States of a CTX-M-15-producing sequence type ST131 Escherichia coli strain resulting in death. *J Clin Microbiol*, 49, 3406-8.
- Oyedemi, B. O., Shinde, V., Shinde, K., Kakalou, D., Stapleton, P. D. & Gibbons, S. 2016. Novel R-plasmid conjugal transfer inhibitory and antibacterial activities of phenolic compounds from Mallotus philippensis (Lam.) Mull. Arg. *J Glob Antimicrob Resist*, 5, 15-21.
- Park, S. C., Shimamura, I., Fukunaga, M., Mori, K. I. & Nakai, T. 2000. Isolation of bacteriophages specific to a fish pathogen, Pseudomonas plecoglossicida, as a candidate for disease control. *Appl Environ Microbiol*, 66, 1416-22.

- Paterson, D. L. & Bonomo, R. A. 2005. Extended-spectrum beta-lactamases: a clinical update. *Clin Microbiol Rev*, 18, 657-86.
- Peng, Z., Li, X., Hu, Z., Li, Z., Lv, Y., Lei, M., Wu, B., Chen, H. & Wang, X. 2019. Characteristics of Carbapenem-Resistant and Colistin-Resistant *Escherichia coli* Co-Producing NDM-1 and MCR-1 from Pig Farms in China. *Microorganisms*, 7.
- Petty, N. K., Foulds, I. J., Pradel, E., Ewbank, J. J. & Salmond, G. P. 2006. A generalized transducing phage (ϕ IF3) for the genomically sequenced *Serratia marcescens* strain Db11: a tool for functional genomics of an opportunistic human pathogen. *Microbiology*, 152, 1701-1708.
- Pitout, J. D. 2010. Infections with extended-spectrum beta-lactamase-producing enterobacteriaceae: changing epidemiology and drug treatment choices. *Drugs*, 70, 313-33.
- Plevka, P., Kazaks, A., Voronkova, T., Kotelovica, S., Dishlers, A., Liljas, L. & Tars, K. 2009. The structure of bacteriophage phiCb5 reveals a role of the RNA genome and metal ions in particle stability and assembly. *J Mol Biol*, 391, 635-47.
- Ploss, M. & Kuhn, A. 2010. Kinetics of filamentous phage assembly. *Phys Biol*, 7, 045002.
- Potron, A., Poirel, L. & Nordmann, P. 2014. Derepressed transfer properties leading to the efficient spread of the plasmid encoding carbapenemase OXA-48. *Antimicrob Agents Chemother*, 58, 467-71.
- Pouillot, F., Chomton, M., Blois, H., Courroux, C., Noelig, J., Bidet, P., Bingen, E. & Bonacorsi, S. 2012. Efficacy of bacteriophage therapy in experimental sepsis and meningitis caused by a clone O25b:H4-ST131 *Escherichia coli* strain producing CTX-M-15. *Antimicrob Agents Chemother*, 56, 3568-75.
- Pulss, S., Semmler, T., Prenger-Berninghoff, E., Bauerfeind, R. & Ewers, C. 2017. First report of an *Escherichia coli* strain from swine carrying an OXA-181 carbapenemase and the colistin resistance determinant MCR-1. *Int J Antimicrob Agents*, 50, 232-236.
- Raetz, C. R. & Whitfield, C. 2002. Lipopolysaccharide endotoxins. *Annu Rev Biochem*, 71, 635-700.
- Rahman, M., Shukla, S. K., Prasad, K. N., Ovejero, C. M., Pati, B. K., Tripathi, A., Singh, A., Srivastava, A. K. & Gonzalez-Zorn, B. 2014. Prevalence and molecular characterisation of New Delhi metallo-beta-lactamases NDM-1, NDM-5, NDM-6 and NDM-7 in multidrug-resistant Enterobacteriaceae from India. *Int J Antimicrob Agents*, 44, 30-7.
- Rakonjac, J. 2012. Filamentous bacteriophages: biology and applications. *e LS*.
- Rakonjac, J., Russel, M., Khanum, S., Brooke, S. J. & Rajic, M. 2017. Filamentous Phage: Structure and Biology. *Adv Exp Med Biol*, 1053, 1-20.
- Ramesh, V., Fralick, J. A. & Rolfe, R. D. 1999. Prevention of *Clostridium difficile*-induced ileocectitis with bacteriophage. *Anaerobe*, 5, 69-78.
- Rasched, I. & Oberer, E. 1986. Ff coliphages: structural and functional relationships. *Microbiol Rev*, 50, 401-27.
- Raya, R. R., Oot, R. A., Moore-Maley, B., Wieland, S., Callaway, T. R., Kutter, E. M. & Brabban, A. D. 2011. Naturally resident and exogenously applied T4-like and

- T5-like bacteriophages can reduce Escherichia coli O157: H7 levels in sheep guts. *Bacteriophage*, 1, 15-24.
- Rice, L. B. 2012. Mechanisms of resistance and clinical relevance of resistance to beta-lactams, glycopeptides, and fluoroquinolones. *Mayo Clin Proc*, 87, 198-208.
- Ripp, S. & Miller, R. 1997. The role of pseudolysogeny in bacteriophage-host interactions in a natural freshwater environment. *Microbiology-(UK)*, 143, 2065-2070.
- Rodrigue, D. C., Cameron, D. N., Puhr, N. D., Brenner, F. W., St Louis, M. E., Wachsmuth, I. K. & Tauxe, R. V. 1992. Comparison of plasmid profiles, phage types, and antimicrobial resistance patterns of Salmonella enteritidis isolates in the United States. *J Clin Microbiol*, 30, 854-7.
- Rozwandowicz, M., Brouwer, M. S. M., Fischer, J., Wagenaar, J. A., Gonzalez-Zorn, B., Guerra, B., Mevius, D. J. & Hordijk, J. 2018. Plasmids carrying antimicrobial resistance genes in Enterobacteriaceae. *J Antimicrob Chemother*, 73, 1121-1137.
- Rumnieks, J. & Tars, K. 2012. Diversity of pili-specific bacteriophages: genome sequence of IncM plasmid-dependent RNA phage M. *BMC Microbiol*, 12, 277.
- Rūmnieks, J. & Tārs, K. 2018. Protein-RNA Interactions in the Single-Stranded RNA Bacteriophages. *Subcell Biochem*, 88, 281-303.
- Russel, M., Lowman, H. B. & Clackson, T. 2004. Introduction to phage biology and phage display. *Phage Display: A practical approach*, 1-26.
- Saitou, N. & Nei, M. 1987. The neighbor-joining method: a new method for reconstructing phylogenetic trees. *Mol Biol Evol*, 4, 406-25.
- Santajit, S. & Indrawattana, N. 2016. Mechanisms of Antimicrobial Resistance in ESKAPE Pathogens. *BioMed Research International*, 2016.
- Scanlan, P. D., Bischofberger, A. M. & Hall, A. R. 2017. Modification of Escherichia coli-bacteriophage interactions by surfactants and antibiotics in vitro. *FEMS microbiology ecology*, 93, fiw211.
- Seemann, T. 2014. Prokka: rapid prokaryotic genome annotation. *Bioinformatics*, 30, 2068-9.
- Shin, H., Lee, J.-H., Kim, H., Choi, Y., Heu, S. & Ryu, S. 2012. Receptor diversity and host interaction of bacteriophages infecting Salmonella enterica serovar Typhimurium.
- Shintani, M., Sanchez, Z. K. & Kimbara, K. 2015. Genomics of microbial plasmids: classification and identification based on replication and transfer systems and host taxonomy. *Front Microbiol*, 6, 242.
- Simonsen, L. 1990. Dynamics of plasmid transfer on surfaces. *Microbiology*, 136, 1001-1007.
- Singleton, R. L., Sanders, C. A., Jones, K., Thorington, B. & Egbo, T. 2018. Function of the RNA Coliphage Q β Proteins in Medical In Vitro Evolution. 1.
- Sklar, I. B. & Joerger, R. D. 2001. Attempts to utilize bacteriophage to combat *Salmonella enterica* serovar enteritidis infection in chickens. *Journal of Food Safety*, 21, 15-29.
- Smith, H. W. 1969. Transfer of antibiotic resistance from animal and human strains of Escherichia coli to resident E. coli in the alimentary tract of man. *Lancet*, 1, 1174-6.

- Smith, H. W. 1970. The transfer of antibiotic resistance between strains of enterobacteria in chicken, calves and pigs. *J Med Microbiol*, 3, 165-80.
- Smith, H. W. & Huggins, M. B. 1982. Successful treatment of experimental Escherichia coli infections in mice using phage: its general superiority over antibiotics. *J Gen Microbiol*, 128, 307-18.
- Smith, H. W. & Huggins, M. B. 1983. Effectiveness of phages in treating experimental Escherichia coli diarrhoea in calves, piglets and lambs. *J Gen Microbiol*, 129, 2659-75.
- Smith, H. W., Huggins, M. B. & Shaw, K. M. 1987a. The control of experimental Escherichia coli diarrhoea in calves by means of bacteriophages. *J Gen Microbiol*, 133, 1111-26.
- Smith, H. W., Huggins, M. B. & Shaw, K. M. 1987b. Factors influencing the survival and multiplication of bacteriophages in calves and in their environment. *J Gen Microbiol*, 133, 1127-35.
- Smith, H. W. & Tucker, J. F. 1975. The effect of antibiotic therapy on the faecal excretion of Salmonella typhimurium by experimentally infected chickens. *J Hyg (Lond)*, 75, 275-92.
- Smith, J. T. & Lewin, C. S. 1993. Mechanisms of antimicrobial resistance and implications for epidemiology. *Vet Microbiol*, 35, 233-42.
- Som, A. 2006. Theoretical foundation to estimate the relative efficiencies of the Jukes-Cantor+gamma model and the Jukes-Cantor model in obtaining the correct phylogenetic tree. *Gene*, 385, 103-10.
- Su, L.-H., Chu, C., Cloeckert, A. & Chiu, C.-H. 2008. An epidemic of plasmids? Dissemination of extended-spectrum cephalosporinases among Salmonella and other Enterobacteriaceae. *FEMS Immunology & Medical Microbiology*, 52, 155-168.
- Sulakvelidze, A., Alavidze, Z. & Morris, J. G., Jr. 2001. Bacteriophage therapy. *Antimicrob Agents Chemother*, 45, 649-59.
- Suttle, C. A. 2005. Viruses in the sea. *Nature*, 437, 356-61.
- Tadesse, D. A., Zhao, S., Tong, E., Ayers, S., Singh, A., Bartholomew, M. J. & Mcdermott, P. F. 2012. Antimicrobial drug resistance in Escherichia coli from humans and food animals, United States, 1950-2002. *Emerging infectious diseases*, 18, 741.
- Tamura, K. & Nei, M. 1993. Estimation of the number of nucleotide substitutions in the control region of mitochondrial DNA in humans and chimpanzees. *Mol Biol Evol*, 10, 512-26.
- Tamura, K., Nei, M. & Kumar, S. 2004. Prospects for inferring very large phylogenies by using the neighbor-joining method. *Proc Natl Acad Sci U S A*, 101, 11030-5.
- Tars, K. 2020. ssRNA Phages: Life Cycle, Structure and Applications. *Biocommunication of Phages*. Springer.
- Thomas, C. M. & Nielsen, K. M. 2005. Mechanisms of, and barriers to, horizontal gene transfer between bacteria. *Nat Rev Microbiol*, 3, 711-21.
- Thompson, J. D., Higgins, D. G. & Gibson, T. J. 1994. CLUSTAL W: improving the sensitivity of progressive multiple sequence alignment through sequence weighting, position-specific gap penalties and weight matrix choice. *Nucleic Acids Res*, 22, 4673-80.

- Tiseo, K., Huber, L., Gilbert, M., Robinson, T. P. & Van Boeckel, T. P. 2020. Global trends in antimicrobial use in food animals from 2017 to 2030. *Antibiotics*, 9, 918.
- Tsukada, K., Okazaki, M., Kita, H., Inokuchi, Y., Urabe, I. & Yomo, T. 2009. Quantitative analysis of the bacteriophage Qbeta infection cycle. *Biochim Biophys Acta*, 1790, 65-70.
- Twort, F. W. 1915. An investigation on the nature of ultra-microscopic viruses. *The Lancet*, 186, 1241-1243.
- Unterholzner, S. J., Poppenberger, B. & Rozhon, W. 2013. Toxin-antitoxin systems: biology, identification, and application. *Mobile genetic elements*, 3, e26219.
- Van Biesen, T. & Frost, L. S. 1994. The FinO protein of IncF plasmids binds FinP antisense RNA and its target, traJ mRNA, and promotes duplex formation. *Mol Microbiol*, 14, 427-36.
- Van Boeckel, T. P., Glennon, E. E., Chen, D., Gilbert, M., Robinson, T. P., Grenfell, B. T., Levin, S. A., Bonhoeffer, S. & Laxminarayan, R. 2017. Reducing antimicrobial use in food animals. *Science*, 357, 1350-1352.
- Van Boeckel, T. P. & Pires, J. 2019. Global trends in antimicrobial resistance in animals in low- and middle-income countries. 365.
- Van Duin, J. & Tsareva, N. 2006. Single-stranded RNA phages, p 175-196. *The bacteriophages*. Oxford University Press, New York, NY.
- Virolle, C., Goldlust, K., Djermoun, S., Bigot, S. & Lesterlin, C. 2020. Plasmid transfer by conjugation in Gram-negative bacteria: from the cellular to the community level. *Genes*, 11, 1239.
- Walker, P. J. & Siddell, S. G. 2020. Changes to virus taxonomy and the Statutes ratified by the International Committee on Taxonomy of Viruses (2020). 165, 2737-2748.
- Wang, J., Hu, B., Xu, M., Yan, Q., Liu, S., Zhu, X., Sun, Z., Reed, E., Ding, L., Gong, J., Li, Q. Q. & Hu, J. 2006a. Use of bacteriophage in the treatment of experimental animal bacteremia from imipenem-resistant *Pseudomonas aeruginosa*. *Int J Mol Med*, 17, 309-17.
- Wang, J., Hu, B., Xu, M., Yan, Q., Liu, S., Zhu, X., Sun, Z., Tao, D., Ding, L., Reed, E., Gong, J., Li, Q. Q. & Hu, J. 2006b. Therapeutic effectiveness of bacteriophages in the rescue of mice with extended spectrum beta-lactamase-producing *Escherichia coli* bacteremia. *Int J Mol Med*, 17, 347-55.
- Wang, R., Liu, Y., Zhang, Q., Jin, L., Wang, Q., Zhang, Y., Wang, X., Hu, M., Li, L., Qi, J., Luo, Y. & Wang, H. 2018. The prevalence of colistin resistance in *Escherichia coli* and *Klebsiella pneumoniae* isolated from food animals in China: coexistence of mcr-1 and bla_{NDM} with low fitness cost. *Int J Antimicrob Agents*, 51, 739-744.
- Watanabe, I., Miyake, T., Sakurai, T., Shiba, T. & Ohno, T. 1967. Isolation and grouping of RNA phages. *Proceedings of the Japan Academy*, 43, 204-209.
- Watanabe, R., Matsumoto, T., Sano, G., Ishii, Y., Tateda, K., Sumiyama, Y., Uchiyama, J., Sakurai, S., Matsuzaki, S., Imai, S. & Yamaguchi, K. 2007. Efficacy of bacteriophage therapy against gut-derived sepsis caused by *Pseudomonas aeruginosa* in mice. *Antimicrob Agents Chemother*, 51, 446-52.
- Waters, V. L. 1999. Conjugative transfer in the dissemination of beta-lactam and aminoglycoside resistance. *Front Biosci*, 4, D433-56.

- Weiner, A. M. & Weber, K. 1973. A single UGA codon functions as a natural termination signal in the coliphage ϕ beta coat protein cistron. *J Mol Biol*, 80, 837-55.
- Wernicki, A., Nowaczek, A. & Urban-Chmiel, R. 2017. Bacteriophage therapy to combat bacterial infections in poultry. *Virology*, 14, 179.
- Willetts, N. 1977. The transcriptional control of fertility in F-like plasmids. *J Mol Biol*, 112, 141-8.
- Wills, Q. F., Kerrigan, C. & Soothill, J. S. 2005. Experimental bacteriophage protection against *Staphylococcus aureus* abscesses in a rabbit model. *Antimicrob Agents Chemother*, 49, 1220-1.
- Wood, D. E. & Salzberg, S. L. 2014. Kraken: ultrafast metagenomic sequence classification using exact alignments. *Genome Biol*, 15, R46.
- World Health Organization. 2016. *Antimicrobial Resistance Fact sheet* [Online]. Available: <http://www.who.int/mediacentre/factsheets/fs194/en/> [Accessed May 31, 2017].
- Wright, A., Hawkins, C. H., Anggard, E. E. & Harper, D. R. 2009. A controlled clinical trial of a therapeutic bacteriophage preparation in chronic otitis due to antibiotic-resistant *Pseudomonas aeruginosa*; a preliminary report of efficacy. *Clin Otolaryngol*, 34, 349-57.
- Xia, G., Corrigan, R. M., Winstel, V., Goerke, C., Gründling, A. & Peschel, A. 2011. Wall teichoic acid-dependent adsorption of staphylococcal siphovirus and myovirus. *Journal of bacteriology*, 193, 4006-4009.
- Ye, H. Y., Li, Y. H., Li, Z. C., Gao, R. S., Zhang, H., Wen, R. H., Gao, G. F., Hu, Q. H. & Feng, Y. J. 2016. Diversified mcr-1-Harboring Plasmid Reservoirs Confer Resistance to Colistin in Human Gut Microbiota. *Mbio*, 7.
- Yoshioka, Y., Ohtsubo, H. & Ohtsubo, E. 1987. Repressor gene finO in plasmids R100 and F: Constitutive transfer of plasmid F is caused by insertion of IS3 into F finO. *Journal of Bacteriology*, 169, 619-623.
- Zatyka, M. & Thomas, C. M. 1998. Control of genes for conjugative transfer of plasmids and other mobile elements. *FEMS Microbiology Reviews*, 21, 291-319.
- Zhang, L., Bao, H., Wei, C., Zhang, H., Zhou, Y. & Wang, R. 2015. Characterization and partial genomic analysis of a lytic Myoviridae bacteriophage against *Staphylococcus aureus* isolated from dairy cows with mastitis in Mid-east of China. *Virus Genes*, 50, 111-7.

